AWARD NUMBER: W81XWH-12-1-0538

TITLE: Treatment of the Cornea Using Transcytotic Delivery into the Tear Film

PRINCIPAL INVESTIGATOR: J. Andrew MacKay

CONTRACTING ORGANIZATION: University of Southern California
Los Angeles, CA 90089

REPORT DATE: December 2015

TYPE OF REPORT: Final

PREPARED FOR: U.S. Army Medical Research and Materiel Command
Fort Detrick, Maryland 21702-5012

REPORT DOCUMENTATION PAGE

Form Approved
OMB No. 0704-0188

1. REPORT DATE	2. REPORT TYPE	3. DATES COVERED
December 2015	Final	27 Sep 2012 - 26 Sep 2015

4. TITLE AND SUBTITLE

Treatment of the Cornea Using Transcytotic Delivery into the Tear Film

5a. CONTRACT NUMBER

5b. GRANT NUMBER
W81XWH-12-1-0538

5c. PROGRAM ELEMENT NUMBER

6. AUTHOR(S)

J.A. Mackay, Wan Wang, Maria C. Edman, Pang-Yu Hseuh, Sarah Hamm-Alvarez

E-Mail: jamackay@usc.edu

5d. PROJECT NUMBER

5e. TASK NUMBER

5f. WORK UNIT NUMBER

7. PERFORMING ORGANIZATION NAME(S) AND ADDRESS(ES)
University of Southern California,
School of Pharmacy,
Dep. Of Pharmacology and
Pharmaceutical Sciences
1985 Zonal Ave
Los Angeles CA 90033

8. PERFORMING ORGANIZATION REPORT NUMBER

9. SPONSORING / MONITORING AGENCY NAME(S) AND ADDRESS(ES)

U.S. Army Medical Research and Materiel Command
Fort Detrick, Maryland 21702-5012

10. SPONSOR/MONITOR'S ACRONYM(S)

11. SPONSOR/MONITOR'S REPORT NUMBER(S)

12. DISTRIBUTION / AVAILABILITY STATEMENT

Approved for Public Release; Distribution Unlimited

13. SUPPLEMENTARY NOTES

14. ABSTRACT

The aim of this study is to develop therapeutics that are retained at the ocular surface and stimulate corneal wound healing using a biodegradable and biocompatible drug delivery platform technology to treat combat-related eye injuries. Utilizing a local delivery approach with direct intra lacrimal injection combined with an unique drug delivery platform, consisting of biodegradable nanoparticles targeted to facilitate uptake into the lacrimal gland, we have been able to form local drug depots in the lacrimal gland. In addition, we have observed transcytosis of related nanoparticles across the polarized lacrimal gland acinar cells. The therapeutic agent used in these studies has a strong prosecretory effect on the lacrimal gland and a mitogenic effect on corneal wound healing. These findings pave the way for a unique strategy of drug delivery to the lacrimal gland and the anterior segment of the eye, enabling a quick treatment promoting wound healing that is sustainable until an injured soldier in the field can reach a hospital setting for further treatment.

15. SUBJECT TERMS

transcytosis, dry eye disease, lacrimal gland, elastin-like polypeptide, protein polymer, nanomedicine, drug delivery, lacritin, adenovirus, knob

16. SECURITY CLASSIFICATION OF:			17. LIMITATION OF ABSTRACT	18. NUMBER OF PAGES	19a. NAME OF RESPONSIBLE PERSON
a. REPORT	b. ABSTRACT	c. THIS PAGE			USAMRMC
Unclassified	Unclassified	Unclassified	Unclassified	20	19b. TELEPHONE NUMBER *(include area code)*

Table of contents

1. Introduction

The goal of this study was to develop therapeutics that are retained at the ocular surface and stimulate corneal wound healing using a biodegradable and biocompatible drug delivery platform technology to treat combat-related eye injuries. To accomplish this, we set out to use protein engineering to modify the ocular targeting of a human tear protein called lacritin in fusion with a small library of repetitive protein-polymers derived from human tropoelastin. **During this period of study, we were successfully able to study receptor-mediated transcytosis of the rabbit and mouse lacrimal glands, as well as possible therapeutic activity on a human corneal epithelial cell line and on both mouse lacrimal gland cells and corneal epithelium.** These findings have been published as three separate works and we are working to develop these into a viable therapeutic.

The LG is a specialized exocrine gland responsible for the secretion of proteins and fluid, which together comprise the aqueous layer of the tear film. This gland is largely comprised of acinar epithelial cells joined by tight junctions at lateral membranes near cell apices to create lumina lined with apical plasma membrane [1, 2] Robust exocytotic and transcytotic transport mechanisms in acinar cells facilitate release of proteins and fluid into the lumina, which drain through ducts to the ocular surface. The LG is critical for supplying nutrients, antibodies and antibacterial proteins to sustain the integrity of the cornea and ocular surface system. As a high capacity excretory organ with output directed to the ocular surface, the LG represents an unexplored target for sustained release of drugs into the tear film for treatment of acute ocular surface trauma.

Once rarely used for medical treatments, protein therapeutics have become more popular because of their great target specificity and minimum immune response [3]. Here we are utilizing a unique local (intra-lacrimal) strategy for delivery of biological therapeutics encapsulated in a biocompatible and biodegradable protein-polymer based nanoparticle delivery system targeted to the LG that will enable sustained release of drugs, specifically lacritin [4], through endogenous LG transport pathways. Lacritin is a bifunctional protein secreted naturally by the LG that both stimulates LG acinar secretion [4-6] and is thought to function as a promitogenic factor for promoting epithelial renewal on the ocular surface [7]. Its cell specificity is generated by a unique 'off-on' switch controlled by heparanase deglycanation of cell surface Syndecan 1(SDC1) [8]. Detected by 2-D PAGE, nano-LC-MS/MS and SELDI studies, lacritin shows a common down regulation in blepharitis (chronic inflammation of the eyelid) *vs.* normal tears [9]. LG-targeted delivery of this therapeutic within our novel delivery system is chosen for its ability to sustain release over the time period immediately following injury, when it may not be possible to manually administer the therapy directly to the ocular surface at a frequency sufficient for therapeutic effect. A major shortcoming of current ocular surface-targeted therapies for diseases or trauma to the anterior segment is that the nasolacrimal ducts efficiently drain tear fluid from the eye surface, such that the effectiveness of topical treatment is often short-lived. For agents that require sustained exposure to the ocular surface in treatment of acute infection or trauma, patients must utilize excessively frequent administration, installation of a cumbersome continual infusion pump, or hospitalization. None of these options may be available in a combat situation.

To overcome these obstacles, the present study targets lacritin to the LG and tears using a combination of molecular and physical mechanisms. To facilitate both approaches, we propose to use a novel class of polypeptides that are biologically inspired from a five amino acid motif identified in tropoelastin, a human extracellular matrix protein. These elastin-like polypeptides (ELPs) [10] are ideal for LG targeting because they can: (i) be tuned to self-assemble into multivalent polypeptide nanoparticles to modulate cellular uptake [11, 12], (ii) be seamlessly fused to proteins (in this case, both a targeting protein and a therapeutic protein) without the need for bioconjugate chemistry [13]; (iii) undergo slow proteolytic biodegradation [14]; and (iv) be non-immunogenic [15]. As a platform technology, ELP nanoparticles are unique in that they are entirely genetically engineered. They provide an innovative and powerful approach to assemble multivalent core-shell nanoparticles with protein or peptide targeting ligands such as the knob protein, and therapeutic proteins, such as lacritin, within a single nanoparticle. The ability to co-assemble bi-functional nanoparticles in a controlled manner is of critical importance to easily and cheaply access more complex nano-architecture with multiple functions [16, 17]. Our strategy to co-assemble LSI-KSI micelle simply takes advantage of the specific targeting property of Knob domain and prosecretory/mitogenic efficacy of lacritin to achieve novel drug properties.

2. Keywords

Transcytosis, dry eye disease, lacrimal gland, elastin-like polypeptide, protein polymer, nanomedicine, drug delivery, lacritin, adenovirus, knob

3. Overall project summary

During this three-year project, we made substantial progress on the proposed study, which includes making strides to publish our results from aims 1, 2, and 3. This project has been largely successful in that we have proceeded to confirm and characterize the transcytosis of the lacrimal gland utilizing both the CAR receptor and an unknown receptor for the human tear protein lacritin. Further, we demonstrated that engineered variations on the human tear protein lacritin appear to have prosecretory activity in the mouse lacrimal gland as well as regenerative potential at the corneal epithelium. We have produced three important publications documenting this work, and have shared these results at major international meetings. The following report summarizes findings from years 1-3 resulting from this work.

Aim 1) characterize the transcytotic behavior of knob-ELP nanoparticles in LG.

Our **first milestone** was to confirm "**transcytosis of LG targeted ELP nanoparticles using in vitro cultured rabbit lacrimal gland acinar cells and ex vivo murine lacrimal gland perfusion**". Over this project we have extensively characterized the intracellular trafficking pathways of transcytosing knob-ELP, as follows. In milestone 1 we confirmed transcytosis of LG targeted ELP nanoparticles using *in vitro* cultured rabbit lacrimal gland acinar cells and ex vivo murine lacrimal gland perfusion. We reconfirmed data in the original grant application with additional controls and also made a surprising finding. Previously, we confirmed that knob-S48I48 (KSI), an ELP nanoparticle targeted against the coxsackie and adenovirus receptor (CAR) binds to lacrimal gland acinar cells (LGACs), which have high expression of CAR (7). Under this grant, we determined that these particles do in fact traffic to low pH compartments; however, only the KSI nanoparticles continued to traffic to the lumen within LGAC clusters (**Fig. 1**). We then proceeded to investigate the exact mechanisms for transcytosis (**Fig. 2**), which revealed that Rab5A coated vesicles are responsible for transcytotic transport across the LGACs.

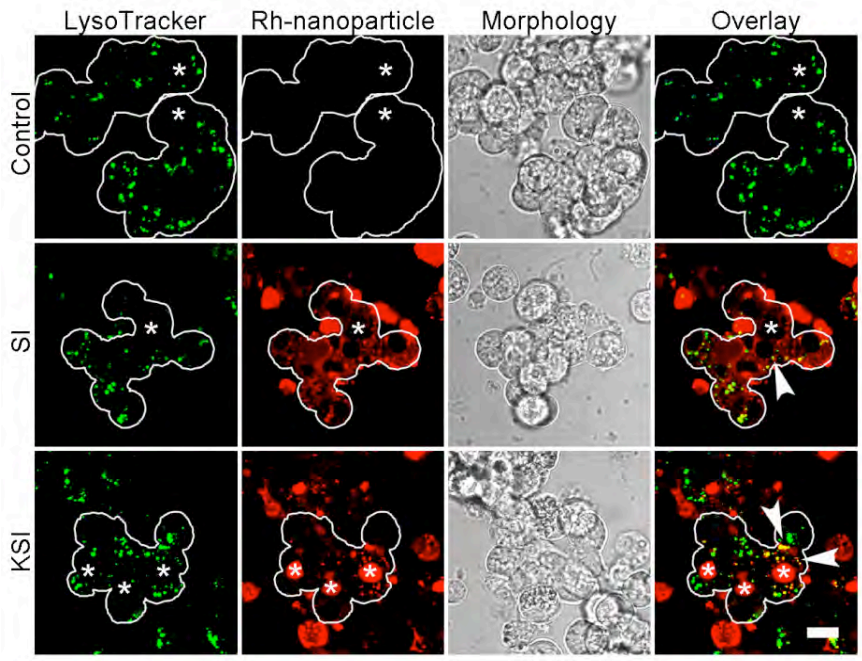

Figure 1. ELP nanoparticles traffic to low pH compartments in rabbit LGACs. 30 μM of Rh-coupled SI or KSI were incubated with rabbit LGACs at 37 °C for 1 hr, and imaged using confocal fluorescence microscopy. KSI (red) exhibited significant co-localization with acidic compartments labelled by LysoTracker green (green) as well as lumenal (*) accumulation. SI showed significant surface binding and also some internalization to acidic compartments labelled by LysoTracker green. Arrowheads indicate the co-localization of SI or KSI with acidic compartments. White lines delineate the BLM of LG acinar clusters. *, lumena. Scale bar indicates 10 μm.

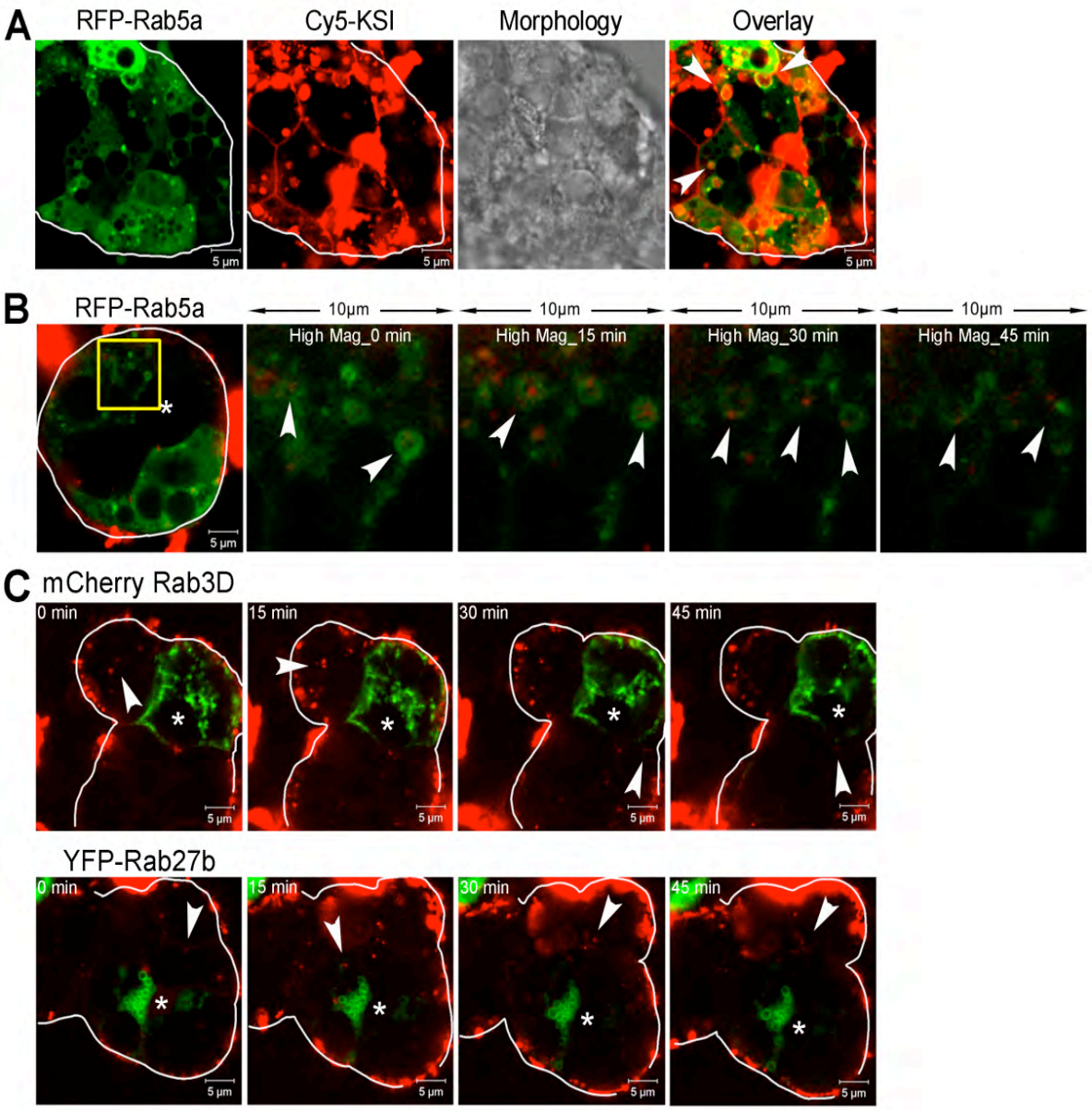

Figure 2. Intracellular trafficking of KSI nanoparticles in LGACs. (A) Internalization of KSI to early endosomes in live rabbit LGACs expressing RFP-Rab5a, a marker of early endosomes. LGACs transduced with RFP-Rab5a (green) were treated with 30 μM of Cy5-KSI (red) at 37 ^{o}C for 1 hr, washed with DPBS twice, and analyzed by confocal fluorescence microscopy. Arrowheads indicate Cy5-KSI in early endosomes. (B) LGACs transduced with RFP-Rab5a (green) were pulsed with 30 μM of Cy5-KSI (red) at 37 ^{o}C for 10 min, rinsed and followed by a 45 min chase in fresh PCM at 37 ^{o}C. The yellow-boxed region is expanded in time-lapse images shown successively to the right. Arrowheads indicate early endosomes that include Cy5-KSI at earlier times but show label dissipating at later times of incubation. White lines depict the periphery of the reconstituted cluster of LGAC obtained by phase contrast imaging. (C) LGACs expressing mCherry-Rab3D (red) or YFP-Rab27b (red) were pulsed with 30 μM of Cy5-KSI (green) at 37 ^{o}C for 10 min and imaged for 45 min in fresh PCM at 37 ^{o}C. Internalized KSI did not associate with either Rab3D or Rab27b in live rabbit LGACs. Data were presented at the indicated time points. White lines depict the periphery of the reconstituted cluster of LGACs. Arrowheads indicate internalized Cy5-KSI. Scale bars indicate 5 μm.

We further characterized and quantified the degree of transcytosis by overexpression of the Myosin V b motor protein tail. Overexpression of this tail has a dominant negative effect, which was successfully able to inhibit transcytosis across the LGACs (**Fig. 3**), which is consistent with active transport across the cell.

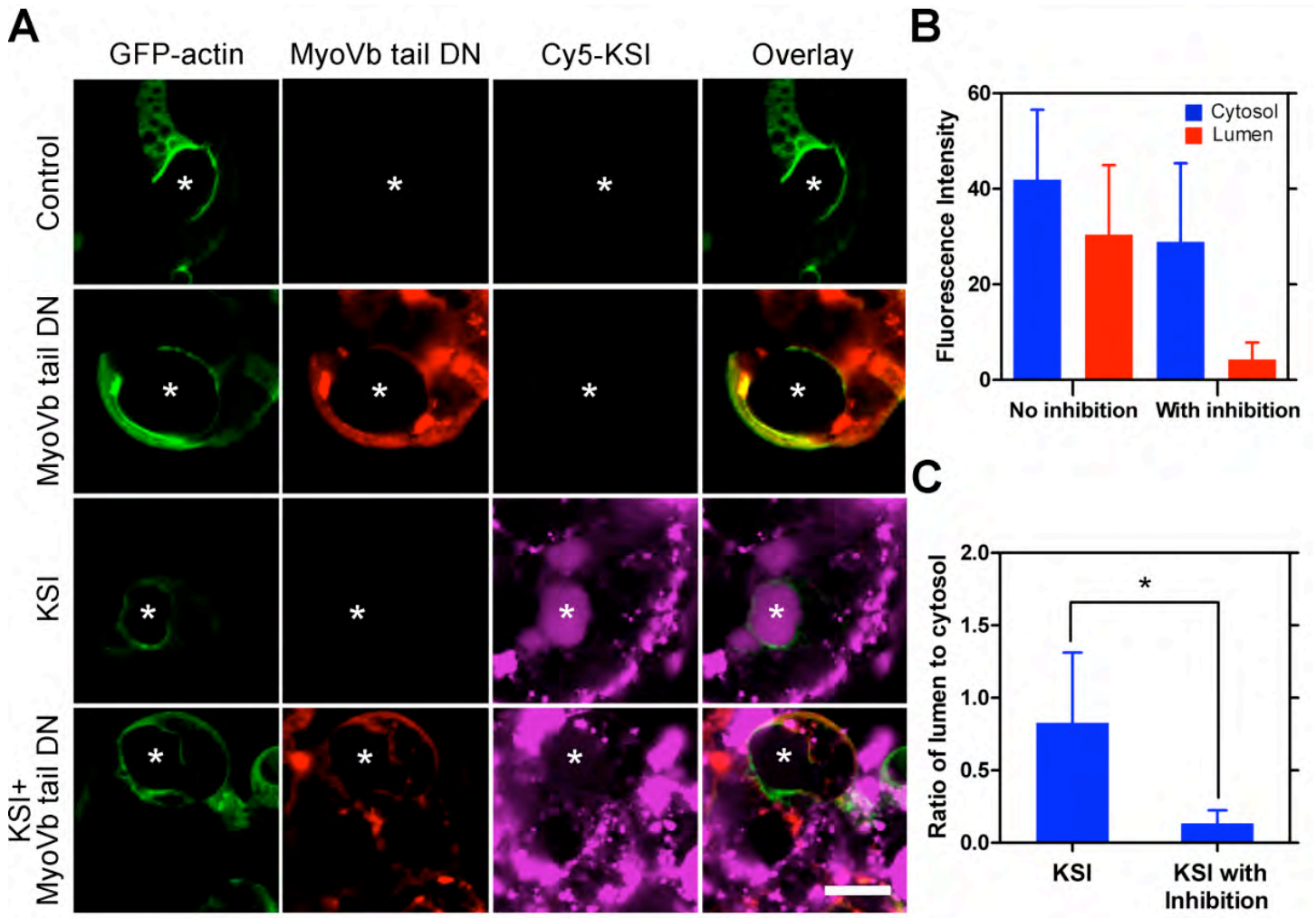

Figure 3. Overexpression of a dominant negative Myosin Vb tail impairs basolateral-to-apical transcytosis of KSI in LGACs. (A) Reconstituted rabbit LGACs, co-transduced with AdGFP-actin (green) to delineate morphology, Ad mCherry Myosin Vb tail DN (red), and Ad helper virus, were incubated with 30 μM of Cy5-KSI nanoparticles (purple) at 37 ^{o}C for 1 hr before analysis. *, lumenal region of LGACs. Scale bar indicates 10 μm. (B) Quantification of fluorescence intensity in lumen and cytosol of LGACs with or without the dominant negative myosin Vb tail, which inhibits transcytosis. Data were expressed as Mean ± SEM (N=4). (C) Quantification of fluorescence intensity as a ratio of lumenal to cytosolic fluorescence. Data were expressed as Mean ± SEM (N=4). KSI, 0.83± 0.24; KSI with inhibition, 0.13 ± 0.05; p value < 0.05.

In milestone 2 we set out to purify 1 gram of ELP KSI nanoparticles sufficient to support the significant *in vivo* murine studies in the subsequent aims. This task was accomplished in early April 2013; however, we continue to produce additional material as required (**Fig. 4**).

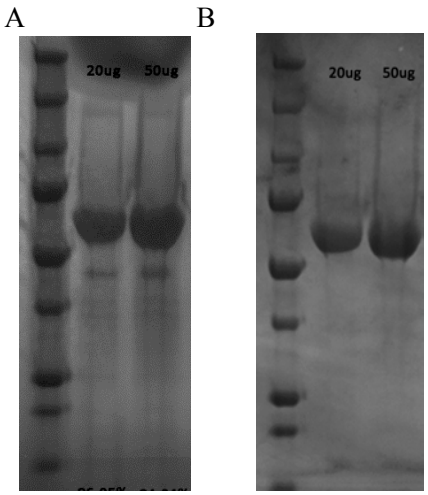

Figure 4. SDS-PAGE of Knob-S48I48 (KSI). Purified KSI was mixed with SDS sample buffer, heated at 95°C for 5 min, and resolved by SDS-PAGE. The gel was stained with copper chloride (5g/50ml) and then stained with Coomassie brilliant blue after removal of copper chloride by de-staining. Molecular weights in the marker lane are 250, 150, 100, 75, 50, 37, 25, and 20 kDa. **A**) Copper Staining; B) Coomassie Staining.

In milestone 3 we initiated ***in vivo* evaluation of ELP nanoparticles and confirmed that transcytosis can be observed with intra-lacrimal injection using fluorescently tagged ELP nanoparticles**. First we attempted direct intra-lacrimal injection of rhodamine labeled knob S48I48 (SI) or knob-S48I48 (KSI) nanoparticles. The lacrimal glands were removed 1h after injection, the glands were fixed, sectioned and analyzed under confocal microscopy (**Fig. 5**). The results suggested that knob-mediates cell surface binding to intact lacrimal glands; furthermore, they appear to stain possible ductal structures within the core of each acinar cluster that is consistent with transcytosis across the lacrimal gland. These preliminary results were later confirmed with a similar intra lacrimal injection approach but with detection through TEM instead of the fluorescence label. With this approach we were able to confirm the presence of KSI in intracellular structures of LGAC as well as in the acinar lumen (**Fig. 6**). The untargeted ELP nanoparticle S48I48 (SI) was only present in the lateral extra cellular space. A publication reporting this finding has been published at the Journal of Controlled Release[18].

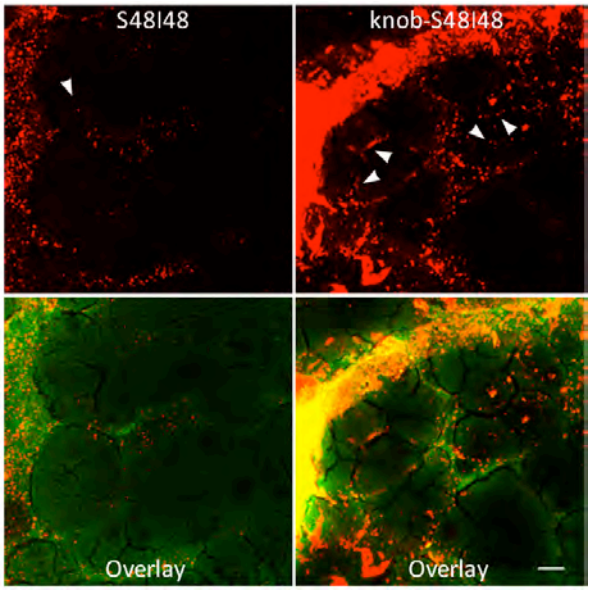

Figure 5. Potential ductal transcytosis of intact murine lacrimal gland. ELP nanoparticles (red) without and with the knob targeting ligand were administered via intra-lacrimal injection to BALB/c mice. To identify the injection site, a carboxyfluorescein dextran (green) was co-administered. *In vivo* accumulation of knob-S48I48 appears to be greater than S48I48. 5 µL of 50 µM rhodamine-labelled S48I48 or rhodamine-labelled knob-S48I48 combined with 50 µg/mL CF-dextran (MW: 10kD) was injected into the LG of BALB/c mouse. After 60 minutes, the glands were retrieved and frozen on dry ice. The frozen glands were cut into 10 µm thick sections and mounted on glass slides. Sections were examined using confocal fluorescence microscopy. The white arrowheads indicate the endocytosed S48I48 or potentially transcytosed knob-S48I48 nanoparticles. The scale bar represents 10 µm.

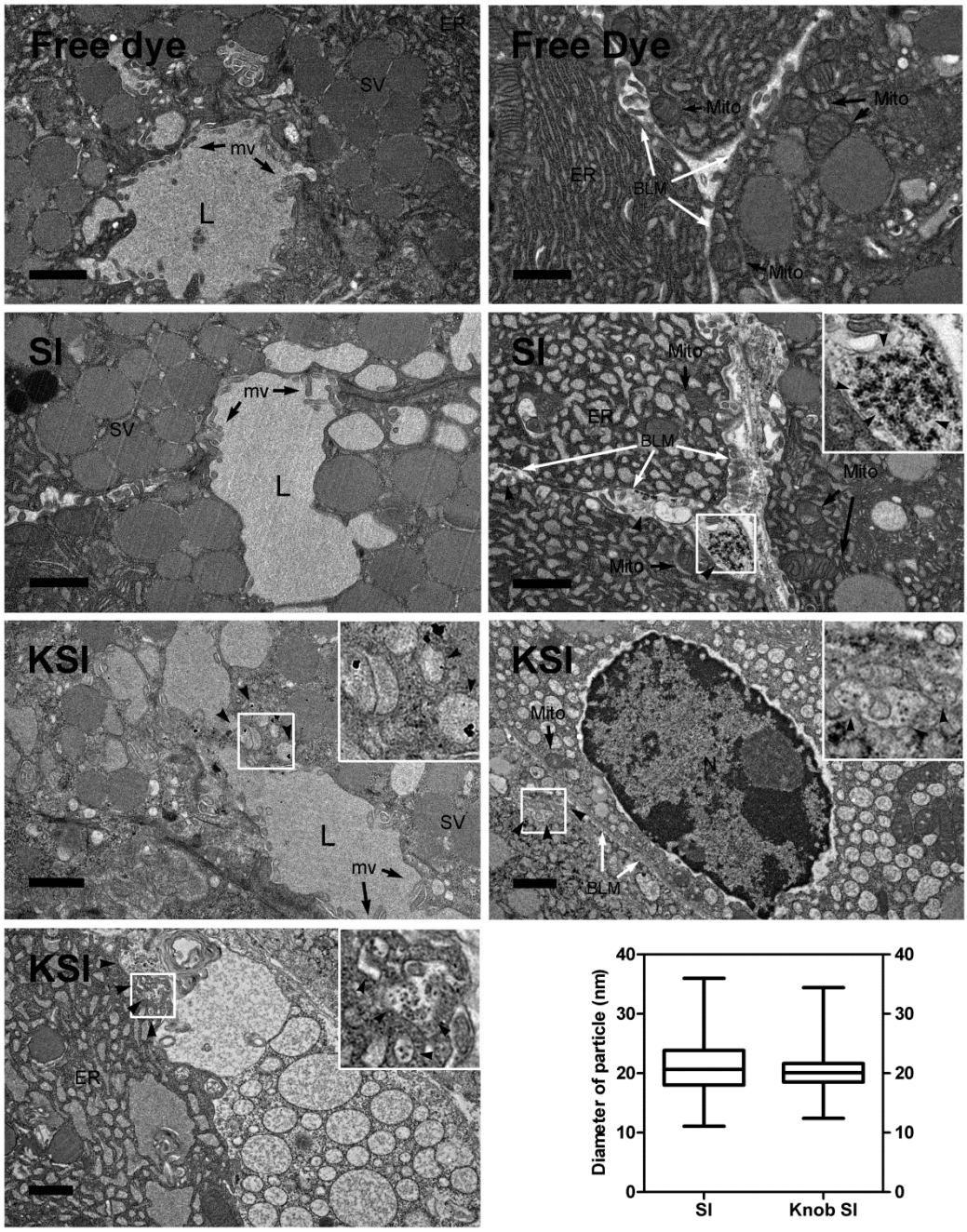

Figure 6. Transmission electron microscopy (TEM)-imaging reveals that knob ELP nanoparticles traffic to vesicles at the apical membrane of the lacrimal gland. Balb/c mouse lacrimal glands (LG) were administered with free rhodamine, S48I48 (SI), or Knob-S48I48 (KSI). LGs from 12-week-old Balb/c mice were given with 50μM of rhodamine (Rh) dye on ELP nanoparticles via intra-lacrimal gland injection. Black arrows represent either mitochondria (Mito) or epithelial microvilli (mv). Black arrowheads indicate the ELP nanoparticles. White arrows show the basolateral membrane (BLM) of LGACs. White boxes, equal to 1 μm^2, are used to highlight locations of ELP nanoparticles. L, lumen; SV, secretory vesicles; ER, endoplasmic reticulum. Scale bars are 1 μm. The box-and-whisker plot is used to summarize identified particle sizes, which are 21.1±0.3 nm (N=178) for SI and 20.2±0.2 nm (N=205) for Knob SI (KSI). Boxes are expressed as the mean± SEM and the whisker shows minimum and maximum values. For SI, the minimum and maximum values are 11.1 and 36.0. For Knob SI, the minimum and maximum values are 12.4 and 34.4.

Aim 2) characterize Lacritin-ELP fusion proteins and evaluate as therapeutic agents in vitro.

Our effort to complete Aim 2 began with **Milestone 4**, confirmation of in vitro prosecretory activity of Lac-ELPs using primary rabbit lacrimal gland acinar cells (LGACs), which was completed. We have continued to study lacritin, finding that it shows a surprising level of activity in various ocular tissues. In the process, we have made the discovery that purified lacritin alone, undergoes a proteolytic cleavage of an unknown origin (**Fig. 7**). In brief, we removed lacritin from the ELP tag and have demonstrated that it can generate smaller peptide fragments predicted by cleavage between lysine residues. This biodegradation process occurs with a half-life about one day; furthermore, it was possible to inhibit it with a cocktail of protease inhibitors (data not shown). We further characterized the cellular internalization for a plain ELP (V96) compared to a lacritin ELP (LV96), and found that only LV96 was able to bind and internalize into LGACs. This level of binding was similar to that observed for free lacritin alone (**Fig. 8**).

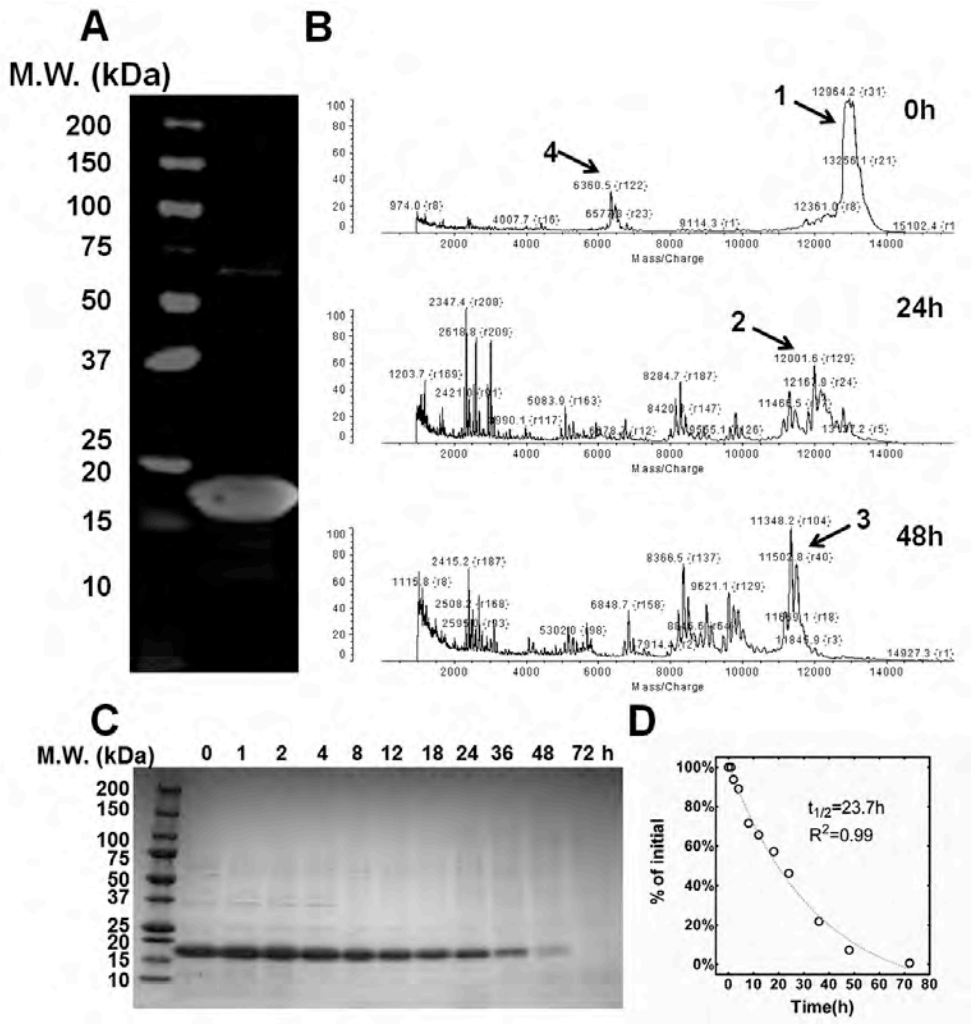

Figure 7. Purified lacritin is susceptible to proteolysis of an unidentified origin. A) Western blot of purified Lacrt probed with an anti-lacritin antibody (raised against Lacrt lacking 65 amino acids at the amino terminus) revealed a major band around 18 kDa, which is consistent with that observed previously for purified Lacrt. **B**) MALDI-TOF analysis of Lacrt revealed the appearance of major lower molecular weight fragments (Table 2) upon incubation at 37 °C in PBS. **C**) Time dependent disappearance of the purified Lacrt band by was tracked by SDS-PAGE stained with Coomassie blue. **D**) Lacrt disappearance was quantified and fitted to a single exponential decay model, which yielded a half-life 23.7 h (R^2=0.99).

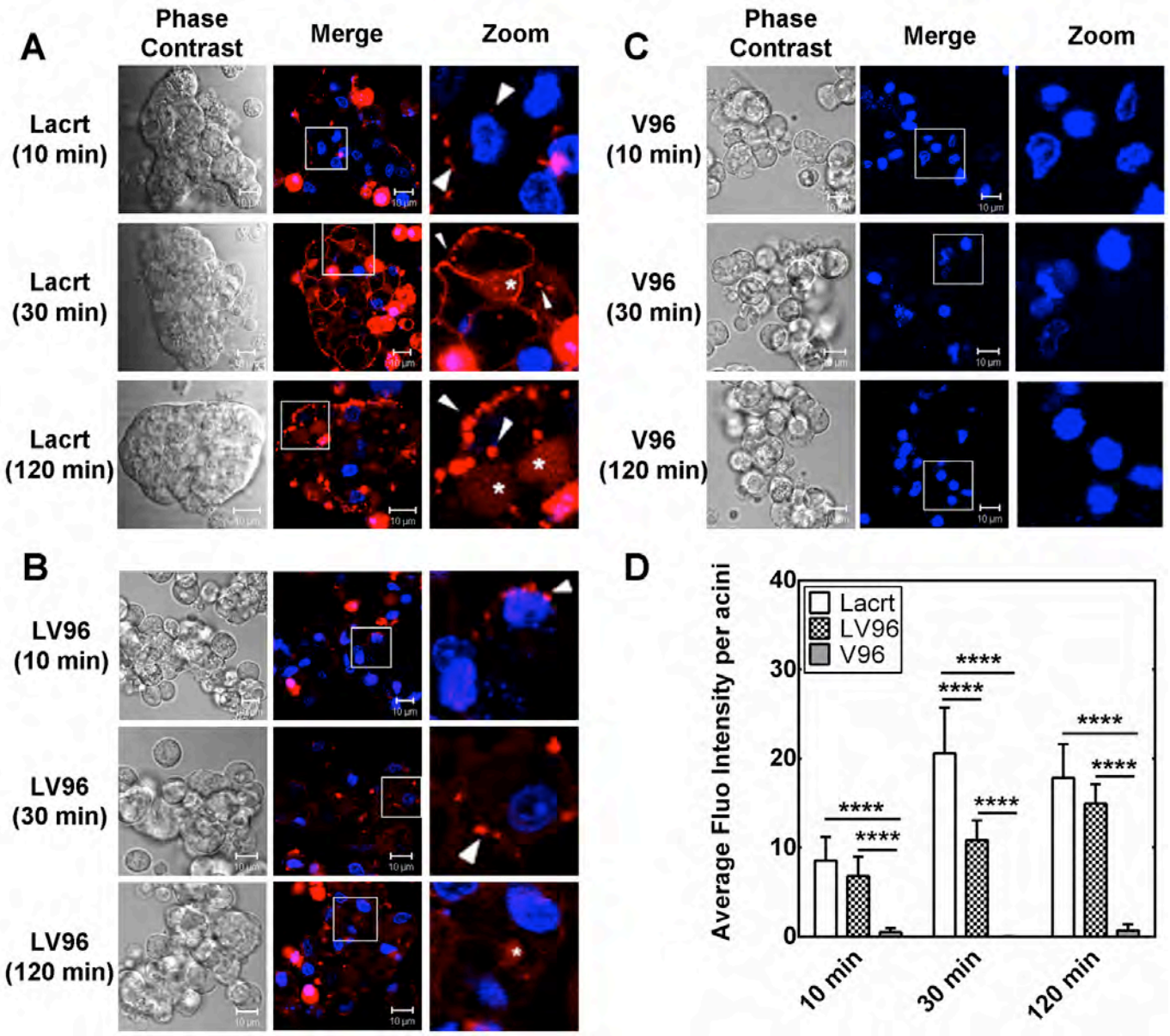

Figure 8. Fusion with V96 influences uptake of exogenous Lacritin into LGACs. A) Time-dependent uptake of rhodamine-labeled Lacrt into rabbit LGACs was assessed by live-cell confocal microscopy. After 30 min, significant numbers of fluorescent puncta were detected in the cytosol proximal to the basolateral membrane (white arrow). More diffuse staining was observed within the lumen encircled by the apical membrane (white *), which suggest possible transcytosis. After 2 h, basolateral binding became less uniformly distributed. **B**) Time-dependent uptake of LV96 revealed a less intense labeling pattern at the basolateral membranes; however, there were significant levels of intracellular puncta (white arrows). Diffuse accumulation was detected in the apical lumen by 2 h (white *), although this effect was less pronounced than for free Lacrt. **C**) A negative control V96 did not show significant uptake into LGACs. Scale bar: 10 μm. **D**) Lacrt, LV96 and V96 intensity in LGACs was quantified at three time points. Both Lacrt and LV96 exhibited significantly (****$p<0.0001$) higher uptake than V96. Lacrt entered LGACs to a greater extent than LV96, most obviously at 30 min (****$p<0.0001$). Data were analyzed by a two-way ANOVA followed by Tukey's multiple comparisons test (n=9).

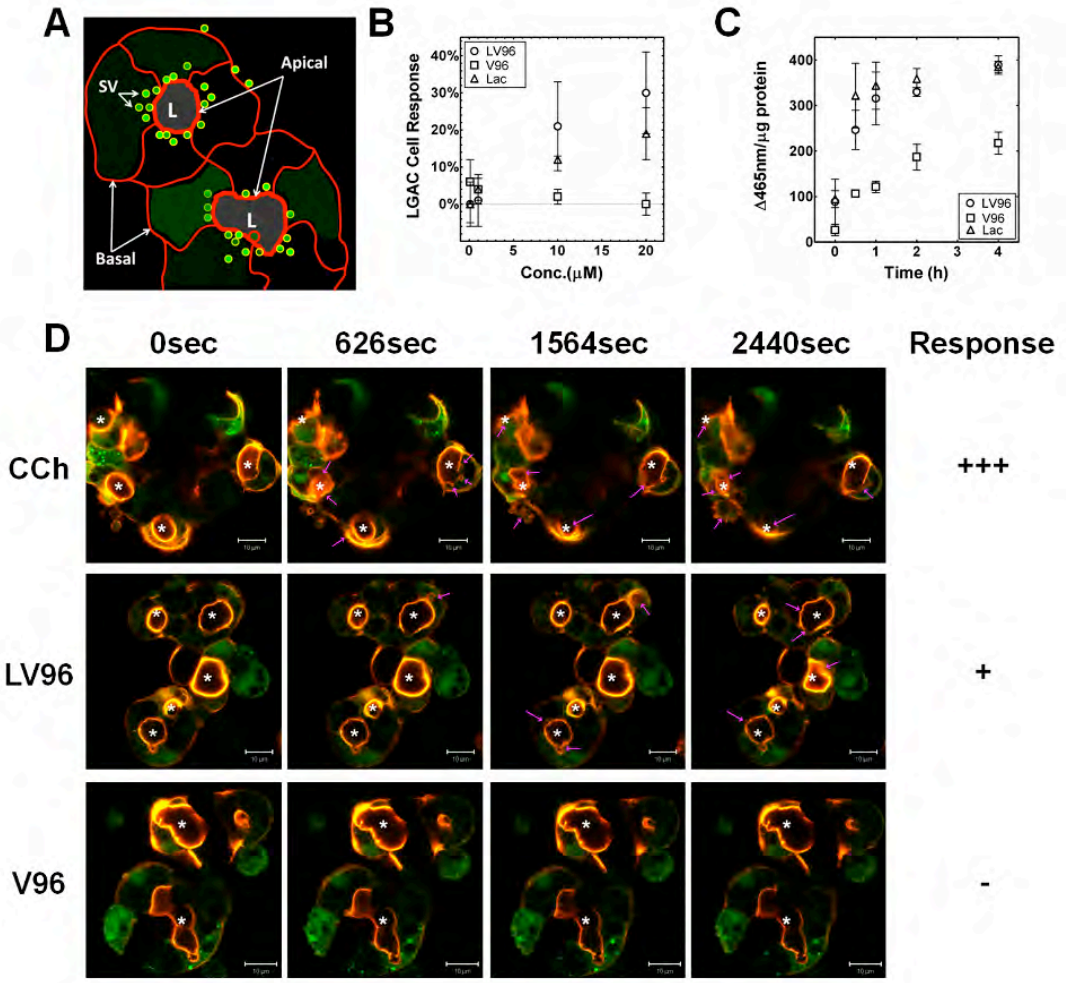

Figure 9. Lacritin ELP fusion proteins stimulate lacrimal gland acinar cells (LGACs) in a time and dose dependent manner. A) Cartoon showing structure *ex vivo* clusters of LGACs obtained from of rabbits. These primary cultures remain polarized towards an apical lumen (L). **B)** Rabbit secretory vesicles (SV) release β-hexosaminidase in a time and dose dependent manner in response to secretagogues. Percentage of cell response compared to a positive control that was defined as 100% (Carbachol stimulation). LGACs were treated with 20 to 0.1 μM of LV96, Lacritin, V96, or control for 1 h at 37 °C. 10 to 20 μM LV96 significantly enhanced β-hexosaminidase secretion compared to the V96 group ($p<0.01$). Similar prosecretory effects were observed for 20 μM lacritin ($p<0.05$). **C)** Representative time dependent LGAC response treated with 10 μM LV96, Lacritin, V96, or control. LV96 and Lacritin stimulate β-hexosaminidase secretion as early as 30 min ($p<0.001$). **D)** Representative live-cell imaging of LGACs stained for actin (red) and syncollin (green). Actin-RFP localizes at the apical membrane surrounding the lumen. Syncollin-GFP is a marker for apical secretion. 20 μM LV96 induces substantial time-dependent actin remodeling in LGAC cultures, with increased irregularity in the continuity of apical actin filaments and formation of actin-coated structures beneath the apical and basal membrane (magenta arrows). White asterisk*: lumen.

Having evaluated the lacritin-ELP fusion in rabbit lacrimal gland acinar cells (**Fig. 9**), *the in vitro* mitogenic activity of the lacritin ELP fusion proteins **(Milestone 5)** was tested using SV40-transformed human corneal epithelial cells (HCE-Ts). In year 2, we successfully published a report of these findings [19], which for the first time demonstrate that lacritin ELPs can form nanoparticles; furthermore, these can stimulate mitogenesis and calcium dependent signaling in a transformed human corneal epithelial cell line. Having been derived from the corneal epithelium, these cells retain some endogenous receptors present in the anterior segment of the eye. First, we demonstrated the transient intracellular concentration of Ca2+ as triggered by Lac-ELPs (**Fig. 10A-C**).

As an early secondary messenger of lacritin-mediated mitogenesis, Ca2+ signal propagation in HCE-Ts prompted us to explore Lac-ELP influence on cell proliferation/migration. To investigate this, we developed an *in vitro* wound-healing model based on a scratch applied to a monolayer of HCE-T cells (**Fig. 10D**). We then demonstrated the feasibility of quantitative comparison among treating groups using lacritin and epidermal growth factor (EGF) (**Fig. 10E**).

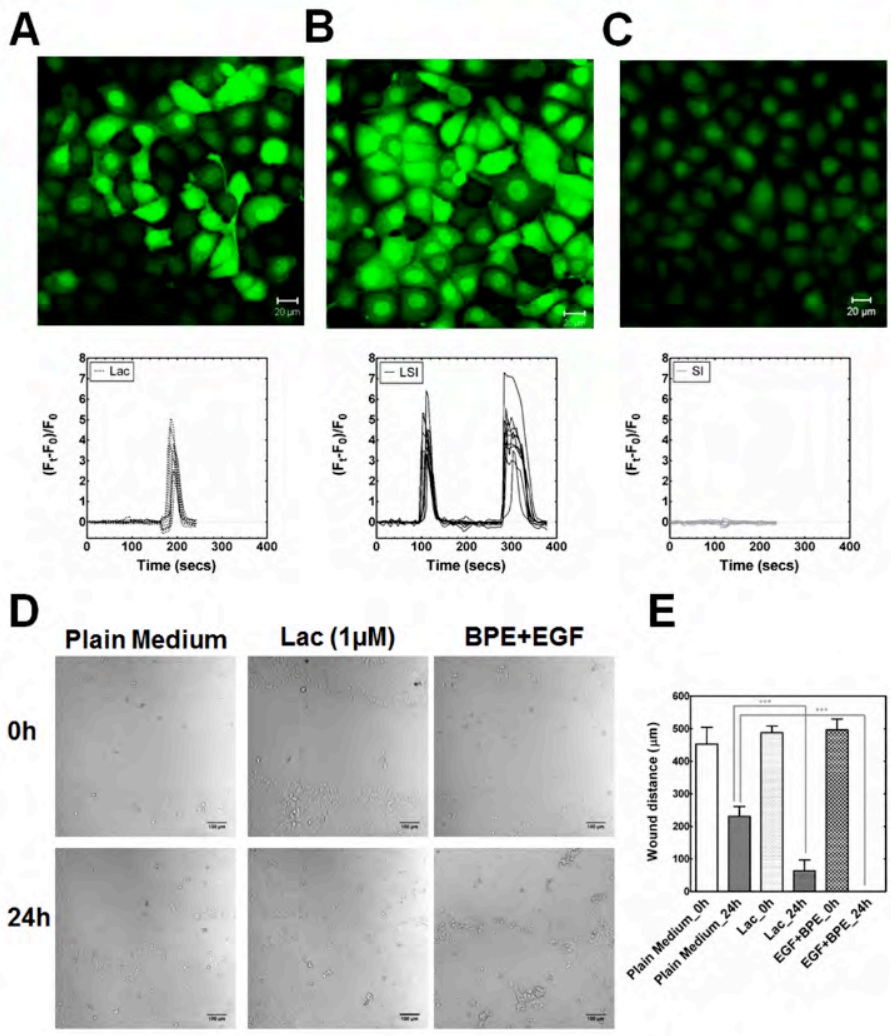

Figure 10. Lacritin and lacritin ELP fusions induce calcium mediated mitogenesis in a human corneal epithelial cell line (HCE-T) A-C) Lacritin (10 μM) and lacritin ELP nanoparticles (LSI) (40 μM×2) triggered a 3-6 fold increase in intracellular Ca^{2+} while the ELP SI, which lacks lacritin, did not induce signaling. **D)** Representative images from a scratch assay on HCE-T cells, which show that lacritin exhibits a scratch closure effect similar to EGF (5ng/ml) and BPE (50μg/ml). **E)** The wound distance was quantified and shows that lacritin significantly reduces the scratch width after 24 h compared to plain medium (n=3). ***P<0.05)

Unexpectedly, cell uptake of exogenous Lac-ELPs was also observed in HCE-Ts (**Fig. 12A**). The structure of Lac-ELPs not only played a role in intracellular uptake level (**Fig. 12B**) but also influenced the kinetics of internalization (**Fig. 12C**). Lacritin is reported to be preferentially mitogenic or prosecretory for the cell types that it normally contacts during its glandular outward flow. Its effect on cells is thought to be mediated by Syndecan-1 (SDC1), which can be turned on or off by deglycanation. The 25 amino acids at the C terminus of lacritin are necessary for binding to deglycanated SDC1; however, fusion to a bulky ELP tag at C-terminus appears to have a slight effect on reducing the internalization of lacritin fusion proteins. While this may slightly influence the efficacy, other data suggests that lacritin appears to efficiently self-cleave from ELPs with a half life on the order of a day (**Fig. 7**). From a controlled release perspective, this observation inspired us to further utilize LSI micelle and LV96 coacervate as local drug depot for sustained release of lacritin payload.

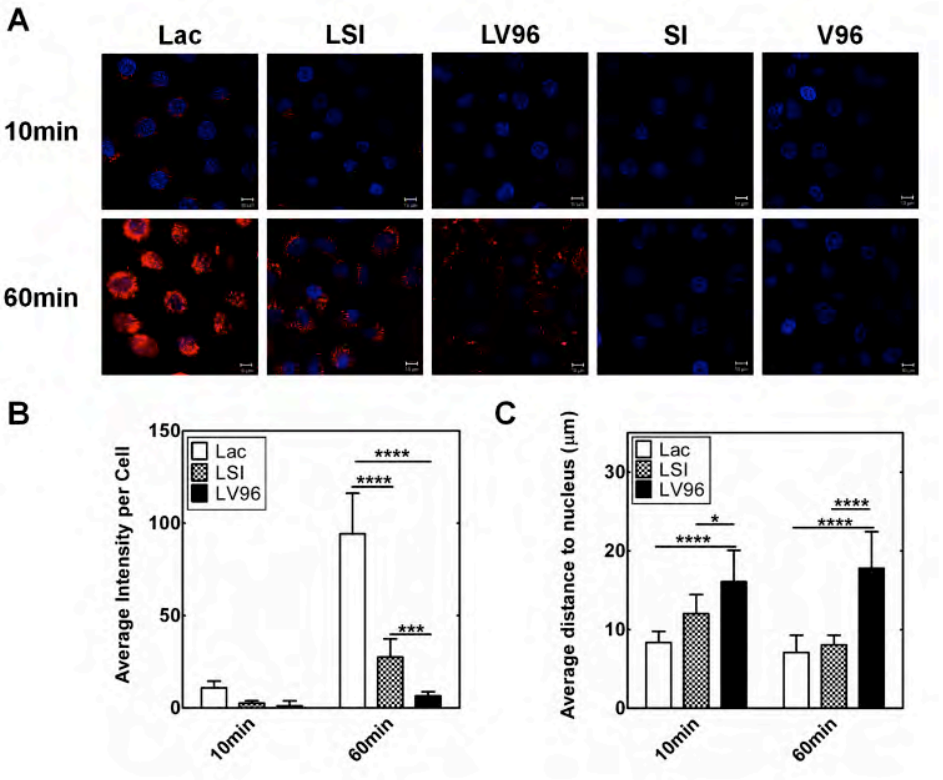

Figure 12. Fusion to ELP reduces the binding and internalization of lacritin on HCE-T cells. A) Representative confocal images showing time dependent uptake of Lac-ELPs into HCE-T cells; plain ELPs SI or V96 did not exhibit uptake effect. Red: rhodamine labeled exogenous Lac-ELPs; Blue: DAPI staining of nuclei. **B)** Quantification of HCE-Ts uptake showing at 60 minutes, both LSI and LV96 exhibited significantly lower uptake level than native Lac (****$p<0.0001$). Cell uptake of LSI nanoparticles was stronger than viscous microparticles formed by LV96 (***$p<0.001$). **C)** Quantification of imaging data was obtained by measuring the distance from Lac-ELP particles to the nucleus. At 10 minutes and 60 minutes, exogenous LV96 significantly trafficked slower than LSI nanoparticles and native Lac (*$p<0.05$). Images were quantified using ImageJ (n=9).

We completed **milestone 6** to purify of 1 gram of Lacritin-ELP fusion protein for *in vivo* evaluation. This was accomplished using the protein purification strategy reported in the original grant application, which is inverse phase transition cycling (ITC) followed by size-exclusion separation. In year 2, we have continued to produce additional lacritin-ELPs as needed for study. In particular, we used our second year to investigate the scale-up of production using a 14 liter bioreactor and a 300 mL bed volume size exclusion chromatography column.

Aim 3) Evaluate the tear targeting of lacritin using ELP nanoparticles and in vivo efficacy studies.

For **Milestone 7, we continued the *in vivo* characterization of the efficacy of lacritin fusion proteins placed directly on the ocular surface utilizing a murine corneal epithelial abrasion model**. We began with briefly characterizing plain ELPs that phase separate on the ocular surface. As shown (**Fig. 13**), a corneal defect was created on the mouse eye. This defect remains open up to 24 hrs without treatment. Two ELPs were evaluated to assist this healing. The first was a control nanoparticle, called SI, that does not have lacritin. The other was a lacritin nanoparticle LSI, which is assembled by a fusion of lacritin to the SI ELP. We found that only LSI was able to rapidly close the size of the defect (**Fig. 13B**); furthermore, the histology of the corneal epithelium healed to a smooth surface with treatment with LSI. Treatment with SI alone resulted in the eventual recovery of a distorted epithelium above the cornea (**Fig. 13C**).

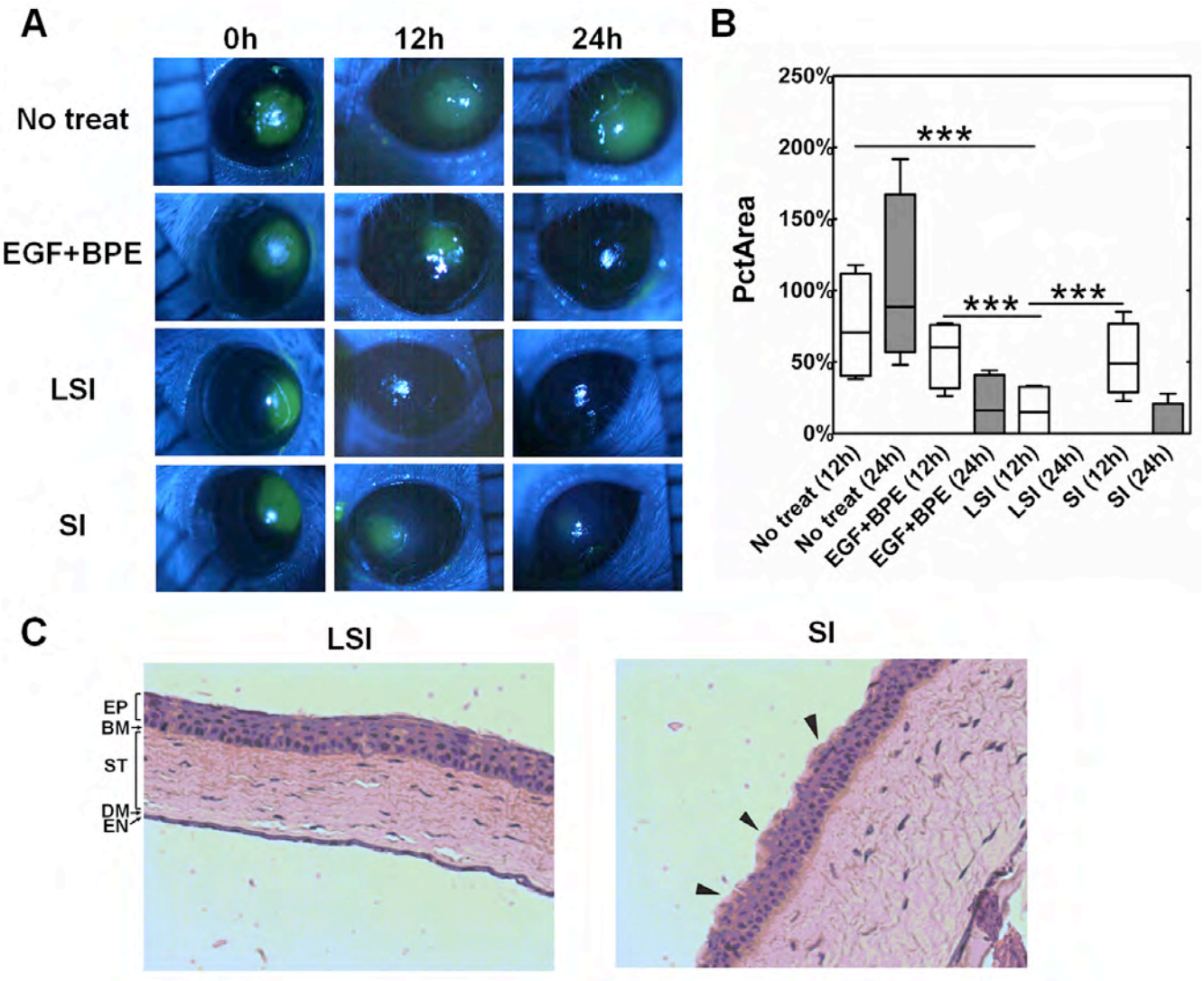

Figure 13. LSI nanoparticles heal corneal abrasions on female NOD mice. (**A**) Representative fluorescein staining images showing time-dependent healing closure of wounds on the ocular surface. (**B**) Analysis of abrasion wound area change using Kruskal-Wallis non-parametric testing showing LSI at both 12 and 24 h significantly decrease the percentage of initial wound area (PctArea) compared to SI, EGF+BPE, and no treatment groups (p=0.001, n=4). *PctArea was evaluated by a blind reviewer for objective justification of wound healing efficacy. (**C**) H&E staining showing 24 h after wound initiation, corneal epithelium of LSI treating group completely healed with no observed inflammation. Although reduced fluorescein staining was observed in SI group, corneal epithelium did not recover fully with a smooth monolayer surface (black arrow). EP: epithelium; BM: Bowman's membrane; ST: Stroma; DM: Descenet's membrane; EN: Endothelium.

Having determined that the LSI nanoparticle successfully resulted in healing of the corneal epithelium, we next determined if this effect differed from that of a soluble lacritin-ELP fusion, which we called LS96 (**Fig. 14**). LS96 contains lacritin and an ELP; however, the ELP S96 does not undergo ELP-mediated assembly of a nanoparticle. To our surprise, we found that the LSI nanoparticles closed a corneal defect significantly faster than the soluble LS96 lacritin control. This result suggests that the lacritin nanoparticles have unique potential to enhance lacritin-mediated therapies.

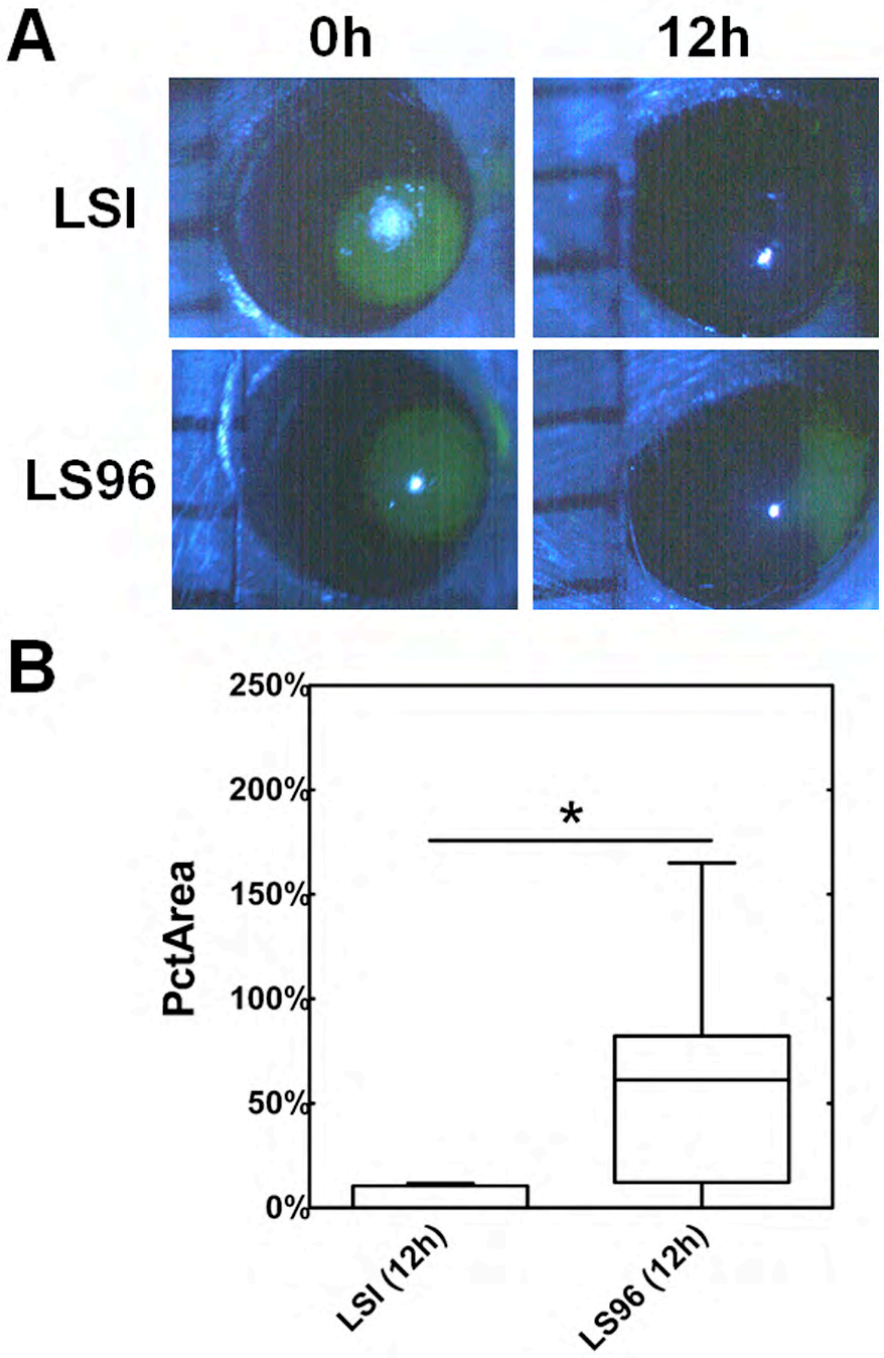

Figure 14. LSI nanoparticles heal corneal abrasions faster than a soluble lacritin-ELP control, called LS96. (**A**) Representative fluorescein staining images showing healing of abrasions to the corneal epithelium for NOD mice after 12 h. (**B**) Analysis of abrasion wound area change using Mann-Whitney U test showing LSI at 12 significantly decrease the percentage of initial wound area (PctArea) compared to LS96 ($p=0.028$, $n=8$). *PctArea was evaluated by a blind reviewer for objective justification of wound healing efficacy.

In **Milestone 8**, we proposed to characterize the delivery and efficacy of lacritin in a mixed nanoparticle containing both Lacritin-ELP (LSI) plus ELP-knob (KSI). In year 2, we initiated this work by looking at the intralacrimal injection of a lacritin-ELP fusion (LV96). LV96 does not assemble a nanoparticle in response to temperature; however, it does phase separate at physiological temperatures. We found that LV96 injected directly into the mouse lacrimal gland forms a fluorescent depot that is nearly undiminished even 24 hours after administration (**Fig. 15A**). In comparison, injection of free lacritin (Lacrt) resulted in a short-lived depot that rapidly was cleared from the site (**Fig. 15C**).

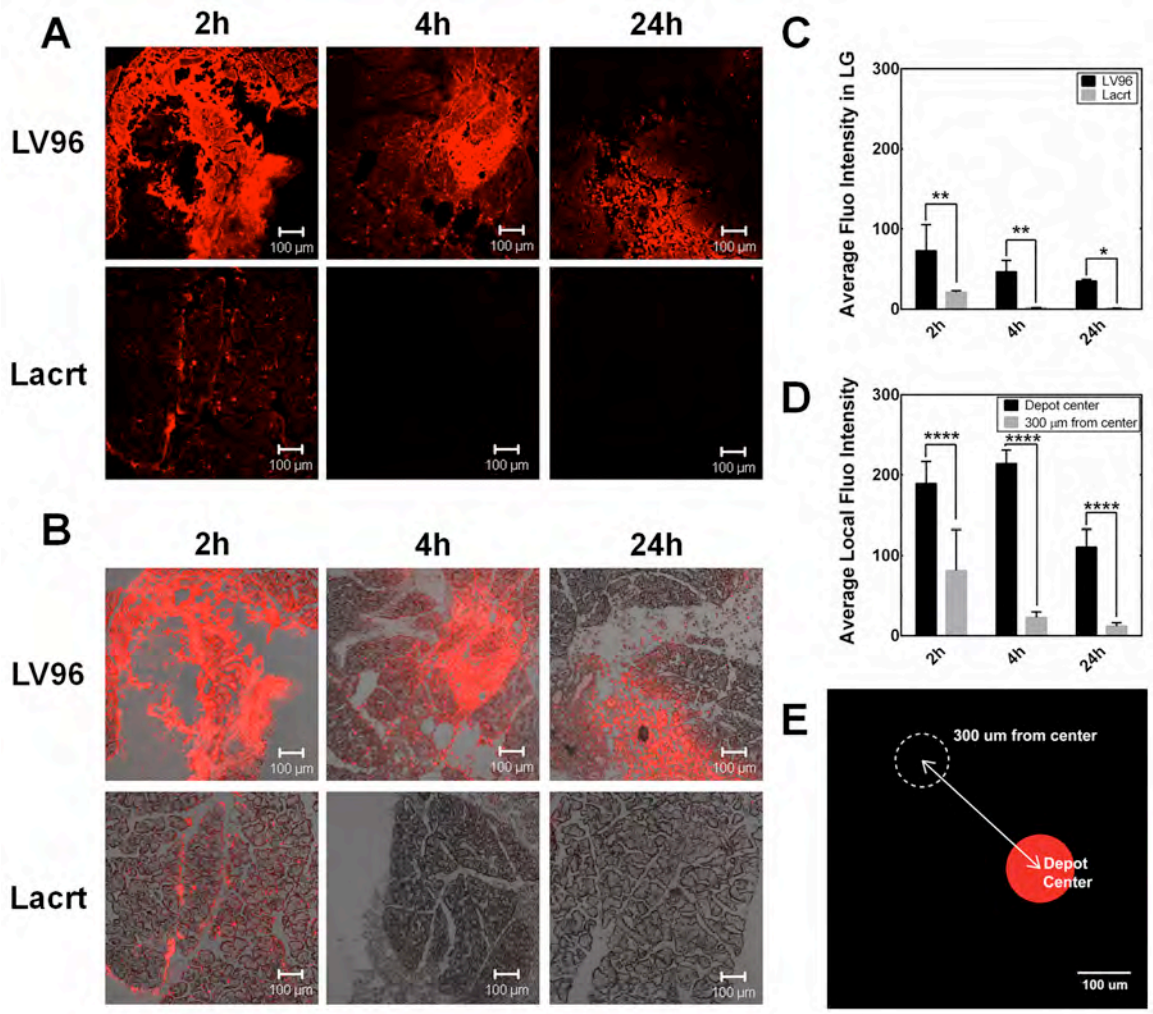

Figure 15. Intra-lacrimal injection of Lacrt-ELP fusion protein produces a depot. A,B) Representative confocal images showing exogenous rhodamine-labeled LV96 forms a depot in the LG of female C57BL/6 mice. LV96 was strongly retained over the 24 h time course, while free Lacrt was not observed after just 4 hours. **A**) Rhodamine signal alone. **B**) Merged combination of phase contrast and rhodamine signal. **C**) Quantification of average fluorescence intensity in the section of LG centered on the injection, which shows that LV96 is retained longer than free Lacrt (*p<0.05, **p<0.01). **D&E**) After injection, depots of LV96 maintained a lower concentration (****<0.0001) at a distance of 300 mm from the depot center; however, this fluorescence was greater than that detected either in surrounding or untreated acini. Scale bar: 100 µm.

We further evaluated the potential therapeutic effect of this lacritin-ELP in the lacrimal glands of non-obese diabetic mice (NOD), which experience diminished tear secretion due to an inflammation of the lacrimal glands (**Fig. 16**). We found that in both male and female NOD mice, the injection of the lacritin ELP called LV96 produced a significant volume of tears (**Fig. 16E,F**). The level of tear production was almost half of that obtained by a positive control called carbachol (CCh). This acute injection also was used to evaluate free lacritin. Under this short duration study, injection of free lacritin produced a similar tear volume as that obtained by LV96, which demonstrates that fusion of lacritin to an ELP does not inhibit its activity.

Milestone 9, In year 3, three manuscripts have been published reporting our work, entitled "Lacritin-mediated regeneration of the corneal epithelia by protein polymer nanoparticles"[19]"; "*Tear-mediated delivery of nanoparticles through transcytosis of the lacrimal gland[18]"*; and "*A thermo-responsive protein treatment for dry eyes* [20]*."* Dr. MacKay's lab has partnered with a company EyeRx to develop lacritin therapeutics. We successfully completed an NIH/NEI STTR grant phase I, and we are investigating the possibilities for an expanded Phase II submission.

Milestone 10, In years 2 and 3, we have worked under a related subcontract from EyeRx (LLC) to study the scaleup and purification of a lacritin ELP. This resulted from an NIH/NEI sponsored award facilitated by data generated in Dr. MacKay's research group.

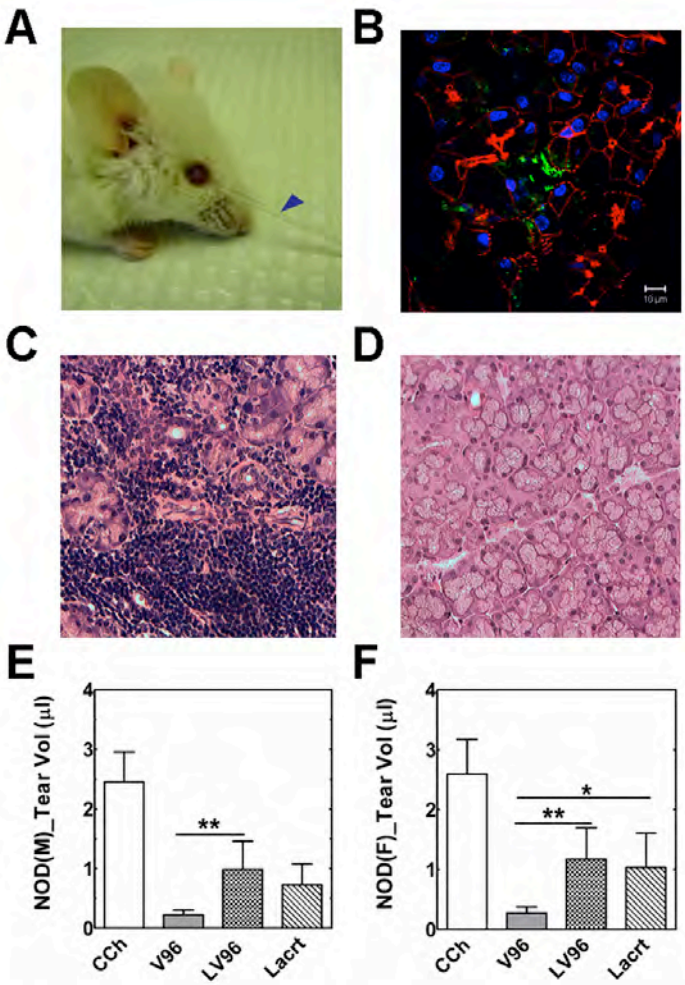

Figure 16. Lacrt-ELP fusion proteins stimulate tear secretion in NOD mice. A) Representative pictures showing tear secretion stimulated by 100 µM LV96 (5 µl) after an intra-lacrimal injection in a male NOD mouse. Blue arrow: collected tear volume after 30 min. **B**) Lacrimal glands injected with LV96 were collected after infusion and visualized using immunofluorescence to identify Lacrt by anti-C terminus lacritin antibody. Green: anti-Lacritin antibody; Red: actin stained using Rho-phalloidin; Blue: nucleus stained by DAPI. Scale bar: 10 µm. **C-D**) Representative H&E staining images of NOD mice lacrimal gland. **C**) Severe lymphocytic infiltration was observed in male NOD mice LG. **D**) Female NOD mice exhibited normal morphology. **E-F**) Tear volume quantification showing significant enhancement of tear secretion by LV96 and Lacrt compared to negative V96 controls (**p<0.01, *p<0.05, n=9). Data are shown as mean ± S.D. and are compared by ANOVA followed by Tukey's Post Hoc Test. **E**) Male NOD mice; **F**) Female NOD mice.

4. Key research accomplishments

- Confirmation of KSI transcytosis *in vitro* and *in vivo*
- Discovery of cell binding, uptake and possible transcytosis of lacritin in rabbit LGACs
- Discovery of cell binding and uptake of lacritin in HCE-T cells
- Confirmation of Lac-ELP structural influence on cellular uptake
- Confirmation of Lac-ELP *in vitro* prosecretory activity based on LGAC β-hexosaminidase secretion and live cell imaging studies
- Discovery of Lac-ELP *in vivo* prosecretory activity in NOD mice via a single bolus intra-lacrimal gland injection
- Confirmation of local drug depot formation of for viscous coacervates LV96 and LI96

- Confirmation of dose dependent Ca^{2+} signal mediated by Lac-ELPs in HCE-T cells
- Completion of fusion protein purification that will enable co-assembly and therapeutic studies
- Completion of *in vitro* mitogenic activity model using HCE-T cells
- Completion of *in vivo* evaluation of Lac-ELPs activity on the ocular surface
- Initiation of combination transcytosis studies of the lacritin (LSI) and knob (KSI) ELP nanoparticles

5. Conclusions

Development of better drugs requires both safety and efficacy [21]; furthermore, local ocular delivery provides unique opportunities to enhance the therapeutic index (TI) of ophthalmic drugs by extending local residence time while minimizing off-target effects and dose frequency [22]. To facilitate this process, we confirmed the cell targeting and transcytosis properties of Knob-SI nanoparticles and evaluated Lac-ELPs' prosecretory/mitogenic effect *in vitro* and *in vivo*. After successful completion of protein purification, we have completed the *in vivo* ocular surface wound healing evaluation. In our third, it proved unnecessary to combine the Knob targeting with the lacritin construct. Surprisingly, the lacritin nanoparticles demonstrated prosecretory activity in the lacrimal gland of mice, transcytosis similar to that found for the knob domain, and even showed evidence of rejuvenation of damaged corneal epithelium in mice. The findings reported here inspire us to continue the proposed strategy to heal the anterior segment of the eye using targeting and/or local drug delivery while investigating the underlying mechanisms of this novel platform in the eye.

6. Publications, abstracts, and presentations

a. manuscripts

1. lay press: none
2. peer reviewed scientific journals
   I. Wang W, Despanie J, Shi P, Edman-Woolcott MC, Lin Y-A, Cui H, J. Heur M, Fini E, Hamm-Alvarez SF, **MacKay JA**. Lacritin-mediated regeneration of the corneal epithelia by protein polymer nanoparticles J. Mater Chem B. 2014. DOI: 10.1039/C4TB00979G (PMC Pending).
   II. Wang W, Jashnani A, Aluri SR, Gustafson JA, Hsueh PY, Yarber F, McKown RL, Laurie GW, Hamm-Alvarez SF, MacKay JA. A thermo-responsive protein treatment for dry eyes. J Cont Rel. 2015 Feb 10;199:156-67. (PMC4456095)
   III. Hsueh PY, Edman MC, Sun G, Shi P, Xu S, Lin Y-A, Cui H, Hamm-Alvarez SF, MacKay JA. Tear-mediated delivery of nanoparticles through transcytosis of the lacrimal gland. J Cont Rel. 2015 Jun 28;208:2-13. (PMC4456098)
3. invited articles: none
4. abstracts
   I. Hsueh P, Edman-Woolcott MC, Sun G, Shi P, **Mackay JA**, Hamm-Alvarez SF. Intracellular trafficking and transcytosis of elastin-based nanoparticles displaying adenovirus knob domain in lacrimal gland acini. Nano Drug Delivery Symposium. San Diego, CA. October, 2013. Poster.
   II. Wang W, Shi P, Aluri S, Hsueh P, Edman-Woolcott MC, Ryan D, McKown RL, Laurie GW, Hamm-Alvarez SF, **MacKay JA**. Bridging ocular therapeutics and contact lenses via thermo-responsive protein polymers. Nano Drug Delivery Symposium. San Diego, CA. October 2013. Poster.
   III. Wang W, Shi P, Aluri S, Hsueh P, Edman-Woolcott MC, Ryan D, McKown RL, Laurie GW, Hamm-Alvarez SF, **MacKay JA**. Bridging ocular therapeutics and contact lenses via thermo-responsive protein polymers. UCLA-USC-Caltech Nanotechnology & Nanomedicine Symposium, Los Angeles, October 2013. Poster.
   IV. **MacKay JA**, Wang W, Hsueh P, Edman-Woolcott MC, Hamm-Alvarez SF. Ocular delivery of a model biopharmaceutical, lacritin, using protein polymers. Annual Meeting of the Society for Controlled Release. Chicago, IL. July, 2014.

7. Inventions, patents and licenses

1. Patents
   I. **MacKay JA**, Wang W. Controlled release of ocular biopharmaceuticals using bioresponsive protein polymers. USC Stevens Institute (USC Ref: 11-692). Filed July 26, 2012. US Patent App. 13/559,053. WO Patent 2,013,016,578
   II. Hamm-Alvarez SF, **MacKay JA**, Sun G. Methods and Therapeutics Comprising Ligand Targeted ELPs. USC Stevens Institute (USC Ref: 11-358). Filed February 11, 2013. US Patent App. 13/764,476.
   III. **MacKay JA,** Wang W, Laurie G. Compositions and methods for the delivery of drugs to the ocular surface by contact lenses. USC Stevens Institute (USC Ref: 13-532). Filed March 31, 2014. US Patent App. 61/806,558

8. Reportable outcomes

- LSI micelle paper manuscript published[19]
- Thermo-responsive lacritin paper manuscript published[20]
- KSI paper manuscript published[18]
- 3 related patents filed

9. Other achievements

nothing additional

10. References

[1] X.D. Li, K.J. Wu, M. Edman, K. Schenke-Layland, M. MacVeigh-Aloni, S.R. Janga, B. Schulz, S.F. Hamm-Alvarez, Increased Expression of Cathepsins and Obesity-Induced Proinflammatory Cytokines in Lacrimal Glands of Male NOD Mouse, Invest Ophth Vis Sci, 51 (2010) 5019-5029.
[2] M.C. Edman, R.R. Marchelletta, S.F. Hamm-Alvarez, Lacrimal Gland Overview, in: D.A. Dartt, J.C. Besharse, M.R. Dana (Eds.) Encyclopedia of the Eye, Elsevier, Oxford, 2010, pp. 522-527.
[3] B. Leader, Q.J. Baca, D.E. Golan, Protein therapeutics: A summary and pharmacological classification, Nat Rev Drug Discov, 7 (2008) 21-39.
[4] S. Sanghi, R. Kumar, A. Lumsden, D. Dickinson, V. Klepeis, V. Trinkaus-Randall, H.F. Frierson, G.W. Laurie, cDNA and genomic cloning of lacritin, a novel secretion enhancing factor from the human lacrimal gland, J Mol Biol, 310 (2001) 127-139.
[5] R.L. McKown, N.N. Wang, R.W. Raab, R. Karnati, Y.H. Zhang, P.B. Williams, G.W. Laurie, Lacritin and other new proteins of the lacrimal functional unit, Exp Eye Res, 88 (2009) 848-858.
[6] S. Samudre, F.A. Lattanzio, V. Lossen, A. Hosseini, J.D. Sheppard, R.L. McKown, G.W. Laurie, P.B. Williams, Lacritin, a Novel Human Tear Glycoprotein, Promotes Sustained Basal Tearing and Is Well Tolerated, Invest Ophth Vis Sci, 52 (2011) 6265-6270.
[7] C. Ding, N. Chang, Y.C. Fong, Y. Wang, M.D. Trousdale, A.K. Mircheff, J.E. Schechter, Interacting influences of pregnancy and corneal injury on rabbit lacrimal gland immunoarchitecture and function, Invest Ophthalmol Vis Sci, 47 (2006) 1368-1375.
[8] E. Macia, M. Ehrlich, R. Massol, E. Boucrot, C. Brunner, T. Kirchhausen, Dynasore, a cell-permeable inhibitor of dynamin, Dev Cell, 10 (2006) 839-850.
[9] O.J. Baker, J.M. Camden, D.E. Rome, C.I. Seye, G.A. Weisman, P2Y(2) nucleotide receptor activation up-regulates vascular cell adhesion molecular-1 expression and enhances lymphocyte adherence to a human submandibular gland cell line, Mol Immunol, 45 (2008) 65-75.
[10] J.A. Hubbell, A. Chilkoti, Chemistry. Nanomaterials for drug delivery, Science, 337 (2012) 303-305.
[11] G. Sun, P.Y. Hsueh, S.M. Janib, S. Hamm-Alvarez, J.A. MacKay, Design and cellular internalization of genetically engineered polypeptide nanoparticles displaying adenovirus knob domain, J Control Release, 155 (2011) 218-226.

[12] M.R. Dreher, A.J. Simnick, K. Fischer, R.J. Smith, A. Patel, M. Schmidt, A. Chilkoti, Temperature triggered self-assembly of polypeptides into multivalent spherical micelles, J Am Chem Soc, 130 (2008) 687-694.
[13] A. Chilkoti, T. Christensen, J.A. MacKay, Stimulus responsive elastin biopolymers: applications in medicine and biotechnology, Curr Opin Chem Biol, 10 (2006) 652-657.
[14] W.E. Liu, M.R. Dreher, D.Y. Furgeson, K.V. Peixoto, H. Yuan, M.R. Zalutsky, A. Chilkoti, Tumor accumulation, degradation and pharmacokinetics of elastin-like polypeptides in nude mice, Journal of Controlled Release, 116 (2006) 170-178.
[15] J.A. Mackay, A. Chilkoti, Temperature sensitive peptides: Engineering hyperthermia-directed therapeutics, Int J Hyperther, 24 (2008) 483-495.
[16] L. Zhang, F.X. Gu, J.M. Chan, A.Z. Wang, R.S. Langer, O.C. Farokhzad, Nanoparticles in medicine: therapeutic applications and developments, Clinical pharmacology and therapeutics, 83 (2008) 761-769.
[17] S.J. Rowan, Polymer Self-Assembly Micelles Make a Living, Nat Mater, 8 (2009) 89-91.
[18] P.Y. Hsueh, M.C. Edman, G. Sun, P. Shi, S. Xu, Y.A. Lin, H. Cui, S.F. Hamm-Alvarez, J.A. MacKay, Tear-mediated delivery of nanoparticles through transcytosis of the lacrimal gland, J Control Release, 208 (2015) 2-13.
[19] W. Wang, J. Despanie, P. Shi, M.C. Edman-Woolcott, Y.-A. Lin, H. Cui, J. Heur, E. Fini, S.F. Hamm-Alvarez, J.A. MacKay, Lacritin-mediated regeneration of the corneal epithelia by protein polymer nanoparticles, J. Mater Chem B, (2014).
[20] W. Wang, A. Jashnani, S.R. Aluri, J.A. Gustafson, P.Y. Hsueh, F. Yarber, R.L. McKown, G.W. Laurie, S.F. Hamm-Alvarez, J.A. MacKay, A thermo-responsive protein treatment for dry eyes, J Control Release, 199 (2015) 156-167.
[21] P.Y. Muller, M.N. Milton, The determination and interpretation of the therapeutic index in drug development, Nat Rev Drug Discov, 11 (2012) 751-761.
[22] G.D. Novack, Ophthalmic drug delivery: development and regulatory considerations, Clinical pharmacology and therapeutics, 85 (2009) 539-543.

11. Appendices

Journal of Controlled Release 208 (2015) 2–13

Contents lists available at ScienceDirect

Journal of Controlled Release

journal homepage: www.elsevier.com/locate/jconrel

Tear-mediated delivery of nanoparticles through transcytosis of the lacrimal gland

Pang-Yu Hsueh [a], Maria C. Edman [a], Guoyong Sun [a], Pu Shi [a], Shi Xu [a], Yi-an Lin [c], Honggang Cui [c], Sarah F. Hamm-Alvarez [a], J. Andrew MacKay [a,b,*]

[a] Department of Pharmacology and Pharmaceutical Sciences, University of Southern California, Los Angeles, CA 90033, USA
[b] Department of Biomedical Engineering, University of Southern California, Los Angeles, CA 90089, USA
[c] Department of Chemical and Biomolecular Engineering, John Hopkins University, Baltimore, MD 21218, USA

ARTICLE INFO

Article history:
Received 26 August 2014
Received in revised form 6 December 2014
Accepted 14 December 2014
Available online 16 December 2014

Keywords:
Coxsackievirus and adenovirus receptor
Elastin-like polypeptide
Knob
Transcytosis
Lacrimal gland

ABSTRACT

Rapid clearance from the tears presents a formidable obstacle to the delivery of peptide drugs to the eye surface. This impedes therapies for ocular infections, wound healing, and dry-eye disease that affect the vision of millions worldwide. To overcome this challenge, this manuscript explores a novel strategy to reach the ocular surface *via* receptor-mediated transcytosis across the lacrimal gland (LG), which produces the bulk of human tears. The LG abundantly expresses the coxsackievirus and adenovirus receptor (CAR); furthermore, we recently reported a peptide-based nanoparticle (KSI) that targets CAR on liver cells. This manuscript reports the unexpected finding that KSI both targets and transcytoses into the LG acinar lumen, which drains to tear ducts. When followed using *ex vivo* live cell imaging KSI rapidly accumulates in lumen formed by LG acinar cells. LG transduction with a myosin Vb tail, which is dominant negative towards transcytosis, inhibits lumenal accumulation. Transcytosis of KSI was confirmed *in vivo* by confocal and TEM imaging of LG tissue following administration of KSI nanoparticles. These findings suggest that it is possible to target nanomaterials to the tears by targeting certain receptors on the LG. This design strategy represents a new opportunity to overcome barriers to ocular delivery.

1. Introduction

Controlled drug delivery to the ocular surface seems intuitively straightforward, yet remains a major challenge. Many drugs are delivered as topically-added eye drops, leading to dilution of the added drug due to lacrimation, low contact time caused by rapid tear turnover, poor penetration through native barriers such as the ocular surface mucin layer, and rapid drainage of the added drug through the nasolacrimal ducts [1]. Studies show that applied drug is washed away within 15–30 s, while less than 5% of the drug administered through eye drops reaches the target tissue [2]. In addition to the natural clearance barriers limiting drug absorption, treatment of acute ocular surface disorders such as keratitis [3] as well as chronic diseases including glaucoma [4] may require addition of eye drops up to hourly, challenging patient compliance [5]. In many cases, ocular diseases such as scleritis [6] and fungal [7], bacterial and viral keratitis [8] must be treated systemically through oral or intravenous drug delivery to get enough drug to the target area, resulting in significant drug exposure at non-target sites. To overcome these challenges, various strategies, including invasive and noninvasive approaches [9,10], have been developed to increase ocular bioavailability, improve precorneal residence time, and prolong therapeutic efficacy after topical applications. The noninvasive strategies frequently focus on *in situ* gelling systems and nanoparticle technologies. Several mucoadhesive and viscosity enhancing polymers, such as polyacrylic acid- (Carbopol®) and polysaccharide-, including gellan gum (Timoptic XE®) and xanthan gum (Timolol Gel Forming Solution®), based polymers [11], have been incorporated into ophthalmic formulations now approved by the United States Food and Drug Administration. In addition, colloidal dosage forms have also been developed to increase drug stability, overcome drug efflux in conjunctival cells, and reduce dosing frequency [10]. Invasive strategies include the developments of eroding and noneroding implants, such as collagen shields [12] and pumps, have been reported to continuously deliver to the ocular surface. While promising, these approaches can compromise vision during treatment. Each strategy has its own advantages and

Abbreviations: Ad5, adenovirus serotype 5; Ad, adenovirus; AM, apical membrane; BEE, basolateral early endosome; BLM, basolateral membrane; CAR, coxsackievirus and adenovirus receptor; cryo-TEM, cryogenic transmission electron microscopy; DLS, dynamic light scattering; DN, dominant negative; EE, early endosome; ELP, elastin-like polypeptide; GFP, green fluorescent protein; KSI, knob fusion to an ELP diblock copolymer; LG, lacrimal gland; LGAC, lacrimal gland acinar cell; PCM, Peter's complete medium; RFP, red fluorescent protein; Rh, rhodamine; SI, ELP diblock copolymer; SV, secretory vesicle; TEM, transmission electron microscopy; T_t, transition temperature; YFP, yellow fluorescent protein.

* Corresponding author at: Department of Pharmacology and Pharmaceutical Sciences, University of Southern California, Los Angeles, CA 90033-9121, USA.
E-mail address: jamackay@usc.edu (J.A. MacKay).

http://dx.doi.org/10.1016/j.jconrel.2014.12.017
0168-3659/

drawbacks; furthermore, the choice of strategy depends on the envisaged therapeutic use. Thus, there is a need to explore alternative ophthalmic drug delivery strategies.

The natural source of tear fluid and proteins is the lacrimal gland (LG), an exocrine gland composed largely of acinar epithelial cells (LGACs), polarized epithelial cells that produce and secrete many of the proteins presented in tears [13]. Tear protein release largely occurs from mucous and serous secretory vesicles sequestered in the acinar cells which are mobilized upon stimulation by neurotransmitters released by parasympathetic and sympathetic innervating neurons [14]. Alternatively, some tear proteins are of serum or paracrine origin and are secreted into tear fluid through a vesicular transport process called transcytosis, which involves vesicular transport through the acinar cells. There are two major transcytosis pathways, nonspecific and receptor-mediated. Nonspecific transcytosis mainly applies to abundant macromolecules in plasma [15]. Receptor-mediated transcytosis, on the other hand, is responsible for the uptake and transport of specific protein moieties and their peptide constituents across cellular barriers such as the endothelium or epithelium, and can be utilized for delivery of receptor-targeted drug molecules [16,17].

An alternative strategy for delivery to the ocular surface might harness the body's own mechanisms in the LG for capturing tear constituents from the blood and releasing those constituents into tears *via* transcytosis. To explore this strategy, this manuscript describes genetically engineered elastin-like polypeptides (ELPs) targeted to the LG via the coxsackievirus and adenovirus receptor (CAR). ELPs are composed of the repeated amino acid sequence $(Val\text{-}Pro\text{-}Gly\text{-}Xaa\text{-}Gly)_n$. These biocompatible and biodegradable [18] protein polymers assemble a secondary aqueous phase, known as a coacervate, above a transition temperature (T_t). This T_t can be precisely tuned by selection of the hydrophobicity of Xaa and the number of repeats, n, of the pentamer sequence. When ELPs with different T_ts are combined in the same polymer, they can assemble stable protein nanoparticles at temperatures between the T_t of the two ELPs [19]. ELPs can also be fused to targeting proteins that retain their cell-binding or drug-binding abilities [19–22]. This manuscript explores a specific ELP nanoparticle comprised of the diblock copolymer, SI, which has 48 serine (Xaa = Ser) pentamers at the amino terminus and 48 isoleucine (Xaa = Ile) pentamers at the carboxy terminus.

We have previously shown that the LG expresses CAR at one of the highest levels in the body [23]. CAR is a cell adhesion protein [24] targeted by the fiber capsid protein of adenovirus serotype 5 (Ad5). Tissues with high surface expression of CAR, including the LG and the liver, are highly transducible with Ad5, which suggests that under certain conditions CAR mediates internalization [23]. Although our group was the first to suggest this entry mechanism in the LG, endocytosis of CAR is supported by another study [25]. We and others have subsequently shown that the affinity of fiber protein for CAR can be replicated by truncations of its terminal domain, called knob. In a previous cell-culture study using only liver-derived cells, fusion of the knob domain to SI nanoparticles (KSI) conferred CAR-mediated internalization [19]. In contrast, for the first time this study demonstrates *in vivo* that KSI nanomaterials can be endocytosed into the LG and, surprisingly, that a subpopulation of these nanoparticles are efficiently transcytosed into the lumen.

2. Material and methods

2.1. Materials and reagents

Terrific broth dry powder growth medium was from MO BIO Laboratories, Inc. (Carlsbad, CA). NHS-Rhodamine was from Thermo Fisher Scientific (Rockford, IL). Sulfo-Cy5 NHS ester was from Lumiprobe Corp. (Hallandale Beach, FL). Copper chloride, isopropyl-beta-D-thiogalactopyranoside, and polyethylenimine were from Sigma-Aldrich (St. Louis, MO). The knob domain gene sequence cloned into vector pUC57 was from Integrated DNA Technologies (Coralville, IA). The pET-25b(+) vector was from Novagen (Madison, WI). LysoTracker® Red DND-99, fluorescein 10,000 MW dextran (anionic), and CellLight® RFP-Rab5a BacMam2.0 reagent were from Life Technologies (Grand Island, NY). The QIAprep Spin Miniprep Kit and QIAquick Gel Extraction Kit were from Qiagen (Valencia, CA). Matrigel™ was from Collaborative Biochemicals (Bedford, MA). Doxycycline was from Clontech (Mountain View, CA). 35 mm glass-bottomed culture dishes were from MatTek Corp. (Ashland, MA). 4–20% PAGEr Precast Gels were from Lonza (Rockland, ME). Tissue-Tek® O.C.T™ compound was from Sakura Finetek USA (Torrance, CA).

2.2. Biosynthesis and characterization of ELPs

Recombinant plasmids encoding the ELP diblock copolymers, SI and KSI, were synthesized using plasmid recursive directional ligation [26]. The KSI protein polymer consists of a N-terminal 22nd β-repeat of the Ad5 fiber shaft (15 amino acids) which is necessary for structural folding [27], the full-length Ad5 knob domain (GenBank Number: AB361382.1), a thrombin cleavage site (Gly-Leu-Val-Pro-Arg-Gly-Ser), and a C-terminal $(Val\text{-}Pro\text{-}Gly\text{-}Ser\text{-}Gly)_{48}(Val\text{-}Pro\text{-}Gly\text{-}Ile\text{-}Gly)_{48}Y$ (SI), in order. ELP gene construction was carried out in a pET25b(+) vector in TOP 10 competent cells followed by protein expression in the BLR (DE3) *Escherichia coli* strain. *E. coli* encoding SI was amplified as reported previously [19]. *E. coli* expressing KSI was first grown in 5 mL terrific broth medium supplemented with ampicillin (100 μg/mL) at 37 °C at 250 rpm overnight. 0.5 mL of overnight culture was then incubated in 1 L of terrific broth containing ampicillin. Isopropyl-beta-D-thiogalactopyranoside induction was initiated when the optical density (OD 600 nm) reached 0.5. KSI expression was induced by isopropyl-beta-D-thiogalactopyranoside (0.5–1 mM) at 25 °C for 6 h. ELPs were purified using inverse transition cycling [28]. In general, at least five rounds of cycling were needed to obtain pure ELP samples. The purity of ELP protein polymers was assessed by SDS-PAGE using 4–20% gradient gels stained with a 10% (w/v) $CuCl_2$ staining solution.

2.3. Dynamic light scattering and zeta potential measurement of ELPs

Hydrodynamic diameters and polydispersity for each construct were measured using dynamic light scattering (DLS). Samples were prepared at 25 μM in PBS and filtered through a Whatman Anotop filter with a 0.02 μm pore size at 4 °C. 90 μl of each sample was transferred to a pre-chilled 384 well microplate, centrifuged at 4 °C to remove air bubbles, and covered with 20 μl of mineral oil to prevent evaporation. Samples were then measured by a Wyatt DynaPro plate reader (Santa Barbara, CA) over a range of temperature from 10 °C to 37 °C in 1 °C increments. Surface charge (zeta potential) of ELP protein polymers was determined on a Zetasizer (Malvern, Worcestershire, UK). Similarly, samples were prepared at 25 μM in PBS and passed through a 0.02 μm filter at 4 °C. 1 mL of each sample was applied to the disposable measurement cell. Zeta potential was estimated from the electrophoretic mobility across an applied electric current at temperatures above and below the assembly temperature for the SI and KSI nanoparticles (Supplementary Table S1).

2.4. Fluorescent labeling of ELPs

ELP samples were labeled with rhodamine (Rh) or sulfo-Cy5 using N-hydroxysuccinimide chemistry. For Rh and Cy5 conjugation of ELPs, reactions were performed in 0.1 M sodium bicarbonate solution (pH 8.3–8.5) at 4 °C for 3 h for KSI or overnight for SI, and the conjugated ELPs were separated by size exclusion chromatography on a PD10 desalting column (GE Healthcare, Piscataway, NJ).

2.5. Animals and animal procedures

Female New Zealand White rabbits weighing between 1.8 and 2.2 kg were obtained from Irish Farms (Norco, CA). Male BALB/c mice aged 12–14 weeks were purchased from Charles River Laboratories (Hollister, CA). All animal procedures were approved by the University of Southern California Institutional Animal Care and Use Committee and followed the Guide for the Care and Use of Laboratory Animals (NIH publication No. 85–23, Revised 1996). For intra-lacrimal injection of SI and KSI and evaluation of fluorescence distribution by confocal fluorescence microscopy, male BALB/c mice were anesthetized with an *i.p.* injection of xylazine 8 mg/kg and ketamine 60 mg/kg. The LG was exposed by a small incision along the axis between the lateral canthus of the eye and the ear. 5 μl of 50 μM Rh-labeled SI or KSI and 50 μg of fluorescein 10 k dextran were injected directly into the LG using a NanoFil syringe with a 33 gauge needle (World Precision Instruments, Sarasota, FL). For analysis of fluorescence distribution by confocal fluorescence microscopy, the injected LGs were removed after 1 h, placed in Tissue-Tek® O.C.T™ compound, snap frozen in liquid nitrogen, cut into 10-μm-thick sections, mounted to slides, and stored at −80 °C. For intra-lacrimal injection of SI and KSI and evaluation of nanoparticle distribution by transmission electron microscopy (TEM), male BALB/c mice were similarly anesthetized and injected with 5 μl of 50 μM Rh-KSI, 50 μM Rh-SI, or 5 μl of free rhodamine dye in PBS. The LGs were removed and processed for TEM as described below.

2.6. Acinar cell isolation and primary culture

Primary acinar cells were collected from LGs from female New Zealand white rabbits using previously established protocols [29]. The isolated LGACs were plated on 35 mm glass-bottomed dishes, coated with Matrigel™ diluted 1:50 in Dulbecco's PBS, at a density of 6.0×10^7 cell/dish and cultured for 2–3 days in Peter's complete medium (PCM) before analysis. Rabbit LGACs prepared in this way reconstitute to form acinus-like structures with distinct basal–lateral and apical domains, a defined actin network enriched beneath the apical plasma membrane (AM) and produce mature secretory vesicles located in the subapical region beneath the lumena [30].

2.7. Adenovirus and baculovirus transduction and real-time fluorescence imaging

Adenoviral (Ad) constructs used in this study include genes that are constitutively expressed (e.g. Ad mCherry-myosin Vb tail DN and Ad YFP-Rab27b) and others which are inducible upon addition of doxycycline (e.g. Ad GFP-actin and Ad mCherry-Rab3D). The inducible Ad constructs required co-transduction with the Tet-on Ad helper virus and addition of doxycycline to express regulatory proteins recognizing the reverse Tet repressor and allowing expression of the gene of interest. Transduction of LGACs with Ad constructs was done on the second day of culture. All Ad constructs were used at a multiplicity of infection of 5 and analyzed 16–18 h after transfection. To study the internalization of KSI, reconstituted rabbit LGACs co-transduced with Ad GFP-actin and Tet-On Ad helper virus at 37 °C were utilized to highlight the basolateral membrane (BLM) and apical membrane (AM) regions, as described previously [31]. To inhibit the transcytosis of KSI, Ad mCherry-myosin Vb tail DN was utilized, a truncated mutant of myosin Vb N′-terminally fused with a mCherry fluorescent protein tag [32]. Other constructs were also utilized to label specific intracellular trafficking pathways. To label early endosomes, LGACs were incubated with Cell Light RFP-Rab5a BacMam 2.0, a modified baculovirus expressing a fusion construct of the early endosome marker, Rab5a, and red fluorescent protein (RFP), at a final concentration of 30 particles per cell on day 2 of culture followed by 16 to 18 h incubation at 37 °C. The transduced cells could be identified visually by the expressed vesicular red fluorescence. For intracellular trafficking studies, these transduced LGACs were incubated with 30 μM of Cy5-KSI at 37 °C for 60 min before imaging or, alternatively, pulsed with 30 μM of Cy5-KSI at 37 °C for 10 min. The Cy5-KSI was then removed and LGACs were chased for 45 min with simultaneous imaging by confocal fluorescence microscopy utilizing a Zeiss LSM 510 Meta NLO imaging system (Thornwood, NY) equipped with Argon, red HeNe, and green HeNe laser, and a Coherent Chameleon Ti-Sapphire laser mounted on a vibration-free table.

2.8. Quantification of fluorescence signal

For evaluation of the percentage of fluorescence recovered within the cellular area versus the lumenal region, the lumenal and cytosolic areas within each LGAC cluster were selected by defining the regions of interest. The fluorescence intensities within these regions were analyzed using ImageJ v1.43u (US National Institutes of Health, Bethesda, MD); fluorescence intensity within each region of interest was determined by calculating the integrated fluorescence intensity corrected for background. The ratio of fluorescence intensity in the lumen to that in the cytosol was calculated. For optimal resolution, each fluorescent image was converted from an RGB to an 8-bit grayscale image before analysis. The fluorescent intensities, presented in the X-axis of Figs. 2, 5 and 6 are expressed as pixels/area.

2.9. Transmission electron microscopy

The morphology of the SI and KSI nanoparticles was observed by cryogenic transmission electron microscopy (cryo-TEM). ELP solutions were kept in an ice bath (4 °C) before processing and then raised to 37 °C immediately prior to cryo-TEM sample preparation using an FEI Vitrobot. A typical procedure involves several steps as described below. In brief, ~6 μL of the sample solution was first loaded on a TEM copper grid coated with a lacey carbon film, and the grid was placed in the Vitrobot chamber with controlled temperature and humidity. After blotting of the excess solution using preset Vitrobot parameters, the grid containing a thin solution layer (~less than 300 nm) was plunged into a liquid ethane reservoir that was cooled and surrounded by liquid nitrogen. After approximately 30 s, the sample was carefully transferred to a liquid nitrogen Dewar and stored in liquid nitrogen temperature before imaging. Throughout the imaging process, the cryo-TEM samples were kept at a temperature below −170 °C. For analysis of ELPs *in vivo* by transmission electron microscopy (TEM) the LG in male BALB/c mice was injected with Rh-KSI, Rh-SI, or free rhodamine dye as described above. The LGs were removed and fixed in half-strength Karnovsky's fixative solution at 4 °C overnight. After fixation, the samples were carefully minced into 1-mm^3 pieces, rinsed three times in 0.1 M cacodylate buffer, postfixed in 2% osmium tetroxide on ice for 2 h, and stained en bloc with 1% uranyl acetate overnight. The samples were dehydrated in serially graded ethanol and infiltrated in eponate resin prior to embedding. The sections were cut at a thickness of 75 nm, placed on copper grids and examined at 100 kV. To compare the size of two types of nanoparticles obtained from cryo-TEM and TEM, SI and KSI were randomly selected and quantified with ImageJ.

2.10. Statistics

Values are presented as mean ± SD. Data from different experiments with only two groups were analyzed using an unpaired two-tailed Student t-test (GraphPad Prism 5.0.1). Experiments with four groups were compared with a global ANOVA followed by the Tukey post-hoc test. To satisfy the homogeneity of variance assumption, the raw intensity values were transformed by the Log_{10} function prior to ANOVA. The criterion for statistical significance was $p \leq 0.05$.

3. Results and discussion

3.1. Characterization of ELP diblock copolymer nanoparticles

The immediate goal of this study was to explore the internalization pathways of ELP nanoparticles displaying the Ad5 fiber knob domain in LGACs. SI and KSI are diblock copolymer ELPs, consisting of the N-terminal hydrophilic $(Val\text{-}Pro\text{-}Gly\text{-}Ser\text{-}Gly)_{48}$ moieties and C-terminal hydrophobic $(Val\text{-}Pro\text{-}Gly\text{-}Ile\text{-}Gly)_{48}$ moieties. Above a critical micelle temperature, both constructs assemble monodisperse nanoparticles (PDI < 0.1) with slightly negative zeta potentials (−5.9 to −7.9 mV) (Supplementary Table S1, Supplementary Fig. S1A). At neutral pH the amino and carboxy termini of SI carry positive and negative charges respectively; however, nanoparticle assembly has no effect on zeta potential. As SI lacks charged amino acids, this suggests that SI nanoparticles are stabilized by steric repulsion provided by the hydrophilic ELP, and not by electrostatic repulsion. With the addition of the adenoviral knob protein, KSI showed a slightly negative shift in zeta potential, which suggests that it may be stabilized by a combination of steric and electrostatic forces. Since cell surfaces are negatively charged, the stabilization of KSI may help prevent nonspecific electrostatic adsorption and promote CAR-mediated specificity. Then, SDS-PAGE was used to characterize the molecular weights of ELP constructs (Supplementary Fig. S1B) revealing a molecular mass of ~38 kDa for SI and ~60 kDa for KSI, consistent with the theoretical molecular masses reported in Supplementary Table 1. The image was analyzed using ImageJ to reveal the purity as 98.5% for SI and 94.5% for KSI.

3.2. Dimensions and size homogeneity of ELP nanoparticles with and without the knob domain

We next determined the size homogeneity and morphology of KSI compared to that of its SI counterpart. The hydrodynamic diameters of nanoparticles assembled by SI and KSI, determined by dynamic light scattering (DLS), were 47.1 ± 1.8 nm and 43.2 ± 0.6 nm, respectively ($p < 0.0001$) (Supplementary Table S1). In prior reports, the addition of the Ad5 knob domain reduced the critical micelle temperature slightly; however, the hydrodynamic diameter and stability at physiological temperatures were nearly unaffected by the fusion of Ad 5 knob domain [19]. Despite the increased molecular weight for monomers of KSI compared to SI, the resulting nanoparticles have nearly identical sizes. This suggests that KSI nanoparticles stabilize at a lower number of polymers per particle compared to SI. If so, this might result from a larger hydrophilic fraction for KSI (66% *vs.* 48% for SI), which could result in a larger radius of curvature per polymer [33,34].

To explore any confounding difference between SI and KSI nanoparticles, cryo-TEM was employed (Fig. 1A). For this analysis, particles suspended in PBS were shock-frozen in liquid ethane. The suspension was supercooled to form a vitrified thin layer so that the particles could be directly studied *in situ*. Fig. 1A shows that SI and KSI formed nearly spherical particles with similar size homogeneity. Particle sizes of SI and KSI, measured by DLS and cryo-TEM, are presented in Fig. 1B. The diameter of the KSI nanoparticles (32.0 ± 3.5 nm) from cryo-TEM was similar to that of the SI nanoparticles (32.4 ± 4.2 nm) and there is no statistically significant difference between the two constructs (Fig. 1B). The particle sizes determined by cryo-TEM are slightly smaller than the sizes reported from DLS, a difference possibly resulting from the presence of the hydration layer on the surface of core–shell ELP nanoparticles. This shell can be detected by DLS but is not visible by cryo-TEM. A similar phenomenon is observed for soft colloidal nanoparticles but not hard shell particles [35]. Moreover, the hydrodynamic diameter from DLS measures an average that is also influenced by the slight irregularity in the shape of the particles. Despite the slight differences in size, morphologies of both KSI and SI from cryo-TEM are generally consistent with the results from DLS. These observations suggest that fusion of Ad5 knob domain to the SI core nanoparticle minimally influences the nanoparticle diameter and morphology and that differences in their cellular trafficking result from receptor-mediated interactions.

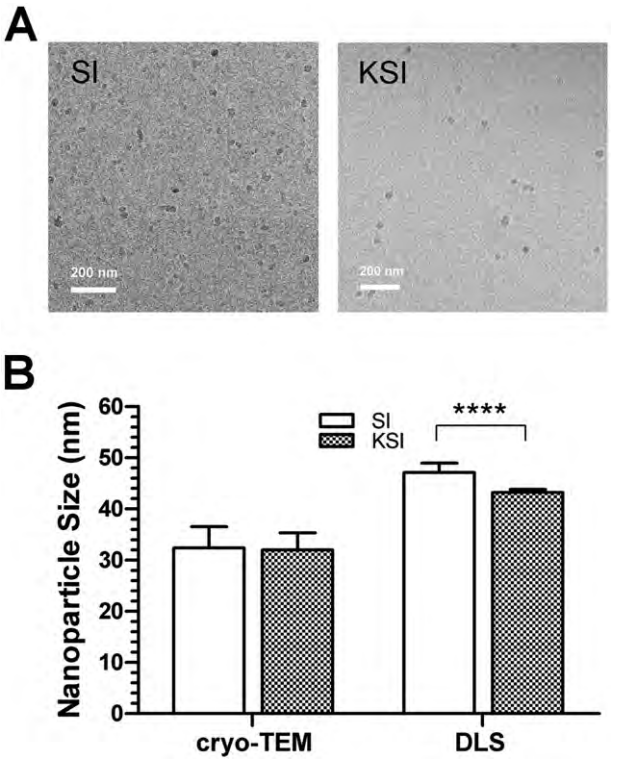

Fig. 1. Genetic fusion of the Ad5 knob domain to SI has minimal impact on the morphology of ELP nanoparticles. (A) Cryo-TEM micrographs of ELP nanoparticles with and without the Ad5 knob domain. (B) A comparison of diameters from ELP nanoparticles imaged by cryo-TEM and DLS. For cryo-TEM, the average diameters of SI and KSI, measured with ImageJ, were 32.4 ± 4.2 nm and 32.0 ± 3.5 nm, respectively. Values are expressed as mean ± SD (n = 15). For DLS, the average diameters of SI and KSI were 47.1 ± 1.8 nm and 43.2 ± 0.6 nm, respectively. Values are expressed as mean ± SD (n = 10). p value < 0.0001 (Student t-test). Statistical comparison was not performed between cryo-TEM and DLS techniques because they measured different aspects of particle formation.

3.3. Internalization and transcytosis of ELP fusions in LG acini

KSI exhibits a fiber knob-dependent and CAR-mediated endocytosis in transformed mouse hepatocytes; however, prior to this report it was unknown if these particles would interact with the LG. Similarly to hepatocytes, cells of the LG abundantly express CAR; therefore, LG CAR could be an excellent target for the selective delivery of KSI. To explore this hypothesis, three-dimensional cultures obtained from rabbit LGs were used to investigate the targeting and internalization of KSI. As documented in previous studies, isolated primary LGACs assemble into ovoid clusters after two days in culture, mimicking the acinar-like structures present in the LG [36]. A schematic of a typical reconstituted acinus comprised of LGACs is shown in Fig. 2A (right) with several reference points, including a central lumen bounded by the apical membrane (AM) of adjacent cells, mature secretory vesicles (SVs) in the sub-apical region, beneath the basolateral membrane (BLM).

As shown in Fig. 2A, fluorescently labeled Rh-SI or Rh-KSI was incubated with LGACs transduced with Ad GFP-actin. GFP-actin was used to delineate the apical lumen of reconstituted LG clusters due to its incorporation into the dense sub-apical meshwork of actin filaments proximal to the lumen. In addition to detection of intracellular puncta, presumed to be membrane compartments, Rh-KSI was clearly observed within the lumenal area of LG clusters, compared with control Rh-SI.

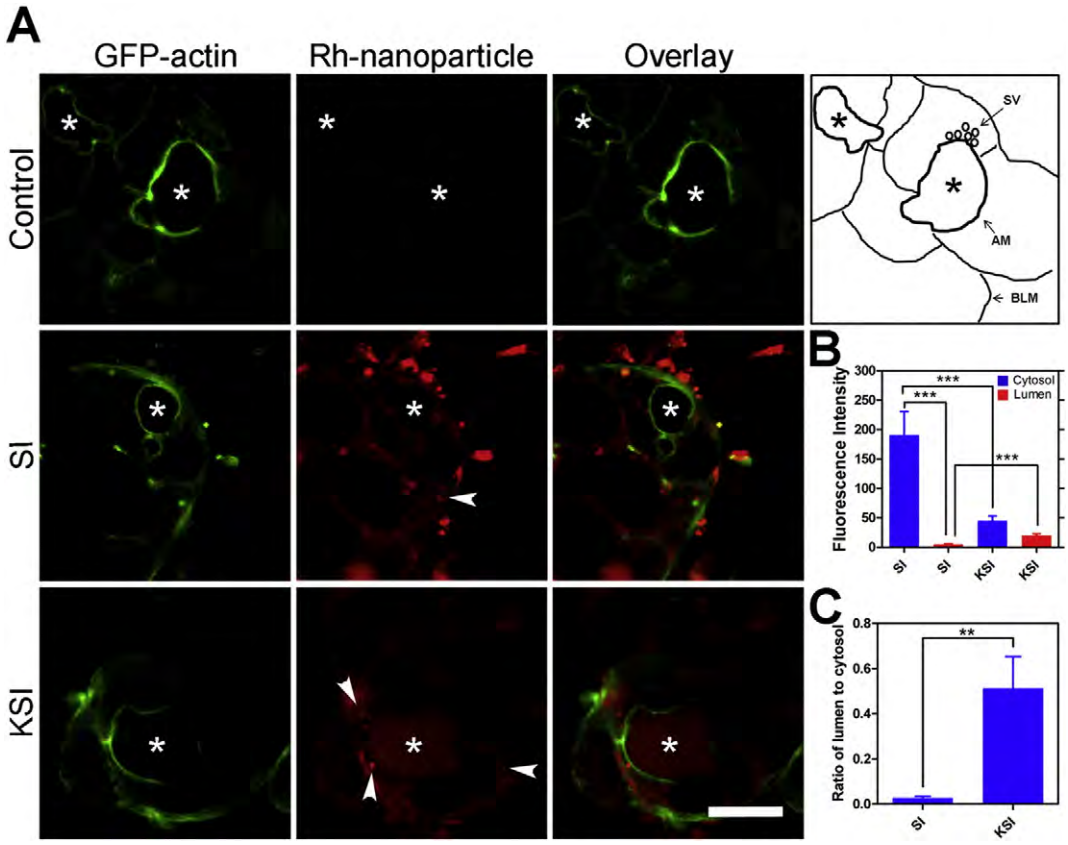

Fig. 2. KSI is internalized and accumulates in the cytosol and lumena of rabbit LGAC expressing GFP-actin. (A) Live cell imaging comparing the intracellular distribution of ELPs with and without Ad5 knob after 1 h incubation at 37 °C. Green, GFP-actin; red, Rh-conjugated SI or KSI; *, lumenal space; scale bar indicates 10 μm. Schematic diagram on the top right depicts reconstituted rabbit LGACs shown on the first row (Control), and indicates the presence of apical plasma membrane (AM), secretory vesicles (SV) and the basolateral membrane (BLM). *, acinar lumen. (B) Quantification of fluorescent intensity in LGACs treated with SI and KSI. ***, p value < 0.005 (ANOVA followed by Tukey post-hoc test). (C) Quantification of the fluorescence intensity expressed as a ratio of lumenal to cytosolic fluorescence. **, p value = 0.009 (Student t-test). For (B) (C), fluorescence intensity was analyzed using ImageJ. Data are presented as mean ± SD (n = 5).

This suggests that an active transport mechanism moves KSI from the basolateral to the apical membrane in these polarized LGAC cultures. The confocal fluorescence images of LGAC clusters were quantified by ImageJ to compare average fluorescent intensities in cytosol and lumen (Fig. 2B) and estimate the ratio of nanoparticles between the lumen to cytosol (Fig. 2C). The fluorescence intensity in the lumen of acini exposed to KSI was much higher than that in cytosol, while for acini exposed to SI, the fluorescence intensity in the lumen was lower than that in the cytosol ($p = 0.001$). When the lumen intensity was normalized by the cytosolic intensity, the ratio for KSI was significantly ($p = 0.009$) higher than for the SI control. This finding suggests that the addition of the knob domain to SI enhances the basolateral-to-apical transcytosis of the ELP nanoparticles, which possibly paves a way to utilize the KSI nanoparticle to selectively deliver therapeutic agents to lacrimal epithelial cells, tear ducts, and the ocular surface.

3.4. Characterization of KSI intracellular trafficking in LGACs

Previous reports have suggested that the Ad5 knob domain administered through intravenous injection is internalized in the liver and sorted into acidic compartments of hepatocytes for degradation [37]. We hypothesized that the uptake of KSI in rabbit LGACs should involve the classical endosomal pathway and further that KSI remaining in acini that did not appear to pass to the lumen would be recovered in acidic lysosomal compartments. To evaluate this, Rh-SI or Rh-KSI was incubated with rabbit LGACs at 37 °C for 60 min before confocal fluorescence microscopy imaging (Fig. 3). LysoTracker green was used as an acidic compartment marker for late endosomes and lysosomes in LGACs. As can be seen in Fig. 3, LGACs without any ELP treatment showed no fluorescence signal (absence of red label). LGACs incubated with Rh-SI showed significant surface association as well as enhanced labeling of single cells present in the preparation. Some internalization was seen in puncta that colocalized with LysoTracker-labeled compartments (arrowheads). In contrast, almost no surface labeling of acini was seen for Rh-KSI which instead mainly internalized to puncta partially co-localized with LysoTracker green; furthermore, Rh-KSI again showed significant lumenal accumulation. Based on these findings, we proposed that the internalized SI and KSI are partially transported to late endosomes and lysosomes, but that KSI internalization occurs more efficiently and is further transported *via* transcytosis.

Early endosomes are well-established recipients of endocytosed material in many cell types [38]. In epithelial cells internalized cargos are first trafficked into basolateral early endosomes (BEEs), where they can either be transported to common recycling endosomes and apical recycling endosomes consecutively before the release of cargos into the apical lumen, or alternatively they may be delivered to late endosomes and then lysosomes [39]. To investigate whether internalized KSI traffics to BEEs in the LG, reconstituted LGACs, transduced with the BEE marker, RFP-Rab5a, were incubated with fluorescence labeled Cy5-KSI and analyzed by time-lapse confocal fluorescence microscopy (Fig. 4 and Supplementary Video S1). Similarly to Rh-KSI, Cy5-KSI was also trafficked to the lumen of LGACs, indicating that this effect was dye independent. Fig. 4A shows that the Cy5-KSI was enclosed by Rab5a-enriched vesicles by 60 min, indicative of the delivery of internalized KSI into Rab5a-enriched BEEs. As seen in Fig. 4B, a pulse-chase experiment with labeled KSI over a time course of 45 min of incubation

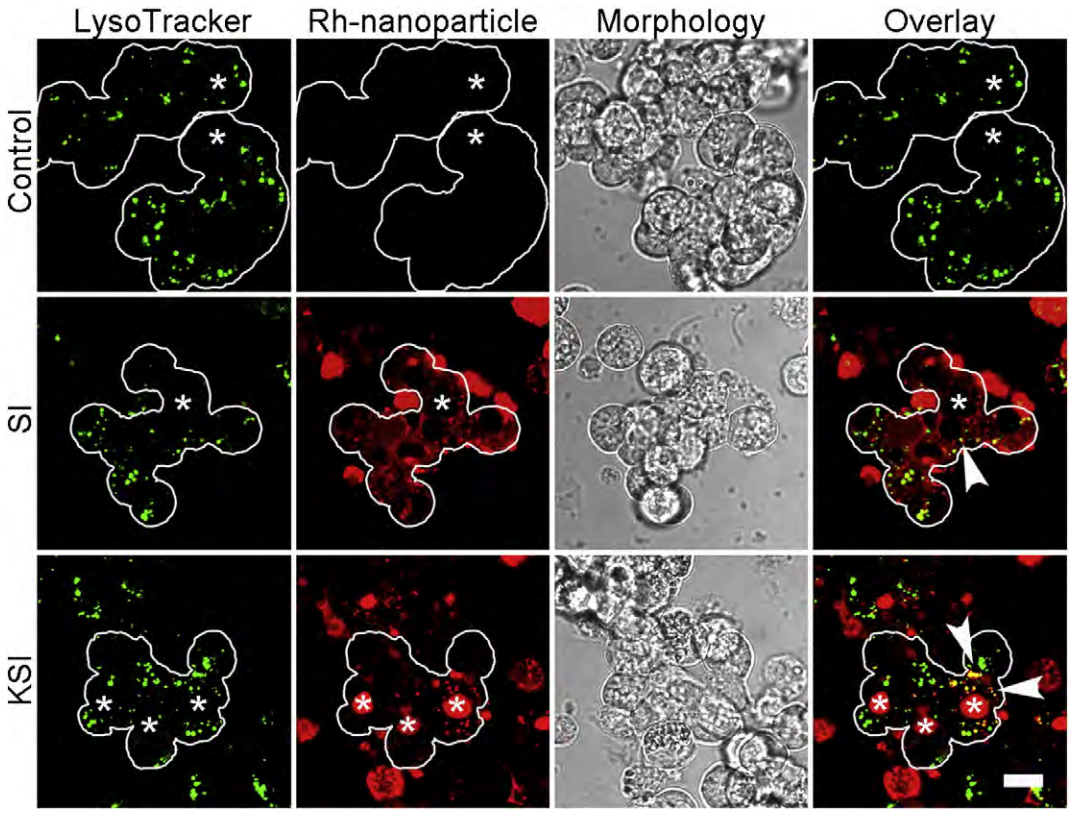

Fig. 3. ELP nanoparticles traffic to low pH compartments in rabbit LGACs. 30 μM of Rh-coupled SI or KSI was incubated with rabbit LGACs at 37 °C for 1 h, and imaged using confocal fluorescence microscopy. KSI (red) exhibited significant co-localization with acidic compartments labeled by LysoTracker green (green) as well as lumenal (*) accumulation. SI showed significant surface binding and also some internalization to acidic compartments labeled by LysoTracker green. Arrowheads indicate the co-localization of SI or KSI with acidic compartments. White lines delineate the BLM of LG acinar clusters. *, lumena. Scale bar indicates 10 μm.

showed that the internalization of KSI to BEEs was observed by 10 min. In particular, the internalized KSI underwent a dynamic continuous exchange and redistribution from smaller BEEs to larger BEEs, possibly through homotypic fusion of early endosomes (Supplementary Video S1). A loss of fluorescence signal, possibly due to photobleaching or transfer of some KSI from early endosomes to proximal trafficking compartments, was observed at later time points. Combined with data in Fig. 3, these results suggest that KSI internalized by receptor-mediated endocytosis was first sorted into Rab5a-enriched BEEs, and then a fraction of this endocytosed material was delivered to late endosomes and lysosomes.

Having identified the primary routing steps for endocytosed KSI in LGACs, we next explored the subsequent trafficking steps involved in release of KSI into the apical lumen. Previous studies from our laboratory have identified at least three pathways for apically directed secretion of tear proteins in LGACs: the Rab11a/myosin Vb mediated transcytotic pathway [32] and the Rab3D and/or Rab27b regulated secretory pathways [40–42]. Rab3D and Rab27b are predominantly localized to distinct populations of secretory vesicles in the subapical region of LGAC that originate from the trans-Golgi network, although a subpopulation expressing both Rab proteins may exist. To investigate whether the Rab3D and Rab27b regulated secretory pathways are involved in the release of KSI into the acinar lumen of LG, LGACs were transduced with either YFP-Rab27b or mCherry-Rab3D followed by imaging of cells subjected to pulse chase uptake experiments. Fig. 5C shows that the internalized Cy5-KSI (red) did not co-localize with YFP-Rab27b or mCherry-Rab3D (green), indicating that the secretion of KSI is not mediated through secretory vesicles enriched in Rab3D or 27b.

We next evaluated the role of the Rab11a/myosin Vb regulated transcytotic pathway. We have shown that expression of dominant negative (DN) myosin Vb tail directly impairs the movement of transcytotic vesicles and their cargos from Rab11a-enriched apical endosomes to the apical membrane, thus inhibiting transcytosis in LGACs [32]. The Rab11a-enriched apical endosome is well established in the trafficking of another transcytotic cargo receptor, the polymeric immunoglobulin A receptor, responsible for transcytosis of dimeric IgA into tears [42]. In Fig. 5, LGACs were transduced with recombinant adenovirus encoding GFP-actin (green) with or without mCherry-myosin Vb tail DN (red), an N-terminal mCherry fluorescent protein fused to a truncated mutant of myosin Vb motor, which associates with vesicle cargo but does not have motor function. Transduced acini were then incubated with Cy5-KSI. As can be seen in Fig. 5A, the Cy5 fluorescent signal (purple) recovered within the lumenal regions surrounded by apical GFP-actin was reduced in LGACs co-transduced with Ad mCherry-myosin Vb tail DN compared to that with Ad GFP-actin alone. The fluorescent KSI signal was quantified using ImageJ in the cytosol and lumena (Fig. 5B) and the ratio of lumenal to cytosolic fluorescence was calculated (Fig. 5C). Although the dual transduction of adenovirus slightly reduced the level of KSI internalization compared to single transduction (Fig. 5B), there is a statistically significant ($p = 0.031$) reduction of the KSI signal calculated from the ratio of lumen to cytosol (Fig. 5C). In LGACs in which transcytotic trafficking has been selectively impaired, Cy5-KSI accumulation in the lumenal region was inhibited, demonstrating that its transport to the lumen was *via* the transcytotic pathway.

3.5. Characterization of KSI intracellular trafficking in vivo

To further evaluate the potential of KSI as a targeted vehicle *in vivo*, our next step was to confirm the internalization and transcytotic behavior of KSI in a mouse model. First, we confirmed the expression and biodistribution of CAR in the LG of BALB/c mice by immunofluorescence,

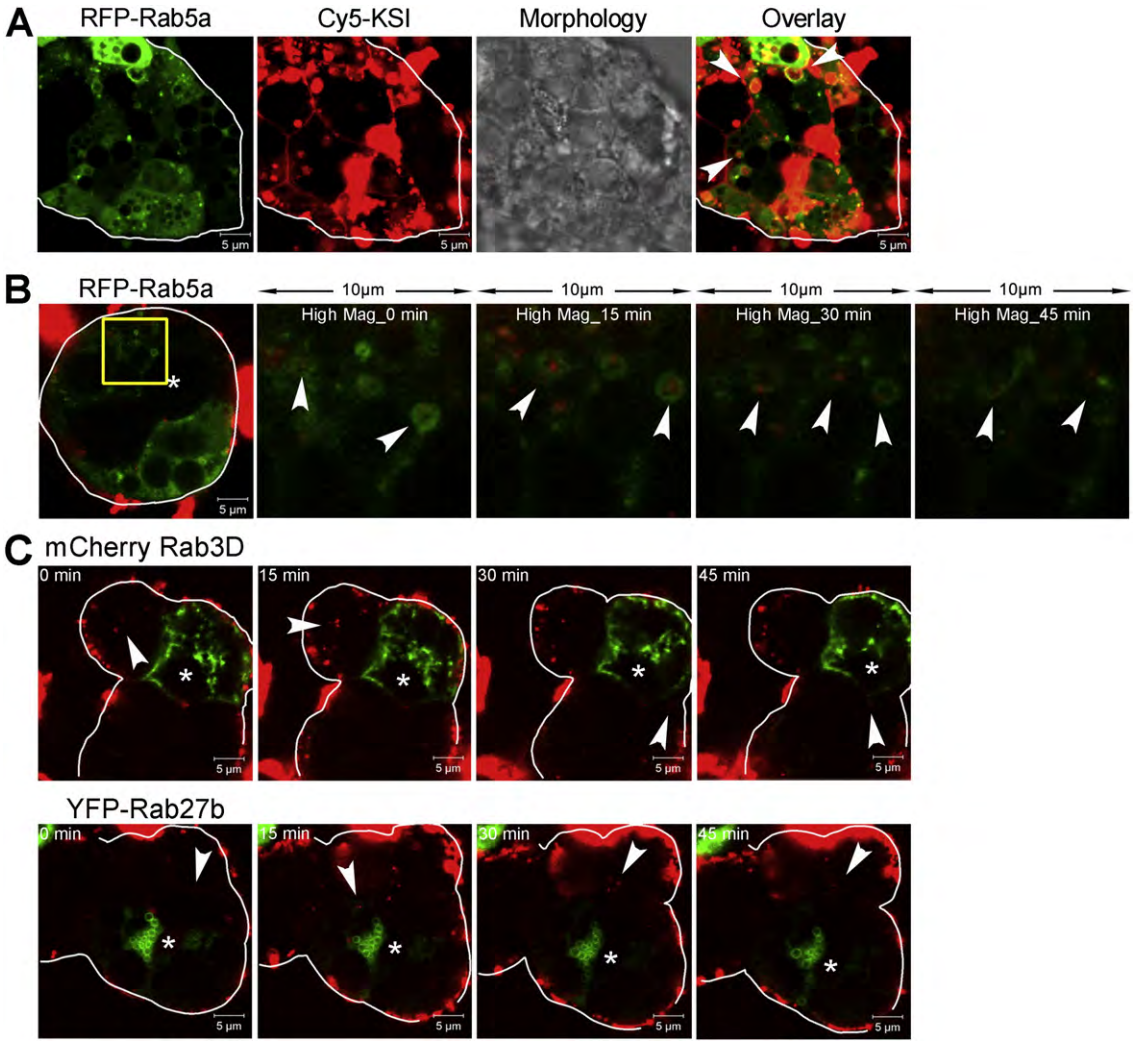

Fig. 4. Intracellular trafficking of KSI nanoparticles in LGACs. (A) Internalization of KSI to early endosomes in live rabbit LGACs expressing RFP-Rab5a, a marker of early endosomes. LGACs transduced with RFP-Rab5a (green) were treated with 30 μM of Cy5-KSI (red) at 37 °C for 1 h, washed with DPBS twice, and analyzed by confocal fluorescence microscopy. Arrowheads indicate Cy5-KSI in early endosomes. (B) LGACs transduced with RFP-Rab5a (green) were pulsed with 30 μM of Cy5-KSI (red) at 37 °C for 10 min, rinsed and followed by a 45 min chase in fresh PCM at 37 °C. The yellow-boxed region is expanded in time-lapse images shown successively to the right. Arrowheads indicate early endosomes that include Cy5-KSI at earlier times but show label dissipating at later times of incubation. White lines depict the periphery of the reconstituted cluster of LGAC obtained by phase contrast imaging. (C) LGACs expressing mCherry-Rab3D (red) or YFP-Rab27b (red) were pulsed with 30 μM of Cy5-KSI (green) at 37 °C for 10 min and imaged for 45 min in fresh PCM at 37 °C. Internalized KSI did not associate with either Rab3D or Rab27b in live rabbit LGACs. Data were presented at the indicated time points. White lines depict the periphery of the reconstituted cluster of LGACs. Arrowheads indicate internalized Cy5-KSI. Scale bars indicate 5 μm.

which revealed primarily basolateral enrichment with traces at the apical membrane (Supplementary Fig. S2). Rh-SI or Rh-KSI, mixed with fluorescein 10 k dextran as a marker of fluid phase uptake, was administered using intra-lacrimal injection. 1 h after injection the LG was retrieved and analyzed (Fig. 6A). Although fluorescein 10 k dextran clearly presented in the LG around the acinar cluster, LGs injected with Rh-SI displayed weak to no fluorescent signal in cytoplasm or lumena of LGAC, indicative of little uptake of SI *in vivo* (Fig. 6A left). However, in the mice injected with Rh-KSI, KSI puncta appeared inside the LGACs where fluorescein 10 k dextran was recovered, suggesting that KSI was internalized. Additionally, the KSI signal was also detected in the apical region of the LGACs, suggesting that the basolateral to apical transcytosis found *in vitro* occurs *in vivo* as well. The images in Fig. 6A were quantified by ImageJ in terms of the fluorescent signals in each LG whole acinus (Fig. 6B) and lumenal region (Fig. 6C). By considering each LG cluster, KSI displayed a 4-fold increased internalization in acini relative to SI ($p < 0.0001$) (Fig. 6B). For those analyzed LG acini, the fluorescent signal in the apical region of LGACs was >7-fold higher with KSI relative to SI ($p = 0.01$) (Fig. 6C). These results suggest that knob enhances the tissue affinity of SI *in vivo*, and that internalized KSI can be transcytosed to the apical region of LGACs and released into the lumen.

To further confirm the internalization and intracellular trafficking of SI and KSI, we repeated the intra-lacrimal injections and analyzed the glands by TEM. The images in Fig. 7 show sections from both apical and basolateral regions of mouse LG after injection with free rhodamine, Rh-SI, and Rh-KSI. The rhodamine label (not shown) was utilized to identify the area around the needle track. LGs injected with free rhodamine were used as a control group. Apical and basolateral membranes were identified based upon the relative locations of mitochondria, nuclei, secretory vesicles, and epithelial microvilli. As shown in Fig. 7, no particles were observed in the control group administered with free rhodamine dye (Fig. 7, free dye panels). For LGs injected with Rh-SI, SI nanoparticles could only be observed in extracellular spaces next to the basolateral membrane of mouse LG; none of these particles were seen in the apical region or lumen (Fig. 7, SI panels), consistent with what we observed *in vitro* and with fluorescent labeling *in vivo*. However, for LGs injected with Rh-KSI, we observed internalized uniform

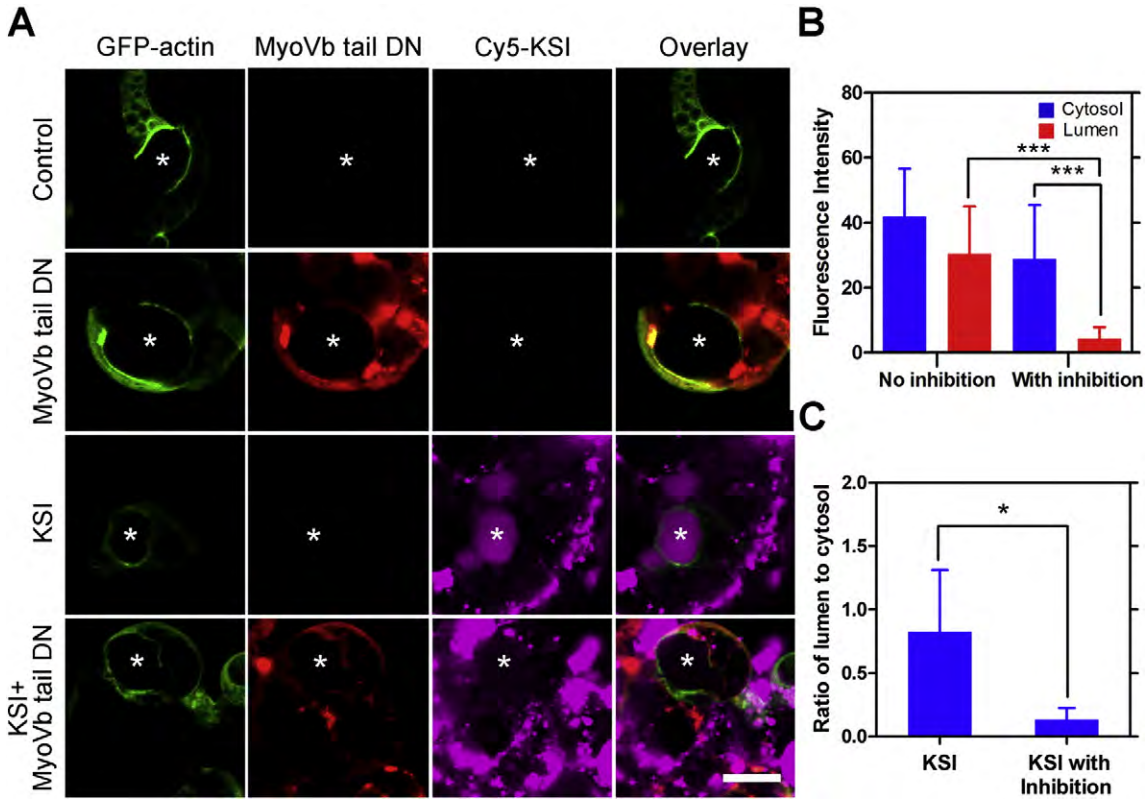

Fig. 5. Overexpression of a dominant negative myosin Vb tail impairs basolateral-to-apical transcytosis of KSI in LGACs. (A) Reconstituted rabbit LGACs, co-transduced with AdGFP-actin (green) to delineate morphology, Ad mCherry myosin Vb tail DN (red), and Ad helper virus, were incubated with 30 μM of Cy5-KSI nanoparticles (purple) at 37 °C for 1 h before analysis. *, lumenal region of LGACs. Scale bar indicates 10 μm. (B) Quantification of fluorescence intensity in lumen and cytosol of LGACs with or without the dominant negative myosin Vb tail, which inhibits transcytosis. ***, p value < 0.005 (ANOVA followed by Tukey post-hoc test). Data were expressed as Mean ± SD (n = 4). (C) Quantification of fluorescence intensity as a ratio of lumenal to cytosolic fluorescence. Data are expressed as Mean ± SD (n = 4). KSI, 0.83 ± 0.48; KSI with inhibition, 0.13 ± 0.09; p value = 0.031 (Student t-test).

nanoparticles enclosed in vesicular structures both at the basolateral and apical membranes of mouse LGs as well as in the lumen (Fig. 7, KSI panels), again confirming the endocytosis and basolateral-to-apical transcytosis of KSI. Some KSI nanoparticles were also observed in autophagosome-like structures close to the basolateral membrane. The box-and-whisker plot shows that the diameter of SI nanoparticles (21.1 ± 4.6 nm) is similar to KSI nanoparticles (20.2 ± 2.8 nm), consistent with cryo-TEM imaging (Fig. 1).

3.6. Hypothesized trafficking model of Knob-ELP

Based on the data collected previously [19] and in this manuscript, the following model is proposed for trafficking KSI in LGAC (Fig. 8). Endocytosis, initiated by the binding of recombinant knob on the KSI nanoparticles to the CAR on the basolateral membrane, is followed by transport to early endosomes enriched in Rab5. Thereafter, KSI is sorted into vesicles utilizing myosin Vb motors for delivery to the apical membrane and released into the lumena. Prior studies have shown that transcytosis of Rab11a vesicles is myosin Vb dependent. [32] The remaining KSI is sorted into late endosomes, autophagosomes and lysosomes.

In this study, we observed a distinct intracellular trafficking pathway of the KSI nanoparticle in primary cells of the lacrimal gland. Prior studies of transformed hepatocytes showed that KSI nanoparticles undergo CAR-dependent internalization and are transported to lysosomes. In contrast, KSI in the LG is transported to the apical membrane and lumen through an intact transcytotic pathway. The mechanisms behind the distinct trafficking behavior in these two cell types remain to be investigated. Both hepatocytes and LGACs are specialized epithelial cells, featuring apical–basal polarity maintained by tight junctions via protein complexes, and are responsible for vectorial transport of ions and solutes across the epithelium. CAR has been identified as a regulator in tight junction permeability for many years, but its biological function and trafficking mechanism in mammalian cells remain unknown. However it is possible that a disparity in CAR function in the hepatocytes and LGACs may play a role in the different trafficking patterns of KSI-CAR complexes between hepatocytes and LGACs. CAR splice-variants have been identified in many tissues [43,44] and each of them may exhibit alternative functions. CAR is expressed as at least two isoforms containing identical extracellular and transmembrane domains, which predict identical serotype preference and adenovirus binding, and differ only in the last 26 (CAR^{ex7}) or 13 (CAR^{ex8}) amino acids of the cytoplasmic domain [45]. CAR^{ex7} and CAR^{ex8} share a similar class of PDZ-binding domain, but interact with different PDZ-domain containing proteins, which may trigger distinct signaling and sorting pathways [46]. For example, CAR^{ex8} interaction with PDZ-domain containing protein MAGI-1b results in CAR^{ex8} degradation, while this interaction cannot be observed in CAR^{ex7} [46]. In addition, the cytoplasmic tail of CAR contains 9 lysines which may serve as ubiquitylation sites for endocytosis and trafficking of CAR to lysosomes for degradation. Deletion of this protein sequence may abolish ubiquitylation, causing resorting of CAR to the cell surface or other intracellular compartments [47].

As model systems, we investigated the intracellular trafficking and transcytosis of KSI nanoparticles in the rabbit LGAC *ex vivo* and evaluated the LG retention of KSI nanoparticles in the mouse LG *in vivo*. Part of the rationale for using two different species was that the *ex vivo* system for LGAC production requires large sources of primary tissue, which can be obtained from rabbits. In contrast, the mouse LG is easily accessible

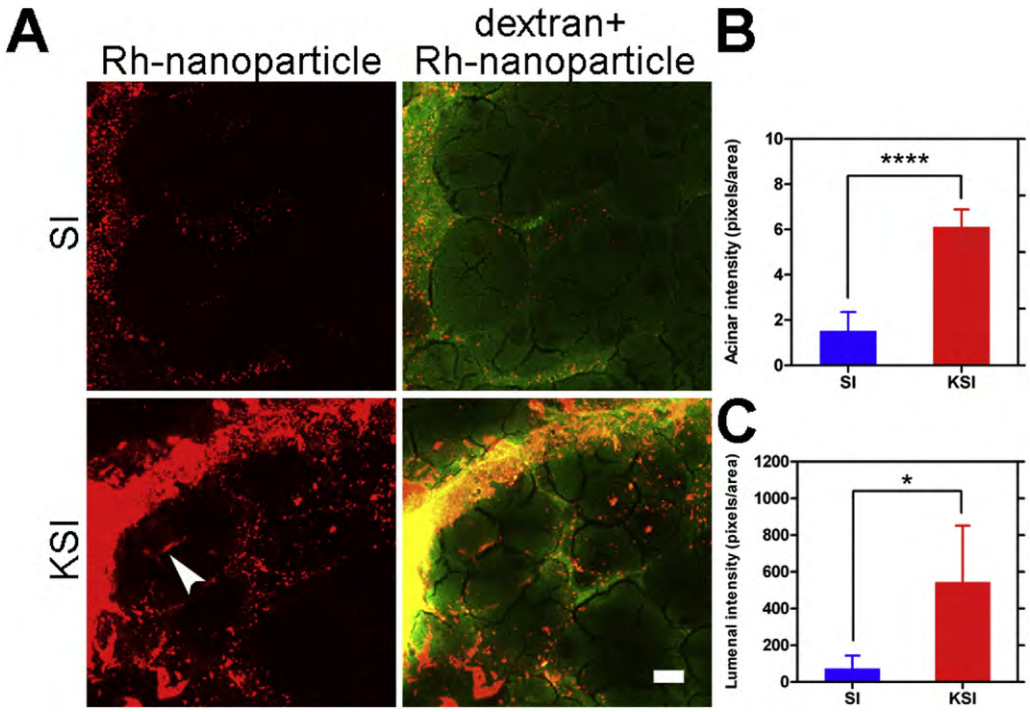

Fig. 6. Comparison of *in vivo* ELP nanoparticle accumulation in LGs from BALB/c mice. (A) Intra-lacrimal gland injection of Rh-coupled KSI (red) into LGs of 12 week BALB/c mice showed significant internalization, LG retention, and lumenal accumulation compared to SI (red). Fluorescein 10 k dextran (green) was used as a control and fluid-phase marker. White arrowhead indicates internalized KSI close to or in the apical/lumenal region of mouse LGACs. Scale bar indicates 10 μm. (B) Quantification of fluorescence intensity for internalized SI and KSI. The fluorescent signals were analyzed in LG acinar clusters and analyzed using ImageJ. ****, p value < 0.0001 (Student t-test). Bar are expressed as mean ± SD (n = 5). (C) Quantification of fluorescence intensity in the subapical membrane and lumenal region of clusters of mouse LGAC. Data are expressed as mean ± SD (n = 5). *, p value = 0.01 (Student t-test).

for direct injection, more so than in a rabbit. While significant anatomical diversity exists between species, many ocular elements are conserved, which suggest the translational potential of these findings. For example, rabbits have a blink rate every 6 min ($10\ s^{-1}$) [48]. Mice and rats share a similar blink rate averaged every 5 min each blink ($12\ s^{-1}$), while human has an average blink rate in every 5 s ($0.15–0.2\ s^{-1}$) [49]. These differences partially result from different eyelid configurations among species. A faster blink rate reduces the precorneal residence time on the ocular surface, increases the tear drainage, and alters the drug absorption of a topically applied therapeutics across the cornea in comparison with a slower blink rate [50]. Cornea is a transparent multilayered epithelium and serves as the primary barrier to drug absorption, especially for hydrophilic drugs. The corneal thickness varies with age, disease, external influences (e.g. contact lenses), damage, and species. Recent research has reported that transporters expressed in the corneal epithelium may involve the transport of some hydrophilic drugs [51]; however, corneal transporter-mediated uptake and elimination can vary largely between species. While parameters such as these clearly suggest major differences between species in ocular pharmacokinetics, the KSI targets the CAR receptor, which is expressed constitutively in the LG across rabbits, mice, and humans [23]. Thus the fact that KSI trancytoses through the LGAC in two different species, suggests the possibility that it may also have this ability in the human LG.

Two different fluorescent dyes (rhodamine, Cy5) were evaluated as labels for KSI in this study. The criteria for fluorescent dye selection were based on two factors: i) the need to label KSI with either red or far red wavelength emissions compatible with other double and triple label microscopy studies; and ii) to demonstrate that KSI transcytosis was conserved across at least two distinct fluorescent probes. Both rhodamine (e.g. TRAMA) and Cyanine dyes (e.g. Cy5) are small molecule derivatives that link to primary amino acids. Rhodamine derivatives have high photostability and little sensitivity in physiological pH range and are suitable for multicolor labeling experiments [52]. In comparison, sulfo-Cy5 shows comparable photostability, more intense emission, and increased water solubility. Therefore, sulfo-Cy5 is well suited for the labeling of proteins that easily denature in the presence of organic co-solvents sometimes used for labeling reactions. Rhodamine is excited by green light; however, Cy5 derivatives are excited by red light (650 nm) and emit in the far-red region (680 nm). Cy5 is well suited for triple label live-cell microscopy experiments alongside probes (RFP-Rab5a, mCherry Rab3D, YFP-Rab27b, mCherry myosin Vb tail DN) with emissions overlapping that of rhodamine. As KSI conjugated with either rhodamine or sulfo-Cy5 displayed comparable internalization and lumenal accumulation in rabbit LGACs, this further supports the contention that KSI mediates transport across the polarized cells of the LG.

Herein, we report for the first time a protein polymer nanoparticle that selectively enters LGAC *in vitro* and *in vivo* and undergoes a basolateral-to-apical transport for secretion into the apical lumen of LGAC. LGAC lumena drain into lacrimal ducts that delivery tear proteins and electrolytes to the surface of the eye. This unusual transcytosing property of the nanoparticle provides a unique capability that may be exploited for sustained delivery of drugs to the ocular surface for those diseases that are currently difficult to treat and require continuous infusion of drug. Transcytosing nanoparticles could be developed for delivery *i.v.* or *s.c.*, or alternatively injected to form a depot in case of acute infection or trauma.

4. Conclusion

As a model for targeted transcytosis to the tear ducts, this strategy has the potential to generate new nanomaterials that act at the LG, the ducts, or the ocular surface. Based on the ELP diblock copolymer

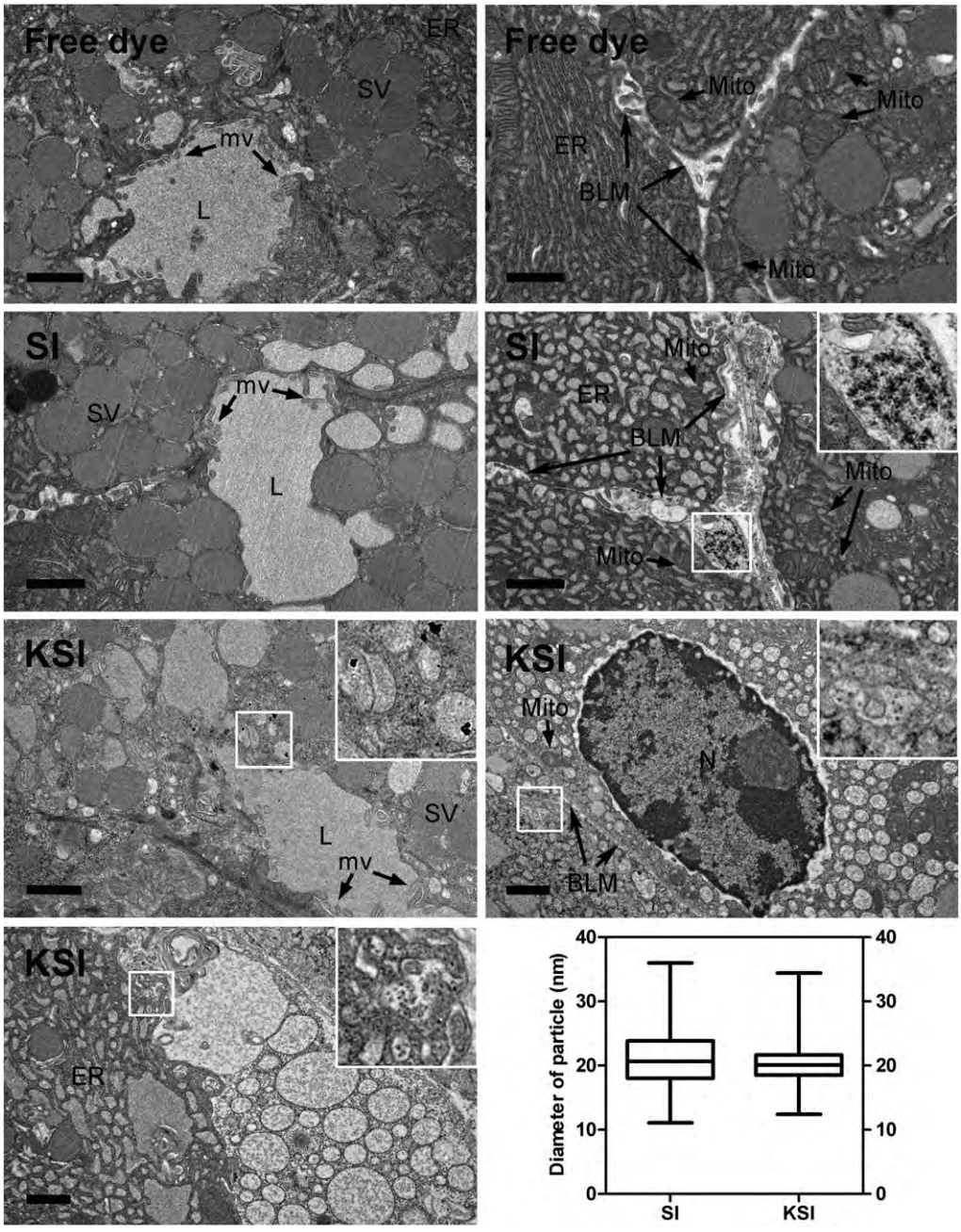

Fig. 7. Transmission electron microscopy confirms KSI transcytosis in LGs from BALB/c mice. Transmission electron microscopy images compared mouse LGs from 12 week BALB/c mice administered with free rhodamine dye, SI or KSI by intra-lacrimal injection. Vesicle-enclosed black puncta close to the apical membrane (AM) of mouse LG acini are KSI nanoparticles. L, lumen; SV, secretory vesicles; M, epithelial microvilli projecting from the AM of LG acini. Scale bars indicate 1 μm. KSI diameters were summarized in a box-and-whisker plot. Particle diameters are expressed as mean ± SD. n = 178 and 205 for SI and KSI, respectively. For the box-and-whisker plot, the box expresses mean ± SD and the whisker shows minimum and maximum values.

template, KSI fusion proteins assemble into stable, monodisperse, and biodegradable nanoparticles at physiological temperature. Genetic fusion of the Ad5 knob domain to SI minimally affects the morphology of the particle but significantly enhances its internalization efficiency. With efficient targeting to CAR on cells of the LG, KSI nanoparticles are internalized and transported from basolateral to apical membranes. KSI nanoparticles represent the first engineered delivery vehicle with potential for selective delivery of therapeutic agents from serum, through the lacrimal gland acinar cells, and to the tears bathing the ocular surface.

Supplementary data to this article can be found online at http://dx.doi.org/10.1016/j.jconrel.2014.12.017.

Acknowledgments

We sincerely appreciate the assistance of F. Yarber and H. Pei for rabbit LGAC preparation and recombinant adenovirus purification. We thank Drs. S. Karvar (Medical University of South Carolina) and L.X. Shu (SUNY-Buffalo) for kindly providing original constructs for Ad-YFP-Rab27b and Ad-mCherry-myosin Vb tail DN, respectively. We thank Dr. Arnold Sipos (Keck School of Medicine of University of Southern California) for his assistance in Zeta potential measurement. We also gratefully acknowledge the help of the USC/Norris Cell and Tissue Imaging Core Facility and their staff, E. Barron, D. Hauser and A. Rodriguez for sample preparation and assistance in TEM imaging. This

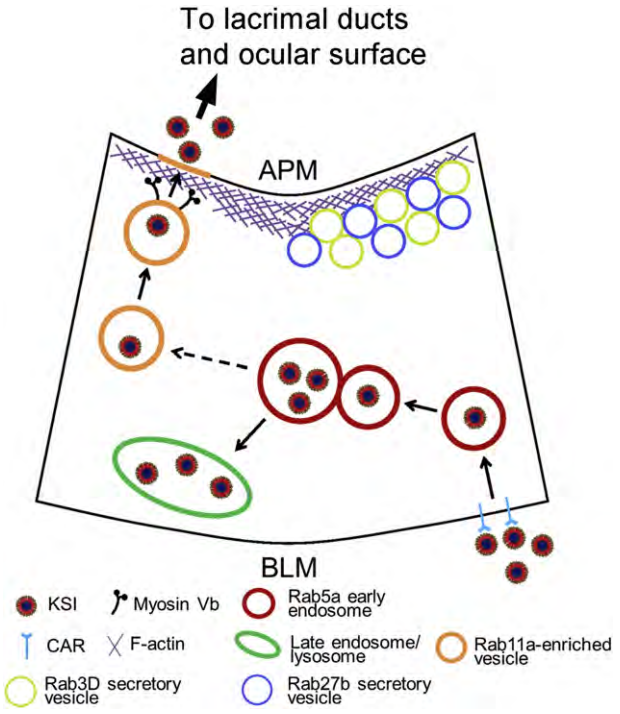

Fig. 8. Working model for intracellular trafficking of KSI ELPs in LGACs. KSI is internalized *via* CAR-mediated endocytosis. KSI is then delivered to Rab5a-early endosomes where some KSI nanoparticles are transported to late endosomes and lysosomes, whereas others are sorted to Rab11a-associated sub-apical intracellular compartments for release to the apical lumen of LG acini. Some KSI remains in intracellular acidic compartments without entering the transcytotic pathway.

study was supported by a Department of Defense grant (TATRC, DOD W81XWH-12-1-0538) to J.A.M. The study was also supported by the following National Institutes of Health grants: RO1EY011386, RO1EY017293, and RO1EY017293S1 to S.F.H.-A.; R21EB012281 to J.A.M., and P30CA014089 to the USC Norris Cancer Center. The content is solely the responsibility of the authors.

References

[1] U.B. Kompella, R.S. Kadam, V.H. Lee, Recent advances in ophthalmic drug delivery, Ther. Deliv. 1 (2010) 435–456.
[2] I. Ahmed, The noncorneal route in ocular drug delivery, in: A.K. Mitra (Ed.), Ophthalmic Drug Delivery Systems, Marcel Dekker, New York, 2003, pp. 335–363.
[3] P.K. Shukla, M. Kumar, G.B. Keshava, Mycotic keratitis: an overview of diagnosis and therapy, Mycoses 51 (2008) 183–199.
[4] H.A. Quigley, Glaucoma, Lancet 377 (2011) 1367–1377.
[5] C.M. Olthoff, J.S. Schouten, B.W. van de Borne, C.A. Webers, Noncompliance with ocular hypotensive treatment in patients with glaucoma or ocular hypertension an evidence-based review, Ophthalmology 112 (2005) 953–961.
[6] A. Galor, J.E. Thorne, Scleritis and peripheral ulcerative keratitis, Rheum. Dis. Clin. N. Am. 33 (2007) 835–854 (vii).
[7] P.A. Thomas, J. Kaliamurthy, Mycotic keratitis: epidemiology, diagnosis and management, Clin. Microbiol. Infect. 19 (2013) 210–220.
[8] K.R. Wilhelmus, Antiviral treatment and other therapeutic interventions for herpes simplex virus epithelial keratitis, The Cochrane Database of Systematic Reviews, 2010, p. CD002898.
[9] A.L. Weiner, B.C. Gilger, Advancements in ocular drug delivery, Vet. Ophthalmol. 13 (2010) 395–406.
[10] K. Cholkar, S.P. Patel, A.D. Vadlapudi, A.K. Mitra, Novel strategies for anterior segment ocular drug delivery, J. Ocul. Pharmacol. Ther. 29 (2013) 106–123.
[11] A. Ludwig, The use of mucoadhesive polymers in ocular drug delivery, Adv. Drug Deliv. Rev. 57 (2005) 1595–1639.
[12] M.R. Sawusch, T.P. O'Brien, J.D. Dick, J.D. Gottsch, Use of collagen corneal shields in the treatment of bacterial keratitis, Am J. Ophthalmol. 106 (1988) 279–281.
[13] M.C. Edman, R.R. Marchelletta, S.F. Hamm-Alvarez, Lacrimal gland overview, in: D.A. Dartt, J.C. Besharse, M.R. Dana (Eds.), Encyclopedia of the Eye, Elsevier, Oxford, 2010, pp. 522–527.
[14] R.R. Hodges, D.A. Dartt, Regulatory pathways in lacrimal gland epithelium, Int. Rev. Cytol. 231 (2003) 129–196.
[15] N. Simionescu, The microvascular endothelium: segmental differentiations, transcytosis, selective distribution of anionic sites, in: B.S.G. Weissman, R. Paoletti (Eds.), Advances in Inflammatory Research, Raven Press, New York, 1979, pp. 61–70.
[16] Z.B. Zhu, S.K. Makhija, B. Lu, M. Wang, A.A. Rivera, M. Preuss, F. Zhou, G.P. Siegal, R.D. Alvarez, D.T. Curiel, Transport across a polarized monolayer of Caco-2 cells by transferrin receptor-mediated adenovirus transcytosis, Virology 325 (2004) 116–128.
[17] J.R. Zhang, K.E. Mostov, M.E. Lamm, M. Nanno, S. Shimida, M. Ohwaki, E. Tuomanen, The polymeric immunoglobulin receptor translocates pneumococci across human nasopharyngeal epithelial cells, Cell 102 (2000) 827–837.
[18] M. Shah, P.Y. Hsueh, G. Sun, H.Y. Chang, S.M. Janib, J.A. MacKay, Biodegradation of elastin-like polypeptide nanoparticles, Protein Sci. 21 (2012) 743–750.
[19] G. Sun, P.Y. Hsueh, S.M. Janib, S. Hamm-Alvarez, J.A. MacKay, Design and cellular internalization of genetically engineered polypeptide nanoparticles displaying adenovirus knob domain, J. Control. Release 155 (2011) 218–226.
[20] A. Chilkoti, M.R. Dreher, D.E. Meyer, Design of thermally responsive, recombinant polypeptide carriers for targeted drug delivery, Adv. Drug Deliv. Rev. 54 (2002) 1093–1111.
[21] M. Shah, M.C. Edman, S.R. Janga, P. Shi, J. Dhandhukia, S. Liu, S.G. Louie, K. Rodgers, J.A. Mackay, S.F. Hamm-Alvarez, A rapamycin-binding protein polymer nanoparticle shows potent therapeutic activity in suppressing autoimmune dacryoadenitis in a mouse model of Sjogren's syndrome, J. Control. Release 171 (2013) 269–279.
[22] P. Shi, S. Aluri, Y.A. Lin, M. Shah, M. Edman-Woolcott, J. Dhandhukia, H. Cui, J.A. Mackay, Elastin-based protein polymer nanoparticles carrying drug at both corona and core suppress tumor growth in vivo, J. Control. Release 171 (2013) 330–338.
[23] J. Xie, L. Chiang, J. Contreras, K. Wu, J.A. Garner, L. Medina-Kauwe, S.F. Hamm-Alvarez, Novel fiber-dependent entry mechanism for adenovirus serotype 5 in lacrimal acini, J. Virol. 80 (2006) 11833–11851.
[24] R.W. Walters, P. Freimuth, T.O. Moninger, I. Ganske, J. Zabner, M.J. Welsh, Adenovirus fiber disrupts CAR-mediated intercellular adhesion allowing virus escape, Cell 110 (2002) 789–799.
[25] S.K. Chung, J.Y. Kim, I.B. Kim, S.I. Park, K.H. Paek, J.H. Nam, Internalization and trafficking mechanisms of coxsackievirus B3 in HeLa cells, Virology 333 (2005) 31–40.
[26] J.R. McDaniel, J.A. Mackay, F.G. Quiroz, A. Chilkoti, Recursive directional ligation by plasmid reconstruction allows rapid and seamless cloning of oligomeric genes, Biomacromolecules 11 (2010) 944–952.
[27] N.M. Green, N.G. Wrigley, W.C. Russell, S.R. Martin, A.D. McLachlan, Evidence for a repeating cross-beta sheet structure in the adenovirus fibre, EMBO J. 2 (1983) 1357–1365.
[28] W. Hassouneh, T. Christensen, A. Chilkoti, Elastin-like polypeptides as a purification tag for recombinant proteins, Current Protocols in Protein Science/Editorial Board, John E. Coligan … [et al.], 2010 (Chapter 6, Unit 6 11).
[29] J.P. Gierow, T. Yang, A. Bekmezian, N. Liu, J.M. Norian, S.A. Kim, S. Rafisolyman, H. Zeng, C.T. Okamoto, R.L. Wood, A.K. Mircheff, Na-K-ATPase in lacrimal gland acinar cell endosomal system: correcting a case of mistaken identity, Am. J. Physiol. 271 (1996) C1685–C1698.
[30] S.F. Hamm-Alvarez, S. Da Costa, T. Yang, X. Wei, J.P. Gierow, A.K. Mircheff, Cholinergic stimulation of lacrimal acinar cells promotes redistribution of membrane-associated kinesin and the secretory protein, beta-hexosaminidase, and increases kinesin motor activity, Exp. Eye Res. 64 (1997) 141–156.
[31] G.V. Jerdeva, K. Wu, F.A. Yarber, C.J. Rhodes, D. Kalman, J.E. Schechter, S.F. Hamm-Alvarez, Actin and non-muscle myosin II facilitate apical exocytosis of tear proteins in rabbit lacrimal acinar epithelial cells, J. Cell Sci. 118 (2005) 4797–4812.
[32] S. Xu, M. Edman, M.S. Kothawala, G. Sun, L. Chiang, A. Mircheff, L. Zhu, C. Okamoto, S. Hamm-Alvarez, A Rab11a-enriched subapical membrane compartment regulates a cytoskeleton-dependent transcytotic pathway in secretory epithelial cells of the lacrimal gland, J. Cell Sci. 124 (2011) 3503–3514.
[33] P.N. Hurter, J. Scheutjens, T.A. Hatton, Molecular modeling of micelle formation and solubilization in block-copolymer micelles. 1. A self-consistent mean-field lattice theory, Macromolecules 26 (1993) 5592–5601.
[34] P. Alexandridis, T.A. Hatton, Poly(ethylene oxide)-poly(propylene oxide)–poly(ethylene oxide) block-copolymer surfactants in aqueous-solutions and at interfaces — thermodynamics, structure, dynamics, and modeling, Colloids Surf. A Physicochem. Eng. Asp. 96 (1995) 1–46.
[35] H. Cui, T.K. Hodgdon, E.W. Kaler, L. Abezgauz, D. Danino, M. Lubovsky, Y. Talmon, D.J. Pochan, Elucidating the assembled structure of amphiphiles in solution via cryogenic transmission electron microscopy, Soft Matter 3 (2007) 945–955.
[36] E. Evans, W. Zhang, G. Jerdeva, C.Y. Chen, X. Chen, S.F. Hamm-Alvarez, C. Okamoto, Direct interaction between Rab3d and the polymeric immunoglobulin receptor and trafficking through regulated secretory vesicles in lacrimal gland acinar cells, Am. J. Physiol. Cell Physiol. 294 (2008) C662–C674.
[37] V. Awasthi, G. Meinken, K. Springer, S.C. Srivastava, P. Freimuth, Biodistribution of radioiodinated adenovirus fiber protein knob domain after intravenous injection in mice, J. Virol. 78 (2004) 6431–6438.
[38] S.O. Rizzoli, I. Bethani, D. Zwilling, D. Wenzel, T.J. Siddiqui, D. Brandhorst, R. Jahn, Evidence for early endosome-like fusion of recently endocytosed synaptic vesicles, Traffic 7 (2006) 1163–1176.
[39] J.M. Carvajal-Gonzalez, D. Gravotta, R. Mattera, F. Diaz, A. Perez Bay, A.C. Roman, R.P. Schreiner, R. Thuenauer, J.S. Bonifacino, E. Rodriguez-Boulan, Basolateral sorting of the coxsackie and adenovirus receptor through interaction of a canonical YXXPhi motif with the clathrin adaptors AP-1A and AP-1B, Proc. Natl. Acad. Sci. U. S. A. 109 (2012) 3820–3825.
[40] L. Chiang, S. Karvar, S.F. Hamm-Alvarez, Direct imaging of RAB27B-enriched secretory vesicle biogenesis in lacrimal acinar cells reveals origins on a nascent vesicle budding site, PLoS One 7 (2012) e31789.

[41] L. Chiang, J. Ngo, J.E. Schechter, S. Karvar, T. Tolmachova, M.C. Seabra, A.N. Hume, S.F. Hamm-Alvarez, Rab27b regulates exocytosis of secretory vesicles in acinar epithelial cells from the lacrimal gland, Am. J. Physiol. Cell Physiol. 301 (2011) C507–C521.
[42] S. Xu, L. Ma, E. Evans, C.T. Okamoto, S.F. Hamm-Alvarez, Polymeric immunoglobulin receptor traffics through two distinct apically targeted pathways in primary lacrimal gland acinar cells, J. Cell Sci. 126 (2013) 2704–2717.
[43] K.C. Huang, Z. Yasruel, C. Guerin, P.C. Holland, J. Nalbantoglu, Interaction of the coxsackie and adenovirus receptor (CAR) with the cytoskeleton: binding to actin, FEBS Lett. 581 (2007) 2702–2708.
[44] J.W. Chen, R. Ghosh, R.W. Finberg, J.M. Bergelson, Structure and chromosomal localization of the murine coxsackievirus and adenovirus receptor gene, DNA Cell Biol. 22 (2003) 253–259.
[45] K.J. Excoffon, N.D. Gansemer, M.E. Mobily, P.H. Karp, K.R. Parekh, J. Zabner, Isoform-specific regulation and localization of the coxsackie and adenovirus receptor in human airway epithelia, PLoS One 5 (2010) e9909.
[46] A.O. Kolawole, P. Sharma, R. Yan, K.J. Lewis, Z. Xu, H.A. Hostetler, K.J. Ashbourne Excoffon, The PDZ1 and PDZ3 domains of MAGI-1 regulate the eight-exon isoform of the coxsackievirus and adenovirus receptor, J. Virol. 86 (2012) 9244–9254.
[47] S.A. Marvin, C.M. Wiethoff, Emerging roles for ubiquitin in adenovirus cell entry, Biol. Cell 104 (2012) 188–198.
[48] H. Toshida, D.H. Nguyen, R.W. Beuerman, A. Murakami, Neurologic evaluation of acute lacrimomimetic effect of cyclosporine in an experimental rabbit dry eye model, Invest. Ophthalmol. Vis. Sci. 50 (2009) 2736–2741.
[49] R. Tutt, A. Bradley, C. Begley, L.N. Thibos, Optical and visual impact of tear break-up in human eyes, Invest. Ophthalmol. Vis. Sci. 41 (2000) 4117–4123.
[50] A. Urtti, L. Salminen, Minimizing systemic absorption of topically administered ophthalmic drugs, Surv. Ophthalmol. 37 (1993) 435–456.
[51] E. Mannermaa, K.S. Vellonen, A. Urtti, Drug transport in corneal epithelium and blood–retina barrier: emerging role of transporters in ocular pharmacokinetics, Adv. Drug Deliv. Rev. 58 (2006) 1136–1163.
[52] M.W. Wessendorf, T.C. Brelje, Which fluorophore is brightest? A comparison of the staining obtained using fluorescein, tetramethylrhodamine, lissamine rhodamine, Texas red, and cyanine 3.18, Histochemistry 98 (1992) 81–85.

Journal of Controlled Release 199 (2015) 156–167

Contents lists available at ScienceDirect

Journal of Controlled Release

journal homepage: www.elsevier.com/locate/jconrel

A thermo-responsive protein treatment for dry eyes

Wan Wang [a], Aarti Jashnani [a], Suhaas R. Aluri [a], Joshua A. Gustafson [a], Pang-Yu Hsueh [a], Frances Yarber [a], Robert L. McKown [b], Gordon W. Laurie [c], Sarah F. Hamm-Alvarez [a,d], J. Andrew MacKay [a,e,*]

[a] Department of Pharmacology and Pharmaceutical Sciences, University of Southern California, Los Angeles, CA, United States
[b] Department of Integrated Science and Technology, James Madison University, Harrisonburg, VA, United States
[c] Department of Cell Biology, School of Medicine of the University of Virginia, Charlottesville, VA, United States
[d] Department of Physiology and Biophysics, Keck School of Medicine of the University of Southern California, Los Angeles, CA, United States
[e] Department of Biomedical Engineering, University of Southern California, Los Angeles, CA, United States

ARTICLE INFO

Article history:
Received 26 April 2014
Accepted 17 November 2014
Available online 3 December 2014

Keywords:
Elastin-like polypeptides (ELPs)
Lacritin
Lacrimal gland
Thermo-responsive
Prosecretory
Uptake

ABSTRACT

Millions of Americans suffer from dry eye disease, and there are few effective therapies capable of treating these patients. A decade ago, an abundant protein component of human tears was discovered and named lacritin (Lacrt). Lacrt has prosecretory activity in the lacrimal gland and mitogenic activity at the corneal epithelium. Similar to other proteins placed on the ocular surface, the durability of its effect is limited by rapid tear turnover. Motivated by the rationale that a thermo-responsive coacervate containing Lacrt would have better retention upon administration, we have constructed and tested the activity of a thermo-responsive Lacrt fused to an elastin-like polypeptide (ELP). Inspired from the human tropoelastin protein, ELP protein polymers reversibly phase separate into viscous coacervates above a tunable transition temperature. This fusion construct exhibited the prosecretory function of native Lacrt as illustrated by its ability to stimulate β-hexosaminidase secretion from primary rabbit lacrimal gland acinar cells. It also increased tear secretion from non-obese diabetic (NOD) mice, a model of autoimmune dacryoadenitis, when administered via intra-lacrimal injection. Lacrt ELP fusion proteins undergo temperature-mediated assembly to form a depot inside the lacrimal gland. We propose that these Lacrt ELP fusion proteins represent a potential therapy for dry eye disease and the strategy of ELP-mediated phase separation may have applicability to other diseases of the ocular surface.

1. Introduction

The lacrimal gland–corneal axis plays a critical role in maintaining ocular surface health. While the avascular cornea serves as both a protective barrier and the main refractive element of the visual system, the lacrimal gland (LG) is the major organ secreting key proteins and electrolytes into the tear film that bathes the cornea and, through nutrient and antimicrobial proteins, sustains its function [1,2]. Dry eye disease (DED) is a multifactorial disease of the ocular surface causing visual disturbance and tear film instability [3] and can be due to either aqueous tear insufficiency originating with defects in aqueous tear production by the LG [4] or evaporative dry eye associated with meibomian gland insufficiency [5,6]. According to reports, severe DED affects approximately 5 million Americans above age 50 and its global prevalence ranges from 5% to 35% of the population [3]. Traditional approaches to treat DED include topical administration of artificial tears or the conservation of secreted tears using tear plugs [7] and eye-shields [8]. Since many cases of DED are associated with inflammation [9,10], some treatments for DED have been proposed that inhibit inflammation of the LG [11]. None of these methods are satisfactory in replacing the lost regulatory functions provided by the many components found in normal tears. To better sustain the health and homeostasis of the ocular surface there remains a need for efficient, sustained and targeted DED therapy. In humans, the inferior palpebral lobe of the LG is accessible for injection beneath the eyelid; furthermore, if coupled with a sustained release strategy this route of administration might have clinical relevance, similar to intra-vitreal injection or subconjunctival injection.

The discovery of the glycosylated human tear protein, lacritin (Lacrt), provided critical insight into the potential use of regulatory tear proteins to treat DED [12,13]. Lacrt was found in a systematic oligonucleotide screen of a human LG cDNA library and exhibited LG specific-expression [14]. Subsequent studies have proven its efficacy in stimulating peroxidase secretion in cultured rat [14], and both lactoferrin and lipocalin secretion in cultured monkey lacrimal acinar cells [15]. Lacrt also promotes constitutive tear secretion by New Zealand white rabbits and Aire KO mice via topical treatment [16,17], proliferation of transformed human corneal epithelial cells [14,18], and restored health of

Abbreviations: DED, dry eye disease; ELP, elastin-like polypeptide; Lacrt, lacritin; T_t, transition temperature; LG, lacrimal gland; LGACs, lacrimal gland acinar cells; NOD, non-obese diabetic; CCh, carbachol.

* Corresponding author at: Department of Pharmacology and Pharmaceutical Sciences, University of Southern California, Los Angeles, CA 90033-9121, United States.
E-mail address: jamackay@usc.edu (J.A. MacKay).

http://dx.doi.org/10.1016/j.jconrel.2014.11.016
0168-3659/

transformed human corneal epithelial cells, primary human corneal epithelial cells [19] and primary monkey lacrimal acinar cells [15] that had been stressed with the inflammatory cytokines interferon-γ and tumor necrosis factor. Interestingly, Lacrt displays growth factor-like behavior; however, its specificity for target cells of the ocular surface system results from a unique 'off–on' switch controlled by heparanase deglycanation of the cell surface protein, syndecan-1 [20], which both exposes and generates a Lacrt binding site [21] as a prerequisite for mitogenic signaling. Confirmed by 2-D electrophoresis, mass spectrometry and surface-enhanced laser desorption/ionization studies, Lacrt [22] is down regulated in blepharitis (chronic inflammation of the eyelid) vs. normal tears [23], and most aqueous deficient dry eye [24]. Whether down regulation of Lacrt provokes disease is a key unresolved question, but its prosecretory and corneal mitogenic activity suggest that it might have activity as a protein therapeutic for ocular surface diseases.

Great strides have been made to improve the bioavailability and simplify the administration of existing drugs, which include depot formulations that deliver short peptides such as leuprolide and bioadhesive polymers used in buccal drug-delivery systems [25]. Recently, stimuli-responsive polypeptides have emerged as an attractive controlled release strategy. One such type of biomaterial is the elastin-like-polypeptide (ELP) [26]. Biologically inspired from human tropoelastin, ELPs are composed of a pentapeptide repeat $(VPGXG)_n$, where the 'guest residue' *X* can be any amino acid and *n* determines molecular weight. One unique property of ELPs is their inverse phase transition temperature behavior. ELPs are soluble in aqueous solutions below their transition temperature (T_t) and self-assemble into various-sized particles above T_t [27]. T_t can be precisely modulated by adjusting the number of pentapeptide repeats, *n*, and the hydrophobicity of the guest residue, *X*, which can determine whether the ELP remains a soluble macromolecular drug carrier [28], assembles a nanoparticle [29], or phase separates into micron-sized coacervates [30] at physiological temperatures. With their distinctive thermo-responsive, elastic, and biocompatible properties, ELPs have impacted fields such as protein purification [31], stimuli responsive hydrogels [32], tissue engineering [33,34], and targeted cancer treatment [35,36]. Yet, the application of ELPs in ophthalmology has just started [37,38].

To explore the concept of a thermo-responsive drug reservoir as a potential novel treatment for DED [7], we generated a novel Lacrt–ELP fusion with T_t below physiological temperature. The construct exhibits thermo-responsiveness of the parent ELPs while retaining prosecretory efficacy of native Lacrt, as demonstrated by its ability to stimulate dose-dependent β-hexosaminidase secretion from primary rabbit lacrimal gland acinar cells (LGACs). Moreover, the Lacrt–ELP fusion enhanced tear secretion from the non-obese diabetic (NOD) mouse model of autoimmune dacryoadenitis when given via intra-lacrimal injection. This treatment formed a depot that lasted over 24 h inside the LG, which was confirmed by confocal laser scanning microscopy. Finally, we captured the intracellular trafficking and transcytosis of exogenous Lacrt in LGACs using time-lapse confocal fluorescence microscopy, which was prolonged by fusion to the ELP. These findings support the potential enhancement of Lacrt therapeutics via the linkage to a thermo-responsive ELP, which may have broader implications in the treatment of DED.

2. Material and methods

2.1. Animals

In vitro studies were conducted using LG from Female New Zealand White rabbits (2.2–2.5 kg) obtained from Irish Farms (Norco, CA). *In vivo* studies were conducted using LG isolated from 12-week old male/female C57BL/6 (Jackson Labs, Bar Harbor/ME, USA) or in house bred non-obese diabetic (NOD) (Taconic Farms, Germantown/NY, USA) mice. All procedures performed were in accordance to the university approved IACUC protocol.

2.2. Instruments and reagents

Terrific broth dry powder growth medium was purchased from MO BIO Laboratories, Inc. (Carlsbad, CA). Isopropyl β-D-1-thiogalactopyranoside, OmniPur*. 99.0% min. was purchased from VWR (Visalia, CA). Amicon Ultra concentrators were purchased from Millipore (Billerica, MA). Thrombin CleanCleave™ Kit, carbachol (CCh) and insulin–transferrin–sodium selenite media supplement were purchased from Sigma-Aldrich (St. Louis, MO). 4–20% Tris-Glycine PAGEr gels were purchased from LONZA (Allendale, NJ). Cell culture reagents were from Life-Technologies (Carlsbad, CA). Peter's Complete Medium (PCM) consisted of 50% Ham's F-12 plus 50% DME (low glucose) supplemented with penicillin (100 U/ml), streptomycin (0.1 mg/ml), glutamine (4 mM), hydrocortisone (5 nM), transferrin (5 μg/ml), insulin (5 μg/ml), butyrate (2 mM), linoleic acid (0.084 mg/l), carbachol (1 μM), laminin (5 mg/l) and insulin–transferrin–sodium selenite (ITS) media supplement (5 μg/ml).

2.3. Biosynthesis of Lacrt–ELP fusions

A sequence encoding human Lacrt without a secretion signal peptide was designed using the best *Escherichia coli* codons in EditSeq (DNAStar Lasergene, WI) [39]. A thrombin cleavage site was encoded between the Lacrt sequence and ELP tag via insertion at the *BseRI* site. A custom gene flanked by *NdeI* and *BamHI* restriction digestions sites at the 5′ and 3′ ends was purchased in the pIDTSmart-KAN vector from Integrated DNA Technologies (IDT) as follows:

5′-**CATATG**GAAGACGCTTCTTCTGACTCTACCGGTGCTGACCCGGCTC
AGGAAGCTGGTACCTCTAAACCGAACGAAGAAATCTCTGGTCCGGCTG
AACCGGCTTCTCCGCCGGAAACCACCACCACCGCTCAGGAAACCTCTG
CTGCTGCTGTTCAGGGTACCGCTAAAGTTACCTCTTCTCGTCAGGAAC
TGAACCCGCTGAAATCTATCGTTGAAAAATCTATCCTGCTGACCGAAC
AGGCTCTGGCTAAAGCTGGTAAAGGTATGCACGGTGGTGTTCCGGGTG
GTAAACAGTTCATCGAAAACGGTTCTGAATTCGCTCAGAAACTGCTGA
AAAAATTCTCTCTGCTGAAACCGTGGGCTGGTCTGGTTCCGCGTGGTT
CTGGTTACTGATCTCCTC**GGATCC**-3′.

The gene encoding for V96 was synthesized by recursive directional ligation in a modified pET25b(+) vector as previously reported [40,41]. The Lacrt-thrombin gene was subcloned into the pET25b(+) vector between the *NdeI* and *BamHI* sites. LV96 gene fusions were synthesized by ligation of a gene encoding for the ELP V96 via the *BseRI* restriction site, resulting in placement of the thrombin cleavage site between Lacrt and ELP. Correct cloning of the fusion protein gene was confirmed by DNA sequencing. The amino acid sequences of ELPs used in this study are described in Table 1.

2.4. Expression and purification of Lacrt ELP fusion protein

Plain ELP V96 and the Lacrt fusion LV96 were expressed in BLR (DE3) *E. coli* (Novagen Inc., Milwaukee, WI). Briefly, V96 was expressed for 24 h in an orbital shaker at 37 °C at 250 rpm. For LV96, 500 μM Isopropyl β-D-1-thiogalactopyranoside (IPTG) was added to the culture when the OD 600 nm reached 0.5, at which point the temperature was decreased to 25 °C for protein expression for 3 h. Cell cultures were harvested and re-suspended in phosphate buffer saline (PBS). Proteins were purified from the clarified cell supernatant by inverse transition cycling [39] until ELP purity was determined to be approximately 99% by SDS-PAGE stained with $CuCl_2$. Due to partial proteolysis of LV96 during biosynthesis, fusion proteins were further purified to homogeneity using a Superose 6 (GE Healthcare Bio-Sciences, Piscataway, NJ) size exclusion column at 4 °C. After equilibration with PBS (pH 7.4), 10 mg LV96 was loaded onto the column and washed out by isocratic flow of PBS at 0.5 ml/min. P1, representing LV96 (Supplementary Fig. S1), was collected and concentrated using an Amicon Ultra

Table 1
Nomenclature, amino acid sequence, and phase behavior of expressed proteins.

Protein label	Amino acid sequence[a]	M.W.		Phase behavior[b]	
		Exp[c] [kDa]	Obs[d] [kDa]	Intercept, b [°C]	Slope, m[°C] $[Log_{10}(\mu M)]^{-1}$
V96	$G(VPGVG)_{96}Y$	39.6	39.5	36.1	3.25
LV96	GEDASSDSTGADPAQEAGTSKPNEEISGPAEPASPPETTTTAQETSAAAVQGTAKVTSSRQELNPLKSIVE KSILLTEQALAKAGKGMHGGVPGGKQFIENGSEFAQKLLKKFSLLKPWAGLVPRGSG$(VPGVG)_{96}Y$	52.5	52.3	28.6	1.19
Lacrt	GEDASSDSTGADPAQEAGTSKPNEEISGPAEPASPPETTTTAQETSAAAVQGTAKVTSSRQELNPLKSIVE KSILLTEQALAKAGKGMHGGVPGGKQFIENGSEFAQKLLKKFSLLKPWAGLVPR	12.8	12.7	NA	NA

Not applicable (NA).
[a] After the start codon, a glycine spacer was added during cloning, which is not present on human Lacrt.
[b] ELPs in PBS phase separate above a line with slope m and intercept b as defined by Eq. (1).
[c] Expected M.W. was estimated for each sequence, which excludes the methionine start codon.
[d] Observed M.W. was measured by MALDI-TOF.

concentrator (10 kD). When desired, free Lacrt was released by thrombin cleavage of LV96 fusion protein. Briefly, 300 μl of thrombin bead slurry (Sigma-Aldrich) was added to 200 mg of purified LV96 and incubated at room temperature for 3 h. After pelleting the thrombin beads at 250 rpm, the solution was warmed up to 37 °C and centrifuged at 4000 rpm for 10 min to remove ELP coacervates. The supernatant was then concentrated using an Amicon Ultra concentrator with a 3 kD M.W. cut-off (MWCO). Protein concentrations were determined by UV–VIS spectroscopy at 280 nm ($\varepsilon_{ELP} = 1285\ M^{-1}\ cm^{-1}$, $\varepsilon_{LV96} = 6990\ M^{-1}\ cm^{-1}$, $\varepsilon_{Lacrt} = 5500\ M^{-1}\ cm^{-1}$). Protein molecular weight was further confirmed by MALDI-TOF mass spectrometry (AXIMA Assurance, Shimadzu).

2.5. Thermal characterization of Lacrt ELP fusion proteins

Self-assembly of purified V96 and LV96 fusion proteins was characterized by optical density using a DU800 UV–VIS spectrophotometer outfitted with the High Performance Transport and Peltier Temperature-Controlled Cell Holder (Beckman Coulter, Brea, CA). Consistent with previous reports [27,28,36], optical density was measured at 350 nm as a function of temperature, a wavelength at which LV96 and V96 contribute little absorption. ELPs (5 to 100 μM) were observed in PBS under a temperature gradient of 1 °C/min (10 to 45 °C). The cuvette provides minimal insulation between the sample and the cell holder. At this slow temperature gradient, the sample and cell holder are engineered to remain in close agreement to avoid over or under heating. The inverse transition temperature (T_t) of each solution was defined as the temperature at which the first derivative of the optical density with respect to the temperature reached a maximum. The ELP transition temperature has been observed as a function of concentration as follows:

$$T_t = b - m\mathrm{Log}_{10}[C_{ELP}] \quad (1)$$

where b is the intercept at a concentration of 1 μM ELP, m is the slope, and C_{ELP} is the ELP concentration. Eq. (1) was fit to data obtained for V96 and LV96 (Table 1).

2.6. Dynamic light scattering

To characterize the assembly process of LV96 coacervates, the hydrodynamic radius (R_h) was monitored as a function of temperature. Samples were suspended (25 μM) in PBS and were filtered through Whatman Anotop 10 syringe filters with a pore size of 0.02 μm (GE Healthcare Bio-Sciences, Piscataway, NJ) at 4 °C. Light scattering data were collected at regular temperature intervals (1 °C) as solutions were heated from 5 to 60 °C using a DynaPro-LSR Plate Reader (Wyatt Technology, Santa Barbara, CA). The results were then analyzed using a Rayleigh sphere model.

2.7. Stability of Lacrt

To determine the cleavage half-life of Lacrt, the purified proteins (20 μg) were incubated in PBS at 37 °C for 72 h followed by SDS-PAGE analysis. Peptide sequence analysis was performed using MALDI-TOF (AXIMA Assurance, Shimadzu). Cleavage products were assigned by MALDI-TOF mass by comparison of measured with predicted mass to charge ratios (m/z) with +1 charge ionization ($[M + H]^+$). For Western blotting of purified Lacrt, 50 μg purified protein was loaded onto 4–20% Tris–HCl polyacrylamide gels; with blocking buffer at room temperature for 1 h and blotted with rabbit anti-N-terminal or anti-C-terminal (1:200) Lacrt antibody [42] overnight at 4 °C followed by blotting with IRDye800 Donkey anti-rabbit IgG (H + L) (Rockland) (1:3000) at room temperature for 1 h. Images were taken using the Odyssey infrared imaging system (Li-Cor, Lincoln, NE).

2.8. Cell isolation, culture and treatments

Isolation of primary cultured LGAC from female New Zealand white rabbits was performed in accordance with the Guiding Principles for Use of Animals in Research. Specifically, LGACs were isolated from rabbit LGAC and cultured by the method of da Costa [43] in Peter's Complete Medium (PCM) medium for 2–3 days.

2.9. Secretion of β-hexosaminidase

Fresh PCM medium was added to wells containing LGAC and incubations were continued for an additional 2 h. Baseline samples were then taken from each well, and the cells were stimulated with 100 μM carbachol (CCh), Lacrt, V96, or LV96 at various concentrations as indicated for 1 h. After stimulation, the cell supernatant was collected and β-hexosaminidase activity in each aliquot was measured against a model substrate, methylumbelliferyl-N-acetyl-β-D-glucosaminide. Assays of catalytic activity were performed in 96-well plates, and reaction product absorbance was determined with a plate reader at 460 nm (Tecan Genios Plus; Phenix Research Products, Candler, NC); signals were analyzed with the manufacturer's software package (Magellan v6.6; Phenix Research Products). Medium was then aspirated from all wells and 500 μl 0.5 M NaOH was added into each well and incubated at 4 °C for overnight to lyse the acini and solubilize all protein. Total protein in each well was measured by the bicinchoninic acid assay (BCA) assay using a bovine serum albumin standard curve. Secreted β-hexosaminidase level was expressed as ΔOD465 nm (post–pre)/μg total protein. Each treatment was performed in triplicate and these assays were repeated 3 times. The secretion was normalized to the secretion induced by CCh as follows:

$$\beta\mathrm{hex}_{\mathrm{Secretion}} = \frac{\beta\mathrm{hex}_{\mathrm{Treatment}} - \beta\mathrm{hex}_{\mathrm{CCh-}}}{\beta\mathrm{hex}_{\mathrm{CCh+}} - \beta\mathrm{hex}_{\mathrm{CCh-}}} 100\% \quad (2)$$

where $\beta hex_{Treatment}$ is the sample activity, βhex_{CCh-} is the activity released in the absence of stimulation, and βhex_{CCh+} is the activity released upon stimulation with CCh.

2.10. Live cell imaging of actin remodeling

LifeAct-RFP adenovirus was generated as described previously [44]. For amplification, QB1 cells, a derivative of HEK293 cells, were infected with the virus and grown at 37 °C and 5% CO_2 in Dulbecco's Modified Eagle's Medium (DMEM, high glucose) containing 10% fetal bovine serum for 66 h until completely detached from the flask surface. The Adeno-X™ virus purification kit (Clontech, CA) was used for virus purification and the Adeno-X™ rapid titer kit for viral titration. LGACs were transduced at a multiplicity of infection of 8–10 for 2 h at 37 °C and then rinsed and cultured in fresh medium overnight to allow for protein expression. Live cell images upon Lacrt/LV96 stimulation were captured using a Zeiss LSM 510 Meta confocal fluorescence microscopy system.

2.11. Cellular uptake of Lacrt and Lacrt ELP fusion proteins

Lacrt, V96 and LV96 were conjugated with NHS-rhodamine (Thermo Fisher Scientific Inc, Rockford, IL) via covalent modification of the amino terminus. Conjugation was performed in 100 mM borate buffer (pH 8.0) for 2 h (LV96 and Lacrt) or overnight (V96) at 4 °C followed by desalting on a PD10 column (GE Healthcare Bio-Sciences, Piscataway, NJ) to remove free dye. Degree of labeling was estimated following the manufacturer's instructions as follows:

$$C_{rhodamine} = \frac{A_{555}}{\varepsilon_{rhodamine}} \quad (3)$$

$$C_{protein} = \frac{A_{280} - (A_{555} CF_{rhodamine})}{\varepsilon_{protein}} \quad (4)$$

where $\varepsilon_{rhodamine} = 80{,}000\ M^{-1}\ cm^{-1}$; $CF_{rhodamine} = 0.34$. Cellular uptake was studied on 35 mm glass coverslip-bottomed dishes. Briefly, after washing with warm fresh medium, LGACs were cultured in medium containing 10 μM of proteins conjugated with rhodamine. After incubation at 37 °C for different time points, the cells were rinsed three times with room temperature medium and images were acquired using confocal fluorescence microscopy. The washing step does not conserve coacervate particles, which are disrupted below 27 °C, but does enable the observation of their intracellular uptake and trafficking.

2.12. Intra-lacrimal administration, retention, and tear secretion in mice

For intra-lacrimal injection, mice were anesthetized with an i.p. injection of xylazine/ketamine (60–70 mg + 5 mg/kg), administered a subcutaneous injection of buprenorphine (0.02 mg/kg), and placed on a heating pad. After removing fur from the cheek and cleansing the area with alcohol, a small incision (5 mm) was made to visualize the LG. 5 μl of 50 μM carbachol (CCh), 100 μM LV96, 100 μM V96 or 100 μM Lacrt was injected into the LG using a 33 gauge blunt needle. The mice were monitored on the heating pad until fully recovered from anesthesia. For quantification of tear secretion, a glass capillary (Microcaps Drummond disposable micropipettes 2 μl) was placed on the lower eyelid of the mice to collect tears (2 LG/each mouse, 30 min/each gland). To evaluate protein retention in the LG after intra-lacrimal injection, the incision was closed with a 6.0 synthetic suture (MERSILENE® Polyester Fiber Suture, ETHICON). Mice were euthanized after different time points, and LG were processed in one of two ways: i) fixed in 4% paraformaldehyde and 4% sucrose in PBS for 2–3 h at room temperature followed by cryoprotection in 30% sucrose at 4 °C overnight before freezing the sample in O.C.T. for immunohistochemistry analysis; ii) fixed overnight in 10% neutral buffered formalin and transferred to 70% ethanol for paraffin-embedded histology and staining by hematoxylin and eosin.

2.13. Statistical analysis

All experiments were replicated at least three times. Values are expressed as the mean ± SD. For β-hexosaminidase secretion, data were analyzed using two-way ANOVA followed by the Bonferroni post-hoc analysis (GraphPad Prism). Within each experiment, each treatment was performed in triplicate and three independent experiments have been performed (n = 9). For LGAC uptake studies, treatments were performed in triplicate and three representative acini in each plate were evaluated (n = 9). Data were then analyzed using two-way ANOVA followed by Tukey's post-hoc test (GraphPad Prism). For mouse tear secretion studies, each treatment was performed on three mice and three independent experiments were performed (n = 9). The results were analyzed using one-way ANOVA followed by Tukey's post-hoc test (GraphPad Prism). To evaluate protein retention in the LG, each time point was repeated in three LGs and a representative image was shown. Three sections from each sample were imaged and quantified using ImageJ (n = 9). Data were then analyzed using two-way ANOVA followed by the Bonferroni post-hoc analysis (GraphPad Prism). A p value less than 0.05 was considered statistically significant.

3. Results

3.1. Construction and purification of a Lacrt ELP fusion protein

We designed the a gene encoding LV96 in the pET25b(+) vector resulting in the amino acid sequence shown in Table 1. V96 forms viscous coacervates with T_t below physiological temperatures of 37 °C [41] and thus was chosen as the ELP backbone for depot formation. LV96 was also used to generate free a Lacrt control protein utilizing selective cleavage of a thrombin cleavage site (Fig. 1A). In contrast to the previously reported intein system for Lacrt purification [14], LV96 fermentation yielded more than 40 mg/l using the inverse transition cycling purification approach followed by size exclusion chromatography at high purity (Fig. 1B). Interestingly, SDS-PAGE analysis of purified LV96 (Supplementary Fig. S1) suggested the spontaneous cleavage of ELP (V96) from the fusion construct, which yielded a combination of fusion protein and the ELP tag after purification. After optimization, a size exclusion chromatography was used to remove free ELP tags as a final purification step (Supplementary Fig. S1). Similar to previous reports [23], free Lacrt ran higher on SDS-PAGE than the expected M.W. of 12 kDa (Fig. 1B); however, its expected mass was confirmed by mass spectrometry (Table 1).

Optical density was used to characterize the phase behavior for all three constructs (Table 1), which revealed that only LV96 and V96 phase separate at physiological temperatures (Fig. 1C). The phase separation for LV96 was similarly confirmed using confocal microscopy and also dynamic light scattering (Supplementary Fig. S2) The LV96 phase transition curve at 25 μM (Fig. 1C) was consistent with the phase transition behavior of the parent V96 with an ~5 °C decrease. Further characterization of the concentration–temperature phase diagrams shows that LV96 is less dependent on concentration compared to V96 as fit by a log-linear regression line (Fig. 1D). Western blotting with antisera raised against the carboxy terminus of Lacrt (N-65) (Fig. 2A) further confirmed the successful production of Lacrt as a band that runs near 18 kDa [45]. To explore the stability of purified Lacrt, it was incubated for up to 2 days at physiological temperatures, which resulted in the appearance of major fragments (Fig. 2B), which were consistent with proteolysis at lysine residues (Table 2). At physiological temperatures, the cleavage half-life of disappearance for Lacrt is about one day (Fig. 2D); furthermore, this cleavage could be inhibited by a protease inhibitor cocktail (Supplementary Fig. S3). Despite this apparent biodegradation,

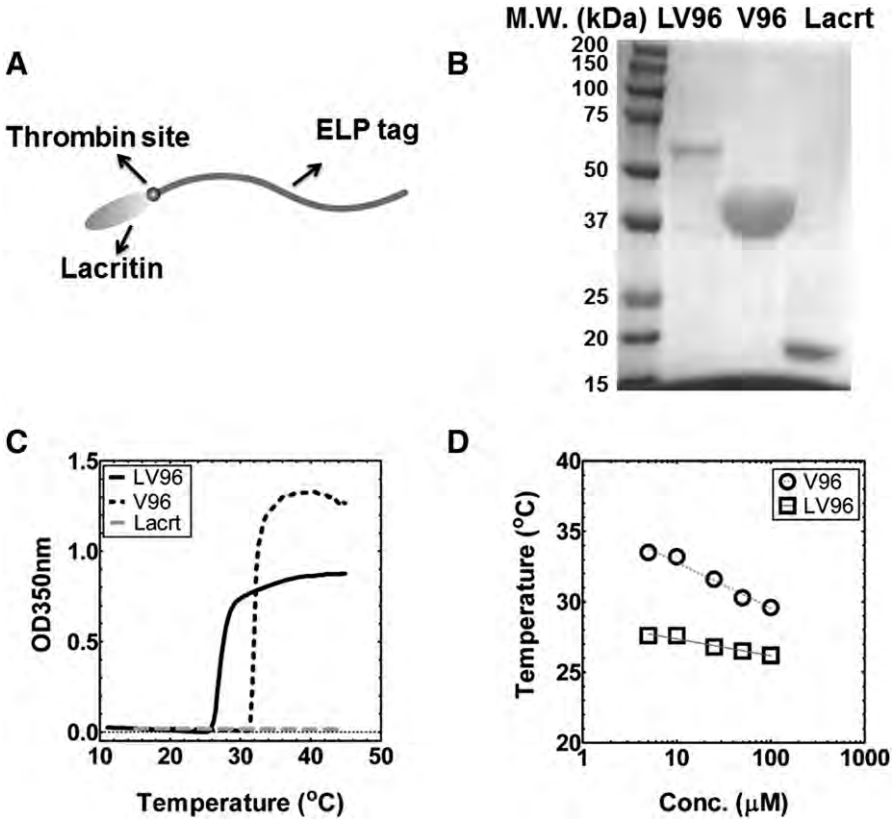

Fig. 1. Purification and thermal characterization of LV96. A) Cartoon of the LV96 fusion protein showing Lacrt at the N-terminus and an ELP tag at the C-terminus, with a thrombin recognition site between the two moieties. B) SDS-PAGE of purified LV96, ELP alone (V96) and free Lacrt. Gels were stained using $CuCl_2$. C) Representative optical density profiles for LV96, V96 and Lacrt at 25 μM as a function of temperature, which indicate a phase separation at 26.8 (LV96) and 31.6 °C (V96) respectively. Lacrt alone remains soluble, and does not increase optical density. D) A concentration temperature phase diagram was constructed. Best fit lines are indicated that follow Eq. (1) (Table 1).

by optimizing the purification strategy and maintaining proteins on ice, both Lacrt and LV96 were available at high purity and yields necessary for further study (Fig. 1B).

3.2. LV96 stimulates β-hexosaminidase secretion from primary rabbit LGACs

The concentration-dependent prosecretory activity of recombinant human Lacrt was first reported using freshly isolated rat lacrimal acinar cells with peroxidase as the marker of secretory activity [14]. Signaling was effective in cells exposed to 10 to 20 μM Lacrt as a coating solution and at 0.8 to 13 nM when presented as soluble Lacrt. The latter was confirmed in assays of several cultured human cell lines over a broad dose range [18]. Yet, Lacrt partially purified from monkey tears is apparently optimal at 1 μM. Further *in vivo* studies indicated that 0.8 to 8 μM Lacrt topically administered either as a single dose or chronically over two weeks elevated basal tearing of healthy New Zealand White adult female rabbits [46]. Rabbit LGACs do not secrete peroxidase; therefore, β-hexosaminidase secretion, an alternative secretory marker, was monitored from primary rabbit LGACs treated with a similar dose range for Lacrt or LV96 (Fig. 3). For all secretory studies, the small molecule carbachol (CCh) was used as a positive control. CCh acts on a broad spectrum of muscarinic and nicotinic acetylcholine GPCRs, including targets in the LG. This non-specificity makes CCh a poor therapeutic; however, as a positive control it can be used to assess maximal prosecretory capacity for the LG. With respect to no treatment or CCh, three treatment groups (Lacrt, LV96 and V96) were evaluated at four concentrations (0.1 to 20 μM) using a two-way ANOVA followed by Bonferroni post-hoc analysis (GraphPad Prism). Each treatment was performed in triplicate and three independent experiments were performed ($n = 9$). Compared to V96, the LV96 coacervate significantly stimulated secretion at a concentration of 10 μM ($p < 0.01$) and 20 μM ($p < 0.001$) while significant Lacrt-triggered stimulation was observed at 20 μM ($p < 0.05$) (Fig. 3B); the effects of either Lacrt or LV96 at 1 μM or 0.1 μM were not statistically significant. This data suggests that receptors exist on rabbit LGACs that respond to human Lacrt delivered by an ELP fusion.

In response to secretagogues, LGACs exocytose mature secretory vesicles containing tear proteins at their apical membranes for release into the acinar lumen, an event that involves F-actin remodeling around secretory vesicles at the luminal region [47]. Motivated to understand the cellular mechanisms of LGAC secretory activity in response to LV96, cellular morphology was tracked in live LGACs transduced with adenovirus Ad-LifeAct-RFP to observe changes in F-actin filament rearrangement at the apical and basolateral membranes during exocytosis (Fig. 3C). CCh acutely increased significant F-actin filament turnover and promoted transient actin coat assembly around apparent fusion intermediates within 10 min, as previously reported [47]. In contrast, LV96 exhibited a slower and sustained effect on F-actin remodeling, which triggered increased irregularity in the actin filaments around the lumen and formation of actin-coated structures beneath apical membranes (white arrows) after 26 min. No significant remodeling of actin filaments was observed in the V96 control group. This data confirms that LV96, even when incubated above its phase transition temperature, induces F-actin remodeling in rabbit LGACs, which is consistent with their secretion of β-hexosaminidase (Fig. 3B).

3.3. Fusion with V96 influences cellular uptake of exogenous Lacrt into LGACs

Secreted by LGAC, transported via ducts and deposited onto rapidly renewing ocular surface epithelia, Lacrt is thought to be preferentially

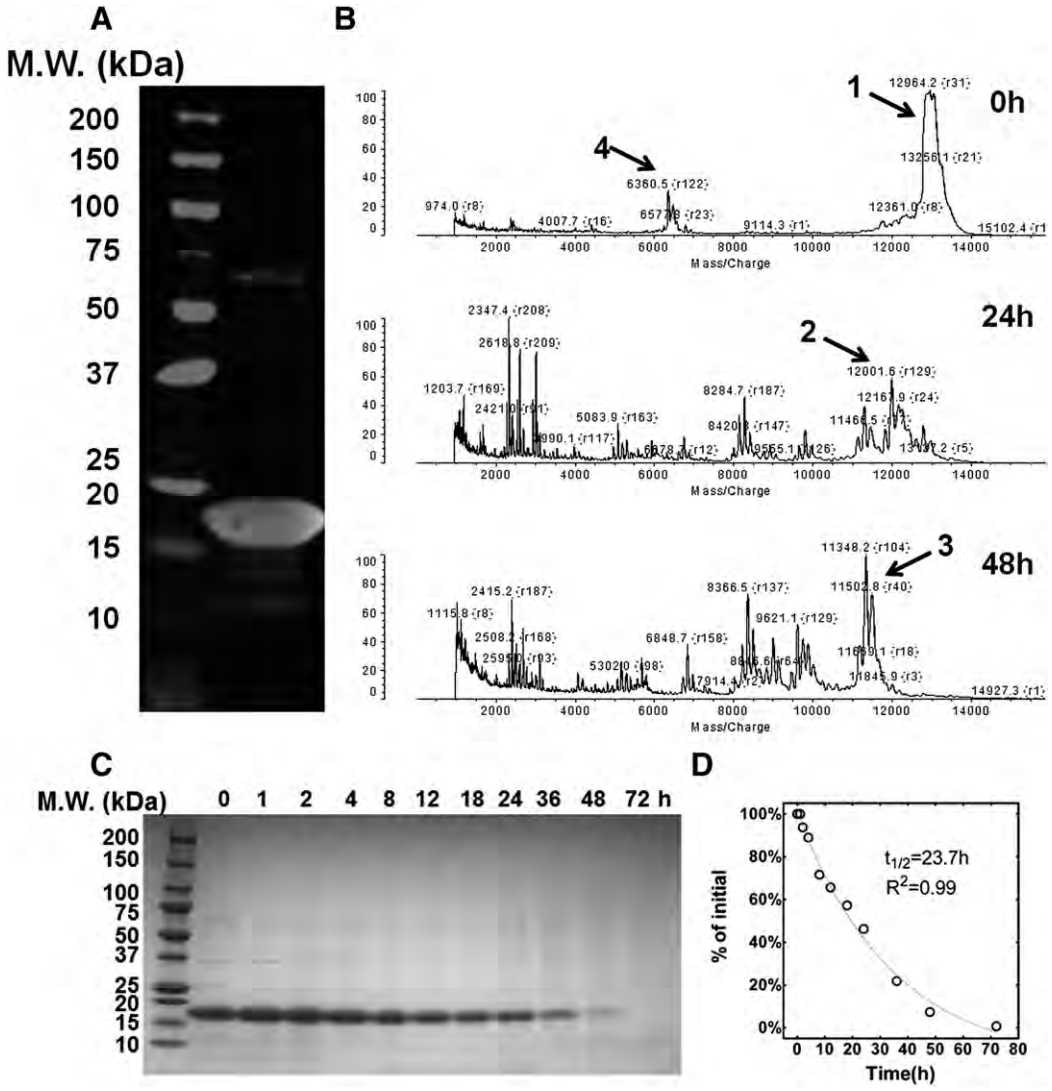

Fig. 2. Purified lacritin is susceptible to proteolysis of an unidentified origin. A) Western blot of purified Lacrt probed with an anti-Lacrt antibody (raised against Lacrt lacking 65 amino acids at the amino terminus) revealed a major band around 18 kDa, which is consistent with that observed previously for purified Lacrt. B) MALDI-TOF analysis of Lacrt revealed the appearance of major lower molecular weight fragments (Table 2) upon incubation at 37 °C in PBS. C) Time dependent disappearance of the purified Lacrt band by was tracked by SDS-PAGE stained with Coomassie blue. D) Lacrt disappearance was quantified and fitted to a single exponential decay model, which yielded a half-life of 23.7 h ($R^2 = 0.99$).

mitogenic or prosecretory for the cell types that it normally contacts during its glandular outward flow, such as the corneal, limbal and conjunctival epithelial cells, meibomian and LG epithelium, retina, and retinal pigmented epithelium/choroid [48]. Yet, no previous studies have captured the real-time binding and transport of Lacrt in live cells. Herein, live-cell confocal microscopy was used to document the time-dependent uptake of exogenous Lacrt and LV96 in rabbit LGACs (Fig. 4). Binding of native Lacrt to the basolateral membrane of LGAC was observed from 10 min of exposure (Fig. 4A). Significant levels of fluorescent puncta were observed in the cytosol after 30 min. Interestingly, there was an increase in accumulation in the apical lumen (white *), which suggests possible transcytosis of Lacrt from the basolateral to the apical membranes in LGACs. Similarly, LV96 was observed in intracellular puncta within LGACs, while LV96 treated cells showed lower levels of basolateral staining than Lacrt (Fig. 4B). The unmodified ELP, V96, did not undergo significant internalization into these

Table 2
Representative Lacritin cleavage sequences identified by MALDI-TOF.

Fragment	Amino acid sequence[a]	Exp. M.W.[b] [kDa]	Obs. M.W.[c] [kDa]
1	GEDASSDSTGADPAQEAGTSKPNEEISGPAEPASPPETTTTAQETSAAAVQGTAKVTSSRQELN PLKSIVEKSILLTEQALAKAGKGMHGGVPGGKQFIENGSEFAQKLLKKFSLLKPWAGLVPR	12.84	12.96
2	GEDASSDSTGADPAQEAGTSKPNEEISGPAEPASPPETTTTAQETSAAAVQGTAKVTSSRQELN PLKSIVEKSILLTEQALAKAGKGMHGGVPGGKQFIENGSEFAQKLLKKFSLLK	11.84/11.97	12.00
3	GEDASSDSTGADPAQEAGTSKPNEEISGPAEPASPPETTTTAQETSAAAVQGTAKVTSSRQELN PLKSIVEKSILLTEQALAKAGKGMHGGVPGGKQFIENGSEFAQKLLKK	11.25/11.38	11.35/11.47/11.50
4	PNEEISGPAEPASPPETTTTAQETSAAAVQGTAKVTSSRQELNPLKSIVEKSILLTEQALAK	6.42	6.36

[a] Underlined sequence: Syndecan-1 binding site.
[b] Expected M.W. (kDa) for fragments was calculated by DNAStar Lasergene Editseq.
[c] Observed M.W. (kDa) was measured by MALDI-TOF.

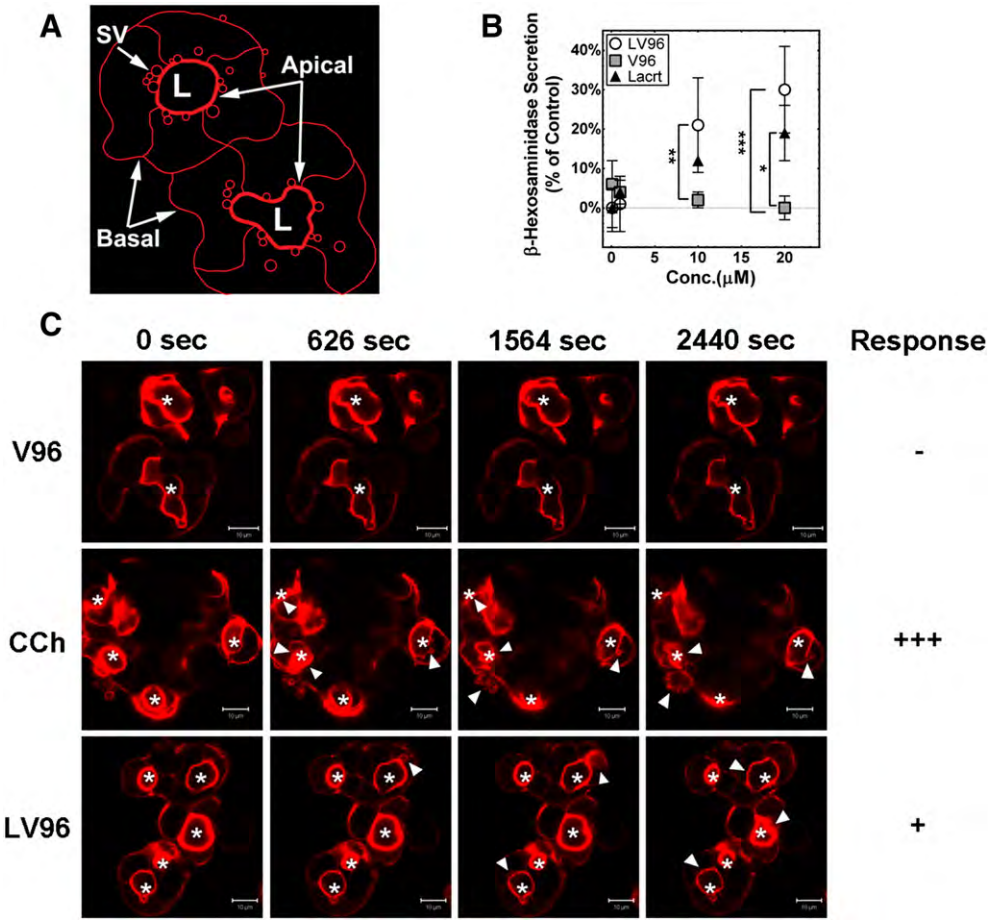

Fig. 3. Lacrt–ELP fusion proteins are prosecretory in LGACs. A) A cartoon depicts structure for *ex vivo* clusters of LGACs obtained from rabbits. These primary cultures form an apical lumen (L) that is bounded by a thick network of actin filaments. SV: secretory vesicles. B) Rabbit secretory vesicles (SV) release β-hexosaminidase in a dose dependent manner in response to secretagogues. The percentage of cellular secretion for each treatment (Eq. (2)) has been normalized to a positive control defined by CCh-stimulation, which is defined as 100%. LGACs were treated with 0.1 to 20 μM of LV96, Lacrt, V96, or no treatment for 1 h at 37 °C. 10 and 20 μM LV96 significantly enhanced secretion compared to the V96 group (**$p < 0.01$), and a similar effect was found with 20 μM Lacrt (*$p < 0.05$). Data were shown as mean ± S.D. and analyzed by ANOVA followed by Bonferroni's post-hoc test. C) Live-cell confocal microscopy was performed using LGACs labeled for F-actin (red). Actin-RFP is enriched beneath the apical membrane surrounding the lumen. Shortly after 10 min, increased irregularity of apical actin filaments and actin-coated secretory vesicle (SV) formation beneath the apical membrane (white arrows) were observed in CCh treated cells (100 μM). Similarly LV96 (20 μM) induced time-dependent actin remodeling after 26 min, which increased the irregularity of apical actin filaments and formation of secretory vesicles (white arrows). No significant remodeling of actin filaments was observed in a V96 treated control group. Apical lumen are indicated (white *). Scale bar: 10 μm.

cells (Fig. 4C). This fluorescent signal was quantified using image analysis and analyzed using a two-way ANOVA followed by Tukey's Post-hoc test (GraphPad Prism). At 10 min, both Lacrt and LV96 exhibited higher cellular uptake than V96. After 30 min, Lacrt underwent significantly higher uptake into LGACs (****$p < 0.0001$) than LV96 (Fig. 4D). After 2 h accumulation of Lacrt and LV96 in the acini was similar, although red puncta were slightly more prevalent in the Lacrt treated cells. The lower intracellular accumulation relative to free Lacrt is possibly caused by its phase separation, which could delay endocytosis [20].

3.4. LV96 stimulates tear secretion from non-obese diabetic (NOD) mice

To explore Lacrt's efficacy as a secretagogue in a murine model, Lacrt and LV96 were administered into non-obese diabetic (NOD) mice via intra-lacrimal injection and assessed for tear secretion (Fig. 5A). NOD mice have been established as a model for type-1 insulin-dependent diabetes mellitus [49] and one of the most utilized models for the study of DED symptomatic of Sjögren's syndrome [50–52], which is characterized by reduced production of aqueous tears [53] and autoimmune infiltration of LGs and salivary tissues [54]. Paradoxically, although Sjögren's syndrome is more prevalent in female patients, the 10–12 week male NOD mice feature earlier symptoms of autoimmune inflammation in LG, including severe lymphocytic infiltration (Fig. 5C), decreased production of lacrimal fluid, significant extracellular matrix degradation and increased expression of matrix metalloproteinases [55]. At 10–12 weeks of age female NOD mice maintain normal LG morphology (Fig. 5D); however, they do develop severe pathology in salivary tissues [54].

Using 10–12 week old NOD mice, four treatments were compared in an acute tear secretion study: CCh, V96, LV96 and Lacrt. Within each experiment, treatments were performed on three mice, and this experiment was repeated three times ($n = 9$). In each mouse, both LGs were treated. The tears were collected for 30 min from each eye and pooled to obtain the volume secreted per mouse. Results were then analyzed using a one-way ANOVA followed by Tukey's post-hoc test (GraphPad Prism). Immunohistochemistry revealed that intra-lacrimal injection of LV96 generates a local depot that is positive for human Lacrt immediately after injection (Fig. 5B). This depot was independently observed following intra-lacrimal injection into healthy mice, which revealed significantly more staining for LV96 than for free Lacrt (Supplementary Fig. S4). In normal mice, there was a small increase in tear volume for LV96 compared to the negative control V96; however, it was not significant (Supplementary Fig. S4). In contrast, for the NOD disease model LV96 and free Lacrt produced strong prosecretory activity in both

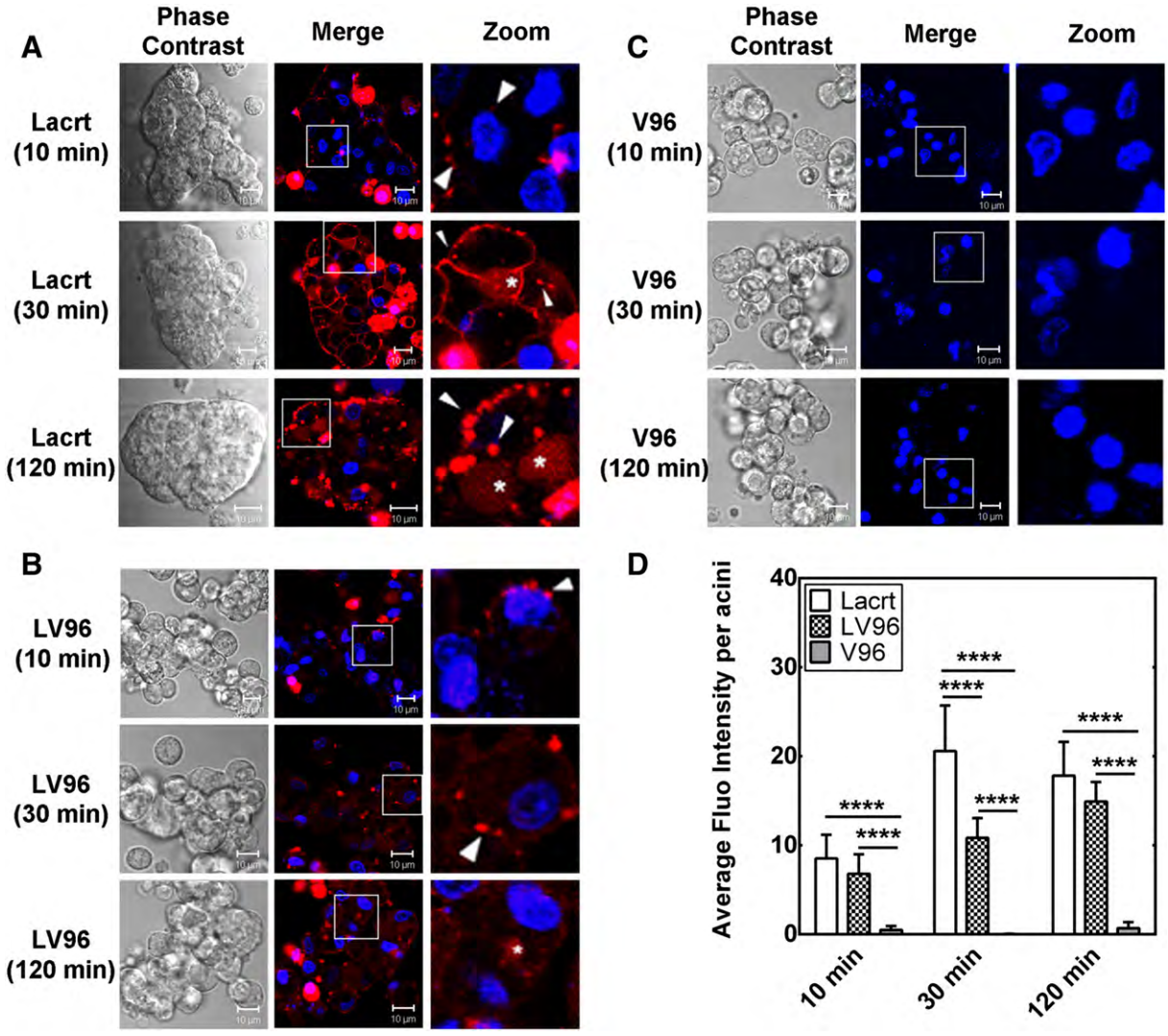

Fig. 4. Fusion with V96 influences uptake of exogenous Lacrt into LGACs. A) Time-dependent uptake of rhodamine-labeled Lacrt into rabbit LGACs was assessed by live-cell confocal microscopy. After 30 min, significant numbers of fluorescent puncta were detected in the cytosol proximal to the basolateral membrane (white arrow). More diffuse staining was observed within the lumen encircled by the apical membrane (white *), which suggest possible transcytosis. After 2 h, basolateral binding became less uniformly distributed. B) Time-dependent uptake of LV96 revealed a less intense labeling pattern at the basolateral membranes; however, there were significant levels of intracellular puncta (white arrows). Diffuse accumulation was detected in the apical lumen by 2 h (white *), although this effect was less pronounced than for free Lacrt. C) A negative control V96 did not show significant uptake into LGACs. Scale bar: 10 μm. D) Lacrt, LV96 and V96 intensity in LGACs was quantified at three time points. Both Lacrt and LV96 exhibited significantly (****$p < 0.0001$) higher uptake than V96. Lacrt entered LGACs to a greater extent than LV96, most obviously at 30 min (****$p < 0.0001$). Data were analyzed by a two-way ANOVA followed by Tukey's post-hoc test ($n = 9$).

males and females (Fig. 5E, F). Compared to CCh stimulation (100%), LV96's prosecretory effect was 40.9% in males and 50.0% in females, both significantly higher than V96 treatment ($p < 0.01$). Lacrt's efficacy was 29.6% in males and 42.9% in females. This data confirms the surprising *in vitro* finding (Fig. 3) that the phase separation of LV96 does not inhibit Lacrt-specific activity. Due to the acute nature of this assay, it was not expected that LV96 would produce a greater tear volume than free Lacrt.

To differentiate the *in vivo* potential of LV96 and free Lacrt, it was necessary to follow the LG up to a day after intra-lacrimal injection. In humans, the inferior palpebral lobe of the lacrimal gland is accessible for injection beneath the eyelid, which makes it a clinically relevant location for sustained release formulations. Unfortunately, in a murine model injection of the lacrimal gland requires surgical exposure of the injection site. This invasive procedure near the eye makes it challenging to attribute differences in basal tear production to the formulations. Therefore, to obtain evidence supporting the sustained retention of LV96, as compared to free Lacrt, the LG biodistributions of rhodamine labeled LV96 and Lacrt were assessed as a function of time at 2, 4, and 24 h after intra-LG injection (Fig. 6). Typically, eight slices (thickness: 8 μm/slice) of each sample with an interval of 80 μm were imaged to reflect the protein distribution in the whole LG. Each treatment and time point has been repeated in three independent LGs. Fluorescence intensity of the entire view or within a defined area was quantified using ImageJ. As shown in Figs. 6, 2 h after implantation LV96 remained in a deposit at the site of injection, which was more intense compared to Lacrt alone (Fig. 6A, B). This effect was quantified by image analysis (Fig. 6C). After 24 h LV96 coacervates remained obvious and showed little decrease in fluorescent intensity. In contrast, signal from free Lacrt was undetectable after 2 h (Fig. 6C). In addition, the depot maintains significant signal both at the center of the injection and also at a reference point taken 300 μm away (Fig. 6D, E). Between 4 and 24 h the intensity taken at the reference point changed minimally, which suggests the possibility that fluorescent LV96 is being released from the depot. In contrast, free Lacrt was not observed anywhere within the gland at 4 or 24 h.

4. Discussion

The eye is now a frequent target for development of new drugs, especially novel biological therapies [56] due to the increased numbers of

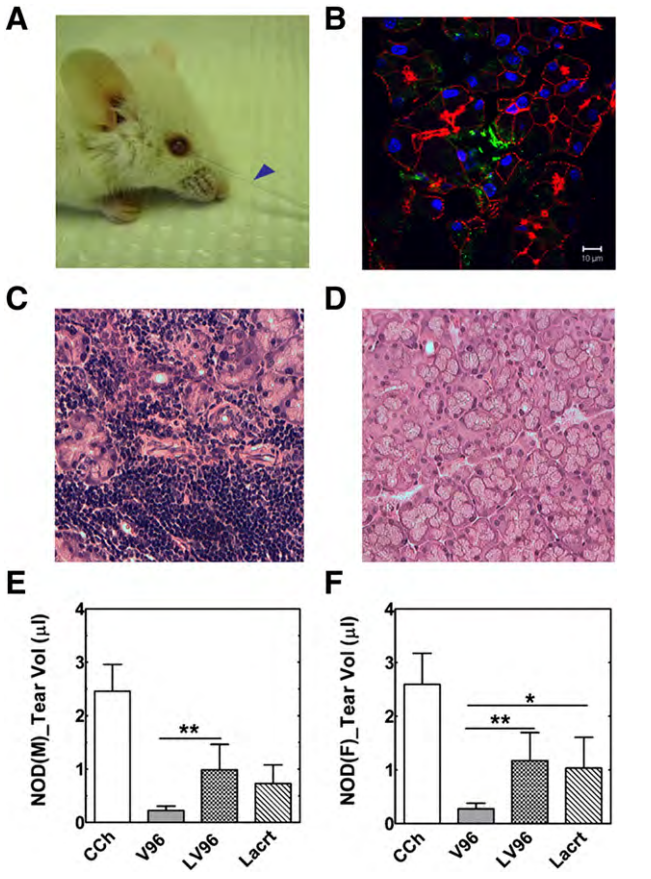

Fig. 5. Lacrt–ELP fusion proteins stimulate tear secretion in NOD mice. A) Representative pictures showing tear secretion stimulated by 100 μM LV96 (5 μl) after an intra-lacrimal injection in a male NOD mouse. Blue arrow: collected tear volume after 30 min. B) Lacrimal glands injected with LV96 were collected after infusion and visualized using immunofluorescence to identify Lacrt by an anti-C terminus Lacrt antibody. Green: anti-Lacrt antibody; Red: actin stained using Rho-phalloidin; Blue: nucleus stained by DAPI. Scale bar: 10 μm. C–D) Representative H&E staining images of NOD mouse lacrimal glands. C) Severe lymphocytic infiltration was observed in male NOD mice LG. D) Female NOD mice exhibited normal morphology. E–F) Tear volume quantification showing significant enhancement of tear secretion by LV96 and Lacrt compared to negative V96 controls ($^{**}p < 0.01$, $^{*}p < 0.05$, $n = 9$). Data are shown as mean ± S.D. and are compared by ANOVA followed by Tukey's Post Hoc Test. E) Male NOD mice; F) Female NOD mice.

patients with aging, ocular allergies and DED [57]. Local ocular delivery provides unique opportunities to enhance the therapeutic index of ophthalmic drugs by extending local residence time while minimizing off-target effects and dose frequency [58]. Over the past several decades, protein therapeutics have become highly successful because of their high target specificity, reduced interference with normal biological processes and minimal immune responses to human self-proteins [59]. The discovery of Lacrt offers a new therapeutic opportunity for DED and an alternative to conventional approaches [12]. Its basic structural features [12], prosecretory and mitogenic significance [14], as well as associated downstream signaling transduction mechanisms [18,20] have been gradually elucidated over the past decade.

As a proof of concept, this study characterizes a thermo-responsive Lacrt–ELP fusion protein for extended retention. The ELP V96 was fused to Lacrt to confer multiple functions: i) re-engineer Lacrt with the ability to form an intra-lacrimal depot at physiological temperatures; ii) to maintain Lacrt-mediated cell signaling. Together, these properties support the further development of Lacrt or other biologicals into sustained-release biopharmaceuticals for ophthalmology. The transition temperature (Fig. 1C, D) and thermo-responsive assembly of LV96 (Supplementary Fig. S2) supports the hypothesis that Lacrt fused to an ELP exhibits similar phase separation and self-assembly properties relative to the parent ELP. Significantly enhanced β-hexosaminidase secretion and actin remodeling from primary rabbit LGACs (Fig. 3) and increased tear secretion from both male and female NOD mice (Fig. 5) corroborated the prosecretory activity of LV96, even above its phase transition temperature. Despite having similar prosecretory activity, cellular internalization studies revealed a distinctly slower pattern of uptake for LV96 coacervates compared to free Lacrt (Fig. 4). Based on this assessment, the microbiodistribution of LV96 following intra-lacrimal administration was characterized via indirect immunofluorescence (Fig. 5B, Supplementary Fig. S4) and by covalent labeling (Fig. 6). These data definitively show that Lacrt fused to an ELP maintains significantly more fluorescence than free Lacrt at all times post-injection. In other disease models, it was recently shown that phase separation of ELPs in a tumor slowed the local half-life of clearance by more than an order of magnitude [60]. Similarly, extended control over blood glucose level was observed using a depot of a therapeutic ELP [61]. Thus, the ocular data presented here support the hypothesis that Lacrt fused to an ELP remains prosecretory both *in vitro* and *in vivo*; furthermore, its ability to form a local depot is consistent with previous literature in other disease models.

Interestingly, Lacrt demonstrated a susceptibility to protease degradation based on MALDI-TOF analysis (Fig. 2B) and time-dependent analysis of degradation by SDS-PAGE (Fig. 2C), which together suggest that native Lacrt has a cleavage half-life of about one day at 37 °C (Fig. 2D). The biodegradation of Lacrt was consistent with the generation of peptides that were cleaved between lysine residues found in human Lacrt (Table 2). Trypsin-like serine proteases cleave peptide bonds next to lysine or arginine residues, with serine performing the nucleophilic attack and negatively charged aspartic acid controlling the specificity [62–64]. *In silico* analysis by the Protease Specificity Prediction Server suggested Lacrt's serine protease sensitivity liberates the C-terminal amphipathic α-helix intact for downstream co-receptor binding to syndecan-1 (Table 2) [65]. Recent reports suggest that this proteolysis releases an α-helical carboxy terminal peptide from Lacrt that displays bactericidal activity, which may represent an innate defensive immunity on the ocular surface [66]. The cleavage may be regulated by serine proteases, as specific protease inhibitors (chymostatin, leupeptin) or boiling were reported to inhibit proteolysis. This report confirms that this proteolytic activity can be inhibited by a standard cocktail of protease inhibitors (Supplemental Fig. S3). This proteolysis was also observed for LV96 during purification (Supplemental Fig. S1). To maintain a single band by SDS-PAGE for purified LV96 (Fig. 1B), sample aliquots were frozen after purification and thawed on ice. Future studies are required to determine the source of this proteolysis, which may be attributed to either: i) trace proteases from bacterial fermentation; or ii) the possibility that Lacrt exhibits autolytic activation similar to trypsin [67]. In addition, the impact of glycosylation or other regulatory mechanisms to control the cleavage of native Lacrt remain to be determined.

Previously, Lacrt's *in vivo* prosecretory activity has been reported using New Zealand white rabbits via topical administration [16]. Recently, Vijmasi and coworkers tested Aire-knockout mice and proved that a long-term topical Lacrt treatment promoted tear secretion, restored ocular surface integrity, and reduced CD4+ T cell infiltration of the LG [17]. Aire-knockout mice are an aqueous-deficient dry eye mouse model that is deficient in the autoimmune regulator (Aire) gene. This model was derived from the non-obese diabetic (NOD) and Balb/c mice background. Here we found that the NOD mouse strain also was highly responsive to the effect of exogenous Lacrt (Fig. 5); furthermore these effects were significantly greater than those observed in a normal mouse (Supplementary Fig. S4). The disparities associated with the NOD disease mice and the C57BL/6 healthy mouse models suggest that features of aqueous tear deficiency may sensitize the diseased LG to therapy with Lacrt. Although the molecular mechanism for Lacrt's prosecretory signaling remains under study, its carboxy-terminus is

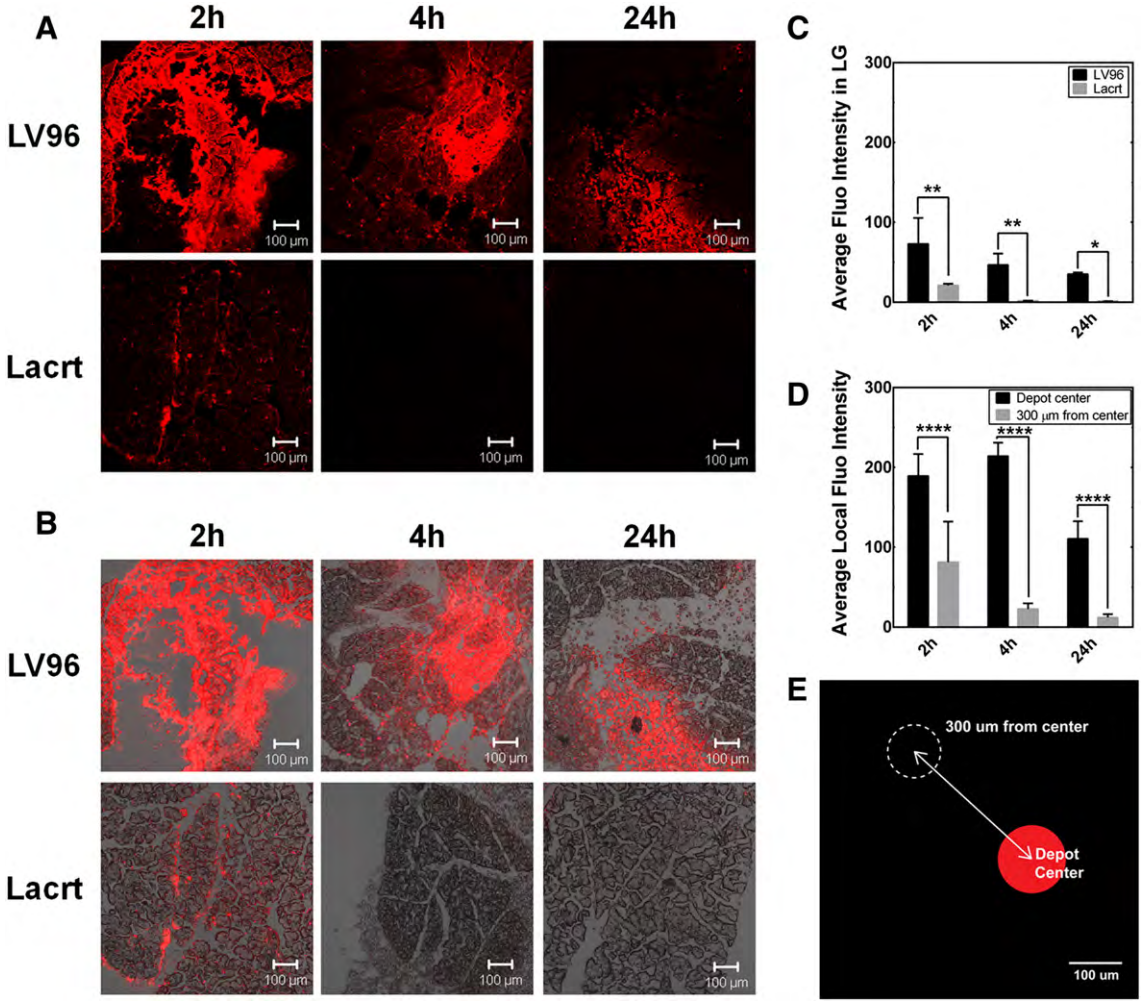

Fig. 6. Intra-lacrimal injection of Lacrt–ELP fusion protein produces a depot. A, B) Representative confocal images showing exogenous rhodamine-labeled LV96, which forms a depot in the LG of female C57BL/6 mice. LV96 was strongly retained over the 24 h time course, while free Lacrt was not observed after just 4 h. A) Rhodamine signal alone. B) Merged combinations of phase contrast and rhodamine signal. C) Quantification of average fluorescence intensity in the section of LG centered on the injection, which shows that LV96 is retained longer than free Lacrt (*$p < 0.05$, **$p < 0.01$). D & E) After injection, depots of LV96 maintained a lower concentration (**** < 0.0001) at a distance of 300 μm from the depot center; however, this fluorescence was greater than that detected either in surrounding or untreated acini. Scale bar: 100 μm.

known to bind specifically to heparanase activated syndecan-1 [20]. Vijmasi and coworkers hypothesized that via topical administration, Lacrt may play a functional role in maintaining corneal innervation during homeostasis, interrupting or mitigating the inflammatory cycle, and thus protecting the LG from focal infiltration of auto-antigen primed CD4+ T cells [17]. This report provides the first *in vivo* evidence of Lacrt's prosecretory effect upon direct interaction with the LG. Further investigations regarding syndecan-1 and heparanase expression level in different mice LGs, Lacrt's affinity towards receptors expressed in the LG, its neuronal stimulation mechanism and differences among various mice strains will be necessary to better understand the mechanism of Lacrt therapies.

Exhibiting prosecretory, mitogenic, cytoprotective and bactericidal functions, Lacrt may recruit different signaling pathways for each of these activities. For example, previous reports have explored intracellular Ca^{2+} changes in response to Lacrt, which is readily evident in the corneal epithelium [39]. Being an important early messenger in signal transduction cascades, Ca^{2+} can indicate different signals by changing its transient cytosolic oscillation frequency [68]. In the LG acinar cells, cholinergic agonists stimulate protein secretion by binding to receptors in the basolateral membrane of secretory cells and activating phospholipase C to break down phosphatidylinositol bisphosphate into 1,4,5-inositol trisphosphate (1,4,5-IP3) and diacylglycerol (DAG). 1,4,5-IP3 causes intracellular release of Ca^{2+}, which works together with calmodulin and further activates specific protein kinases that may be involved in secretion [69]. Interestingly, of all the treatment groups tested herein, only carbachol (CCh) triggered cytoplasmic Ca^{2+} concentration change in LGACs (Supplementary Fig. S5), while no significant signals were observed in EGF, Lacrt or LV96 treatment groups. Consistent with this observation, Sanghi and coworkers discussed a similar loss of Ca^{2+} activation in Lacrt's prosecretory activity pathway [14]. Although Lacrt and LV96 only exhibited 10–30% of the control CCh response in the β-hexosaminidase secretion assay (Fig. 3B), these findings are consistent with the possibility that Lacrt may recruit alternative pathways for its prosecretory function. While CCh acts on a broad spectrum of muscarinic acetylcholine G-protein coupled receptors (GPCRs) as well as nicotinic acetylcholine receptors (ligand-gated ion channels), Lacrt's signaling pathway may be more specific.

This specificity may be due to its involvement with deglycanated syndecan-1, which enables it to act on an as of yet unidentified GPCR [12]. The carboxy-terminal amphipathic α-helix of Lacrt has been reported to associate with co-receptor syndecan-1, which thus regulates functional specificity [20] and maintains corneal epithelium homeostasis [19]. New data suggested that the same region undergoes proteolytic processing and demonstrates crucial bactericidal activity in tears [66]. Similar to our recent reports in SV40-transduced human

corneal epithelial cells (HCE-Ts) [39], Lacrt triggers a cascade of mitogenic events involving Gαi or Gαo–PKCα-PLC–Ca^{2+}–calcineurin–NFATC1 and Gαi or Gαo–PKCα–PLC–phospholipase D (PLD)–mTOR pathways [18].

The concept of a 'reservoir drug' [70] is intended to tackle the problem of inefficient target delivery and rapid payload clearance. By modulating the precise location and residence time of the therapeutic agent, side effects (such as those produced by CCh) can be reduced and efficacy may be enhanced [71]. ELPs have shown promise as reservoir scaffolds [30,34], and now provide an emerging alternative to PLGA [72] or catechol-based gels [73]. Prior to this study, it was unclear if polymer modification and phase separation would sterically hinder Lacrt and thus impair its activity. Thus, we have now verified both *in vitro* and *in vivo* that LV96 is equivalent in potency to free Lacrt. Moreover, the phase separation of the V96 tag slows cellular uptake and promotes retention in the LG. Based on this report, and of those noted above for free Lacrt, we can propose a mechanism of action for an LV96 drug depot (Supplementary Fig. S6); however, additional studies will be required to confirm this model. Further study of Lacrt ELP fusions are require required that explore the local and systemic pharmacokinetics as well as the molecular mechanisms of Lacrt release, receptor-mediated binding, and cellular signaling involved with tear secretion.

5. Conclusion

Achieving sustained delivery of therapeutic proteins is one of the major challenges of ophthalmology. In pursuing this goal, ELPs were fused with the model dry eye disease biopharmaceutical, Lacrt. Lacrt–ELP fusion proteins demonstrated thermo-responsive phase separation, similar to that exhibited by the parent ELPs. They also gained the prosecretory activity of human Lacrt. ELP modification influenced cell uptake speed, enhanced local retention time in the LG, and provided Lacrt-mediated signaling. If successful, this approach may be useful to deliver a variety of proteins to ocular targets.

Acknowledgments

This study is supported by the USAMRMC/TATRC grant W81XWH1210538, NIH EY011386, and the USC Whittier foundation. The authors appreciate the excellent technical support of rabbit lacrimal gland acinar cells (LGACs) preparation by Hua Pei.

Appendix A. Supplementary data

Supplementary data to this article can be found online at http://dx.doi.org/10.1016/j.jconrel.2014.11.016.

References

[1] D.A. Dartt, Neural regulation of lacrimal gland secretory processes: relevance in dry eye diseases, Prog. Retin. Eye Res. 28 (2009) 155–177.
[2] G.W. Laurie, L.A. Olsakovsky, B.P. Conway, R.L. McKown, K. Kitagawa, J.J. Nichols, Dry eye and designer ophthalmics, Optom. Vis. Sci. 85 (2008) 643–652.
[3] N.J. Friedman, Impact of dry eye disease and treatment on quality of life, Curr. Opin. Ophthalmol. 21 (2010) 310–316.
[4] M.E. Stern, R.W. Beuerman, R.I. Fox, J.P. Gao, A.K. Mircheff, S.C. Pflugfelder, The pathology of dry eye: the interaction between the ocular surface and lacrimal glands, Cornea 17 (1998) 584–589.
[5] M.A. Javadi, S. Feizi, Dry eye syndrome, J. Ophthalmic Vis. Res. 6 (2011) 192–198.
[6] J. Qiao, X. Yan, Emerging treatment options for meibomian gland dysfunction, Clin. Ophthalmol. 7 (2013) 1797–1803.
[7] T. Kojima, Y. Matsumoto, O.M. Ibrahim, T.H. Wakamatsu, M. Dogru, K. Tsubota, Evaluation of a thermosensitive atelocollagen punctal plug treatment for dry eye disease, Am J. Ophthalmol. 157 (2014) 311–317 (e311).
[8] H.E. Kaufman, T.L. Steinemann, E. Lehman, H.W. Thompson, E.D. Varnell, J.T. Jacob-LaBarre, B.M. Gebhardt, Collagen-based drug delivery and artificial tears, J. Ocul. Pharmacol. 10 (1994) 17–27.
[9] R. Lu, R. Huang, K. Li, X. Zhang, H. Yang, Y. Quan, Q. Li, The influence of benign essential blepharospasm on dry eye disease and ocular inflammation, Am J. Ophthalmol. 157 (2014) 591–597 (e591–592).
[10] Y. Wei, N. Gadaria-Rathod, S. Epstein, P. Asbell, Tear cytokine profile as a noninvasive biomarker of inflammation for ocular surface diseases: standard operating procedures, Invest. Ophthalmol. Vis. Sci. 54 (2013) 8327–8336.
[11] E.K. Akpek, K.B. Lindsley, R.S. Adyanthaya, R. Swamy, A.N. Baer, P.J. McDonnell, Treatment of Sjogren's syndrome-associated dry eye an evidence-based review, Ophthalmology 118 (2011) 1242–1252.
[12] R.L. McKown, N. Wang, R.W. Raab, R. Karnati, Y. Zhang, P.B. Williams, G.W. Laurie, Lacritin and other new proteins of the lacrimal functional unit, Exp. Eye Res. 88 (2009) 848–858.
[13] R. Karnati, D.E. Laurie, G.W. Laurie, Lacritin and the tear proteome as natural replacement therapy for dry eye, Exp. Eye Res. 117 (2013) 39–52.
[14] S. Sanghi, R. Kumar, A. Lumsden, D. Dickinson, V. Klepeis, V. Trinkaus-Randall, H.F. Frierson Jr., G.W. Laurie, cDNA and genomic cloning of lacritin, a novel secretion enhancing factor from the human lacrimal gland, J. Mol. Biol. 310 (2001) 127–139.
[15] A. Fujii, A. Morimoto-Tochigi, R.D. Walkup, T.R. Shearer, M. Azuma, Lacritin-induced secretion of tear proteins from cultured monkey lacrimal acinar cells, Invest. Ophthalmol. Vis. Sci. 54 (2013) 2533–2540.
[16] S. Samudre, F.A. Lattanzio Jr., V. Lossen, A. Hosseini, J.D. Sheppard Jr., R.L. McKown, G.W. Laurie, P.B. Williams, Lacritin, a novel human tear glycoprotein, promotes sustained basal tearing and is well tolerated, Invest. Ophthalmol. Vis. Sci. 52 (2011) 6265–6270.
[17] T. Vijmasi, F.Y. Chen, S. Balasubbu, M. Gallup, R.L. McKown, G.W. Laurie, N.A. McNamara, Topical administration of lacritin is a novel therapy for aqueous-deficient dry eye disease, Invest. Ophthalmol. Vis. Sci. 55 (8) (2014 Jul 17) 5401–5409.
[18] J. Wang, N. Wang, J. Xie, S.C. Walton, R.L. McKown, R.W. Raab, P. Ma, S.L. Beck, G.L. Coffman, I.M. Hussaini, G.W. Laurie, Restricted epithelial proliferation by lacritin via PKCalpha-dependent NFAT and mTOR pathways, J. Cell Biol. 174 (2006) 689–700.
[19] N. Wang, K. Zimmerman, R.W. Raab, R.L. McKown, C.M. Hutnik, V. Talla, M.F.t. Tyler, J.K. Lee, G.W. Laurie, Lacritin rescues stressed epithelia via rapid forkhead box O3 (FOXO3)-associated autophagy that restores metabolism, J. Biol. Chem. 288 (2013) 18146–18161.
[20] P. Ma, S.L. Beck, R.W. Raab, R.L. McKown, G.L. Coffman, A. Utani, W.J. Chirico, A.C. Rapraeger, G.W. Laurie, Heparanase deglycanation of syndecan-1 is required for binding of the epithelial-restricted prosecretory mitogen lacritin, J. Cell Biol. 174 (2006) 1097–1106.
[21] Y. Zhang, N. Wang, R.W. Raab, R.L. McKown, J.A. Irwin, I. Kwon, T.H. van Kuppevelt, G.W. Laurie, Targeting of heparanase-modified syndecan-1 by prosecretory mitogen lacritin requires conserved core GAGAL plus heparan and chondroitin sulfate as a novel hybrid binding site that enhances selectivity, J. Biol. Chem. 288 (2013) 12090–12101.
[22] V.F. Velez, J.A. Romano, R.L. McKown, K. Green, L.W. Zhang, R.W. Raab, D.S. Ryan, C.M.L. Hutnik, H.F. Frierson, G.W. Laurie, Tissue transglutaminase is a negative regulator of monomeric lacritin bioactivity, Invest. Ophthalmol. Vis. Sci. 54 (2013) 2123–2132.
[23] P. Ma, N. Wang, R.L. McKown, R.W. Raab, G.W. Laurie, Focus on molecules: lacritin, Exp. Eye Res. 86 (2008) 457–458.
[24] S.V. Aluru, S. Agarwal, B. Srinivasan, G.K. Iyer, S.M. Rajappa, U. Tatu, P. Padmanabhan, N. Subramanian, A. Narayanasamy, Lacrimal proline rich 4 (LPRR4) protein in the tear fluid is a potential biomarker of dry eye syndrome, PLoS One 7 (2012).
[25] H. Rosen, T. Abribat, The rise and rise of drug delivery, Nat. Rev. Drug Discov. 4 (2005) 381–385.
[26] J.A. Hubbell, A. Chilkoti, Chemistry. Nanomaterials for drug delivery, Science 337 (2012) 303–305.
[27] J. Dhandhukia, I. Weitzhandler, W. Wang, J.A. MacKay, Switchable elastin-like polypeptides that respond to chemical inducers of dimerization, Biomacromolecules 14 (2013) 976–985.
[28] S.R. Aluri, P. Shi, J.A. Gustafson, W. Wang, Y.A. Lin, H. Cui, S. Liu, P.S. Conti, Z. Li, P. Hu, A.L. Epstein, J.A. MacKay, A hybrid protein–polymer nanoworm potentiates apoptosis better than a monoclonal antibody, ACS Nano 8 (2014) 2064–2076.
[29] P. Shi, S. Aluri, Y.A. Lin, M. Shah, M. Edman, J. Dhandhukia, H. Cui, J.A. Mackay, Elastin-based protein polymer nanoparticles carrying drug at both corona and core suppress tumor growth in vivo, J. Control. Release 171 (3) (2013 Nov 10) 330–338.
[30] M. Amiram, K.M. Luginbuhl, X. Li, M.N. Feinglos, A. Chilkoti, Injectable protease-operated depots of glucagon-like peptide-1 provide extended and tunable glucose control, Proc. Natl. Acad. Sci. U. S. A. 110 (2013) 2792–2797.
[31] D.E. Meyer, A. Chilkoti, Purification of recombinant proteins by fusion with thermally-responsive polypeptides, Nat. Biotechnol. 17 (1999) 1112–1115.
[32] E. Wang, M.S. Desai, S.W. Lee, Light-controlled graphene–elastin composite hydrogel actuators, Nano Lett. 13 (2013) 2826–2830.
[33] D.L. Nettles, A. Chilkoti, L.A. Setton, Applications of elastin-like polypeptides in tissue engineering, Adv. Drug Deliv. Rev. 62 (2010) 1479–1485.
[34] P. Koria, H. Yagi, Y. Kitagawa, Z. Megeed, Y. Nahmias, R. Sheridan, M.L. Yarmush, Self-assembling elastin-like peptides growth factor chimeric nanoparticles for the treatment of chronic wounds, Proc. Natl. Acad. Sci. U. S. A. 108 (2011) 1034–1039.
[35] D.J. Callahan, W. Liu, X. Li, M.R. Dreher, W. Hassouneh, M. Kim, P. Marszalek, A. Chilkoti, Triple stimulus-responsive polypeptide nanoparticles that enhance intratumoral spatial distribution, Nano Lett. 12 (2012) 2165–2170.
[36] J.A. MacKay, M. Chen, J.R. McDaniel, W. Liu, A.J. Simnick, A. Chilkoti, Self-assembling chimeric polypeptide–doxorubicin conjugate nanoparticles that abolish tumours after a single injection, Nat. Mater. 8 (2009) 993–999.
[37] M. Shah, M.C. Edman, S.R. Janga, P. Shi, J. Dhandhukia, S. Liu, S.G. Louie, K. Rodgers, J.A. Mackay, S.F. Hamm-Alvarez, A rapamycin-binding protein polymer nanoparticle

shows potent therapeutic activity in suppressing autoimmune dacryoadenitis in a mouse model of Sjogren's syndrome, J. Control. Release 171 (3) (2013 Nov 10) 269–279.
[38] W. Wang, P.G. Sreekumar, V. Valluripalli, P. Shi, J. Wang, Y.A. Lin, H. Cui, R. Kannan, D.R. Hinton, J.A. Mackay, Protein polymer nanoparticles engineered as chaperones protect against apoptosis in human retinal pigment epithelial cells, J. Control. Release (2014).
[39] W. Wang, J. Despanie, P. Shi, M.C. Edman-Woolcott, Y.-A. Lin, H. Cui, J. Heur, E. Fini, S.F. Hamm-Alvarez, J.A. MacKay, Lacritin-mediated regeneration of the corneal epithelia by protein polymer nanoparticles, J. Mater. Chem. B 2 (2014) 8131–8141.
[40] J.R. McDaniel, J.A. Mackay, F.G. Quiroz, A. Chilkoti, Recursive directional ligation by plasmid reconstruction allows rapid and seamless cloning of oligomeric genes, Biomacromolecules 11 (2010) 944–952.
[41] S.M. Janib, M. Pastuszka, S. Aluri, Z. Folchman-Wagner, P.Y. Hsueh, P. Shi, A. Yi, H. Cui, J.A. Mackay, A quantitative recipe for engineering protein polymer nanoparticles, Polym. Chem. 5 (2014) 1614–1625.
[42] D.E. Laurie, R.K. Splan, K. Green, K.M. Still, R.L. McKown, G.W. Laurie, Detection of prosecretory mitogen lacritin in nonprimate tears primarily as a C-terminal-like fragment, Invest. Ophthalmol. Vis. Sci. 53 (2012) 6130–6136.
[43] S.R. da Costa, F.A. Yarber, L. Zhang, M. Sonee, S.F. Hamm-Alvarez, Microtubules facilitate the stimulated secretion of beta-hexosaminidase in lacrimal acinar cells, J. Cell Sci. 111 (Pt 9) (1998) 1267–1276.
[44] L. Chiang, J. Ngo, J.E. Schechter, S. Karvar, T. Tolmachova, M.C. Seabra, A.N. Hume, S.F. Hamm-Alvarez, Rab27b regulates exocytosis of secretory vesicles in acinar epithelial cells from the lacrimal gland, Am. J. Physiol. Cell Physiol. 301 (2011) C507–C521.
[45] K. Seifert, N.C. Gandia, J.K. Wilburn, K.S. Bower, R.K. Sia, D.S. Ryan, M.L. Deaton, K.M. Still, V.C. Vassilev, G.W. Laurie, R.L. McKown, Tear lacritin levels by age, sex, and time of day in healthy adults, Invest. Ophthalmol. Vis. Sci. 53 (2012) 6610–6616.
[46] D. Kurzbach, W. Hassouneh, J.R. McDaniel, E.A. Jaumann, A. Chilkoti, D. Hinderberger, Hydration layer coupling and cooperativity in phase behavior of stimulus responsive peptide polymers, J. Am. Chem. Soc. 135 (2013) 11299–11308.
[47] G.V. Jerdeva, K. Wu, F.A. Yarber, C.J. Rhodes, D. Kalman, J.E. Schechter, S.F. Hamm-Alvarez, Actin and non-muscle myosin II facilitate apical exocytosis of tear proteins in rabbit lacrimal acinar epithelial cells, J. Cell Sci. 118 (2005) 4797–4812.
[48] Y. Zhang, R.L. McKown, R.W. Raab, A.C. Rapraeger, G.W. Laurie, Focus on molecules: syndecan-1, Exp. Eye Res. 93 (2011) 329–330.
[49] Y. Tochino, The NOD mouse as a model of type I diabetes, Crit. Rev. Immunol. 8 (1987) 49–81.
[50] C.P. Robinson, S. Yamachika, C.E. Alford, C. Cooper, E.L. Pichardo, N. Shah, A.B. Peck, M.G. Humphreys-Beher, Elevated levels of cysteine protease activity in saliva and salivary glands of the nonobese diabetic (NOD) mouse model for Sjogren syndrome, Proc. Natl. Acad. Sci. U. S. A. 94 (1997) 5767–5771.
[51] R.E. Hunger, S. Muller, J.A. Laissue, M.W. Hess, C. Carnaud, I. Garcia, C. Mueller, Inhibition of submandibular and lacrimal gland infiltration in nonobese diabetic mice by transgenic expression of soluble TNF-receptor p55, J. Clin. Invest. 98 (1996) 954–961.
[52] P.A. Moore, D.I. Bounous, R.L. Kaswan, M.G. Humphreys-Beher, Histologic examination of the NOD-mouse lacrimal glands, a potential model for idiopathic autoimmune dacryoadenitis in Sjogren's syndrome, Lab. Anim. Sci. 46 (1996) 125–128.
[53] M.G. Humphreys-Beher, Y. Hu, Y. Nakagawa, P.L. Wang, K.R. Purushotham, Utilization of the non-obese diabetic (NOD) mouse as an animal model for the study of secondary Sjogren's syndrome, Adv. Exp. Med. Biol. 350 (1994) 631–636.
[54] I. Toda, B.D. Sullivan, E.M. Rocha, L.A. Da Silveira, L.A. Wickham, D.A. Sullivan, Impact of gender on exocrine gland inflammation in mouse models of Sjogren's syndrome, Exp. Eye Res. 69 (1999) 355–366.
[55] K. Schenke-Layland, J. Xie, M. Magnusson, E. Angelis, X. Li, K. Wu, D.P. Reinhardt, W.R. Maclellan, S.F. Hamm-Alvarez, Lymphocytic infiltration leads to degradation of lacrimal gland extracellular matrix structures in NOD mice exhibiting a Sjogren's syndrome-like exocrinopathy, Exp. Eye Res. 90 (2010) 223–237.
[56] K. Garber, Biotech in a blink, Nat. Biotechnol. 28 (2010) 311–314.
[57] A.F. Clark, T. Yorio, Ophthalmic drug discovery, Nat. Rev. Drug Discov. 2 (2003) 448–459.
[58] G.D. Novack, Ophthalmic drug delivery: development and regulatory considerations, Clin. Pharmacol. Ther. 85 (2009) 539–543.
[59] B. Leader, Q.J. Baca, D.E. Golan, Protein therapeutics: a summary and pharmacological classification, Nat. Rev. Drug Discov. 7 (2008) 21–39.
[60] W. Liu, J.A. MacKay, M.R. Dreher, M. Chen, J.R. McDaniel, A.J. Simnick, D.J. Callahan, M.R. Zalutsky, A. Chilkoti, Injectable intratumoral depot of thermally responsive polypeptide–radionuclide conjugates delays tumor progression in a mouse model, J. Control. Release 144 (2010) 2–9.
[61] M. Amiram, K.M. Luginbuhl, X. Li, M.N. Feinglos, A. Chilkoti, A depot-forming glucagon-like peptide-1 fusion protein reduces blood glucose for five days with a single injection, J. Control. Release 172 (2013) 144–151.
[62] L. Hedstrom, Serine protease mechanism and specificity, Chem. Rev. 102 (2002) 4501–4524.
[63] L.B. Evnin, J.R. Vasquez, C.S. Craik, Substrate specificity of trypsin investigated by using a genetic selection, Proc. Natl. Acad. Sci. U. S. A. 87 (1990) 6659–6663.
[64] L. Polgar, The catalytic triad of serine peptidases, Cell Mol. Life Sci. 62 (2005) 2161–2172.
[65] J. Song, H. Tan, A.J. Perry, T. Akutsu, G.I. Webb, J.C. Whisstock, R.N. Pike, PROSPER: an integrated feature-based tool for predicting protease substrate cleavage sites, PLoS One 7 (2012) e50300.
[66] R.L. McKown, E.V. Coleman Frazier, K.K. Zadrozny, A.M. Deleault, R.W. Raab, D.S. Ryan, R.K. Sia, J.K. Lee, G.W. Laurie, A cleavage potentiated fragment of tear lacritin is bactericidal, J. Biol. Chem. 289 (32) (2014 Aug 8) 22172–22182.
[67] M.M. Vestling, C.M. Murphy, C. Fenselau, Recognition of trypsin autolysis products by high-performance liquid chromatography and mass spectrometry, Anal. Chem. 62 (1990) 2391–2394.
[68] D. Kraus, I. Kaiserman, J. Frucht-Pery, R. Rahamimoff, Calcium—an "all-round player" in the cornea, Isr. Med. Assoc. J. 3 (2001) 269–274.
[69] D.A. Dartt, Signal transduction and control of lacrimal gland protein secretion: a review, Curr. Eye Res. 8 (1989) 619–636.
[70] L. Setton, Polymer therapeutics: reservoir drugs, Nat. Mater. 7 (2008) 172–174.
[71] R. Langer, Drug delivery. Drugs on target, Science 293 (2001) 58–59.
[72] M. Parent, C. Nouvel, M. Koerber, A. Sapin, P. Maincent, A. Boudier, PLGA in situ implants formed by phase inversion: critical physicochemical parameters to modulate drug release, J. Control. Release 172 (2013) 292–304.
[73] C.J. Kastrup, M. Nahrendorf, J.L. Figueiredo, H. Lee, S. Kambhampati, T. Lee, S.W. Cho, R. Gorbatov, Y. Iwamoto, T.T. Dang, P. Dutta, J.H. Yeon, H. Cheng, C.D. Pritchard, A.J. Vegas, C.D. Siegel, S. MacDougall, M. Okonkwo, A. Thai, J.R. Stone, A.J. Coury, R. Weissleder, R. Langer, D.G. Anderson, Painting blood vessels and atherosclerotic plaques with an adhesive drug depot, Proc. Natl. Acad. Sci. U. S. A. 109 (2012) 21444–21449.

Journal of Materials Chemistry B

PAPER

View Article Online
View Journal

Cite this: DOI: 10.1039/c4tb00979g

Lacritin-mediated regeneration of the corneal epithelia by protein polymer nanoparticles

Wan Wang,[a] Jordan Despanie,[a] Pu Shi,[a] Maria C. Edman,[a] Yi-An Lin,[d] Honggang Cui,[d] Martin Heur,[e] M. Elizabeth Fini,[f] Sarah F. Hamm-Alvarez[ab] and J. Andrew MacKay*[ac]

Received 17th June 2014
Accepted 30th July 2014

DOI: 10.1039/c4tb00979g

www.rsc.org/MaterialsB

The avascular corneal epithelium plays an important role in maintaining normal vision and protecting the corneal interior from environmental infections. Delayed recovery of ocular wounds caused by trauma or refractive surgery strengthens the need to accelerate corneal wound healing and better restore the ocular surface. To address this need, we fused elastin-like polypeptide (ELP) based nanoparticles SI with a model mitogenic protein called lacritin. Lacritin fused at the N-terminus of the SI diblock copolymer is called LSI. This LSI fusion protein undergoes thermo-responsive assembly of nanoparticles at physiologically relevant temperatures. In comparison to ELP nanoparticles without lacritin, LSI showed potent signs of lacritin specific effects on a human corneal epithelial cell line (HCE-T), which included enhancement of cellular uptake, calcium-mediated signaling, and closure of a scratch. *In vivo*, the corneas of non-obese diabetic mice (NOD) were found to be highly responsive to LSI. Fluorescein imaging and corneal histology suggested that topical administration of LSI onto the ocular surface significantly promoted corneal wound healing and epithelial integrity compared to mice treated with or without plain ELP. Most interestingly, it appears that ELP-mediated assembly of LSI is essential to produce this potent activity. This was confirmed by comparison to a control lacritin ELP fusion called LS96, which does not undergo thermally-mediated assembly at relevant temperatures. In summary, fusion of a mitogenic protein to ELP nanoparticles appears to be a promising new strategy to bioengineer more potent biopharmaceuticals with potential applications in corneal wound healing.

1. Introduction

Eye injury is reported to be the second most common cause of visual impairment in the United States after cataracts.[1] Back in 2006, emergency room (ER) visits for eye injuries represented 1.4% of all ER visits.[1] To maintain corneal transparency and rigidity, the corneal epithelium serves as an important barrier between the external environment and the delicate internal ocular tissues.[2] Although the corneal epithelium normally recovers rapidly from damage, certain clinical conditions including diabetic retinopathy, herpes simplex virus infection, neurotrophic keratopathy, and corneal transplants result in delayed wound healing, often precipitating sight-threatening complications.[3] Thus, there remains a need for more effective therapies to facilitate epithelial healing on the ocular surface. Moreover, recovery times following popular refractive procedures, such as photorefractive keratectomy (PRK) and laser *in situ* keratomileusis (LASIK), directly rely on the patients' corneal wound healing response; however these procedures may lead to haze, dry eye disease, nerve damage, and Diffuse Lamellar Keratitis.[4]

Corneal epithelium recovery after injury involves apoptosis, migration, proliferation, and differentiation of multiple cells in a cascade mediated by cytokines, growth factors, and chemokines.[3] Naturally present in the anterior segment of the eye and responsible for the migration and proliferation of corneal epithelial cells, growth factors have become a class of promising therapeutic candidates in treating visual impairments.[5] An enhanced wound healing effect has been observed in primate models and clinical trials *via* topical treatment with epidermal growth factor (EGF),[6,7] keratinocyte growth factor,[8] nerve growth factor,[9] *etc.* As such, it would be of great clinical value to rationally bioengineer growth factor-like proteins into therapies using a robust formulation process. Successful earlier trials include increased tensile strength of full thickness corneal wounds after topical epidermal growth factor (EGF) treatment[10]

[a]Department of Pharmacology and Pharmaceutical Sciences, University of Southern California Los Angeles, CA, 90033-9121, USA. E-mail: jamackay@usc.edu; Tel: +1-323-442-4118

[b]Department of Physiology and Biophysics, Keck School of Medicine of The University of Southern California, Los Angeles, CA, 90033-9121, USA

[c]Department of Biomedical Engineering, University of Southern California, Los Angeles, CA, 90033, USA

[d]Department of Chemical and Biomolecular Engineering, Johns Hopkins University, Baltimore, MD, 21218, USA

[e]Department of Ophthalmology, Keck School of Medicine of The University of Southern California, Los Angeles, CA, 90033-9121, USA

[f]Institute for Genetic Medicine, Keck School of Medicine of The University of Southern California, Los Angeles, CA, 90033-9121, USA

and better ulcer healing in diabetic patients from platelet-derived growth factor-BB in a topical gel formulation.[11] One novel candidate to stimulate wound healing on the ocular surface is the mitogen known as lacritin.[12] Lacritin is the most severely downregulated protein in contact lens related dry eye and is similarly deficient in blepharitis (a common inflammation of the eyelid).[13] Previous *in vitro* tests have shown that, on the ocular surface, lacritin triggers Ca^{2+} wave propagation,[13] in addition to promoting the survival of primary and cultured human corneal epithelial cells stressed with interferon-γ, tumor necrosis factor,[14] and benzalkonium chloride,[15] indicative of both mitogenic and cytoprotective activity. This cell targeting specificity is triggered by a unique 'off-on' switch controlled by heparanase deglycanation of the cell surface protein, syndecan-1, which exposes a lacritin binding site as a prerequisite for its downstream mitogenic signaling.[16,17]

Although topical application of ophthalmic products has remained the most popular and well-tolerated administration route for patient compliance, the bioavailability of eye drops is severely hindered by blinking, baseline and reflex lacrimation, and nasolacrimal drainage.[18] One solution to enhance the therapeutic index of topical treatments is through the application of polymeric nanoparticles as drug carriers.[19–21] Polymeric nanoparticles displaying therapeutic ligands at the corona can interact with complex biomolecular architectures through multiple simultaneous interactions (multivalency) and exhibit the well-defined sizes required for efficient tissue penetration.[22] One such material capable of being employed as the scaffold are thermo-responsive elastin-like polypeptides (ELPs).[23] ELPs are composed of the repetitive pentapeptide motif (Val-Pro-Gly-Xaa-Gly)$_n$ and exhibit unique reversible inverse phase transition temperatures, T_t, below which they solubilize and above which they phase separate.[24] T_t can be modulated through guest residue (Xaa) selection and changes in the number of pentameric repeats, n.[25,26] We have previously reported the successful bioengineering of diblock ELP nanoparticles to suppress tumor growth with rapamycin binding at both the corona as well as in the core;[27] uptake of ELP nanoparticles displaying adenovirus knob domain into hepatocytes and acinar cells has also been described.[28] Moreover, Callahan and coworkers have demonstrated enhanced intratumoral spatial distribution of ELP nanoparticles *via* triple stimuli[29] while MacEwan and coworkers observed controlled cellular uptake in HeLa, MCF7, and primary HUVEC cells using local Arg density modulation on ELP nanoparticles.[30] Collectively, these studies illustrate the potential of ELP nanoparticles to enhance both local and systemic therapeutic effects as a drug carrier.

Inspired by the motivation to further explore lacritin's function on the ocular surface, enhance its bioavailability, and better target the corneal epithelium, we utilized a diblock ELP (SI) nanoparticle scaffold to bioengineer LSI nanoparticles with multivalent presentation of lacritin at the surface (Table 1). The thermo-responsiveness and self-assembly of LSI nanoparticles was investigated by UV-Vis turbidity analysis, dynamic light scattering (DLS), and transmission electron microscopy (TEM). LSI exhibited mitogenic activity *in vitro* as confirmed by Ca^{2+} wave propagation and scratch wound healing using SV40-transduced human corneal epithelial cells (HCE-Ts). To further explore the *in vivo* efficacy of LSI nanoparticles, we created abrasion wounds on the ocular surface of female NOD mice mimicking the PRK procedure and topically treated the eye with two doses of LSI nanoparticles within 12 h after the surgery. The LSI treated group exhibited significantly faster wound healing compared to SI, epidermal growth factor (EGF), and bovine pituitary extract (BPE) co-treatment, and no treatment. To address the importance of multivalency, we also included a control lacritin ELP fusion that does not undergo thermally mediated assembly, called LS96. Murine corneal abrasion recovery study strongly supported enhanced healing efficacy of LSI nanoparticles over LS96 in a 12 h timeframe. Histology analysis revealed that, after LSI treatment, no significant corneal inflammation was observed and the reconstituted ocular surface appeared as smooth as pre-procedure following 24 h. For the first time, we have successfully bioengineered multivalent self-assembling LSI nanoparticles based on the thermo-responsive SI nanoparticle scaffold, confirmed its *in vitro* mitogenic activity using HCE-Ts, and corroborated the efficacy using a novel murine corneal abrasion model. This report provides the first *in vivo* verification of lacritin's wound healing potential and can be further applied to rationally bioengineer other peptide therapeutics into self-assembling

Table 1 Nomenclature, amino acid sequence, and physicochemical property of expressed proteins

Protein label	Amino acid sequence[a]	Expected M.W.[b] (kDa)	Observed M.W.[c] (kDa)	T_{t1}[d] (°C)	T_{t2} (°C)
SI	$G(VPGSG)_{48}(VPGIG)_{48}Y$	39.65	39.54	32.3	73.1
LSI	GEDASSDSTGADPAQEAGTSKPNEEISGPAEPASPPETTTTAQETSAAAVQGTAK VTSSRQELNPLKSIVEKSILLTEQALAKAGKGMHGGVPGGKQFIENGSEFAQKLL KKFSLLKPWAGLVPRGSG$(VPGSG)_{48}(VPGIG)_{48}Y$	52.61	52.21	18.7	n.d.
LS96	GEDASSDSTGADPAQEAGTSKPNEEISGPAEPASPPETTTTAQETSAAAVQGTA KVTSSRQELNPLKSIVEKSILLTEQALAKAGKGMHGGVPGGKQFIENGSEFAQK LLKKFSLLKPWAGLVPRGSG$(VPGSG)_{96}Y$	51.36	51.15	n.d.	n.d.

[a] After the start codon, a glycine spacer was added during cloning which is not present on human lacritin. [b] Expected M.W. (kDa) was calculated by DNAStar Lasergene Editseq. [c] Observed M.W. (kDa) was measured by MALDI-TOF. [d] T_t (°C) was defined at the point of the maximum first derivative of 25 μM protein solution turbidity change at 350 nm in phosphate buffer saline (PBS). n.d. not detected.

nanoparticles for treating visual impairments using the ELP delivery system.

2. Materials and methods

2.1. Materials and equipment

TB DRY® Powder Growth Media was purchased from MO BIO Laboratories, Inc. (Carlsbad, CA). NHS-rhodamine was purchased from Thermo Fisher Scientific (Rockford, IL). SV40-Adeno vector transformed cornea cells (RCB 2280, HCE-T) were purchased from Riken Cell Bank, Japan. Keratinocyte-SFM medium supplied with Bovine Pituitary Extract (BPE) and pre-qualified human recombinant Epidermal Growth Factor 1-53 (EGF) was purchased from Gibco Invitrogen (Life Technologies, NY). Calcium Indicator Fluo-4, AM, cell permeant was purchased from Life Technologies (NY). Algerbrush II with a 0.5 mm burr was purchased from The Alger Company, Inc., TX. *In vivo* studies were conducted using in house bred 12 week female non-obese diabetic (NOD) (Taconic Farms, Germantown/NY, USA) mice. All procedures performed were in accordance with IACUC approval and oversight.

2.2. Construction of LSI nanoparticles

Genes encoding for ELPs (SI) were synthesized by recursive directional ligation in pET25b(+) vector as previous reported.[27] A sequence encoding human lacritin without secretion signal peptide was designed using the best *E. coli* codons in EditSeq (DNAStar Lasergene, WI). A thrombin cleavage site was designed between the lacritin sequence and ELP tag *via* insertion at the *BseRI* site. Lacritin gene flanked by *NdeI* and *BamHI* restriction digestions sites at the 5′ and 3′ ends was purchased in the pIDTSmart-KAN vector from Integrated DNA Technologies (IDT) as follows:

5′-**CATATG**GAAGACGCTTCTTCTGACTCTACCGGTGCTGACC
CGGCTCAGGAAGCTGGTACCTCTAAACCGAACGAAGAAATCTC
TGGTCCGGCTGAACCGGCTTCTCCGCCGGAAACCACCACCACC
GCTCAGGAAACCTCTGCTGCTGCTGTTCAGGGTACCGCTAAAG
TTACCTCTTCTCGTCAGGAACTGAACCCGCTGAAATCTATCGTT
GAAAAATCTATCCTGCTGACCGAACAGGCTCTGGCTAAAGCTG
GTAAAGGTATGCACGGTGGTGTTCCGGGTGGTAAACAGTTCAT
CGAAAACGGTTCTGAATTCGCTCAGAAACTGCTGAAAAAATTCT
CTCTGCTGAAACCGTGGGCTGGTCTGGTTCCGCGTGGTTCTG
GTTACTGATCTCCTC**GGATCC**-3′.

The above gene was subcloned into the pET25b(+) vector and the LSI gene was synthesized by ligation of ELP SI gene *via* the *BseRI* restriction site. Correct cloning of the fusion protein gene was confirmed by DNA sequencing. LSI fusion proteins were expressed in BLR (DE3) *E. coli* (Novagen Inc., Milwaukee, WI) for 24 h in an orbital shaker at 37 °C at 250 rpm and purified *via* inverse phase transition cycling as previously reported.[31]

2.3. Characterization of LSI phase behavior and nanoparticle formation

The phase diagram for LSI fusion protein was characterized by optical density change at 350 nm as a function of solution temperature using a DU800 UV-Vis Spectrophotometer (Beckman Coulter, Brea, CA). T_t was defined at the point of the maximum first derivative. Self-assembly of nanoparticles was measured using dynamic light scattering (DLS) using a DynaPro-LSR Plate Reader (Wyatt Technology, Santa Barbara, CA). Light scattering data were collected at regular temperature intervals (1 °C) as solutions were heated from 5 to 50 °C. The results were analyzed using a Rayleigh sphere model and fitted into a cumulant algorithm based on the sum-of-squares value. The critical micelle temperature (CMT) was defined as the lowest temperature at which the R_h is significantly greater than the average monomer R_h.

2.4. TEM imaging of LSI nanoparticles

The TEM imaging was carried out on a FEI Tecnai 12 TWIN microscope (Hillsboro, OR) at 100 kV. Briefly, a 100 μM solution (5 μL) was initially deposited on a copper grid with carbon film (CF400-Cu, Election Microscopy Sciences, Hatfield, PA). After removing the excess amount of solution with filter paper, the samples were negatively stained with 2% uranyl acetate, followed by removing excess uranyl acetate after 30 s. The samples were then dried under room temperature for at least 3 h before use in imaging.

2.5. SV40-immortalized human corneal epithelial cell (HCE-T) culture

SV40-immortalized HCE-T cells (Riken Cell Bank, Japan) were grown in keratinocyte-SFM media (KSFM, Life Technologies, Rockville, MD) containing bovine pituitary extract (BPE, 50 μg ml^{-1}) and epidermal growth factor (EGF, 5 ng ml^{-1}). Cell passages 4–6 were used for Ca^{2+} imaging, scratch and uptake assays in 35 mm coverslip-bottomed dishes. To optimize responsiveness upon stimuli, cells were starved with EGF and BPE free medium for 24 h before experimentation.

2.6. Ca^{2+} imaging

HCE-Ts were rinsed twice with Ca^{2+} and Mg^{2+} free phosphate buffer saline (PBS) and incubated at 37 °C for 20 m in fresh KSFM medium containing 2.5 μM calcium probe Fluo-4 AM (Invitrogen Life technologies, NY). The cells were then rinsed twice with NaCl Ringer buffer (145 mM NaCl, 5 mM KCl, 1 mM $CaCl_2$, 1 mM KH_2PO_4, 1 mM $MgCl_2$, 10 mM glucose, and 10 mM HEPES, osmolarity 300, pH 7.4) and kept in the same buffer at room temperature for 30 m. For Ca^{2+} free medium, 1 mM Ca^{2+} was replaced with 0.5 mM EGTA. The cells were illuminated at 488 nm, and their emission was monitored every 3.15 s at 510 nm using Zeiss LSM 510 Meta confocal microscope system. The field of interest contained 24 to 45 cells, and the fluorescent intensity change was calculated for each region with image-analysis software. Ca^{2+} dynamics were evaluated using the changes in fluorescence intensity of Fluo-4AM. The data are presented as percentage change in fluorescence intensity at each time point (F_t) to the first time point (F_0) reading: $(F_t - F_0)/F_0 \times 100\%$.

2.7. *In vitro* scratch closure assay

For a scratch assay, confluent HCE-T monolayers were scraped in a straight line to create a scratch wound with a p200 pipet

tip.[32] Cells were rinsed with KSFM medium without BPE or EGF to remove debris and then incubated with fresh KSFM medium containing BPE (50 μg ml^{-1}) and EGF (5 ng ml^{-1}), LSI, or medium without growth factors (No treat). Phase contrast images of the wound at the beginning and after 24 h treatment were captured using Zeiss LSM 510 Meta confocal microscope system.

2.8. Exogenous cell uptake assay

SI and LSI nanoparticles were conjugated with NHS-rhodamine (Thermo Fisher Scientific Inc, Rockford, IL) *via* covalent modification of the amino terminus. Conjugation was performed in 100 mM borate buffer (pH 8.0) for 2 h (LSI) or overnight (SI) at 4 °C followed by desalting on a PD10 column (GE Healthcare, Piscataway, NJ) to remove free dye. Briefly, after the cells were rinsed with fresh medium without BPE and EGF, 10 μM rhodamine labeled proteins were added into the dish. After incubation at 37 °C for different time points, the cells were rinsed and images were acquired using Zeiss LSM 510 Meta confocal microscope system.

2.9. Murine corneal abrasion and recovery study

Briefly, 12 week female NOD mice were anesthetized with an i.p. injection of xylaxine/ketamine (60–70 mg + 5 mg kg^{-1}) and placed on a heating pad. After cleaning the ocular surface with eye wash (OCuSOFT, Inc., TX), the corneal epithelium of the right eye was removed down to the basement membrane using an algerbrush II (The Alger Company, Inc., TX); the left eye was left intact as a contra lateral control. Mice were allowed to heal for 24 h with 2 doses (5 μl) of KSFM medium containing BPE (50 μg ml^{-1}) and EGF (5 ng ml^{-1}), 100 μM LSI, 100 μM SI, or no treatment at 12 h intervals. After staining the ocular surface with 5 μl 0.6 mg ml^{-1} fluorescein (Akorn, IL), images of the abrasion wound were captured using a Moticam 2300 camera after 12 h and 24 h.

2.10. Statistics

All experiments were replicated at least three times. Maximum fluorescence intensity change in Ca^{2+}-mediated fluorescence was analyzed using a non-paired *t*-test. Scratch wound healing quantification was analyzed using a one-way ANOVA followed by Tukey's *post hoc* test. HCE-T uptake was analyzed using two-way ANOVA followed by Bonferroni post-test and murine corneal epithelium recovery from abrasion wound were analyzed using Kruskal–Wallis non-parametric ANOVA. Corneal wound healing comparison between LSI and LS96 after 12 h treatment was analyzed using Mann–Whitney *U* test. A *p* value less than 0.05 was considered statistically significant.

3. Results and discussion

3.1. The ELP lacritin fusion called LSI forms thermo-responsive nanoparticles

Lacritin moderates homeostasis through receptor-mediated events across the anterior segment of the eye.[12] In principle, it is possible to further enhance the activity of receptor-mediated events through the deliberate formation of multivalent protein polymer nanoparticles (Fig. 1A).[28,30,33] While targeting ligands have been explored using ELP based nanoparticles similar to SI (Table 1), to the best of our knowledge, this approach has never been used to modulate the activity of a cell signaling protein such as lacritin. To explore this possibility, LSI and LS96 (Table 1) were cloned into a pET25(+) vector, expressed in *E. coli*, and purified using inverse phase transition cycling (Fig. 1B). As shown in Fig. 1A, a chemically synthesized gene encoding lacritin was fused to the ELP diblock copolymer called SI and expressed as a fusion protein called LSI. LSI was expected to undergo thermally-mediated assembly similar to SI and form nanoparticles above its phase transition temperature (T_t), while LS96, with lacritin gene fused to the soluble macromolecule S96, was developed as a control that does not phase separate until significantly above physiological temperatures. After confirming the purity and molecular weight of expressed proteins,

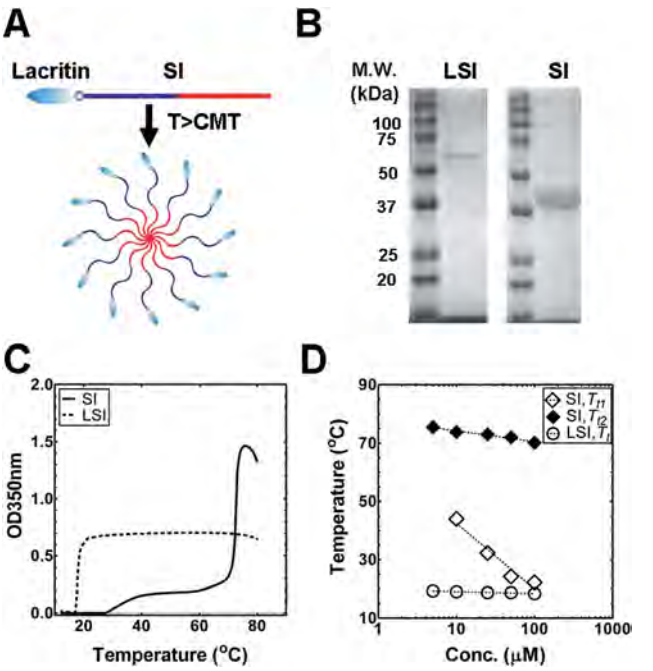

Fig. 1 Construction of a thermo-responsive nanoparticle decorated with a mitogenic protein. (A) A gene encoding lacritin was fused to an ELP diblock copolymer called SI and expressed as a protein called LSI. LSI undergoes temperature-dependent assembly of a nanoparticle above its phase transition temperature (T_t). (B) After purification, gel electrophoresis (SDS-PAGE) was used to confirm the molecular weight for expressed LSI and SI. (C) An optical density profile was obtained upon heating purified polymers in phosphate buffered saline (25 μM). SI shows two inflections, where the first represents the assembly of a nanoparticle (T_{t1}) and the second represents the bulk phase separation (T_{t2}) of that nanoparticle. In contrast, LSI shows only a single inflection and does not undergo bulk phase separation. (D) Optical density data was compiled to create a concentration–temperature phase diagram for LSI and SI. Dashed lines indicate the fit of T_t to the following equation: $T_t = m \log_{10}[C_{ELP}] + b$ where C_{ELP} is the concentration, m is the slope, and b is the transition temperature at 1 μM. For T_t of LSI, $b = 19.69$ °C and $m = -0.64$ °C (log 10[μM])$^{-1}$. For T_{t1} of SI, $b = 65.06$ °C, $m = -22.56$ °C (log 10[μM])$^{-1}$. For T_{t2} of SI, $b = 77.98$ °C, $m = -3.72$ °C (log 10[μM])$^{-1}$.

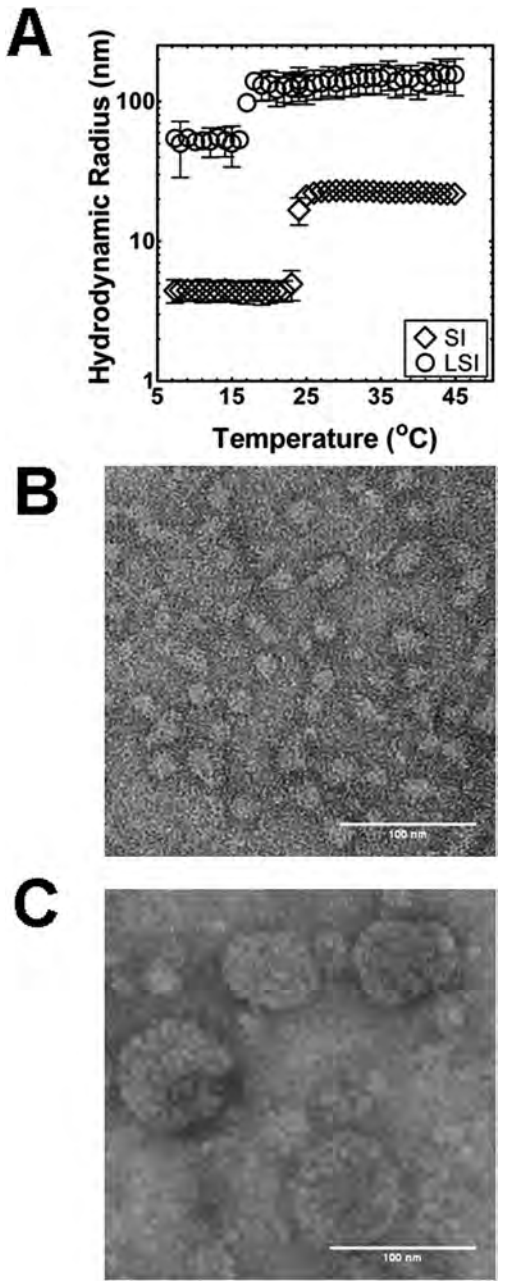

Fig. 2 LSI and SI assemble nanoparticles at physiological temperatures. (A) Dynamic Light Scattering (DLS) was performed during heating, which shows that SI assemble nanoparticles with a R_h of 22.3 ± 1.1 nm at 37 °C. Below T_{t1} LSI form 30–40 nm structures; however, above T_t these reconstitute into stable 147 ± 36 nm nanoparticles at 37 °C. (B and C) TEM images of (B) SI and (C) LSI nanoparticles, with average diameter of 36.5 ± 5.8 nm and 67.1 ± 11.5 nm accordingly. The scale bar represents 100 nm.

their phase diagrams were characterized using optical density as a function of temperature (Fig. 1C). While monomeric ELPs undergo a single phase transition from solubility to coacervate, certain ELP diblock copolymers display two steps of assembly in response to heating: (i) soluble monomers assemble into stable nanoparticles above T_{t1}; and (ii) at a higher temperature, T_{t2}, the nanoparticles themselves coacervate (Fig. 1D). For ELPs such as SI, T_{t1} is thus defined as the critical micelle temperature (CMT) above which nanoparticles are favorable (32.3 °C at 25 μM). T_{t2}, or the bulk phase transition temperature, represents the temperature at which these nanoparticles further assemble into coacervates.[34] In striking contrast to its SI scaffold, LSI only shows one phase transition at 18.4 °C (25 μM). Moreover, LSI illustrated less concentration dependent phase transition compared to the SI scaffold, as demonstrated by a decreased slope when T_t was fit by the equation:

$$T_t = m \log[C_{ELP}] + b, \quad (1)$$

where C_{ELP} is the concentration, m is the slope, and b is the transition temperature at 1 μM (Fig. 1D). Eqn (1) permits the estimation of T_t over a broad range of concentrations, which may be encountered *in vivo*. In our recent reports, suppression of the ELP concentration dependence correlates with assembly mediated by the fusion domain itself, which we have reported in fusion between a single chain antibody and also a disintegrin.[31]

Based on the unexpected observation that LSI exhibits a single phase transition, dynamic light scattering (DLS) was used to determine whether particles form above or below this T_t. Both constructs were thus compared by DLS to monitor the

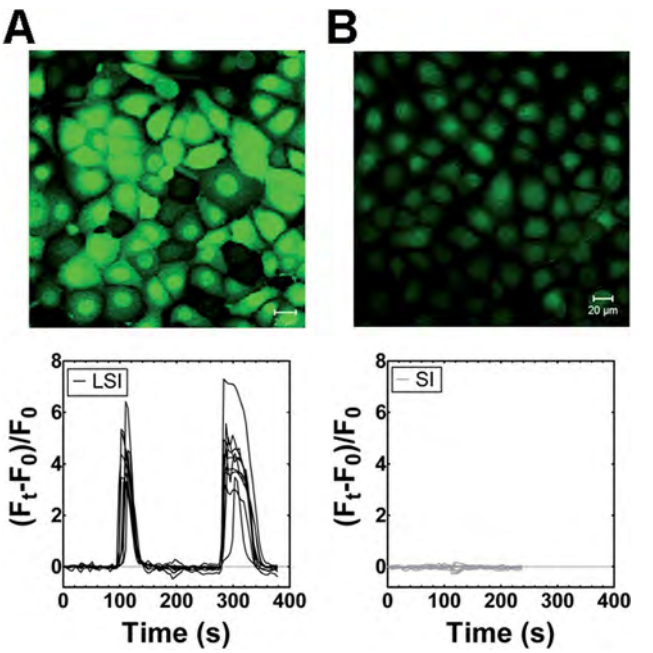

Fig. 3 LSI nanoparticles stimulate Ca^{2+}-mediated signaling in corneal epithelial cells. HCE-T cells were treated with Fluo-4AM to detect calcium-mediated signaling and imaged using live cell confocal microscopy. The upper images are representative of the peak intensity following the administration of either LSI or SI (40 μM). The lower plot presents the fluorescence intensity as a function of time in ten individual cells. The percentage change in fluorescence intensity, F_t, compared to the initial time point, F_0, was estimated as follows: $F_t = (F_t - F_0)/F_0 \times 100\%$. (A) LSI nanoparticles were administered twice, each time triggering a 3–6 fold increase in intracellular Ca^{2+}. (B) In contrast, the same concentration of SI did not elicit a significant effect (****$p < 0.0001$, $n = 10$). The scale bar represents 20 μm. Maximum fluorescence intensity changes were analyzed using an un-paired t-test.

temperature dependent assembly process (Fig. 2A). Surprisingly, LSI preassembled into 30–40 nm nanoparticles even below T_t. Above T_t, it began to favor larger nanoparticles ranging from 130–140 nm. Consistent with our previous reports, SI remained as 20–30 nm micelles at physiologically relevant temperatures (Fig. 2A). In combination with the optical density data, this suggests that lacritin itself mediates partial assembly of small aggregates that proceed to assemble larger structures above the T_{t1} mediated by SI. To further examine the dominant structures formed by LSI and SI, we observed their morphologies when dried from room temperature using transmission electron microscopy (TEM). Consistent with DLS, while SI formed a mono-dispersed micelle structure with an average diameter of 36.5 ± 5.8 nm (Fig. 2B) and LSI formed larger nanoparticles that exhibit average diameters of 67.1 ± 11.5 nm (Fig. 2C). Regardless, both SI and LSI appear capable of forming nanostructures; therefore, we proceeded to investigate the potential for these lacritin functionalized nanoparticles to participate in lacritin-mediated signaling and healing relevant to the corneal epithelium.

3.2. LSI nanoparticles exhibit mitogenic activity using SV-40 transduced human corneal epithelial cells

Upon injury, one of the earliest reactions of many epithelial cells is a transient Ca^{2+} wave spreading across the monolayer

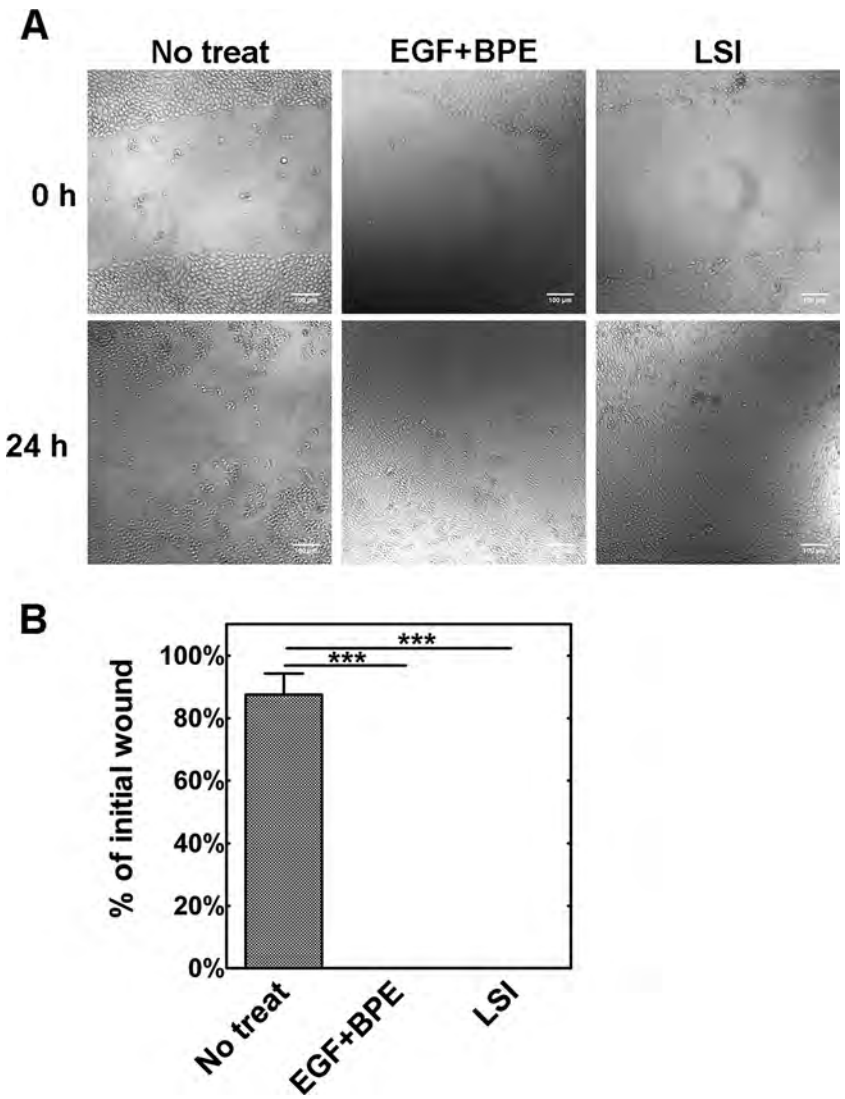

Fig. 4 LSI nanoparticles mediate scratch closure in corneal epithelial cells. HCE-T cells were grown to confluence on tissue culture polystyrene, scratched, and imaged for 24 h to observe the rate of closure. (A) At low concentrations, 10 nM LSI nanoparticles completely closed the scratch. This finding was similar to that obtained by a positive control containing epidermal growth factor (EGF) (5 ng ml^{-1}) and bovine pituitary extract (BPE) (50 μg ml^{-1}). In contrast, the no treatment group (medium only) failed to close the scratch. The scale bar represents 100 μm. (B) The scratch closure at 24 h was quantified to show that LSI nanoparticles induce an effect similar to control EGF and BPE. The no treatment group retained more than 80% of initial scratch width. Each treatment condition was performed in triplicate and four representative distances in each well were measured for statistical analysis (***$p < 0.001$, $n = 12$). Data were analyzed by a blind reviewer. Images were quantified using ImageJ and analyzed using one-way ANOVA followed by Tukey's post-test.

cell sheet.[35] The Ca^{2+} wave triggers downstream signaling pathways responsible for cell migration, proliferation and other events associated with wound repair.[36,37] Sanghi *et al.* first reported lacritin's ability to stimulate Ca^{2+} wave propagation throughout HCE-Ts while initially exploring its efficacy on the ocular surface.[13] Further studies have confirmed that this Ca^{2+} signal is associated with lacritin's protection of HCE cells stressed with benzalkonium chloride[15] and maintenance of cultured corneal epithelia homeostasis.[14] To confirm whether LSI maintains mitogenic activity of lacritin, we tested both calcium transients and scratch wound healing assays based on the reported HCE-T model.[38] We first tested intracellular Ca^{2+} wave propagation in HCE-T cells loaded with Fluo-4 AM under either LSI or SI treatment. The fields of interest containing 24 to 45 cells were chosen and the fluorescent intensity change of ten individual cells was calculated using LSM 510 image-analysis software. Percentage change in fluorescence intensity at each time point (F_t) to the first time point (F_0) reading: $(F_t - F_0)/F_0 \times 100\%$ was used to quantify Ca^{2+} signal. The signal triggered by SI was negligible, evoking only a 0.054 ± 0.049 fold maximum fluorescence intensity change compared to baseline. The addition of LSI nanoparticles, however, resulted in a significantly rapid calcium influx into the cells with a maximum fluorescence intensity 4.399 ± 1.043 fold of F_0 ($p < 0.0001$, Fig. 3). Moreover, HCE-T cells appeared to have 'memory' for exogenous LSI treatment, as treating the same group of cells for the second time with the same concentration resulted in a broader peak for Ca^{2+} influx, which extended peak duration from 40 to 70 s (Fig. 3A). Downstream of Ca^{2+} mediated signaling,[39] HCE-Ts are known to initiate more rapid motility and proliferation,[14,15] which can be visualized during the closure of a scratch made on a confluent sheet of cells. To visualize the *in vitro* effect of LSI, we applied a scratch to a sheet of cells and captured the time-lapse healing process (Fig. 4A). Each treatment was performed in triplicate and four independent wound distances in each well were measured for analysis. After 24 h of treatment, a very low concentration of LSI (10 nM) significantly accelerated scratch wound healing compared to plain medium without growth-factors (***$p < 0.001$). This effect was comparable to a positive control containing BPE and EGF.

3.3. LSI nanoparticles undergo uptake into HCE-Ts

Encouraged by LSI's *in vitro* mitogenic activity, we further explored whether exogenous LSI can enter the HCE-Ts. The cells were thus incubated with NHS-rhodamine labeled LSI and SI nanoparticles for different time points and representative images were shown in Fig. 5. Consistent with lacritin-mediated uptake, LSI underwent cell uptake into HCE-Ts in a time dependent manner (Fig. 5A). Significant cell entry was observed 10 m following incubation, and after 1 h, LSI nanoparticles accumulated within the peri-nuclear region. Upon quantification, LSI exhibited significantly higher cytosolic fluorescence than SI nanoparticles ($p < 0.0001$, Fig. 5B). Nanomaterials of different sizes, shapes, and charges have been widely used in biomedical imaging, tissue targeting, and cell uptake.[40–42] More recently, the use of nanoparticles to crosslink membrane receptors more efficiently to regulate downstream signaling has attracted enormous attention, especially in antibody mediated receptor crosslinking.[43,44] This data suggests that LSI may be useful as a platform to not only stimulate lacritin-mediated mitogenesis, but could also have applications in the targeted delivery of other agents (antibodies, small molecules) to the cells of the cornea.

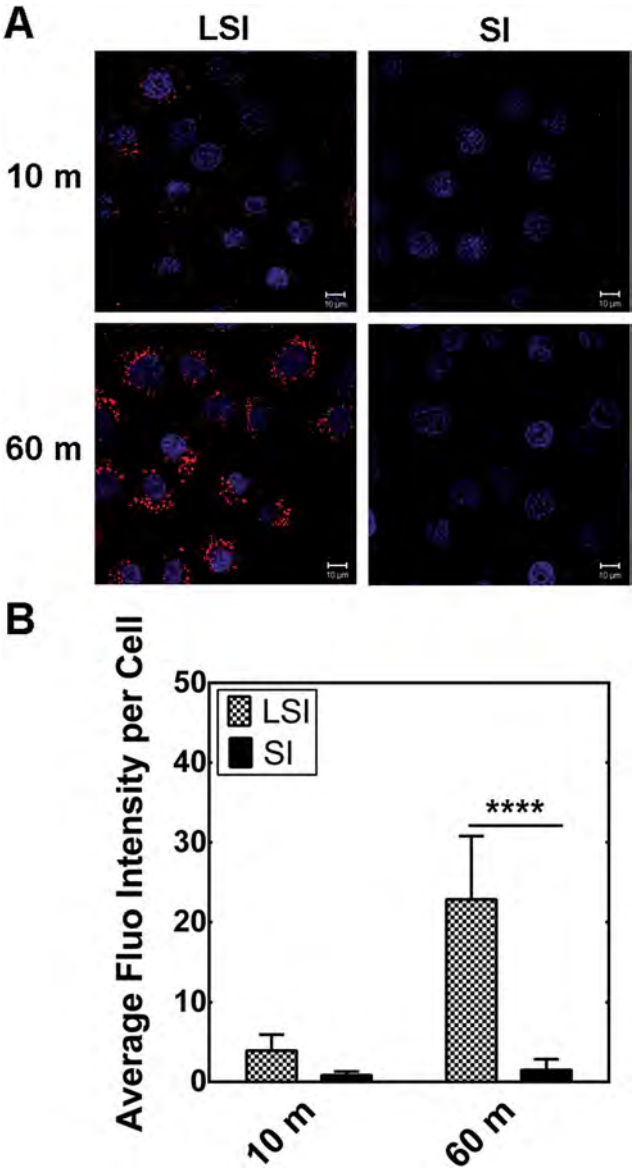

Fig. 5 Lacritin mediates nanoparticle uptake in corneal epithelial cells. HCE-T cells were incubated with rhodamine labeled LSI or SI nanoparticles and imaged using confocal microscopy. (A) Representative images show time dependent uptake of LSI while SI nanoparticles do not internalize to the same degree. Red: rhodamine labeled LSI and SI; blue: DAPI staining of nuclei. The scale bar represents 10 μm. (B) For cell uptake quantification, each treatment was repeated three times and three representative cells on each plate were chosen for analysis purpose. Remarkably, LSI exhibits significantly higher uptake level than SI (****$p < 0.0001$, $n = 9$) at 60 m. Images were quantified using ImageJ and analyzed *via* two-way ANOVA followed by a Bonferroni post-hoc *t*-test.

3.4. LSI nanoparticles heal a corneal abrasion on non-obese diabetic (NOD) mice

While evidence for lacritin's mitogenic activity have been confirmed,[14,15] the *in vivo* mitogenic potential of lacritin has not been previously reported. As such, our *in vitro* results inspired us to investigate the activity of LSI nanoparticles on the ocular surface. To do so, we proceeded to investigate their *in vivo* efficacy *via* the easiest and most well-tolerated delivery approach-topical eye drops. In this study, we developed a corneal epithelial abrasion model on female NOD mice to assess the wound-healing effect of LSI nanoparticles. Non-obese diabetic (NOD) mice are frequently used as an animal model for impaired wound healing in humans. For example, Darby and coworkers have previously compared the skin wound healing process in non-obese diabetic (NOD) mice and C57BL/6 mice. Reduced cell proliferation, retarded onset of the myofibroblast phenotype, reduced procollagen I mRNA expression, and aberrant control of apoptotic cell death were observed in NOD group.[45] Alternatively, Rich and coworkers used NOD mice as an impaired wound healing model to study the pathogenesis of *Staphylococcus aureus* infection.[46] Also, Lee and coworkers have implanted alginate hydrogels loaded with model drug VEGF into NOD mice after femoral artery ligation to increase collateral circulation under cyclic mechanical stimulation.[47]

Based on the above reports, the NOD mouse model was selected for evaluation of the *in vivo* activity of LSI nanoparticles. Briefly, a circular abrasion wound with a diameter of around 2 mm was created on the right eye of the animal with an algerbrush II without damaging the limbal region.[48,49] Immediately after imaging, 5 μl of 100 μM LSI nanoparticles, SI nanoparticles, or control EGF + BPE were topically administered to the ocular surface, and this treatment was repeated once 12 h after wound initiation. Images of the wound were captured at time 0, 12 h, and 24 h using fluorescein staining under cobalt blue light (Fig. 6A). The initial wound healing comparison study included 4 mice under each treatment group, with the left eye intact as a contralateral control. After experimentation, wound-healing images were analyzed using ImageJ. Mean fluorescein intensity, wound area, total fluorescein (total = mean fluorescein intensity × wound area), fluorescein percentage of initial value, wound area percentage of initial value (PctArea), and total fluorescein percentage of initial value were determined by a blind reviewer and compared between groups at 12 h and 24 h using Kruskal–Wallis non-parametric testing. No significant inflammation or any other adverse effects were observed upon treatments.

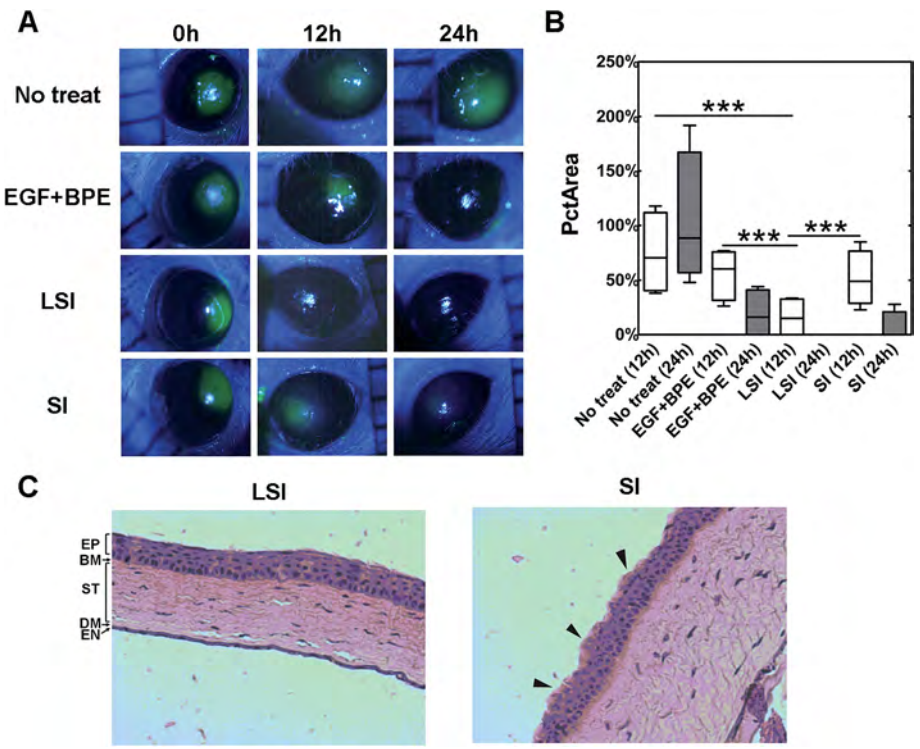

Fig. 6 Lacritin-decorated nanoparticles heal abrasions in the corneal epithelium of mice. An algerbrush II was used to create a 2 mm defect in the corneal epithelium of female non-obese diabetic (NOD) mice, which were monitored using fluorescein staining at 0, 12 and 24 h with or without treatment by LSI, SI, and a positive control EGF + BPE. (A) Representative images showing the time-lapse healing of the defect on the corneal epithelium. (B) The area of the wounds as a percent of the initial wound area (PctArea) was determined by a blind reviewer to ensure objectivity. A Kruskal–Wallis non-parametric test was used to compare groups. These revealed that LSI at both 12 and 24 h significantly (***p = 0.001, n = 4) decreased the percentage of initial wound area (PctArea) compared to SI, EGF + BPE, and no treatment groups. (C) After 24 h, corneas were fixed, sectioned across the defect, and stained by hematoxylin and eosin. The corneal epithelium of the LSI treatment group revealed normal pathology, absent of inflammation. Although reduced fluorescein staining was observed at late times in the SI group, the epithelium did not recover fully, as evidenced by its irregular surface (black arrows). EP: epithelium; BM: Bowman's membrane; ST: stroma; DM: Descenet's membrane; EN: endothelium.

Notably, LSI at both 12 and 24 hours significantly decreased the percentage of initial wound area (PctArea) compared to SI ($p = 0.001$), EGF + BPE ($p = 0.001$), and no treatment groups ($p = 0.001$), suggesting that LSI is the best formulation to accelerate recovery of the corneal epithelium (Fig. 6B). To corroborate the fluorescein imaging result, we further processed the corneal epithelium after 24 h for histology analysis (Fig. 6C). Briefly, corneas were fixed, sectioned across the defect, and stained by hematoxylin and eosin. Pathology of corneal epithelium (EP); Bowman's membrane (BM); stroma (ST); Descenet's membrane (DM); endothelium (EN) was evaluated. Remarkably, the corneal epithelium of the LSI treatment group showed complete recovery with a smooth, reconstituted surface, absent of inflammation. While the fluorescein test revealed partial resistance to staining at 24 h in the SI group, the regenerated corneal epithelium did not complete differentiation as illustrated by a rough, irregular ocular surface (black arrows).

Having demonstrated that the mitogenic lacritin protein remains active when decorated on a protein polymer nanoparticle, we next investigated whether ELP-mediated particle assembly is required to achieve this result. To address the significance of ELP assembly *in vivo*, the efficacy of LSI nanoparticles can be directly compared with a thermally non-responsive lacritin fusion protein called LS96 (Table 1). Both LSI and LS96 contain the lacritin sequence followed by an ELP containing 96 total pentameric repeats; however, the ELP previously characterized as S96 [34,50] does not phase separate until above physiological temperatures. Optical density measurements, in fact, revealed that LS96 does not display any observable phase transitions in phosphate buffered saline (Fig. 7A). In addition, DLS confirmed that LSI has a much larger hydrodynamic radius than LS96 at 37 °C (Fig. 7B). Using these two related formulations of lacritin ELPs, the corneal defect study in NOD mice was both to confirm the ability of LSI to close the epithelium after 12 h and compare this closure with that of LS96. To better evaluate our experimental observation, we further increased the sample size to eight mice per group, with all right eyes receiving the abrasion procedure. Interestingly, LSI healed the abrasion wound significantly ($p < 0.05$) faster than the non thermo-responsive LS96 fusion (Fig. 7D). This finding directly supports the contention that ELP-mediated assembly is involved with the enhancement of LSI. To the best of our knowledge, this is the first definitive study showing that ELP-mediated assembly can be used to boost the activity of a mitogenic peptide.

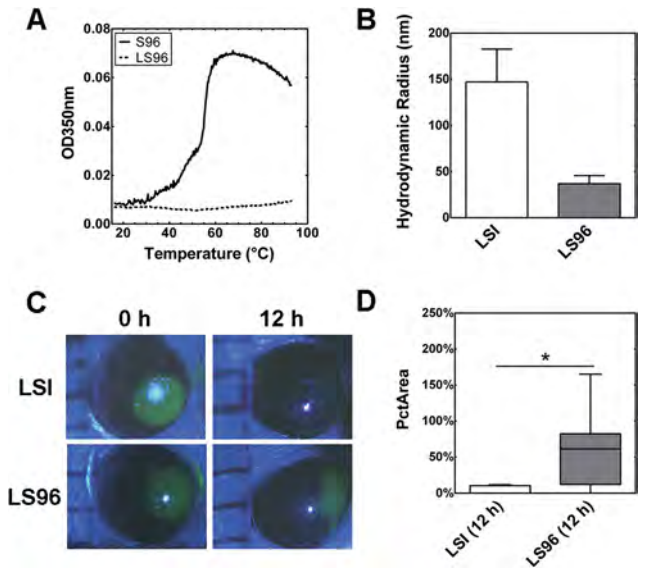

Fig. 7 ELP-mediated assembly is essential for the *in vivo* activity of LSI nanoparticles. To determine whether the potency of LSI nanoparticles depends on ELP-mediated assembly of SI, a control lacritin fusion called LS96 (Table 1) was expressed. (A) Optical density measurements confirmed that LS96 lacks any detectable phase transitions at 25 μM in phosphate buffer saline (PBS). (B) Under the same conditions, Dynamic Light Scattering (DLS) was performed at 37 °C, which confirmed that LSI assembles nanoparticles with a R_h of 147.0 ± 35.8 nm, while LS96 produced particles with a R_h of 37.0 ± 8.8 nm, which is similar to that observed for LSI below T_t (Fig. 2A). (C) A 2 mm corneal defect was induced in female NOD mice, treated with LSI or LS96, stained by fluorescein at 12 h, and quantified by a blind reviewer. A representative image shows superior integrity of the ocular surface treated with LSI after 12 h. (D) Comparison of the PctArea was made by the non-parametric Mann–Whitney *U* test, which confirms that LSI at 12 h significantly decreases the wound area compared to LS96 (*$p < 0.05$, $n = 8$).

4. Conclusions

To accelerate the corneal wound healing process, this manuscript describes a multivalent ELP nanoparticle as a means of delivering a candidate biopharmaceutical, the mitogen lacritin, to the ocular surface. This lacritin ELP fusion, LSI, displays thermo-responsive self-assembly properties similar to the unmodified SI nanoparticle and presents accessible lacritin at its corona at physiologically relevant temperatures. LSI nanoparticles trigger calcium dependent cell signaling, internalize into cells, and facilitate scratch closure in monolayers of a human corneal epithelial cell line (HCE-Ts). When topically applied on the ocular surface of NOD mice following removal of the corneal epithelium, LSI nanoparticles promoted faster wound healing compared to SI and untreated groups. Most importantly, the LSI nanoparticles produce faster regeneration of the corneal epithelium compared to a control lacritin ELP fusion, called LS96, that does not undergo thermally-mediated assembly. Overall, this study highlights the potential of ELPs as nanoparticle scaffolds to effectively deliver protein therapeutics to the ocular surface and repair abrasion wounds. This strategy may have utility in developing other candidate peptides into biopharmaceuticals. To maximize the conversion of biologically active peptides into drugs, this manuscript suggests that it may be beneficial to induce their multivalent presentation on a nanoparticle; furthermore, ELP protein polymers have emerged as a new strategy to directly bioengineer these particles at the genetic level.

Abbreviations

PRK Photorefractive keratectomy
LASIK Laser *in situ* keratomileusis
TEM Transmission electron microscopy

ELPs	Elastin-like polypeptides
T_t	Transition temperature
CMT	Critical micelle temperature
HCE-T	SV40-Adeno vector transformed human corneal epithelial cell
NOD	Non-obese diabetic
BPE	Bovine pituitary extract
EGF	Epidermal growth factor

Acknowledgements

This study is supported by the USAMRMC/TATRC grant W81XWH1210538, NIH EY011386, and the USC Whittier foundation. The authors appreciate important discussions regarding the study with Dr Gordon W. Laurie and Dr Robert L. McKown. The authors thank Frances Yarber and Dr Gabriel Gordon for technical support of the animal studies. The authors thank Dr Tianyi Jiang for cloning the LS96 gene and Dr Benjamin Droese's technical support in cloning the LSI gene.

Notes and references

1 R. I. Haddadin, G. K. Vora and J. Chodosh, *Int. Ophthalmol. Clin.*, 2013, **53**, 23–32.
2 K. Kimura, S. Teranishi, K. Fukuda, K. Kawamoto and T. Nishida, *Invest. Ophthalmol. Visual Sci.*, 2008, **49**, 565–571.
3 K. Suzuki, J. Saito, R. Yanai, N. Yamada, T. Chikama, K. Seki and T. Nishida, *Prog. Retinal. Eye Res.*, 2003, **22**, 113–133.
4 M. V. Netto, R. R. Mohan, R. Ambrosio, A. E. K. Hutcheon, J. D. Zieske and S. E. Wilson, *Cornea*, 2005, **24**, 509–522.
5 B. Klenkler and H. Sheardown, *Exp. Eye Res.*, 2004, **79**, 677–688.
6 T. Kitazawa, S. Kinoshita, K. Fujita, K. Araki, H. Watanabe, Y. Ohashi and R. Manabe, *Invest. Ophthalmol. Visual Sci.*, 1990, **31**, 1773–1778.
7 C. Scardovi, G. P. Defelice and A. Gazzaniga, *Ophthalmologica*, 1993, **206**, 119–124.
8 C. Sotozono, T. Inatomi, M. Nakamura and S. Kinoshita, *Invest. Ophthalmol. Visual Sci.*, 1995, **36**, 1524–1529.
9 A. Lambiase, P. Rama, S. Bonini, G. Caprioglio and L. Aloe, *N. Engl. J. Med.*, 1998, **338**, 1174–1180.
10 H. M. Leibowitz, S. Morello, Jr, M. Stern and A. Kupferman, *Arch. Ophthalmol.*, 1990, **108**, 734–737.
11 J. M. Embil, K. Papp, G. Sibbald, J. Tousignant, J. M. Smiell, B. Wong and C. Y. Lau, *Wound Repair Regen.*, 2000, **8**, 162–168.
12 R. Karnati, D. E. Laurie and G. W. Laurie, *Exp. Eye Res.*, 2013, **117**, 39–52.
13 S. Sanghi, R. Kumar, A. Lumsden, D. Dickinson, V. Klepeis, V. Trinkaus-Randall, H. F. Frierson and G. W. Laurie, *J. Mol. Biol.*, 2001, **310**, 127–139.
14 N. Wang, K. Zimmerman, R. W. Raab, R. L. McKown, C. M. L. Hutnik, V. Talla, M. F. Tyler, J. K. Lee and G. W. Laurie, *J. Biol. Chem.*, 2013, **288**, 18146–18161.
15 M. M. Feng, J. Baryla, H. Liu, G. W. Laurie, R. L. McKown, N. Ashki, D. Bhayana and C. M. Hutnik, *Curr. Eye Res.*, 2014, **39**, 604–610.
16 Y. H. Zhang, N. N. Wang, R. W. Raab, R. L. McKown, J. A. Irwin, I. Kwon, T. H. van Kuppevelt and G. W. Laurie, *J. Biol. Chem.*, 2013, **288**, 12090–12101.
17 P. S. Ma, S. L. Beck, R. W. Raab, R. L. McKown, G. L. Coffman, A. Utani, W. J. Chirico, A. C. Rapraeger and G. W. Laurie, *J. Cell Biol.*, 2006, **174**, 1097–1106.
18 J. C. Lang, *Adv. Drug Delivery Rev.*, 1995, **16**, 39–43.
19 S. K. Sahoo, F. Diinawaz and S. Krishnakumar, *Drug Discovery Today*, 2008, **13**, 144–151.
20 Y. Diebold, M. Jarrin, V. Saez, E. L. Carvalho, M. Orea, M. Calonge, B. Seijo and M. J. Alonso, *Biomaterials*, 2007, **28**, 1553–1564.
21 R. C. Nagarwal, S. Kant, P. N. Singh, P. Maiti and J. K. Pandit, *J. Controlled Release*, 2009, **136**, 2–13.
22 M. P. Monopoli, C. Aberg, A. Salvati and K. A. Dawson, *Nat. Nanotechnol.*, 2012, **7**, 779–786.
23 J. A. Hubbell and A. Chilkoti, *Science*, 2012, **337**, 303–305.
24 D. E. Meyer and A. Chilkoti, *Nat. Biotechnol.*, 1999, **17**, 1112–1115.
25 D. L. Nettles, A. Chilkoti and L. A. Setton, *Adv. Drug Delivery Rev.*, 2010, **62**, 1479–1485.
26 A. Chilkoti, T. Christensen and J. A. MacKay, *Curr. Opin. Chem. Biol.*, 2006, **10**, 652–657.
27 P. Shi, S. Aluri, Y. A. Lin, M. Shah, M. Edman, J. Dhandhukia, H. G. Cui and J. A. MacKay, *J. Controlled Release*, 2013, **171**, 330–338.
28 G. Sun, P. Y. Hsueh, S. M. Janib, S. Hamm-Alvarez and J. A. MacKay, *J. Controlled Release*, 2011, **155**, 218–226.
29 D. J. Callahan, W. E. Liu, X. H. Li, M. R. Dreher, W. Hassouneh, M. Kim, P. Marszalek and A. Chilkoti, *Nano Lett.*, 2012, **12**, 2165–2170.
30 S. R. MacEwan and A. Chilkoti, *Nano Lett.*, 2012, **12**, 3322–3328.
31 S. R. Aluri, P. Shi, J. A. Gustafson, W. Wang, Y. A. Lin, H. G. Cui, S. L. Liu, P. S. Conti, Z. B. Li, P. S. Hu, A. L. Epstein and J. A. MacKay, *ACS Nano*, 2014, **8**, 2064–2076.
32 C. C. Liang, A. Y. Park and J. L. Guan, *Nat. Protoc.*, 2007, **2**, 329–333.
33 A. J. Simnick, M. Amiram, W. Liu, G. Hanna, M. W. Dewhirst, C. D. Kontos and A. Chilkoti, *J. Controlled Release*, 2011, **155**, 144–151.
34 S. M. Janib, M. Pastuszka, S. Aluri, Z. Folchman-Wagner, P. Y. Hsueh, P. Shi, A. Yi, H. Cui and J. A. Mackay, *Polym. Chem.*, 2014, **5**, 1614–1625.
35 M. J. Berridge and G. Dupont, *Curr. Opin. Cell Biol.*, 1994, **6**, 267–274.
36 G. C. Churchill, M. M. Atkinson and C. F. Louis, *J. Cell Sci.*, 1996, **109**(Pt 2), 355–365.
37 Y. J. Sung, Z. Sung, C. L. Ho, M. T. Lin, J. S. Wang, S. C. Yang, Y. J. Chen and C. H. Lin, *Exp. Cell Res.*, 2003, **287**, 209–218.
38 K. Arakisasaki, Y. Ohashi, T. Sasabe, K. Hayashi, H. Watanabe, Y. Tano and H. Handa, *Invest. Ophthalmol. Visual Sci.*, 1995, **36**, 614–621.
39 J. Wang, N. Wang, J. Xie, S. C. Walton, R. L. McKown, R. W. Raab, P. Ma, S. L. Beck, G. L. Coffman, I. M. Hussaini and G. W. Laurie, *J. Cell Biol.*, 2006, **174**, 689–700.

40 R. Weissleder, K. Kelly, E. Y. Sun, T. Shtatland and L. Josephson, *Nat. Biotechnol.*, 2005, **23**, 1418–1423.
41 A. Verma and F. Stellacci, *Small*, 2010, **6**, 12–21.
42 W. Jiang, B. Y. S. Kim, J. T. Rutka and W. C. W. Chan, *Nat. Nanotechnol.*, 2008, **3**, 145–150.
43 P. M. Dubois, J. Stepinski, J. Urbain and C. H. Sibley, *Eur. J. Immunol.*, 1992, **22**, 851–857.
44 S. Barua, J. W. Yoo, P. Kolhar, A. Wakankar, Y. R. Gokarn and S. Mitragotri, *Proc. Natl. Acad. Sci. U. S. A.*, 2013, **110**, 3270–3275.
45 I. A. Darby, T. Bisucci, T. D. Hewitson and D. G. MacLellan, *Int. J. Biochem. Cell Biol.*, 1997, **29**, 191–200.
46 J. Rich and J. C. Lee, *Diabetes*, 2005, **54**, 2904–2910.
47 K. Y. Lee, M. C. Peters, K. W. Anderson and D. J. Mooney, *Nature*, 2000, **408**, 998–1000.
48 R. Mohan, S. K. Chintala, J. C. Jung, W. V. L. Villar, F. McCabe, L. A. Russo, Y. Lee, B. E. McCarthy, K. R. Wollenberg, J. V. Jester, M. Wang, H. G. Welgus, J. M. Shipley, R. M. Senior and M. E. Fini, *J. Biol. Chem.*, 2002, **277**, 2065–2072.
49 G. M. Gordon, J. S. Austin, A. L. Sklar, W. J. Feuer, A. J. Lagier and M. E. Fini, *J. Cell. Physiol.*, 2011, **226**, 1461–1470.
50 W. Wang, P. G. Sreekumar, V. Valluripalli, P. Shi, J. Wang, Y. A. Lin, H. Cui, R. Kannan, D. R. Hinton and J. A. Mackay, *J. Controlled Release*, 2014, DOI: 10.1016/j.jconrel.2014.04.028.

IN THE UNITED STATES PATENT AND TRADEMARK OFFICE

Applicant:	MACKAY, John Andrew
International Application No.:	To be assigned
International Filing Date:	To be assigned
Title of Invention:	COMPOSITIONS AND METHODS FOR THE DELIVERY OF DRUGS TO THE OCULAR SURFACE BY CONTACT LENSES

ASSERTION OF SMALL ENTITY STATUS

Mail Stop PCT
Commissioner for Patents
P.O. Box 1450
Alexandria, VA 22313-1450

Commissioner:

Pursuant to 37 C.F.R. §1.27(c)(1), Applicant hereby asserts entitlement to small entity status in the above-identified application.

Respectfully submitted,

Date: March 31, 2014

By _____

FOLEY & LARDNER LLP
3000 K Street, Suite 600
Washington, DC 20007-5109
Telephone: 650-856-3700
Facsimile: 202-672-5399

Antoinette F. Konski
Attorney for Applicant
U.S. Registration No. 34,202

COMPOSITIONS AND METHODS FOR THE DELIVERY OF DRUGS TO THE OCULAR SURFACE BY CONTACT LENSES

CROSS-REFERENCE TO RELATED APPLICATIONS

[0001] This application claims the benefit under 35 U.S.C. § 119(e) of U.S. Provisional Application Serial No. 61/806,558, filed March 29, 2013, the contents of which is hereby incorporated by reference into the present disclosure.

BACKGROUND

[0002] Accounting for approximately 90% of all ophthalmic medications, topical ophthalmic solutions (eye drops) have long been the most commonly used method of ocular drug delivery. However, eye drops are generally considered an inefficient drug delivery system that is characterized by a transient overdose, followed by a relatively short period of effective therapeutic concentration, and then a prolonged period of insufficient concentration or underdosing.

[0003] Ophthalmic ointments, an alternative to liquid eye drops, have a longer contact time with the cornea and possibly provide higher chance for drug absorption than a solution due to their high viscosity. Nevertheless as each drop is diluted, the majority of the active agent is washed away by reflex tearing, blinking, or drained through the nasolacrimal system so that only 1 to 7% of an eye drop is absorbed by the eye. To remedy this problem, collagen shields have been proposed to absorb and then slowly release a wide variety of medications. In one application, these shields are applied after surgical procedures involving the corneal epithelium promote re-epithelialization and delivery antibiotic prophylaxis. However, collagen shields are not widely used for daily drug delivery because they lack optical clarity, are difficult to self-insert, are uncomfortable to the patient, and degrade quickly.

[0004] Beyond providing millions of people with glasses-free vision correction, contact lenses have been proposed as a more comfortable way to therapeutically manage ocular anterior segment disorders. Indications for using soft contact lenses therapeutically include protecting a compromised ocular surface, pain management, and promoting epithelialization or wound closure. Many studies report that contact lenses improve the corneal penetration and bioavailability of topically applied pharmaceutical agents using two approaches. In the first method, lenses are soaked in the drug solution for a period of time and then placed on the eye, resulting in a high initial release, followed by a slower, long-term release during hours to days of lens wearing. This method is commonly employed with antibiotics and non-steroidal anti-inflammatory drugs (NSAIDs) postoperatively, and with antibiotics for severe infections.

Alternatively, a topical drug can be applied over the lens while the lens is *in situ*. This approach is necessary when a patient wears a contact lens as a protective device (bandage lens) following a corneal injury or a serious infection, in which case a lens is used as a shield or bandage lens to promote wound repair. The lens absorbs drug from the tear film and then acts as a reservoir, slowly releasing the drug into the tears as the overall concentration of the drug in the tear film declines. Both these approaches prolong the contact time of the drug with the cornea and thus improve penetration of drugs into the cornea. Ongoing research of drug-eluting contact lenses includes copolymerizing the contact lens' hydrogel material (p-HEMA) with other polymers, such as PLGA; releasing drug from microemulsions contained in hydrogel prototype lenses; molecularly imprinted hydrogels, and immobilizing drug-containing liposomes onto the surface of contact lenses. However, achieving sustained, long-term drug delivery at the normal physiological temperature, pH, and salinity of human eye still remains a challenge. Furthermore, it would be desirable to develop contact lens drug carriers that are relatively simple in design: which do not require complicated and expensive manufacturing processes; which do not impair or interfere with the patient's vision; and which do not require a substantial change in the practice patterns of ophthalmologists.

SUMMARY

[0005] To develop new treatments and delivery mechanisms for ocular diseases, new drug vehicles are required that are biocompatible, biodegradable and easily modified with bioactive peptides. An emerging approach to this challenge employs protein polymers to drive reversible assembly of nanostructures. As one example, the elastin-like-polypeptides (ELPs) possess unique phase transition behavior, which mediates self-assembly of nanoparticles. As they are composed from amino acids, protein polymers and ELPs may be produced either by chemical synthesis or by biological expression from an engineered gene expressed by a host cell.

[0006] This document discloses the useful interaction between biocompatible polymeric used for contact lenses and therapeutic materials composed from protein polymers, such as ELPs, that adhere to promote long-term delivery of peptide therapeutics for the enhanced treatment of ocular diseases and disorders.

[0007] Thus, in one aspect, this disclosure describes a biocompatible, polymeric material that comprises, or alternatively consists essentially of, or yet further consists of a biocompatible, polymeric material and an ELP. In one aspect, the polymeric material is a material comprising one or more of poly(hydroxyl ethyl methacrylate), methacrylic acid, N-vinyl pyrrolidone, cyclohexyl methacrylate, N,N-dimethyl acrylamide or a contact lens material, non-limiting examples of such are provide in Table 1 although any suitable biocompatible, polymeric material

may be used and therefore, the disclosure is not so limited. In one aspect the ELP is attached to the polymeric material in a random fashion or alternatively, attached in a pre-determined design such one or more concentric rings, or only in the center of the polymeric material or alternatively, only around the periphery of the polymeric material, or alternatively in swirls or stamped blocked or rectangular geometries. In one particular aspect, the ELP is attached to the polymer in one or more concentric rings.

[0008] The ELP component of the polymeric material can be any ELP known in the art which includes those obtained from either chemical or biological synthetic rountes. In one aspect, the ELP is a diblock polypeptide. Non-limiting examples of such include one or more of the ELPs described herein, which optionally includes one or more of SEQ ID NOS: 1 to 6, or a biological equivalent of each thereof. In a further aspect, the polymeric material-ELP is combined with a pharmaceutically acceptable carrier, such as saline or the like, to maintain the polymeric material's biocompatible characteristics.

[0009] In a further aspect, the polymeric material further comprises, or consists essentially of, or yet further consists of a detectable label, e.g., a fluorophore or a detectable dye.

[0010] In one aspect, the polymeric material and ELP further comprises a therapeutic agent bound to the ELP or encapsulated within the ELP. Non-limiting examples of a therapeutic agent include a peptide, a protein, an antibody, an antibody fragment or a small molecule. In a different aspect, the therapeutic acts as a growth factor, an anti-microbial agent or a non-steroidal anti-inflammatory drug. In a further aspect, an effective amount of the therapeutic is bound to the ELP and polymeric material. In different further aspects, the polymeric material-ELP is combined with a pharmaceutically acceptable carrier, such as saline or the like, to maintain the therapeutic agent's effectiveness and/or the polymeric material's biocompatible characteristics.

[0011] Methods to link or encapsulate a therapeutic agent to the ELP are described in International Application No.: PCT/US2013/64719, filed October 11, 2013, incorporated by reference herein. In one embodiment, the therapeutic agent is fused to the ELP by covalent attachment to a cleavable peptide sequence located between the therapeutic agent and the ELP In one aspect, the cleavable peptide sequence is a thrombin cleavable peptide sequence which comprises the amino acid sequence GLVPR$_{\downarrow}$GS (SEQ ID NO.: 7), or a biological equivalent thereof, wherein a biological equivalent is a sequence having at least 80% sequence identity, or alternatively at least 90% sequence identity, or alternatively at least 95 % sequence identity to SEQ ID NO: 7, or a sequence that hybridizes under conditions of high stringency to the polynucleotide that encodes the sequence or its complement.

[0012] In one aspect, the therapeutic agent is the lacritin protein, a fragment of lacritin, or a biological equivalent thereof. This strategy is used to delivery other peptide therapeutics including growth factors, including but not limited to Epidermal Growth Factor (EGF), transforming growth factor beta (TGF-β), human growth factor (HGF). In one embodiment, the lacritin comprises SEQ ID NO.: 8 or 10, or a biological equivalent of each thereof, which is covalently fused to the ELP either directly or via a cleavable peptide sequence located between the therapeutic agent and the ELP. . To biologically express a fusion peptide between an ELP and a therapeutic, DNA encoding a cleavable peptide sequence is inserted between that encoding for the therapeutic agent and ELP sequence. Using conventional molecular biology methodology, the resulting gene fusion can be cloned into a plasmid that encodes for antibiotic resistance and transformed into prokaryotic or eukaryotic host cells, including but not limited to BLR(DE3) competent cells, Origami^{TM} B competent cells, or HEK-293 cells. Transformants expressing the fusion protein can be isolated using antibiotic selection, such as ampicillin, kanamycin, or gentamycin. Alternatively, the cleavage sequence can be added between ELPs and the therapeutic peptide that are produced using solid-phase peptide synthesis. Alternatively, cleavage sequence can be added after/before therapeutic agent protein sequence using solid-phase peptide synthesis. In one aspect, the cleavable peptide sequence is a thrombin cleavable peptide sequence which comprises the amino acid sequence GLVPR↓GS (SEQ ID NO. 7), or a biological equivalent thereof (as defined herein). A non-limiting example of the lacritin-ELP amino acid sequence comprises the amino acid sequence of SEQ ID NO: 9 or a biological equivalent thereof.

[0013] This disclosure also provide the isolated polynucleotides that encode the polypeptide ELPs as described above which can be contained within an expression vector for recombinant expression in a host cell. Accordingly, the isolated host cells comprising the isolated polynucleotides and/or ELP polypeptides, that in one aspect contain the therapeutic peptide, are within the scope of this disclosure. Methods to prepare the ELP alone or in combination with the therapeutic are within the scope of this disclosure and described herein. Methods to prepare the polymeric material of this disclosure is further provided, as is the method comprising absorbing, conjugating, or coating a polymeric material with the ELP, alone or in combination with the therapeutic agent.

[0014] The polymeric materials as described herein are useful for delivering a therapeutic agent, the method comprising contacting the polymeric material topically or internally, with a subject to be treated. As used herein, the term “subject” intends an animal, such as a mammal, e.g., a canine, an equine, a rabbit, or feline, or a human patient. In one aspect, the polymeric

material is in contact with the ocular surface of an eye. Thus, the polymeric material is useful in methods for treating an ocular disease, comprising contacting the polymeric material with the eye of a patient in need of such treatment. Non-limiting examples of an ocular disease that can be treated by this method includes without limitation dry eye, age-related macular degeneration, diabetic retinopathy, retinal venous occlusions, retinal arterial occlusion, macular edema, postoperative inflammation, infection, dryness, uveitis retinitis, proliferative vitreoretinopathy and glaucoma.

[0015] This disclosure also provides a kit comprising one or more polymeric materials, alone or in combination with a therapeutic agent and instructions for use as described herein.

BRIEF DESCRIPTION OF THE FIGURES

[0016] **FIGS. 1A-D** show NHS-Rhodamine labeled V96 (Rho-V96) selectively phase separated onto Proclear Contact lens. A) Rho-V96 on SDS-PAGE. B) Reversible temperature dependent phase transition behavior of Rho-V96 at 500μM. C) Fluorescence image of contact lenses after Rho-V96 phase separation. D) Contact lens modification process at 37ºC. *1. Proclear Compatibles contact lens (CooperVision); 2. Dailies (CIBA Vision); 3. Acuvue OASYS (Johnson & Johnson Vision Care); 4. Acuvue Advance Plus (Johnson & Johnson Vision Care). Pictures were captured using Bio-Rad VersaDoc MP System.

[0017] **FIGS. 2A-D** show that the protein polymer architecture controls rate of release from contact lenses. A) A therapeutic protein, lacritin, fused to an ELP. B) ELPs adhere and release from contact lenses. C) Representative rhodamine-ELP labeled Proclear contact lenses. D) Confocal laser scanning microscopy of rhodamine-labeled ELPs incubated with contact lenses at 37 °C. Soluble ELPs (Rho-S96) washed away immediately. ELP nanoparticles (Rho-S48I48) form embedded puncta within the lens. ELP coacervate (Rho-V96) uniformly stains the lens, which was retained at high levels after 3 days. Scale bar: 50 μm.

[0018] **FIGS. 3A-E** show the ELP phase transition extended retention time of Rho-V96 on contact lens. A) Proclear contact lenses were incubated with equal concentration of Rho-V96 (100μM) at 4°C and 37°C for overnight. 37°C incubation showed significantly higher ELP retention than 4°C. B) Proclear contact lens incubated in Rho-V96 (100μM) at 37°C was cut into two halves and incubated at 37°C or 4°C ddH2O for overnight. Contact lens incubated at 37°C exhibited higher Rho-V96 retention. C, D&E) Rho-V96 phase separation onto Proclear contact lens is a reversible process. Three individual lenses were modified with Rho-V96 at 37°C, gently washed in PBS at 37°C and incubated in 2ml PBS for one week (168h). Equal amount of sample (100 μl) was taken out from incubating solution at each time point (0h, 30 min,

1h, 2h, 4h, 8h, 12h, 24h, 48h, 96h, 168h). After one week, lenses were incubated in 1.5 ml fresh PBS at 4°C for 24 h (Wash 1) with gentle shaking. Washing step was repeated once in another 1.5 ml fresh PBS at 4°C for 24h (Wash 2) with gentle shaking. After measuring fluorescence of all collected samples using fluorescent plate reader (D), samples were concentrated to equal volume using Amicon Ultra protein concentrator (3kD cut-off). Equal volume of samples was loaded onto 4-20% gradient gel and imaged using Bio-Rad VersaDoc MP System (C). Protein retention ratio was characterized using ImageJ (E). 96.2±1.8% of total fluorescence and 99.1±2.3% of total protein was retained on the lens after one week incubation at 37°C.

[0019] **Figures 4A and B** show that ELP selectively phase separate onto Proclear compatibles™ contact lens. A) Among four types of contact lens tested, rhodamine labeled V96 selectively phase separated onto Proclear compatibles™ contact lens. 1: Proclear compatibles™; 2: Dailies (AquaComfort Plus); 3: Acuvue OASYS; 4: Acuvue Advance Plus. B) Different shapes of rhodamine labeled V96 on Proclear compatibles™ contact lens. Upper: white light; lower: fluorescence.

[0020] **Figures 5 A to E** show T_t and temperature dependent affinity of ELPs towards Proclear Compatible™ contact lens. A) Representative picture showing different affinity of V96 and S96 to the lens at 37°C and 4°C after 24 h incubation. B) Total fluorescence intensity quantification result showing ELPs' attachment to the lens was T_t and temperature dependent. C) Group one exhibited high retention on the lens after one week incubation at 37°C. D) Group two, three and four showed similar release pattern and can fit into same two-phase decay model. E) Group five illustrated different release kinetics from group one, with significant lower plateau. ***$p<0.001$; grey line: predicted values using one phase decay model; grey dash line: predicted values using two phase decay model.

[0021] **Figures 6A to G** show spatiotemporal HCE-T cell uptake. A) Representative pictures showing time dependent uptake of Lac and Lac-V96 into HCE-T cells. B-C Quantification result showing V96 tag modulated cell uptake speed and amount of exogenous Lac. D) Cartoon showing rho-Lac-V96 "ring" modified contact lens with three representative regions. 1: rho-Lac-V96 fully covered cell region; 2: cell region half covered by rho-Lac-V96; 3: cell region not covered by the lens. E-G) Representative pictures showing HCE-T cell uptake of rho-Lac-V96 in three regions delivered by contact lens. Red: rhodamine; Blue: DAPI staining of nuclei.

DETAILED DESCRIPTION

Definitions

[0022] The practice of the present invention will employ, unless otherwise indicated, conventional techniques of tissue culture, immunology, molecular biology, microbiology, cell biology and recombinant DNA, which are within the skill of the art. See, e.g., Sambrook et al., (1989) Molecular Cloning: A Laboratory Manual, 2nd edition; Ausubel et al., eds. (1987) Current Protocols In Molecular Biology; MacPherson, B.D. Hames and G.R. Taylor eds., (1995) PCR 2: A Practical Approach; Harlow and Lane, eds. (1988) Antibodies, A Laboratory Manual; Harlow and Lane, eds. (1999) Using Antibodies, a Laboratory Manual; and R.I. Freshney, ed. (1987) Animal Cell Culture.

[0023] All numerical designations, e.g., pH, temperature, time, concentration, and molecular weight, including ranges, are approximations which are varied (+) or (-) by increments of 1.0 or 0.1, as appropriate. It is to be understood, although not always explicitly stated that all numerical designations are preceded by the term “about”. It also is to be understood, although not always explicitly stated, that the reagents described herein are merely exemplary and that equivalents of such are known in the art.

[0024] As used in the specification and claims, the singular form “a,” “an” and “the” include plural references unless the context clearly dictates otherwise.

[0025] As used herein, the term “comprising” is intended to mean that the compositions and methods include the recited elements, but do not exclude others. “Consisting essentially of” when used to define compositions and methods, shall mean excluding other elements of any essential significance to the combination when used for the intended purpose. Thus, a composition consisting essentially of the elements as defined herein would not exclude trace contaminants or inert carriers. “Consisting of” shall mean excluding more than trace elements of other ingredients and substantial method steps. Embodiments defined by each of these transition terms are within the scope of this invention.

[0026] The term "purified protein or peptide" as used herein, is intended to refer to a composition, isolatable from other components, wherein the protein or peptide is purified to any degree relative to its naturally-obtainable state. A purified protein or peptide therefore also refers to a protein or peptide, free from the environment in which it may naturally occur.

[0027] The term “therapeutic agent” refers to an agent or component capable of inducing a biological effect in vivo and/or in vitro, such as for example an anti-inflammation agent, an antibiotic, a polypeptides and diverse protein/antibody therapeutic libraries via encapsulation or

recombinant protein expression, a small molecule, a nucleic acid, a protein, antibody, antibody fragment or a polypeptide. Strategies for incorporation of therapeutic agents are described in International Patent Appl. No: PCT/US2013/64719, filed October 11, 2013. Non-limiting examples of therapeutic agents include lactrintin, cyclosporin A, ketorolac, nepafenac, bromfenac; antibiotics such as Bacitracin, Erythromycin; growth factors such as Epidermal Growth Factor (EGF), Transforming Growth Factor Beta (TGF-β), Hepatocyte Growth Factor (HGF); protease inhibitors such as Matrix Metallopeptidase 2 (MMP-2) or Matrix Metallopeptidase 9 (MMP-9). The biological effect may be useful for treating and/or preventing a condition, disorder, or disease in a subject or patient.

[0028] As used herein, the term "biological equivalent thereof" is used synonymously with "equivalent" unless otherwise specifically intended. When referring to a reference protein, polypeptide or nucleic acid, the term intends those having minimal homology while still maintaining desired structure or functionality. Unless specifically recited herein, it is contemplated that any polynucleotide, polypeptide or protein mentioned herein also includes equivalents thereof. For example, an equivalent intends at least about 60%, or 65%, or 70%, or 75%, or 80 % homology or identity and alternatively, at least about 85 %, or alternatively at least about 90 %, or alternatively at least about 95 %, or alternatively 98 % percent homology or identity and exhibits substantially equivalent biological activity to the reference protein, polypeptide or nucleic acid. Alternatively, a biological equivalent is a peptide encoded by a nucleic acid that hybridizes under stringent conditions to a nucleic acid or complement that encodes the peptide. Hybridization reactions can be performed under conditions of different "stringency". In general, a low stringency hybridization reaction is carried out at about 40°C in about 10 x SSC or a solution of equivalent ionic strength/temperature. A moderate stringency hybridization is typically performed at about 50°C in about 6 x SSC, and a high stringency hybridization reaction is generally performed at about 60°C in about 1 x SSC. Hybridization reactions can also be performed under "physiological conditions" which is well known to one of skill in the art. A non-limiting example of a physiological condition is the temperature, ionic strength, pH and concentration of Mg^{2+} normally found in a cell.

[0029] A polynucleotide or polynucleotide region (or a polypeptide or polypeptide region) having a certain percentage (for example, about 60%, 65%, 70%, 75%, 80%, 85%, 90%, 95% or 97%) of "sequence identity" to another sequence means that, when aligned, that percentage of bases (or amino acids) are the same in comparing the two sequences. The alignment and the percent homology or sequence identity can be determined using software programs known in the art, for example those described in Current Protocols in Molecular Biology (Ausubel et al., eds.

1987) Supplement 30, section 7.7.18, Table 7.7.1. Preferably, default parameters are used for alignment. A preferred alignment program is BLAST, using default parameters. In particular, preferred programs are BLASTN and BLASTP, using the following default parameters: Genetic code = standard; filter = none; strand = both; cutoff = 60; expect = 10; Matrix = BLOSUM62; Descriptions = 50 sequences; sort by = HIGH SCORE; Databases = non-redundant, GenBank + EMBL + DDBJ + PDB + GenBank CDS translations + SwissProtein + SPupdate + PIR. Details of these programs can be found at the following Internet address: ncbi.nlm.nih.gov/cgi-bin/BLAST.

[0030] "Homology" or "identity" or "similarity" refers to sequence similarity between two peptides or between two nucleic acid molecules. Homology can be determined by comparing a position in each sequence which may be aligned for purposes of comparison. When a position in the compared sequence is occupied by the same base or amino acid, then the molecules are homologous at that position. A degree of homology between sequences is a function of the number of matching or homologous positions shared by the sequences. An "unrelated" or "non-homologous" sequence shares less than 40% identity, or alternatively less than 25% identity, with one of the sequences of the present invention.

[0031] An "equivalent" is used in the alternative with "biological equivalent" of a polynucleotide or polypeptide refers to a polynucleotide or a polypeptide having a substantial homology or identity to the reference polynucleotide or polypeptide. In one aspect, a "substantial homology" is greater than about 60%, 65%, 70%, 75%, 80%, 85%, 90%, 95% or 98% homology.

[0032] As used herein, "expression" refers to the process by which polynucleotides are transcribed into mRNA and/or the process by which the transcribed mRNA is subsequently being translated into peptides, polypeptides, or proteins. If the polynucleotide is derived from genomic DNA, expression may include splicing of the mRNA in an eukaryotic cell.

[0033] The term "encode" as it is applied to polynucleotides refers to a polynucleotide which is said to "encode" a polypeptide if, in its native state or when manipulated by methods well known to those skilled in the art, it can be transcribed and/or translated to produce the mRNA for the polypeptide and/or a fragment thereof. The antisense strand is the complement of such a nucleic acid, and the encoding sequence can be deduced therefrom.

[0034] "Regulatory polynucleotide sequences" intends any one or more of promoters, operons, enhancers, as known to those skilled in the art to facilitate and enhance expression of polynucleotides.

[0035] An “expression vehicle” is a vehicle or a vector, non-limiting examples of which include viral vectors or plasmids, that assist with or facilitate expression of a gene or polynucleotide that has been inserted into the vehicle or vector.

[0036] A “delivery vehicle” is a vehicle or a vector that assists with the delivery of an exogenous polynucleotide into a target cell. The delivery vehicle may assist with expression or it may not, such as traditional calcium phosphate transfection compositions.

[0037] A “composition” is intended to mean a combination of active agent and another compound or composition, inert (for example, the polymeric material of this disclosure, a solid support or pharmaceutically acceptable carrier) or active, such as an adjuvant.

[0038] A “pharmaceutical composition” is intended to include the combination of an active agent with a carrier, inert or active (e.g., the polymeric material of this disclosure), making the composition suitable for diagnostic or therapeutic use in vitro, in vivo or ex vivo.

[0039] “An effective amount” refers to the amount of an active agent or a pharmaceutical composition sufficient to induce a desired biological and/or therapeutic result. That result can be alleviation of the signs, symptoms, or causes of a disease, or any other desired alteration of a biological system. The effective amount will vary depending upon the health condition or disease stage of the subject being treated, timing of administration, the manner of administration and the like, all of which can be determined readily by one of ordinary skill in the art.

[0040] As used herein, the terms "treating," "treatment" and the like are used herein to mean obtaining a desired pharmacologic and/or physiologic effect. The effect may be prophylactic in terms of completely or partially preventing a disorder or sign or symptom thereof, and/or may be therapeutic in terms of a partial or complete cure for a disorder and/or adverse effect attributable to the disorder.

[0041] As used herein, to “treat” further includes systemic amelioration of the symptoms associated with the pathology and/or a delay in onset of symptoms. Clinical and sub-clinical evidence of “treatment” will vary with the pathology, the subject and the treatment.

[0042] “Administration” can be effected in one dose, continuously or intermittently throughout the course of treatment. Methods of determining the most effective means and dosage of administration are known to those of skill in the art and will vary with the composition used for therapy, the purpose of the therapy, the target cell being treated, and the subject being treated. Single or multiple administrations can be carried out with the dose level and pattern being selected by the treating physician. Suitable dosage formulations and methods of administering the agents are known in the art.

[0043] The agents and compositions of the present invention can be used in the manufacture of medicaments and for the treatment of humans and other animals by administration in accordance with conventional procedures, such as an active ingredient in pharmaceutical compositions.

[0044] As used herein, the term "detectable label" intends a directly or indirectly detectable compound or composition that is conjugated directly or indirectly to the composition to be detected, e.g., N-terminal histidine tags (N-His), magnetically active isotopes, e.g., ^{115}Sn, ^{117}Sn and ^{119}Sn, a non-radioactive isotopes such as ^{13}C and ^{15}N, polynucleotide or protein such as an antibody so as to generate a "labeled" composition. The term also includes sequences conjugated to the polynucleotide that will provide a signal upon expression of the inserted sequences, such as green fluorescent protein (GFP) and the like. The label may be detectable by itself (e.g. radioisotope labels or fluorescent labels) or, in the case of an enzymatic label, may catalyze chemical alteration of a substrate compound or composition which is detectable. The labels can be suitable for small scale detection or more suitable for high-throughput screening. As such, suitable labels include, but are not limited to magnetically active isotopes, non-radioactive isotopes, radioisotopes, fluorochromes, luminescent compounds, dyes, and proteins, including enzymes. The label may be simply detected or it may be quantified. A response that is simply detected generally comprises a response whose existence merely is confirmed, whereas a response that is quantified generally comprises a response having a quantifiable (e.g., numerically reportable) value such as intensity, polarization, and/or other property. In luminescence or fluorescence assays, the detectable response may be generated directly using a luminophore or fluorophore associated with an assay component actually involved in binding, or indirectly using a luminophore or fluorophore associated with another (e.g., reporter or indicator) component.

[0045] Examples of luminescent labels that produce signals include, but are not limited to bioluminescence and chemiluminescence. Detectable luminescence response generally comprises a change in, or an occurrence of, a luminescence signal. Suitable methods and luminophores for luminescent labeling assay components are known in the art and described for example in Haugland, Richard P. (1996) Handbook of Fluorescent Probes and Research Chemicals (6th ed.). Examples of luminescent probes include, but are not limited to, aequorin and luciferases.

[0046] Examples of suitable fluorescent labels include, but are not limited to, fluorescein, rhodamine, tetramethylrhodamine, eosin, erythrosin, coumarin, methyl-coumarins, pyrene, Malacite green, stilbene, Lucifer Yellow, Cascade Blue^{TM}, and Texas Red. Other suitable

optical dyes are described in the Haugland, Richard P. (1996) Handbook of Fluorescent Probes and Research Chemicals (6th ed.).

[0047] In another aspect, the fluorescent label is functionalized to facilitate covalent attachment to a cellular component present in or on the surface of the cell or tissue such as a cell surface marker. Suitable functional groups, including, but not are limited to, isothiocyanate groups, amino groups, haloacetyl groups, maleimides, succinimidyl esters, and sulfonyl halides, all of which may be used to attach the fluorescent label to a second molecule. The choice of the functional group of the fluorescent label will depend on the site of attachment to either a linker, the agent, the marker, or the second labeling agent.

[0048] The term "contact lens" refers to the entire product that is placed in contact with the cornea. Non-limiting examples of commercially available contact lenses are listed in Table 1. Generally, contact lenses comprise a central lens with a diameter of 7-9 mm. The central lens of conventional contact lenses contains front and back surface curvatures that combine to create the optical power of the lens (after accounting for lens thickness and refractive index of the lens material). In addition to the central lens, contact lenses also conventionally comprise an outer region. The outer region is located between the edge of the central lens and the edge of the contact lens. Conventionally, the outer region of a contact lens is designed to provide a comfortable fitting of the lens to the eye, and causes minimal physiological disruption to the normal functioning of the eye. The contact lenses utilized in the present disclosure may be customized or conventional contact lenses designed based on the unique low and high order aberrations of each individual eye. Conventional contact lenses correct low order aberrations (myopia, hyperopia and astigmatism), whereas customized contact lenses also correct high order aberrations including optical characteristics such as coma, spherical aberration and trefoil. Preferably, the forces applied to the eye by the upper and/or lower eyelid are dispersed so that the optical characteristics of the eye are unchanged by downward gaze or near work. Contact lenses used in the present disclosure may also be corrective (i.e. corrects a vision defect) or non-corrective (i.e. no correction of vision defect). In certain embodiments, the contact lens may be non—corrective and serve as a drug carrier for the efficient delivery of therapeutic agents and proteins to the eye of a patient in need thereof. U.S. patent publication 2011/0230588 describes methods of making hydrogel or soft contact lenses. Table 1 shows a summary of contact lenses commercially available. Both traditional and p-HEMA hydrogel contact lenses and silicone hydrogel contact lenses are included within this disclosure.

Table 1: Contact lens material characteristics

Commercial Name (supplier)	Polymer composition	Listed water content (%)	Measured water volume[a] (mL)	Oxygen permeability (barrers[b])	FDA category
Optima FW (Bausch & Lomb, Rochester, NY)	Polymacon p-HEMA/NVP/CMA	38	0.01048	9	Group I (non-ionic, low water content)
Focus Night & Day (Ciba Vision, Duluth, GA)	Lotrafilcon A DMA/Siloxane macromer	24	0.00448	140	Group I (non-ionic, low water content)
Softlens 66 (Bausch & Lomb, Rochester, NY)	Alphafilcon A p-HEMA/NVP/CMA	66	0.0231	30	Group II (non-ionic, high water content)
Proclear Compatibles (Biocompatibles, Norfolk, VA)	Omafilcon A p-HEMA/phosphorylcholine	59	0.01741	22	Group II (non-ionic, high water content)
PureVision (Bausch & Lomb, Rochester, NY)	Balafilcon A Siloxane macromer/NVP	36	0.00956	99	Group III (ionic, low water content)
Acuvue/Surevue (Johnson & Johnson, Jackonsonville, FL)	Etafilcon A p-HEMA/MA	58	0.01588	21	Group IV (ionic, high water content)
Focus Monthly (Ciba Vision, Duluth, GA)	Vifilcon A p-HEMA/MA/NVP	55	0.01588	19	Group IV (ionic, high water content)

p-HEMA, poly(hydroxyl ethyl methacrylate); MA, methacrylic acid; NVP, N-vinyl pyrrolidone; CMA, cyclohexyl methacrylate; DMA, N,N-dimethyl acrylamide.

[a] Volume of water in the contact lens as obtained by subtracting the wet lens from the dry lens weight.

[b] 1 barrer = 10^{-11} (cm^3mL O_2)/s mL mm Hg), obtained from the contact lens package inserts.

[0049] By "biocompatible," it is meant that the components of the delivery system will not cause tissue injury or injury to the human biological system. To impart biocompatibility, polymers and excipients that have had history of safe use in humans or with GRAS (Generally Accepted As Safe) status, will be used preferentially. For a composition to be biocompatible, and be regarded as non-toxic, it must not cause toxicity to cells.

[0050] The term "polymeric material", refers a material comprising a polymer matrix and a plurality of interconnecting pores. Non-limiting examples of polymeric materials include polymers comprising unsaturated carboxylic acids, such as methacrylic acid and acrylic acid; (meth)acrylic substituted alcohols, such as 2-hydroxyethylmethacrylate and 2-hydroxyethylacrylate; vinyl lactams, such as N-vinyl pyrrolidone; (meth)acrylamides, such as methacrylamide and N,N-dimethylacrylamide, poly(hydroxyl ethyl methacrylate); N-vinyl pyrrolidone; and cyclohexyl methacrylate.

[0051] The term "fuse," "fused" or "link" refers to the covalent linkage between two polypeptides in a fusion protein. The polypeptides are typically joined via a peptide bond, either directly to each other or via an amino acid linker. Optionally, the peptides can be joined via non-peptide covalent linkages known to those of skill in the art.

[0052] The term "cleavable peptide" refers to a peptide that may be cleaved by a molecule or protein. By way of example, cleavable peptide spacers include, without limitation, a peptide sequence recognized by proteases (in vitro or in vivo) of varying type, such as Tev, thrombin, factor Xa, plasmin (blood proteases), metalloproteases, cathepsins (e.g., GFLG, etc.), and proteases found in other corporeal compartments. In some embodiments employing cleavable peptides, the fusion protein (i.e. therapeutic protein) may be inactive, less active, or less potent as a fusion, which is then activated upon cleavage of the spacer *in vivo*.

[0053] As used herein, the term “elastin-like peptide (ELP) component” intends a polypeptide that forms stable nanoparticle (also known as a micelle) above the transition temperature of the ELP. In another aspect, the ELP component comprises, or alternatively consists essentially of, or yet further consists of the polypeptide S48I48 having the sequence G(VPGSG)n(VPGIG)nY (SEQ ID NO: 1)or a biological equivalent thereof, wherein n is an integer that denotes the number of repeats, and can be from about 6 to about 192, or alternatively from about 15 to 75, or alternatively from about 40 to 60, or alternatively from about 45 to 55, or alternatively about 48), wherein in one aspect, S48I48 comprises, or alternatively consists essentially of, or yet further consists of the amino acid sequence $G(VPGSG)_{48}(VPGIG)_{48}Y$, or a biological equivalent thereof. A biological equivalent of polypeptide S48I48 is a peptide that has at least 80% sequence identity to polypeptide S48I48 or a peptide encoded by a polynucleotide that

hybridizes under conditions of high stringency to a polynucleotide that encodes polypeptide S48I48 or its complement, wherein conditions of high stringency comprise hybridization reaction at about 60°C in about 1 x SSC. The biological equivalent will retain the characteristic or function of forming a nanoparticle (also known as a micelle) when the biological equivalent is raised above the transition temperature of the biological equivalent or, for example, the transition temperature of S48I48.

[0054] In another aspect, the ELP comprises, or alternatively consists essentially of, or yet further consists of, the polypeptide (VPGSG)n (SEQ ID NO: 5) or a biological equivalent thereof, wherein n is an integer that denotes the number of repeats, and can be from about 6 to about 192, or alternatively from about 15 to 125, or alternatively from about 50 to 110, or alternatively from about 90 to 100, or alternatively about 96 $(VPGSG)_{96}$ (SEQ ID NO: 2) or a biological equivalent of each thereof. A biological equivalent of polypeptide is a peptide that has at least 80% sequence identity to SEQ ID No: 2 or a peptide encoded by a polynucleotide that hybridizes under conditions of high stringency to a polynucleotide that encodes SEQ ID NOS: 2 or 5, or the respective complements, wherein conditions of high stringency comprise hybridization reaction at about 60°C in about 1 x SSC. The biological equivalent will retain the characteristic or function of forming a nanoparticle (also known as a micelle) when the biological equivalent is raised above the transition temperature of the biological equivalent or, for example, the transition temperature of SEQ ID NOS: 2 or 5.

[0055] In another aspect, the ELP comprises, or alternatively consists essentially of, or yet further consists of, the polypeptide (VPGVG)n (SEQ ID NO: 6) or a biological equivalent thereof, wherein n is an integer that denotes the number of repeats, and can be from about 6 to about 192, or alternatively from about 15 to 125, or alternatively from about 50 to 110, or alternatively from about 90 to 100, or alternatively about 96) $(VPGIG)_{96}$ (SEQ ID NO: 3) or a biological equivalent of each thereof. A biological equivalent of polypeptide is a peptide that has at least 80% sequence identity to SEQ ID NOS: 3 or 6, or a peptide encoded by a polynucleotide that hybridizes under conditions of high stringency to a polynucleotide that encodes SEQ ID NOS: 3 or 6, or its complement, wherein conditions of high stringency comprise hybridization reaction at about 60°C in about 1 x SSC. The biological equivalent will retain the characteristic or function of forming a nanoparticle (also known as a micelle) when the biological equivalent is raised above the transition temperature of the biological equivalent or, for example, the transition temperature of SEQ ID NOS: 3 or 6.

[0056] In another aspect, the ELP comprises, or alternatively consists essentially of, or yet further consists of, the repeated pentapeptide sequences, $(VPGXG)_n$ (SEQ ID NO: 4) or a

biological equivalent thereof, derived from human tropoelastin, where X is the "guest residue" which is any amino acid and n is the number of repeats. In one aspect, n is an integer from about 6 to about 192, or alternatively from about 15 to 75, or alternatively from about 40 to 60, or alternatively from about 45 to 55, or alternatively about 48). A biological equivalent of polypeptide $(VPGXG)_n$ is a peptide that has at least 80% sequence identity to polypeptide, or a peptide encoded by a polynucleotide that hybridizes under conditions of high stringency to a polynucleotide that encodes polypeptide $(VPGXG)_n$ or its complement, wherein conditions of high stringency comprise hybridization reaction at about 60°C in about 1 x SSC. The biological equivalent will retain the characteristic or function of forming a nanoparticle (also known as a micelle) when the biological equivalent is raised above the transition temperature of the biological equivalent or, for example, the transition temperature of $(VPGXG)_n$.

Elastin-like polypeptides (ELPs)

[0057] This disclosure relates to polymeric materials and contact lenses comprising genetically engineered polypeptide nanoparticles. To develop new treatments for ocular diseases, new drug carriers are required that are biocompatible and easily modified with bioactive peptides. An emerging solution to this challenge utilizes genetically engineered polypeptides to drive the assembly of nanostructures.

[0058] Elastin-like-polypeptides (ELPs) are a genetically engineered polypeptide with unique phase behavior (see for e.g. S.R. MacEwan, et al., Biopolymers 94(1) (2010) 60-77) which promotes recombinant expression, protein purification and self-assembly of nanostructures (see for e.g. A. Chilkoti, et al., Advanced Drug Delivery Reviews 54 (2002) 1093-1111). In one aspect, the ELP is as described above, e.g., any one or more of SEQ ID NOS: 1 to 6 or a biological equivalent thereof.

[0059] In another aspect the ELP is composed of repeated pentapeptide sequences, $(VPGXG)_n$ (SEQ ID. NO: 4) derived from human tropoelastin, where X is the "guest residue" which is any amino acid and n is the number of repeats or a biological equivalent thereof. In one aspect, n is an integer from about 6 to about 192, or alternatively from about 15 to 75, or alternatively from about 40 to 60, or alternatively from about 45 to 55, or alternatively about 48). A biological equivalent of polypeptide $(VPGXG)_n$ is a peptide that has at least 80% sequence identity to polypeptide, or a peptide encoded by a polynucleotide that hybridizes under conditions of high stringency to a polynucleotide that encodes polypeptide $(VPGXG)_n$ or its complement, wherein conditions of high stringency comprise hybridization reaction at about 60°C in about 1 x SSC. The biological equivalent will retain the characteristic or function of forming a nanoparticle (also known as a micelle) when the biological equivalent is raised above the transition

temperature of the biological equivalent or, for example, the transition temperature of $(VPGXG)_n$. In one embodiment, X is any amino acid except proline. This peptide motif displays rapid and reversible de-mixing from aqueous solutions above a transition temperature, T_t. Below T_t, ELPs adopt a highly water soluble random coil conformation; however, above T_t, they separate from solution, coalescing into a second aqueous phase. The T_t of ELPs can be tuned by choosing the guest residue and ELP chain length as well as fusion peptides at the design level (see for e.g. MacEwan SR, et al., Biopolymers 94(1): 60-77). The ELP phase is both biocompatible and highly specific for ELPs or ELP fusion proteins, even in complex biological mixtures. Genetically engineered ELPs are monodisperse, biodegradable, non-toxic. Throughout this description, ELPs are identified by the single letter amino acid code of the guest residue followed by the number of repeat units, *n*. For example, S48I48 represents a diblock copolymer ELP with 48 serine (**S**) pentamers ($[VPGSG]_{48}$, SEQ ID. NO: 5) at the amino terminus and 48 isoleucine (**I**) pentamers ($[VPGIG]_{48}$, SEQ ID. NO: 6) at the carboxy terminus. A "diblock" as used herein refers to an ELP with two blocks of repeated polypeptide sequence. For example, the diblock $(VPGSG)_{48}$ $(VPGIG)_{48}$ (SEQ ID. NO: 1) comprises 48 repeated units of a polypeptide having the sequence VPGSG (SEQ ID NO: 5) and 48 repeated units of a polypeptide having the sequence VPGIG (SEQ ID. NO: 6). In one embodiment, the ELP component comprises a polypeptide with the sequence of SEQ ID. NO: 1. In each of the above embodiments, the ELP can comprise a biological equivalent thereof.

[0060] In further embodiments, the ELP component comprises, consists essentially of, or yet consists of, a polypeptide with the sequence $(VPGSG)_{48}(VPGIG)_{48}$ (SEQ ID. NO: 1), $(VPGSG)_{96}$ (SEQ ID. NO: 2) or $(VPGVG)_{96}$ (SEQ ID. NO: 3) or a biological equivalent or each thereof.

[0061] Described herein are ELP fusion proteins, which can be self assembled into nanoparticles. The diameter of the nanoparticle can be from about 1 to about 1000 nm or from about 1 to about 500 nm, or from about 1 to about 100 nm, or from about 1 to about 50 nm, or from about 20 to about 50 nm, or from about 30 to about 50 nm, or from about 35 to about 45 nm. In one embodiment, the diameter is about 40 nm.

[0062] In one embodiment, the ELP component may further comprise a therapeutic agent. ELP fusion proteins are able to conjugate small molecules, such as, for example, chemotherapeutic agents, anti-inflammation agents, antibiotics and polypeptides and other water soluble drugs. In addition, the ELP nanoparticles are useful for carrying DNA, RNA, protein and peptide-based therapeutics.

[0063] ELPs have potential advantages over chemically synthesized polymers as drug delivery agents. First, because they are biosynthesized from a genetically encoded template, ELPs can be made with precise molecular weight. Chemical synthesis of long linear polymers does not typically produce an exact length, but instead a range of lengths. Consequently, fractions containing both small and large polymers yield mixed pharmacokinetics and biodistribution. Second, ELP biosynthesis produces very complex amino acid sequences with nearly perfect reproducibility. This enables very precise selection of the location of drug attachment. The drug can be selectively placed on the corona, buried in the core, or dispersed equally throughout the polymer. Third, ELP can self assemble into multivalent nanoparticles that can have excellent site-specific accumulation and drug carrying properties. Fourth, because ELP are designed from native amino acid sequences found extensively in the human body they are biodegradable, biocompatible, and tolerated by the immune system. Fifth, ELPs undergo an inverse phase transition temperature, T_t, above which they phase separate into large aggregates. By localized heating, additional ELP can be drawn into the target site, which may be beneficial for increasing drug concentrations.

[0064] A therapeutic agent such as a drug, for example, may be attached to the ELP through cysteine, lysine, glutamic acid or aspartic acid residues present in the polymer. In some embodiments, the cysteine, lysine, glutamic acid or aspartic acid residues are generally present throughout the length of the polymer. In some embodiments, the cysteine, lysine, glutamic acid or aspartic acid residues are clustered at the end of the polymer. In some embodiments of the presently described subject matter, therapeutics are attached to the cysteine residues of the ELP using thiol reactive linkers. In some embodiments of the presently described subject matter, therapeutics are attached to the lysine residues of the high molecular weight polymer sequence using NHS (N-hydroxysuccinimide) chemistry to modify the primary amine group present on these residues. In some embodiments of the presently described subject matter, therapeutics are attached to the glutamic acid or aspartic acid residues of the ELP using EDC (1-Ethyl-3-[3-dimethylaminopropyl]carbodiimide Hydrochloride) chemistry to modify the carboxylic acid group present on the ELP residues.

[0065] The therapeutic associated with the ELP may be hydrophobic or hydrophilic. For hydrophobic drugs, attachment to the terminus of the ELP may facilitate formation of the multivalent nanoparticle. The number of drug particles attached to the ELP can be from about 1 to about 30, or from about 1 to about 10, or about 1, 2, 3, 4, 5, 6, 7, 8, 9, or 10. In some embodiments, the attachment points for a therapeutic are equally distributed along the backbone

of the ELP, and the resulting drug-ELP is prevented from forming nanoparticle structures under physiological salt and temperature conditions.

[0066] In certain embodiments, the therapeutic agent is an anti-microbial agent or a non-steroidal anti-inflammatory drug. As used herein, the term "anti-microbial" is meant to include prevention, inhibition, termination, or reduction of virulence factor expression or function of a microbe. "Prevention" can be considered, for example, to be the obstruction or hindrance of any potential microbial growth. "Termination" can be considered, for example, to be actual killing of the microbes by the presence of the composition. "Inhibition" can be considered, for example, to be a reduction in microbial growth or inhibiting virulence factor expression or function of the microbe. As used herein, the term "anti-microbial agent" is meant to encompass any molecule, chemical entity, composition, drug, therapeutic agent, or biological agent capable of preventing or reducing growth of a microbe, or capable of blocking the ability of a microbe to cause disease. An example of an anti-microbial agent is an antibiotic. The term includes small molecule compounds, antisense reagents, siRNA reagents, antibodies, enzymes, peptides, organic or inorganic molecules, natural or synthetic compounds and the like.

[0067] In a further embodiment, the therapeutic agent is a non-steroidal anti-inflammatory drug. The term "non-steroidal anti-inflammatory drug," usually abbreviated to NSAIDs, but also referred to as nonsteroidal anti-inflammatory agents/analgesics (NSAIAs) or nonsteroidal anti-inflammatory medicines (NSAIMs), are a class of drugs that provide analgesic and antipyretic (fever-reducing) effects, and, in higher doses, anti-inflammatory effects. The term "nonsteroidal" distinguishes these drugs from steroids, which, among a broad range of other effects, have a similar eicosanoid-depressing, anti-inflammatory action. As analgesics, NSAIDs are unusual in that they are non-narcotic. Non-limiting examples of NSAIDs include aspirin, ibuprofen, and naproxen.

[0068] The methods, lenses, and compositions of the present invention are effective against bacteria including, for example, gram-positive and gram-negative cocci, gram positive and gram negative straight, curved and helical/vibroid and branched rods, sheathed bacteria, sulfur-oxidizing bacteria, sulfur or sulfate-reducing bacteria, spirochetes, actinomycetes and related genera, myxobacteria, mycoplasmas, rickettsias and chlamydias, cyanobacteria, archea, fungi, parasites, viruses and algae. In particular, the present invention is useful against the Pseudomonas species of bacteria, e.g., Pseudomonas aeruginosa, and other microbes that are found in the eye.

[0069] In addition to therapeutics, the ELPs may also be associated with a detectable label that allows for the visual detection of *in vivo* uptake of the ELPs. Suitable labels include, for

example, fluorescein, rhodamine, tetramethylrhodamine, eosin, erythrosin, coumarin, methyl-coumarins, pyrene, Malacite green, Alexa-Fluor®, stilbene, Lucifer Yellow, Cascade Blue.TM., and Texas Red. Other suitable optical dyes are described in Haugland, Richard P. (1996) Molecular Probes Handbook.

[0070] In certain embodiments, the ELP components include polymeric or oligomeric repeats of the pentapeptide VPGXG (SEQ ID. NO: 4), where the guest residue X is any amino acid, that in one aspect, excludes proline. X may be a naturally occurring or non-naturally occurring amino acid. In some embodiments, X is selected from alanine, arginine, asparagine, aspartic acid, cysteine, glutamic acid, glutamine, glycine, histidine, isoleucine, leucine, lysine, methionine, phenylalanine, serine, threonine, tryptophan, tyrosine and valine. In some embodiments, X is a natural amino acid other than proline or cysteine.

[0071] The guest residue X may be a non-classical (non-genetically encoded) amino acid. Examples of non-classical amino acids include: D-isomers of the common amino acids, 2, 4-diaminobutyric acid, α-amino isobutyric acid, A-aminobutyric acid, Abu, 2-amino butyric acid, γ-Abu, ε-Ahx, 6-amino hexanoic acid, Aib, 2-amino isobutyric acid, 3-amino propionic acid, ornithine, norleucine, norvaline, hydroxyproline, sarcosine, citrulline, homocitrulline, cysteic acid, t-butylglycine, t-butylalanine, phenylglycine, cyclohexylalanine, β-alanine, fluoro-amino acids, designer amino acids such as β -methyl amino acids, C α -methyl amino acids, N α -methyl amino acids, and amino acid analogs in general.

[0072] Selection of X is independent in each ELP structural unit (e.g., for each structural unit defined herein having a guest residue X). For example, X may be independently selected for each structural unit as an amino acid having a positively charged side chain, an amino acid having a negatively charged side chain, or an amino acid having a neutral side chain, including in some embodiments, a hydrophobic side chain.

[0073] In each embodiment, the structural units, or in some cases polymeric or oligomeric repeats, of the ELP sequences may be separated by one or more amino acid residues that do not eliminate the overall effect of the molecule, that is, in imparting certain improvements to the therapeutic component as described. In certain embodiments, such one or more amino acids also do not eliminate or substantially affect the phase transition properties of the ELP component (relative to the deletion of such one or more amino acids).

[0074] The ELP component in some embodiments is selected or designed to provide a T_t ranging from about 10 to about 80°C, such as from about 10 to about 60°C, or from about 38 to about 45°C. The transition temperature, in some embodiments, is above the body temperature of

the subject or patient (e.g., >37°C) thereby remaining soluble in vivo, or in other embodiments, the T_t is below the body temperature (e.g., <37°C) to provide alternative advantages, such as in vivo formation of a drug depot for sustained release of the therapeutic agent.

[0075] The T_t of the ELP component can be modified by varying ELP chain length, as the Tt generally increases with decreasing MW. For polypeptides having a molecular weight >100,000, the hydrophobicity scale developed by Urry et al. (PCT/US96/05186, which is hereby incorporated by reference in its entirety) is preferred for predicting the approximate T_t of a specific ELP sequence. However, in some embodiments, ELP component length can be kept relatively small, while maintaining a target T_t, by incorporating a larger fraction of hydrophobic guest residues (e.g., amino acid residues having hydrophobic side chains) in the ELP sequence. For polypeptides having a molecular weight <100,000, the T_t may be predicted or determined by the following quadratic function: $T_t=M_0+M_1X+M_2X^2$ where X is the MW of the fusion protein, and $M_0=116.21$; $M_1=-1.7499$; $M_2=0.010349$.

[0076] While the T_t of the ELP component, and therefore of the ELP component coupled to a therapeutic component, is affected by the identity and hydrophobicity of the guest residue, X, additional properties of the molecule may also be affected. Such properties include, but are not limited to solubility, bioavailability, persistence, and half-life of the molecule.

Therapeutic peptides

[0077] In certain embodiments of the disclosure, the ELP component further comprises a therapeutic protein. The term "therapeutic protein" as used herein is a protein that may be used to treat a disease, particularly an ocular disease. Non-limiting examples of therapeutic proteins include lacritin, anti-VEGF proteins or antibodies or therapeutics, such as afibercept (Eylea®), bevacizumab (Avasin®), pegaptanib (Macugen®) or ranibuzumab (Lucentis®); Rab Escort Protein-1(REP-1, described in Ophthalmic Genetic. (2012) Jun;33(2):57-65); Retinitis Pigmentosa Related 65 (described in Hum Gene Ther. Clin Dev.(2013) Mar:24(1):23-8); ATP-binding cassette transporter abc4 (ABC4, described in . (Nat Genet. 1997 Mar;15(3):236-46); and MYO7A (associated with The Usher Syndromes (“USH”) (Ophthalmology. 2014 Feb;121(2):580-7.). The therapeutic protein may also be an antibody that provides therapy for a condition of the eye. When therapeutic proteins and/or therapeutic agents are added to the polymeric material or contact lens of the disclosure, they are typically added in an effective amount or a therapeutically effective amount.

[0078] In one embodiment, the therapeutic protein is lacritin or a biological equivalent thereof. Lacritin is a glycoprotein encoded in humans by the LACRT gene. Lacritin is a secreted protein

found in tears and saliva. Lacritin also promotes tear secretion and proliferation of some epithelial cells. Lacritin is thus a prosecretory mitogen. Functional studies suggest a role in epithelial renewal of some nongermative epithelia. By flowing downstream through ducts, it may generate a 'proliferative field'. Lacritin also promotes secretion. This raises the possibility that lacritin may have clinical applications in the treatment of dry eye, the most common eye disease. The lacritin protein sequence is known in the art. For example, the GenBank Accession Nos.: NP_150593 and AAG44392.1 represents the lacritin sequence. The sequence associated with this GenBank Accesion number is herein incorporated by reference in its entirety.

[0079] In one embodiment, lacritin comprises the amino acid sequence of SEQ ID NO: 8 or a biological equivalent thereof:

EDASSDSTGADPAQEAGTSKPNEEISGPAEPASPPETTTTAQETSAAAVQGTAKVTSSRQ ELNPLKSIVEKSILLTEQALAKAGKGMHGGVPGGKQFIENGSEFAQKLLKKFSLLKPWA (SEQ ID. NO: 8). A biological equivalent is as described above.

[0080] In a further embodiment, the lacritin ELP comprises the amino acid sequence of SEQ ID NO: 9 or a biological equivalent thereof as described above:

MGEDASSDSTGADPAQEAGTSKPNEEISGPAEPASPPETTTTAQETSAAAVQGTAKVTSS RQELNPLKSIVEKSILLTEQALAKAGKGMHGGVPGGKQFIENGSEFAQKLLKKFSLLKP WAGLVPR|GSG$(VPGX_1G)_{n1}(VPGX_2G)_{n2}$Y (SEQ ID NO: 9); wherein X_1 and X_2 represent a guest residue as defined herein and n1 and n2 represents the repeat number of pentamers (VPGXG) (SEQ ID NO: 4) as described above.

[0081] In a further embodiment, lacritin comprises the amino acid sequence of SEQ ID NO: 10 or a biological equivalent thereof:

MKFTTLLFLAAVAGALVYAEDASSDSTGADPAQEAGTSKPNEEISGPAEPASPPETTTTA QETSAAAVQGTAKVTSSRQELNPLKSIVEKSILLTEQALAKAGKGMHGGVPGGKQFIEN GSEFAQKLLKKFSLLKPWA (SEQ ID NO: 10).

[0082] The following polynucleotide sequence represents an example of a lacritin polynucleotide sequence:

5'-
CATATGGAAGACGCTTCTTCTGACTCTACCGGTGCTGACCCGGCTCAGGAAGCTGG TACCTCTAAACCGAACGAAGAAATCTCTGGTCCGGCTGAACCGGCTTCTCCGCCGGA AACCACCACCACCGCTCAGGAAACCTCTGCTGCTGCTGTTCAGGGTACCGCTAAAGT TACCTCTTCTCGTCAGGAACTGAACCCGCTGAAATCTATCGTTGAAAAATCTATCCT

GCTGACCGAACAGGCTCTGGCTAAAGCTGGTAAAGGTATGCACGGTGGTGTTCCGG GTGGTAAACAGTTCATCGAAAACGGTTCTGAATTCGCTCAGAAACTGCTGAAAAAA TTCTCTCTGCTGAAACCGTGGGCTGGTCTGGTTCCGCGTGGTTCTGGTTACTGATCTC CTCGGATCC-3' (SEQ ID NO: 11).

[0083] The term "biological equivalent" is defined above. In one aspect, a biological equivalent is a peptide encoded by a nucleic acid that hybrizes to a nucleic acid that encodes the lacritin protein or its complement under conditions of a high stringency hybridization reaction, that is performed at about 60°C in about 1 x SSC that has substantial identical biological activity to the above-noted sequence.

[0084] When a therapeutic protein is part of the ELP component, the therapeutic protein may be fused to the N- or C-terminus of the ELP component. In one embodiment, a cleavable peptide sequence is between the ELP component and the therapeutic peptide or therapeutic agent. In a related embodiment, the cleavable peptide sequence is a protease cleavage site. The term "protease cleavage site" refers to a peptide sequence that is cleaved by a protease. A protease is any enzyme that conducts proteolysis. Protease cleavage proteins and their cleavage sites are known in the art. Non-limiting examples of proteases include, but are not limited to, for example, thrombin, intracellular proteases, including caspases; proteases involved in the regulation of complement activation; proteases involved in the regulation of coagulation; proteases involved in the regulation of signal transduction; and, proteases involved in the expression or activity of prostaglandins (e.g., PGHS-2). Other proteases include, but are not limited to, matrix metalloproteinases, elastase, alpha$_1$-proteinase, proteinase 3, chymotrypsin, trypsin, human mast cell chymase, stratum corneum chymotryptic enzyme, human cathepsin G, bovine chymotrypsin, pig chymotrypsin, tryptase, human leukocyte elastase, pig pancreatic elastase, stratum corneum chymotryptic enzyme. In one embodiment, the protease is thrombin, and the protease cleavage site is a thrombin cleavage site as known in the art and as described herein. In another embodiment, the protease is a protease endogenous to the eye or secretions of the eye (i.e. tears). Proteases endogenous to the eye or eye secretions include, for example, metalloproteinases (MMPs) such as MMP-2 and MMP-9, trypsin-like protease, multicatalytic endopeptidase complex, membrane bound proteases, and calpain.

[0085] To insert the cleavable sequence, the cDNA of cleavable peptide sequences is inserted between the cDNA encoding the therapeutic agent and cDNA encoding ELP sequence. The whole therapeutic-cleavage-ELP cDNA is cloned into a chosen plasmid (such as pIDTSmart, Ampicillin resistance) and expressed in either prokaryotic and/or eukaryotic cells, such as BLR(DE3) competent cells, Origami^{TM} B competent cells and HEK-293 cell line, etc.

Alternatively, cleavage sequence can be added after/before therapeutic agent protein sequence using solid-phase peptide synthesis. In one aspect, the cleavable peptide sequence is a thrombin cleavable peptide sequence which comprises the amino acid sequence GLVPR|GS (SEQ ID NO.: 12), or a biological equivalent thereof (as defined herein).

Expression of Recombinant Proteins

[0086] ELPs and other recombinant proteins described herein can be prepared by expressing polynucleotides encoding the polypeptide sequences of this invention in an appropriate host cell, i.e., a prokaryotic or eukaryotic host cell This can be accomplished by methods of recombinant DNA technology known to those skilled in the art. It is known to those skilled in the art that modifications can be made to any peptide to provide it with altered properties. Polypeptides of the invention can be modified to include unnatural amino acids. Thus, the peptides may comprise D-amino acids, a combination of D- and L-amino acids, and various "designer" amino acids (*e.g.*, β-methyl amino acids, C-α-methyl amino acids, and N-α-methyl amino acids, etc.) to convey special properties to peptides. Additionally, by assigning specific amino acids at specific coupling steps, peptides with α-helices, β turns, β sheets, α-turns, and cyclic peptides can be generated. Generally, it is believed that beta-turn spiral secondary structure or random secondary structure is preferred.

[0087] The ELPs can be expressed and purified from a suitable host cell system. Suitable host cells include prokaryotic and eukaryotic cells, which include, but are not limited to bacterial cells, yeast cells, insect cells, animal cells, mammalian cells, murine cells, rat cells, sheep cells, simian cells and human cells. Examples of bacterial cells include *Escherichia coli, Salmonella enterica* and *Streptococcus gordonii*. In one embodiment, the host cell is *E. coli.* The cells can be purchased from a commercial vendor such as the American Type Culture Collection (ATCC, Rockville Maryland, USA) or cultured from an isolate using methods known in the art. Examples of suitable eukaryotic cells include, but are not limited to 293T HEK cells, as well as the hamster cell line BHK-21; the murine cell lines designated NIH3T3, NS0, C127, the simian cell lines COS, Vero; and the human cell lines HeLa, PER.C6 (commercially available from Crucell) U-937 and Hep G2. A non-limiting example of insect cells include Spodoptera frugiperda. Examples of yeast useful for expression include, but are not limited to Saccharomyces, Schizosaccharomyces, Hansenula, Candida, Torulopsis, Yarrowia, or Pichia. See e.g., U.S. Patent Nos. 4,812,405; 4,818,700; 4,929,555; 5,736,383; 5,955,349; 5,888,768 and 6,258,559.

Protein Purification

[0088] The phase transition behavior of the ELPs allows for easy purification. The ELPs may also be purified from host cells using methods known to those skilled in the art. These techniques involve, at one level, the crude fractionation of the cellular milieu to polypeptide and non-polypeptide fractions. Having separated the polypeptide from other proteins, the polypeptide of interest may be further purified using chromatographic and electrophoretic techniques to achieve partial or complete purification (or purification to homogeneity). Analytical methods particularly suited to the preparation of a pure peptide or polypeptide are filtration, ion-exchange chromatography, exclusion chromatography, polyacrylamide gel electrophoresis, affinity chromatography, or isoelectric focusing. A particularly efficient method of purifying peptides is fast protein liquid chromatography or even HPLC. In the case of ELP compositions protein purification may also be aided by the thermal transition properties of the ELP domain as described in U.S. Pat. No. 6,852,834.

[0089] Generally, "purified" will refer to a protein or peptide composition that has been subjected to fractionation to remove various other components, and which composition substantially retains its expressed biological activity. Where the term "substantially purified" is used, this designation will refer to a composition in which the protein or peptide forms the major component of the composition, such as constituting about 50%, about 60%, about 70%, about 80%, about 90%, about 95% or more of the proteins in the composition.

[0090] Various methods for quantifying the degree of purification of the protein or peptide will be known to those of skill in the art in light of the present disclosure. These include, for example, determining the specific activity of an active fraction, or assessing the amount of polypeptides within a fraction by SDS/PAGE analysis. A preferred method for assessing the purity of a fraction is to calculate the specific activity of the fraction, to compare it to the specific activity of the initial extract, and to thus calculate the degree of purity, herein assessed by a "-fold purification number." The actual units used to represent the amount of activity will, of course, be dependent upon the particular assay technique chosen to follow the purification and whether or not the expressed protein or peptide exhibits a detectable activity.

[0091] Various techniques suitable for use in protein purification will be well known to those of skill in the art. These include, for example, precipitation with ammonium sulfate, PEG, antibodies and the like or by heat denaturation, followed by centrifugation; chromatography steps such as ion exchange, gel filtration, reverse phase, hydroxylapatite and affinity chromatography; isoelectric focusing; gel electrophoresis; and combinations of such and other techniques. As is generally known in the art, it is believed that the order of conducting the

various purification steps may be changed, or that certain steps may be omitted, and still result in a suitable method for the preparation of a substantially purified protein or peptide.

Pharmaceutical Compositions

[0092] Pharmaceutical compositions are further provided. The compositions comprise a carrier and ELPs as described herein. The carriers can be one or more of a solid support or a pharmaceutically acceptable carrier. In one aspect, the compositions are formulated with one or more pharmaceutically acceptable excipients, diluents, carriers and/or adjuvants. In addition, embodiments of the compositions include ELPs, formulated with one or more pharmaceutically acceptable auxiliary substances.

[0093] The invention provides pharmaceutical formulations in which the one or more of an isolated polypeptide of the invention, an isolated polynucleotide of the invention, a vector of the invention, an isolated host cell of the invention, or an antibody of the invention can be formulated into preparations for injection in accordance with the invention by dissolving, suspending or emulsifying them in an aqueous or nonaqueous solvent, such as vegetable or other similar oils, synthetic aliphatic acid glycerides, esters of higher aliphatic acids or propylene glycol; and if desired, with conventional additives such as solubilizers, isotonic agents, suspending agents, emulsifying agents, stabilizers and preservatives or other antimicrobial agents. A non-limiting example of such is a antimicrobial agent such as other vaccine components such as surface antigens, e.g. a Type IV Pilin protein (see Jurcisek and Bakaletz (2007) J. of Bacteriology 189(10):3868-3875) and antibacterial agents.

[0094] Aerosol formulations provided by the invention can be administered via inhalation. For example, embodiments of the pharmaceutical formulations of the invention comprise a compound of the invention formulated into pressurized acceptable propellants such as dichlorodifluoromethane, propane, nitrogen and the like.

[0095] Embodiments of the pharmaceutical formulations of the invention include those in which the ELP is formulated in an injectable composition. Injectable pharmaceutical formulations of the invention are prepared as liquid solutions or suspensions; or as solid forms suitable for solution in, or suspension in, liquid vehicles prior to injection. The preparation may also be emulsified or the active ingredient encapsulated in liposome vehicles in accordance with other embodiments of the pharmaceutical formulations of the invention.

[0096] Suitable excipient vehicles are, for example, water, saline, dextrose, glycerol, ethanol, or the like, and combinations thereof. In addition, if desired, the vehicle may contain minor amounts of auxiliary substances such as wetting or emulsifying agents or pH buffering agents.

Methods of preparing such dosage forms are known, or will be apparent upon consideration of this disclosure, to those skilled in the art. See, e.g., Remington's Pharmaceutical Sciences, Mack Publishing Company, Easton, Pennsylvania, 17th edition, 1985. The composition or formulation to be administered will, in any event, contain a quantity of the compound adequate to achieve the desired state in the subject being treated.

[0097] Routes of administration applicable to the ELP compositions described herein include intranasal, intramuscular, subcutaneous, intradermal, topical application, intravenous, nasal, oral, inhalation, intralacrimal, retrolacrimal profusal along the duct, intralacrimal, and other enteral and parenteral routes of administration. Routes of administration may be combined, if desired, or adjusted depending upon the agent and/or the desired effect. An active agent can be administered in a single dose or in multiple doses. Embodiments of these methods and routes suitable for delivery, include systemic or localized routes. In one embodiment, the composition comprising the ELP is administered intralacrimally through injection. In further embodiments, the composition is administered systemically, topically on top of the eye, by retrolacrimal profusion, or intranasally. In embodiments of the contact lenses as described herein, the route of administration is through the eye.

Treatment of Disease

[0098] Methods and compositions disclosed herein are useful in treating disorders and diseases of the eye (ocular diseases) and may be particularly useful to encapsulate or attach drugs for treating disorders localized to the eye.

[0099] Certain aspects relate to a method for treating an ocular disease, comprising administering to a patient in need of such treatment a polymeric material or contact lens as described herein. The term "ocular disease" refers to any disorder of the eye and/or lacrimal system. It includes non-infectious ocular diseases such as non-infectious ocular surface diseases, e.g., dry eye, and infectious ocular disease such as those ocular diseases caused by microbes. Diseases treatable by the methods of the present invention include, but are not limited to, diseases of the eyelid such as infectious and non-infectious blepharitis, hordeolum, preseptal cellulites, chalazion, herpes zoster ophthalmicus, dacryocystitis, herpes simplex blepharitis, orbital cellulites, and entropion; diseases of the conjunctiva and sclera, such as allergic conjunctivitis, vernal keratoconjunctivitis, viral conjunctivitis, bacterial conjunctivitis, episcleritis, scleritis, pingueculitis, ocular cysticercosis, toxic follicular conjunctivitis, and giant papillary conjunctivitis; diseases of the cornea, such as keratitis sicca or dry eye syndrome, herpes simplex keratitis, bacterial keratitis, sterile corneal infiltrates, and Salzmann's nodular degeneration; diseases of the uvea, such as inflammatory glaucoma and uveitis; and diseases of

the vitreous and retina. Also treated by the contact lenses and methods described herein are contact lens associated diseases or conditions are treatable by the methods of the present invention, e.g., bacterial keratitis, contact lens associated red eye ("CLARE"), contact lens induced peripheral ulcers ("CLPU") and infiltrative keratitis ("IK"). Further examples of ocular disorders treated by the contact lenses and methods disclosed herein are age-related macular degeneration, Sjögren's syndrome, autoimmune exocrinopathy, diabetic retinopathy, graft versus host disease (exocrinopathy associated with) retinal venous occlusions, retinal arterial occlusion, macular edema, postoperative inflammation, uveitis retinitis, proliferative vitreoretinopathy and glaucoma. In one embodiment, the disease is Sjögren's syndrome. In another embodiment, the disease is keratoconjunctivitis sicca (dry eye). In another embodiment the disease is scleritis. In another embodiment the disease is glaucoma.

[0100] Also provided is a method for delivering a drug comprising an elastin-like peptide (ELP) component to the eye, comprising contacting the eye with a contact lens as described herein. In one embodiment, the contact lens is in contact with the ocular surface of the eye.

Combination Treatments

[0101] Administration of the therapeutic agent or substance of the present invention to a patient will follow general protocols for the administration of that particular secondary therapy, taking into account the toxicity, if any, of the treatment. It is expected that the treatment cycles would be repeated as necessary. It also is contemplated that various standard therapies, as well as surgical intervention, may be applied in combination with the described therapy and/or use of the polymeric material

[0102] The following examples are intended to illustrate and not limit the invention.

EXAMPLE 1

[0103] Decorating contact lenses with ELPs will provide a platform for hundreds of potential therapeutic entities (including small molecules, peptides, proteins and monoclonal antibodies) to function in a new format: a bioadhesive drug reservoir. For example, the bio-construction of lacritin-ELP library with various hydrophobicity and nanoparticle sizes ranging from 2-3 nm (lacritin) to 130-140 nm (Lac-S48I48) has been completed. Unique thrombin cleavage site design provides additional release route besides possible cleavage by protease existing in human tears. The thrombin cleavage site may comprise the amino acid sequence: GLVPRGSG (SEQ ID. NO: 7).

ELP protein expression and purification

[0104] Polynucleotides encoding ELPs S48I48 (SEQ ID NO: 1), S96 (SEQ. ID. NO: 2) and V96 (SEQ. ID. NO: 3) were expressed in BLR (DE3) E. coli cells (Novagen Inc., Milwaukee, WI). Briefly, after overnight start culture, protein was expressed for 24 h in an orbital shaker at 37 °C at 250 rpm. Cell culture were harvested and resuspended in phosphate buffer saline (PBS). After sonication and removing insoluble cell debris and nucleic, ELPs were purified from clarified cell supernatant by inverse transition cycling (ITC)15 as follows: the ionic strength of warmed-up soluble lysate (37°C) was increased by adding crystal NaCl to trigger aggregation of ELPs. Aggregated protein was separated from soluble E. coli proteins by centrifugation at moderate temperature (37-40°C). The pellet containing target protein was then dissolved in cold PBS on ice and centrifuged at 4 °C to remove any insoluble contaminants. This aggregation and dissolution process was repeated 6-7 times until proteins was determined to be approximately 99% pure by SDS-PAGE gels stained with coomassie blue. Protein concentrations were determined by UV-visible spectroscopy at 280 nm (ε=1285M-1cm-1). Protein molecular weight is further confirmed by MALDI-TOF analysis.

Fluorescein labeling ELPs and Lacritin-ELPs

[0105] ELPs S48I48, S96 and V96 were conjugated with NHS-Rhodamine (Thermo Fisher Scientific Inc, Rockford, IL) via covalent modification of primary amines at the amino end of the peptide. Briefly, the conjugation was performed in 100 mM borate buffer (pH8.5) for overnight at 4°C, and conjugated protein was desalted using PD10 column (GE Healthcare, Piscataway, NJ) and overnight dialysis against PBS at 4°C. For Lacritin and Lacritin-ELPs, the conjugation time was shortened to 2h at 4°C due to multiple Lysine residues in lacritin sequence.

Labeling Proclear contact lenses with Rho-ELPs

[0106] Proclear compatible contact lens was incubated in 100 μM-500 μM Rho-ELPs (Rho-V96, Rho-S48I48 or Rho-S96) for 48 hours at 4°C or 37°C. After gentle rinse with PBS, contact lens was imaged using Zeiss 510 confocal microscopy or Bio-Rad VersaDoc MP System.

EXAMPLE 2

Rhodamine label ELPs and contact lens decoration

[0107] Briefly, ELPs were covalently modified with NHS-Rhodamine (Thermo Fisher Scientific Inc, Rockford, IL) via the primary amino terminus. The conjugation was performed in 100 mM borate buffer (pH 8.5) overnight at 4 °C. Excess fluorophore was removed using a desalting PD-10 column (GE Healthcare, Piscataway, NJ) and overnight dialysis against PBS at

4 °C. Contact lenses were either incubated with 50μM labeled ELPs overnight at 37°C in a 24-well plate or spot decorated with concentrated labeled ELPs using a 20 μl pipette at 37 °C before transferred to PBS solution.

ELPs inverse phase transition characterization

[0108] The temperature-concentration phase diagrams for rhodamine labeled ELPs/ELP fusion proteins were characterized by optical density observation using a DU800 UV-Vis spectrophotometer at 350 nm as a function of solution temperature. Typically, ELPs (5 – 100 μM) were heated at 1 °C/min from 10 to 85 °C and sampled every 0.3 °C. T_t was defined at the point of the maximum first derivative.

Fluorescence release characterization

[0109] ELP modified contact lens were gently rinsed with PBS and placed in 4 ml of PBS at 37°C or 4°C for 1 week. Samples of the solution (100 μl) were withdrawn at regular intervals and kept at -20°C. After one week, lenses were thoroughly washed in PBS at 4 °C for 24 hours to detach ELPs. Rhodamine intensity of collected samples was measured spectrophotometrically (Ex: 525nm, Em: 575nm) using Synergy™ H1m Monochromator-Based Multi-Mode Microplate Reader (BioTek) and analyzed using Gen5 2.01 Data Analysis Software (BioTek). Total fluorescence on the lens was calculated using Equation 1. Retention rate was calculated using Equation 2. Raw data were then fitted into either a one phase decay model (Equation 3) or two phase decay mode (Equation 4) using SPSS. Goodness of fit and predicted values were collected.

$$Total\ I_{rhodamine} = I_{release_{Total}} + I_{wash_{Total}} \quad (1)$$

$$Retention\ (\%) = \frac{Total\ I_{rhodamine} - \sum_{t=0}^{t} I_{release_t}}{Total\ I_{rhodamine}} \times 100\% \quad (2)$$

$$Retention\ (\%) = (R_0 - Plateau) \times e^{-kt} + Plateau \quad (3)$$

$$Retention\ (\%) = Plateau + Span_{fast} \times e^{-k_{fast}t} + Span_{slow} \times e^{-k_{slow}t} \quad (4)$$

Spatiotemporal HCE-T cell uptake study

[0110] HCE-T cell uptake study was conducted on 35mm glass coverslip-bottomed dishes. Briefly, HCE-T cells were grown to 70-80% confluency and gently rinsed with warm fresh

medium before changed to fresh medium containing either rhodamine labeled lacritin, Lac-V96 or Proclear Compatible™ contact lens modified with rhodamine labeled Lac-V96. After incubation at 37°C for 1 hour, the cells were rinsed with fresh medium and images were immediately acquired using ZEISS 510 confocal microscope system. For uptake quantification comparison, images were analyzed using ImageJ.

Statistical Analysis

[0111] Data presented are representative curves or mean ± S.D. All experiments were repeated at least three times. Statistical analysis was performed by Student t-test or one-way ANOVA by SPSS. Differences between treatments were established with Tukey's post-hoc test. A p value of less than 0.05 was considered statistically significant.

Discussion and Results

[0112] In an extension of Experiment No. 1, Applicant report the surprising discovery of ELPs' thermally-reversible, spatiotemporal and sustained attachment to Proclear Compatibles™ contact lens as an elastic bridge. Moreover, attachment and release of ELPs to/from Proclear contact lens was a T_t and temperature dependent process using rhodamine as a detection probe. For this study, two ELPs, V96 (Tt: ~30°C) and S96 (Tt: ~55°C) were used. When attaching the lens with V96 at 37°C, around 80% of fluorecence remained on the lens after one week incubation in PBS solution at 37°C, while the plateau of fluorescence retention dropped down to below 10% when releasing at 4°C. Lenses modified with S96 did not exhibit significant total fluorescence or release profile differences at either 37°C or 4°C. Interestingly, lenses modified with V96 at 4°C exhibited similar release pattern at 4°C compared to S96 group, both of which can be described using a single two-phase decay model. The lens were further modified with prosecretory mitogenic fusion protein (Lac-V96) and demonstrated spatial cell uptake via contact lens using human corneal epithelial cell model (HCE-Ts).

Discovery of ELPs specific attachment to Proclear Compatible™ contact lens

[0113] Surprising discovery of ELPs' attachment to Proclear Compatible™ contact lens came from a quick screen of four types of market contact lenses, including Acuvue Oasys®, Acuvue Advance Plus®, Dailies AquaComfort Plus™ and Proclear Compatibles™. Unexpectedly, rhodamine labeled V96 selectively attached to Proclear Compatibles™ contact lens at 37°C after overnight incubation in PBS solution and the attachment was stable at 37°C in PBS solution for more than 24 hours. Motivated by the rationale that the delivery system itself should not interfere with normal vision, Applicants investigated whether it was possible to spatially

decorate the lens with ELPs. Interestingly, Applicants were able to modify the lens with various shapes of ELPs according to the need, such as ring, dots, etc (Figure 4B).

T_t and temperature dependent attachment of ELPs to the lens

[0114] Without being bound by theory, Applicants proposed that the attachment of the ELPs to the contact lens was partially T_t and temperature dependent. To further explore the T_t and temperature dependence of ELPs' affinity to Proclear Compatible™ contact lens, Applicants chose two types of representative ELPs: V96 (T_t at around 30°C) and S96 (T_t at around 55°C) for a five group comparison study: i) Group one: lens incubated with V96 at 37°C and release at 37°C (closed circle); ii) Group two: lenses incubated with S96 at 37°C and release at 37°C (closed square); iii) Group three: lenses incubated with V96 at 4°C and release at 4°C (open circle); iv) Group four: lenses incubated with S96 at 4°C and release at 4°C (open square); v) Group five: lenses incubated with V96 at 37°C and release at 4°C (half closed circle). After 24h incubation, total attachment of V96 at 37°C (Group one) was about six fold of S96's attachment at 37°C (Group two) and sixty-nine fold of V96's attachment at 4°C (Group three) (Figures 5A and 5B). Interestingly, S96 incubated at 37°C (Group two), V96 incubated at 4°C (Group three) and S96 incubated at 4°C (Group four) did not exhibit significant different contact lens attachment affinity ($p>0.50$) (Figures 5A and B). After one week release in PBS, only Group one exhibited around 80% of fluorescence retention on the lens while all the other groups released most of the attached ELPs (Figures 5C to 5E). Total fluorescence intensity provided the first clue of the association between contact lens affinity and T_t. To thoroughly compare fluorescence release kinetics of all five groups, Applicants fitted the data using both one phase decay and two phase decay models by SPSS (Table 2). Both Group one and Group five data can be described using a one phase decay model, with R^2 of 0.916 and 0.953 accordingly; while the other three groups did not fit the one phase decay model very well (R^2=0.646). Interestingly, release kinetics of Group two, Group three and Group four can be described using the same two phase decay model (R^2=0.847). The modeling result highly supported our hypothesis about the link between ELPs' attachment to Proclear Compatible™ contact lens and T_t/temperature. Most significant different release profile comes from Group one, which exhibited a predicted plateau of more than 75% retention after one week's incubation at 37°C. Retention of V96 (Group five) on the lens was significant lowered when the incubation temperature was changed to 4°C, with a predicted plateau of less than 10% using either model and a longer half-life of release (Table 2). The link between lens affinity and T_t was further corroborated by Group two, three and four. As when both incubation and release temperatures were below ELPs' T_t, no significant difference

was noticed in either total binding fluorescence intensity (Figure 5B) or release kinetic profiles (Figure 5D).

Table 2.Modeling of release kinetics

	Group 1	Group 2	Group 3	Group 4	Group 5
ELP Type	V96	S96	V96	S96	V96
Label Temp (°C)	37	37	4	4	37
Release Temp (°C)	37	37	4	4	4
Model (one phase decay)	$R=(R_0\text{-Plateau})*\exp(-k*t)+\text{Plateau}$				
Predicted R_0 (%)	100.048±1.722	74.323±4.784	85.585±4.103		
Predicted Plateau (%)	82.222±0.576	29.728±3.397	9.281±3.956		
k (h^{-1})	2.875±0.653	0.174±0.072	0.069±0.018		
$t_{1/2}$ (h)	0.241	3.984	10.046		
R^2	0.916	0.646	0.953		
Model (two phase decay)	$R=\text{Plateau}+\text{Span}_{fast}*\exp(-k_{fast}*t)+\text{Span}_{slow}*\exp(-k_{slow}*t)$				
Predicted Plateau (%)	75.000±36.259	0.000±27.790	6.436±2.669		
Predicted Span_{fast} (%)	8.526±35.885	40.503±6.210	64.419±4.209		
k_{fast} (h^{-1})	0.003±0.017	3.301±1.181	0.040±0.008		
$t_{1/2fast}$ (h)	231.049	0.210	17.329		
Predicted Span_{slow} (%)	16.563±1.569	54.234±26.585	30.398±5.478		
k_{slow} (h^{-1})	3.362±0.744	0.008±0.007	1.943±0.797		
$t_{1/2slow}$ (h)	0.206	86.643	0.357		
R^2	0.957	0.847	0.990		

Lac-V96 ring decorated contact lens mediated spatiotemporal HCE-T cell uptake

[0115] To explore the targeted delivery potential of ELP-contact lens system, Applicants chose one of the potential protein therapies for ocular disease, lacritin, which has shown prosecretory mitogenic activities as dry eye disease and cornea wound healing treatment. Applicants have previously proved that Lac-ELP fusion proteins imparted similar proseceretroy/mitogenic function of lacritin and thermo responsiveness of ELPs. Moreover, by fused to different ELP tags, uptake level and speed of exogenous Lac-ELPs into HCE-Ts could be modulated (Figures

6A-C). The spatiotemporal controlled HCE-T cell uptake effect was enhanced when the lens was ring decorated with rhodamine labeled Lac-V96 (Figure 6D). Three representative regions underneath the lens were chosen to compare cell uptake level and distribution (Figures 6E-G). As illustrated in the figures, Lac-V96 ring decorated contact lens successfully executed its targeted delivery task. Region 1 (Figure 6E) was fully covered by the lens, exhibiting evenly distributed highest cell uptake level. Region 2 (Figure 6F) was partially covered by the lens and thus only showed one section of cell uptake. Region 3 (Figure 6G) was outside of the Lac-V96 ring area, which illustrated the lowest cell uptake level.

[0116] To develop new treatments or delivery mechanisms for ocular diseases and improve the bioavailability, new drug vehicles are required to be biocompatible, biodegradable, easily modified with bioactive peptides, small molecules or antibodies and can work in concert with existing medical devices to provide novel functionality. In this communication, Applicants reported the surprising discovery of thermal responsive ELPs' selective reversible attachment to Proclear Compatibles^{TM} contact lens; Applicants described the T_t and temperature dependence of this attachment and Applicants provided the first proof of concept to spatiotemporally deliver model ocular protein drug lacritin via contact lens. Different from reported contact lens mediated drug delivery systems, the ELP modification on contact lens can be T_t and spatiotemporally modulated so that delivery is more targeted to the disease site and delivery rate can be further fine-tuned using external stimuli such as local cooling for on demand dosing. In this study, the monoblock ELP modified contact lens was fused with fluorescent labeled therapeutic agent for visual detection of release and in vitro cell uptake.

[0117] It should be understood that although the present invention has been specifically disclosed by preferred embodiments and optional features, modification, improvement and variation of the inventions embodied therein herein disclosed may be resorted to by those skilled in the art, and that such modifications, improvements and variations are considered to be within the scope of this invention. The materials, methods, and examples provided here are representative of preferred embodiments, are exemplary, and are not intended as limitations on the scope of the invention.

[0118] The invention has been described broadly and generically herein. Each of the narrower species and subgeneric groupings falling within the generic disclosure also form part of the invention. This includes the generic description of the invention with a proviso or negative limitation removing any subject matter from the genus, regardless of whether or not the excised material is specifically recited herein.

[0119] In addition, where features or aspects of the invention are described in terms of Markush groups, those skilled in the art will recognize that the invention is also thereby described in terms of any individual member or subgroup of members of the Markush group.

[0120] All publications, patent applications, patents, and other references mentioned herein are expressly incorporated by reference in their entirety, to the same extent as if each were incorporated by reference individually. In case of conflict, the present specification, including definitions, will control.

CLAIMS:

1. A biocompatible, polymeric material comprising an elastin-like peptide (ELP).

2. The polymeric material of claim 1, wherein the ELP is attached to the polymeric material randomly or in a pre-determined design.

3. The polymeric material of claim 1 or 2, wherein the ELP comprises one or more of SEQ ID NOs: 1 to 6, or a biological equivalent thereof.

4. The polymeric material of claims 1 or 2, wherein the ELP further comprises a therapeutic agent bound to the ELP or encapsulated within the ELP.

5. The polymeric material of claim 4, wherein the therapeutic agent is lacritin or a biological equivalent thereof.

6. The polymeric material of claim 4, wherein lacritin is fused to the ELP.

7. The polymeric material of claim 4, further comprising a cleavable peptide sequence located between the therapeutic agent and the ELP.

8. The polymeric material of claim 6, further comprising a cleavable peptide sequence located between the therapeutic agent and the ELP.

9. The polymeric material of claim 7, wherein the cleavable peptide sequence is a thrombin cleavable peptide sequence.

10. The polymeric material of claim 8, wherein the cleavable peptide sequence is a thrombin cleavable peptide sequence.

11. The polymeric material of claim 5, wherein the lacritin protein comprises an amino acid sequence corresponding to the amino acid sequence of SEQ ID NO: 8 or 10 or a biological equivalent thereof.

12. The polymeric material of claim 11, wherein the lacritin-ELP comprises an amino acid sequence corresponding to the amino acid sequence of SEQ ID NO: 9 or a biological equivalent thereof.

13. The polymeric material of any one of claims 1-9, further comprising a therapeutic agent.

14. The polymeric material of claim 4, wherein the therapeutic agent is an anti-microbial agent or a non-steroidal anti-inflammatory drug.

15. The polymeric material of claim 1, further comprising a detectable label.

16. The polymeric material of claim 1, wherein the ELP comprises a diblock.

17. A method for preparing the polymeric material of claim 1 comprising absorbing, conjugating, or coating a polymeric material with an ELP.

18. A method for delivering a therapeutic agent, comprising contacting the polymeric material of claim 4 with a subject to be treated.

19. The method of claim 18, wherein the polymeric material is in contact with the ocular surface of an eye.

20. A method for treating an ocular disease, comprising contacting the polymeric material of claim 4 with the eye of a patient in need of such treatment.

21. The method of claim 20, wherein the ocular disease is selected from the group consisting of dry eye, age-related macular degeneration, diabetic retinopathy, retinal venous occlusions, retinal arterial occlusion, macular edema, postoperative inflammation, infection, dryness, uveitis retinitis, proliferative vitreoretinopathy and glaucoma.

22. The method of claim 21, wherein the ocular disease is dry eye.

23. A polypeptide comprising the amino acid sequence corresponding to the amino acid sequence of SEQ ID NO: 9 or a biological equivalent thereof.

24. A method for delivering a therapeutic agent, comprising contacting the polymeric material of claim 23 with a subject to be treated.

25. The method of claim 24, wherein the polymeric material is in contact with the ocular surface of an eye.

26. A method for treating an ocular disease, comprising contacting the polymeric material of claim 23, with the eye of a patient in need of such treatment.

27. The method of claim 26, wherein the ocular disease is dry eye.

28. A polynucleotide encoding the polypeptide of claim 23.

29. A host cell comprising the polynucleotide of claim 24.

30. A composition comprising a carrier and the polypeptide of claim 23.

31. A method for preparing the polypeptide of claim 23, comprising expressing the polynucleotide of claim 24.

32. A method for preparing the polypeptide of claim 23, comprising expressing the polynucleotide of claim 24 in the host cell of claim 25.

33. The method of claim 32, further comprising separating or purifying the drug delivery agent.

34. A kit comprising one or more polymeric materials of any one of claims 1 to 16 and instructions for use.

ABSTRACT

Disclosed herein are novel methods and compositions for targeting ocular diseases. One aspect relates to a contact lens comprising an elastin-like peptide (ELP) component and optionally a therapeutic agent. Also provided are methods for treating ocular diseases comprising administering a contact lens of the disclosure to a subject in need thereof.

PTO/SB/14 (11-08)
Approved for use through 01/31/2014. OMB 0651-0032
U.S. Patent and Trademark Office; U.S. DEPARTMENT OF COMMERCE

Application Data Sheet 37 CFR 1.76	Attorney Docket Number	065715-000038US00
	Application Number	
Title of Invention	CONTROLLED RELEASE OF OCULAR BIOPHARMACEUTICALS USING BIORESPONSIVE PROTEIN POLYMERS	

The application data sheet is part of the provisional or nonprovisional application for which it is being submitted. The following form contains the bibliographic data arranged in a format specified by the United States Patent and Trademark Office as outlined in 37 CFR 1.76.
This document may be completed electronically and submitted to the Office in electronic format using the Electronic Filing System (EFS) or the document may be printed and included in a paper filed application.

Secrecy Order 37 CFR 5.2

☐ Portions or all of the application associated with this Application Data Sheet may fall under a Secrecy Order pursuant to 37 CFR 5.2 (Paper filers only. Applications that fall under Secrecy Order may not be filed electronically.)

Applicant Information:

Applicant 1

Applicant Authority ◉ Inventor ○ Legal Representative under 35 U.S.C. 117 ○ Party of Interest under 35 U.S.C. 118

Prefix	Given Name	Middle Name	Family Name	Suffix
	John	Andrew	MacKay	

Residence Information (Select One) ◉ US Residency ○ Non US Residency ○ Active US Military Service

City	Pasadena	State/Province	CA	Country of Residence	US

Citizenship under 37 CFR 1.41(b) US

Mailing Address of Applicant:

Address 1	2350 E. Woodlyn Road
Address 2	

City	Pasadena	State/Province	CA
Postal Code	91104	Country	US

Applicant 2

Applicant Authority ◉ Inventor ○ Legal Representative under 35 U.S.C. 117 ○ Party of Interest under 35 U.S.C. 118

Prefix	Given Name	Middle Name	Family Name	Suffix
	Wan		Wang	

Residence Information (Select One) ◉ US Residency ○ Non US Residency ○ Active US Military Service

City	Los Angeles	State/Province	CA	Country of Residence	US

Citizenship under 37 CFR 1.41(b) CN

Mailing Address of Applicant:

Address 1	2555 Grand Avenue #1906
Address 2	

City	Los Angeles	State/Province	CA
Postal Code	90012	Country	US

All Inventors Must Be Listed - Additional Inventor Information blocks may be generated within this form by selecting the **Add** button. Add

Correspondence Information:

Enter either Customer Number or complete the Correspondence Information section below.
For further information see 37 CFR 1.33(a).

☐ **An Address is being provided for the correspondence Information of this application.**

PTO/SB/14 (11-08)
Approved for use through 01/31/2014. OMB 0651-0032
U.S. Patent and Trademark Office; U.S. DEPARTMENT OF COMMERCE

Application Data Sheet 37 CFR 1.76	Attorney Docket Number	065715-000038US00
	Application Number	
Title of Invention	CONTROLLED RELEASE OF OCULAR BIOPHARMACEUTICALS USING BIORESPONSIVE PROTEIN POLYMERS	

Customer Number	106303		
Email Address	LAPATENTMB@NIXONPEABODY.COM	Add Email	Remove Email

Application Information:

Title of the Invention	CONTROLLED RELEASE OF OCULAR BIOPHARMACEUTICALS USING BIORESPONSIVE PROTEIN POLYMERS		
Attorney Docket Number	065715-000038US00	**Small Entity Status Claimed**	☒
Application Type	Nonprovisional		
Subject Matter	Utility		
Suggested Class (if any)		**Sub Class (if any)**	
Suggested Technology Center (if any)			
Total Number of Drawing Sheets (if any)	23	**Suggested Figure for Publication (if any)**	

Publication Information:

☐ Request Early Publication (Fee required at time of Request 37 CFR 1.219)

☐ **Request Not to Publish.** I hereby request that the attached application not be published under 35 U.S. C. 122(b) and certify that the invention disclosed in the attached application **has not and will not** be the subject of an application filed in another country, or under a multilateral international agreement, that requires publication at eighteen months after filing.

Representative Information:

Representative information should be provided for all practitioners having a power of attorney in the application. Providing this information in the Application Data Sheet does not constitute a power of attorney in the application (see 37 CFR 1.32).
Enter either Customer Number or complete the Representative Name section below. If both sections are completed the Customer Number will be used for the Representative Information during processing.

Please Select One:	◉ Customer Number	○ US Patent Practitioner	○ Limited Recognition (37 CFR 11.9)
Customer Number	106303		

Domestic Benefit/National Stage Information:

This section allows for the applicant to either claim benefit under 35 U.S.C. 119(e), 120, 121, or 365(c) or indicate National Stage entry from a PCT application. Providing this information in the application data sheet constitutes the specific reference required by 35 U.S.C. 119(e) or 120, and 37 CFR 1.78(a)(2) or CFR 1.78(a)(4), and need not otherwise be made part of the specification.

Prior Application Status	Pending		Remove
Application Number	Continuity Type	Prior Application Number	Filing Date (YYYY-MM-DD)
	non provisional of	61511928	2011-07-26

Additional Domestic Benefit/National Stage Data may be generated within this form by selecting the **Add** button.

Foreign Priority Information:

PTO/SB/14 (11-08)
Approved for use through 01/31/2014. OMB 0651-0032
U.S. Patent and Trademark Office; U.S. DEPARTMENT OF COMMERCE

Application Data Sheet 37 CFR 1.76	Attorney Docket Number	065715-000038US00
	Application Number	
Title of Invention	CONTROLLED RELEASE OF OCULAR BIOPHARMACEUTICALS USING BIORESPONSIVE PROTEIN POLYMERS	

This section allows for the applicant to claim benefit of foreign priority and to identify any prior foreign application for which priority is not claimed. Providing this information in the application data sheet constitutes the claim for priority as required by 35 U.S.C. 119(b) and 37 CFR 1.55(a).

Remove

Application Number	Country[i]	Parent Filing Date (YYYY-MM-DD)	Priority Claimed
			○ Yes ◉ No

Additional Foreign Priority Data may be generated within this form by selecting the **Add** button.

Assignee Information:

Providing this information in the application data sheet does not substitute for compliance with any requirement of part 3 of Title 37 of the CFR to have an assignment recorded in the Office.

Assignee 1

If the Assignee is an Organization check here. ☒

Organization Name	University of Southern California		
Mailing Address Information:			
Address 1	1150 South Olive Street, Suite 2300		
Address 2			
City	Los Angeles	**State/Province**	CA
Country[i]	US	Postal Code	90015
Phone Number		Fax Number	
Email Address			

Additional Assignee Data may be generated within this form by selecting the **Add** button.

Signature:

A signature of the applicant or representative is required in accordance with 37 CFR 1.33 and 10.18. Please see 37 CFR 1.4(d) for the form of the signature.

Signature	/Stephen W. Chen/			Date (YYYY-MM-DD)	2012-07-26
First Name	Stephen	Last Name	Chen	Registration Number	60629

This collection of information is required by 37 CFR 1.76. The information is required to obtain or retain a benefit by the public which is to file (and by the USPTO to process) an application. Confidentiality is governed by 35 U.S.C. 122 and 37 CFR 1.14. This collection is estimated to take 23 minutes to complete, including gathering, preparing, and submitting the completed application data sheet form to the USPTO. Time will vary depending upon the individual case. Any comments on the amount of time you require to complete this form and/or suggestions for reducing this burden, should be sent to the Chief Information Officer, U.S. Patent and Trademark Office, U.S. Department of Commerce, P.O. Box 1450, Alexandria, VA 22313-1450. DO NOT SEND FEES OR COMPLETED FORMS TO THIS ADDRESS. **SEND TO: Commissioner for Patents, P.O. Box 1450, Alexandria, VA 22313-1450.**

CONTROLLED RELEASE OF OCULAR BIOPHARMACEUTICALS USING BIORESPONSIVE PROTEIN POLYMERS

CROSS REFERENCE TO RELATED APPLICATIONS

This application includes a claim of priority under 35 U.S.C. §119(e) to U.S. Patent Application No. 61/511,928, filed July 26, 2011.

GOVERNMENT RIGHTS

This invention was made with government support under Contract No. R21EB012281-01 awarded by the National Institutes of Health. The government has certain rights in the invention.

FIELD OF INVENTION

This invention relates to the use of protein polymers to improve drug delivery to various organs, particularly the eye, and other related uses.

BACKGROUND

All publications herein are incorporated by reference to the same extent as if each individual publication or patent application was specifically and individually indicated to be incorporated by reference. The following description includes information that may be useful in understanding the present invention. It is not an admission that any of the information provided herein is prior art or relevant to the presently claimed invention, or that any publication specifically or implicitly referenced is prior art.

Affecting over 3.2 million Americans, dry eye syndrome is a common disorder of the tear film characterized by decreased tear production. This disease is prevalent among the elderly and is particularly common in postmenopausal women. Typically, dry eye is treated using conventional drops containing small molecule drugs, although recombinant tear protein rescue for dry eye syndrome has become a possibility with the discovery of a novel human tear glycoprotein, lacritin. Lacritin is capable of promoting basal tear peroxidase secretion by rat lacrimal acinar cells *in vitro*, basal tear secretion by rabbit *in vivo* and possibly triggers downstream signaling pathway through tyrosine phosphorylation and calcium release. However, this option has found limited practical application as tears wash drugs away from the eye within

minutes, and less than 2% of the medication is absorbed. As tears rapidly wash away both small and large molecule drugs, this has prevented the development of numerous protein-based drugs. By contrast, protein drugs administered to other sites in the body have continued to be developed into effective therapies. Thus, there is a clear unmet need to develop effective delivery strategies that for administration and retention of biopharmaceuticals in a target organ, such as the surface of the eye.

Accordingly, the inventive compositions and methods disclosed herein establish new and improved techniques for improving drug delivery to organs that are presently limited by biochemical and biomechanical environments due to pH, temperature, hydrodynamic flow, mechanical/structure features, among others. To overcome these obstacles, the inventors have developed temperature sensitive protein polymers and fused these polymers directly to a biopharmaceutical with enhanced therapeutic activity at the eye surface. This strategy allows for retention of drugs in the eye for much longer periods of time, on the order of days to weeks, thereby improving drug efficacy, while reducing cost and eliminating the need for repeated drug application.

SUMMARY OF THE INVENTION

The present invention provides, in one embodiment, an isolated fusion protein including a bioresponse protein polymer, and a therapeutic protein conjugated to the bioresponse protein polymer. In another embodiment, the bioresponse protein polymer is an elastin-like polypeptide (ELP). In another embodiment, the ELP includes amino acid motif $(Val\text{-}Pro\text{-}Gly\text{-}X_{aa}\text{-}Gly)_n$, where n includes 10 to 300 units and X_{aa} is a natural or synthetic amino acid. In another embodiment, n is 96 and X_{aa} is serine, valine, or isoleucine. In another embodiment, therapeutic protein is lacritrin, a functional equivalent or active fragment thereof. In another embodiment, lacritrin, functional equivalent or active fragment thereof includes human lacritrin. In another embodiment, the lacritrin, functional equivalent or active fragment thereof includes amino acid sequence: SEQ ID NO: 3, SEQ ID NO: 4, SEQ ID NO: 5, SEQ ID NO: 6, SEQ ID NO: 7, or SEQ ID NO: 8. In another embodiment, the bioresponse protein polymer and therapeutic protein are conjugated via a linker peptide. In another embodiment, the linker peptide includes amino acid sequence: SEQ ID NO: 9. In another embodiment, the bioresponse protein polymer is ELP, the therapeutic protein is lacritrin, and the ELP is conjugated to the lacritrin via a linker peptide. In another embodiment, the fusion protein includes an ELP including amino acid motif (Val-Pro-

Gly-X_{aa}-Gly)$_n$, n is 96 and X_{aa} is valine, conjugated to a lacritrin, functional equivalent or active fragment thereof including amino acid sequence: SEQ ID NO: 3, SEQ ID NO: 4, SEQ ID NO: 5, SEQ ID NO: 6, SEQ ID NO: 7, or SEQ ID NO: 8, via a linker peptide including SEQ ID NO:9.

Another aspect of the present invention provides, in one embodiment, an isolated nucleotide encoding a fusion protein including a bioresponse protein polymer, and a therapeutic protein conjugated to the bioresponse protein polymer. In another embodiment, the bioresponse protein polymer includes an elastin-like polypeptide (ELP). In another embodiment, the ELP includes amino acid motif (Val-Pro-Gly-X_{aa}-Gly)$_n$, where n includes 10 to 300 repeat units and X_{aa} is a natural or synthetic amino acid. In another embodiment, the therapeutic protein includes lacritrin, a functional equivalent or active fragment thereof. In another embodiment, the isolated nucleotide of is constructed using recursive directional ligation. In another embodiment, the isolated nucleotide encodes for a fusion protein inluding an ELP including amino acid motif (Val-Pro-Gly-X_{aa}-Gly)$_n$, n is 96 and X_{aa} is valine, conjugated to a lacritrin, functional equivalent or active fragment thereof including amino acid sequence: SEQ ID NO: 3, SEQ ID NO: 4, SEQ ID NO: 5, SEQ ID NO: 6, SEQ ID NO: 7, or SEQ ID NO: 8, via a linker peptide including SEQ ID NO:9.

Another aspect of the present invention provides, in one embodiment, a method of treating a disease and/or condition in a human subject, include providing a quantity of a composition, wherein the composition includes a fusion protein, the fusion protein including a bioresponse protein polymer and a therapeutic protein conjugated to the bioresponse protein polymer; and treating a human subject by administering a therapeutically effective dosage of the composition to the subject, thereby treating the subject. In another embodiment, the human subject is in need of treatment for an eye disease and/or condition selected from the group consisting of: acanthamoeba keratitis, allergies, amblyopia, Bell's palsy, blepharitis, cataracts, chalazion, color blindness, corneal ulcer, detached retina, dry eye syndrome, keratoconjunctivitis sicca, eye occlusions, eye twitching, macular hole, nystagmus, ocular migraine, ocular rosacea, optic neuritis, optic neuropathy, photophobia, pinguecula, pterygium, ptosis, Sjogren's syndrome, strabismus, stye, subconjunctival hemorrhage, uveitis, CMV retinitis, conjunctivitis, diabetic retinopathy, eye herpes, glaucoma, karatoconus, macular degeneration, macular dystrophy, ocular hypertension, retinitis pigmentosa, and/or Stargardt's disease. In another embodiment, the bioresponse protein polymer includes an elastin-like polypeptide (ELP), the

therapeutic protein includes lacritrin, and the ELP is conjugated to the lacritrin via a linker peptide.

Another aspect of the present invention provides, in one embodiment, a pharmaceutical composition including a bioresponse protein polymer, a therapeutic protein conjugated to the bioresponse protein polymer, and a pharmaceutically acceptable carrier. In another embodiment, the bioresponse protein polymer includes an elastin-like polypeptide (ELP), the therapeutic protein includes lacritrin, and the ELP is conjugated to the lacritrin via a linker peptide.

Another aspect of the present invention provides, in one embodiment, a a method of using an ELP in a purification process, including: a) providing a sample including a ELP construct, b) inducing phase transition in the sample by adding 0 to 20 M NaCl and heating to temperatures up to about 10, 20, 30, 35, 37, 40, or 45°C, b) centrifuging the sample at 5,000, 6,000, 7,000, 8,000, 9,000 or 10,000 g, c) discarding the supernatant, and d) cooling remaining pellet to about, 1, 2, 3, 4, 5, or 6-10°C.

BRIEF DESCRIPTION OF THE FIGURES

Exemplary embodiments are illustrated in referenced figures. It is intended that the embodiments and figures disclosed herein are to be considered illustrative rather than restrictive.

Figure 1 ELP protein polymers. (A): Cartoon showing Lac-ELP fusion protein stimulates primary rabbit lacrimal gland acinar cells (LGACs) secretion. **(B):** Elastin-like polypeptides (ELPs) phase transition. **(C):** Cartoon showing drug delivery to the eye via topical administration or lacrimal gland injection.

Figure 2. Examples of Lac-ELPs. (A): Cartoon showing structure of a typical Lac-ELP fusion protein. Lacritin and ELP tag are at the N and C terminus of the fusion construct accordingly. A thrombin recognition site (GLVPR|GS) is designed between the two moieties for releasing free lacritin. Four types of ELP tags are chosen: I96, V96, S96 and S48I48. **(B):** Sequence, M.W. and Phase Transition Temperature (T_t) characterization of Lac-ELP library. At T<T_t, ELPs exist as soluble monomers; at T>T_t, monoblock S96 stay soluble as 2-3nm monomers; more hydrophonbic I96, V96 self-assemble into micron-sized coacervates (>1μm). Diblock ELPs (S48I48) undergo two transitions: one smooth transition from 2-3nm monomer to 20nm micelles at CMT (26.6°C) and one sharp bulk phase transition at 75°C. Lac-ELPs exhibit different phase transition behavior from their parent ELPs based on particular guest residues. Both Lac-I96 and Lac-V96 exhibited 5°C decrease of T_t compared to I96 and V96. Lac-S96

completely abolished the phase transition behavior of S96. In contrast to an obvious 2-stage phase transition of S48I48, Lac-S48I48 only shows one sharp phase transition at 18.7°C. *m/z (Expected M.W.) is calculated by DNAStar Lasergene Editseq; [M+H]+ (Observed M.W.) is measured by MALDI-TOF; *T_t is characterized at 25μM in PBS.

Figure 3. Construction of bacterial expression vector encoding for a lacritin ELP fusion protein. (A): A gene encoding the lacritin between the NdeI and BamHI sites was ligated into a pET25B(+) vector. A technique used by our group called Recursive Directional Ligation was used to create ELP genes that can be extracted by cleavage at a BseRI and the BamHI restriction site. Fusion of the appropriate digested vectors, yields a bacterial expression plasmid that encodes for an in frame fusion protein consisting of an amino terminal lacritin and a carboxy terminal ELP. The two domains are linked by a thrombin cleavage recognition site to enable proteolytic cleavage and purification of the free lacritin. **(B):** Size exclusion chromatograph of Lac-V96 purification.

Figure 4. Purity of a lacritin-ELP fusion protein and mass spectrometry analysis. (A): SDS PAGE of copper chloride stained purified lacritin-ELP fusion protein, Lac-V96. Also included are purified ELP alone, V96, and the purified lacritin protein (Lac). **(B):** Matrix assisted laser desorption ion time of flight (MALDI TOF) was used to confirm the exact masses of the ELP and Lac-V96 fusion proteins. Results of this study are indicated in Table 3; however, these results demonstrate that the correct protein has been expressed and purified using our methods. Lac-ELP fusion gene was biosynthesized using pET25b(+) vector. After expression in BLR(DE3) cells, ELPs and Lac-ELP fusion proteins were purified using Inverse phase transition cycling (ITC) and size exclusion chromatography. Free lacritin was released by thrombin cleavage.

Figure 5. Further characterization of purity of a Lacririn-ELP fusion protein and mass spectrometry analysis. (A): Another SDS PAGE of copper chloride stained purified lacritin-ELP fusion protein. Lanes from L to R are 1,7: Marker, 2: Lac-V96 After ITC purification, 3: Lac-V96 After size exclusion column purification, 4: V96 After ITC purification, 5: Lac After thrombin cleavage Before hot spin, 6: Lac After thrombin cleavage After hot spin. **(B):** Another MALDI TOF confirming the exact masses of the ELP and Lac-V96 fusion proteins, demonstrating correct expression of the protein purified using our methods.

Figure 6. Phase diagrams for lacritin ELP fusion proteins. The fusion protein between lacritin and the ELP V96 displays ELP phase transition behavior.**(A):** T_t characterizaiton of V96. **(B):** T_t characterizaiton of Lac-V96. **(C):** Concentration dependent T_t of V96 and Lac-V96. **(D):** Above the line depicted for Lac-V96, the fusion protein undergoes phase separation, around 30 °C. This fusion construct would therefore be soluble at room temperature and undergo phase separation at the temperature of the ocular surface, which is > 32 °C. The fusion of lacritin has a detectable, but minimal effect on the transition temperature compared to unmodified ELP.

Figure 7. Lacritin undergoes degradation at 37°C. (A): Time dependent degradation characterization of Lac, fit into one-phase decay curve. **(B):** Amino acid sequence of Lac, red: K residues. **(C):** MALDI-TOF analysis of purified lacritin and degraded lacritin, K is expected cutting site. For determination of the degradation half-life of purified Lac-ELPs and lacritin, the purified proteins (20μg) were incubated in PBS or rabbit tear at 37°C for 72h. At each time point, an equal volume of 4x SDS-PAGE loading buffer (2% SDS, 0.01% bromophenol blue, and 63 mM Tris-HCl, pH 6.8, with or without 5% β-mercaptoethanol) was added. The samples were boiled for 5 min at 95°C, and then loaded onto precasted 4-20% Tris-HCl polyacrylamide gels (Lonza). β-mercaptoethanol was included in the SDS-PAGE sample buffer to disrupt the possible intrachain and interchain disulfide bonds in protein. The ability of the exogenous protease inhibitors to inactivate degradation was also evaluated. Peptide sequence analysis of degradation was performed using MALDI-TOF. Cleavage products were assigned by MALDI-TOF mass by comparison of measured with predicted mass to charge ratios (m/z) with +1 charge ionization ([M + H]+).

Figure 8. Lacritin influences inverse phase transition behavior of parent ELPs. (A): Representative phase transition turbidity change observed at 350 nm (OD350nm) as a function of solution temperature for Lac-V96 (open circles), V96 (open squares) and lacritin (open triangle) at 25μM. **(B, C&D):** T_t as a function of concentration (100μM, 50μM, 25μM, 10μM, 5μM) for Lac-ELP and ELPs in PBS. Data points were fit into model: T_t = m Log10[CELP] + b, where CELP (μM) is the ELP concentration, m is the slope (°C per Log10[μM]), and b (°C) is the transition temperature at 1 μM. R2 and 95% confidence interval of fitting was shown in red. * **(B):** S96 and Lac-S96. **(C):** V96 and Lac-V96. **(D):** I96 and Lac-I96, E: S48I48 and Lac-S48I48.

Figure 9. Lac-ELPs assemble into nanoparticles at low temperature. **(A):** Free lacritin exhibited as 2-3nm monomers within experiment temperature range. **(B):** V96 stayed as 2-3 monomers until bulk phase transition; Lac-V96 preassembled into 30-40nm particles below T_t and aggregated into micron-sized coacervate above Tt. **(C):** As soluble ELP control, S96 remained as 2-3nm monomers between 10°C and 55°C while Lac-S96 assembled into 30-40nm particles within same temperature range. **(D):** S48I48 existed as soluble monomers and aggregated into stable monodisperse nanoparticles with a Rh of 20-30nm above its CMT (26.6°C). Lac-S48I48 preassembled into 30-40nm particles similar to other Lac-ELPs; above its T_t, Lac-S48I48 further reconstituted into 130-140nm micelles. **(E&F):** TEM images of S48I48 and Lac-S48I48 micelles, with average diameter of 36.5±5.8nm and 67.1±11.5nm accordingly. **(G):** Cartoon showing S48I48 and Lac-S48I48 micelles. **(H&I):** Cryo-TEM images of S48I48 and Lac-S48I48 micelles, with average diameter of 29.1±3.4nm and 56.7±3.1nm accordingly. *Hydrodynamic radius (Rh) of lacritin, Lac-ELPs and parent ELPs were measured at 25μM in PBS (pH.7.4) as a function of temperature by DLS.

Figure 10. Construction and Expression of a functional lacritin ELP fusion protein. **(A):** The lacritin constructs were evaluated for their ability to induce secretion of β-hexosaminidase from primary rabbit LGACs. Carbachol (CCH+) provided a positive control. Lac-V96 and Lac both have significantly (*$p<0.05$) more activity than the negative control (CCH-) or V96 alone. The similarity in efficacy between the isolated lacritin and ELP fusion protein suggests they may have similar activity; however, the phase behavior of the ELP domain may promote ocular retention and enhance activity *in vivo*. **(B):** Steps of recursive directional ligation. **(Ba):** ELP gene is inserted into the pet25b+ vector and dimerized by ligating with another ELP. It is cut at two sites with BseRI (RE-A) and AcuI (RE-B). A linearized gene of the ELP is obtained by cutting only at the A site. **(Bb):** The steps are repeated until the desired ELP chain length is obtained. **(Bc):** ELP is inserted into a plasmid containing the lacritin gene to form a lacritin ELP fusion protein.

Figure 11. Lac-V96 and Lac stimulate LGAC secretion. **(A):** Time dependent LGAC secretion, bhex level is normalized to total protein secreted using BCA assay, N=3. **(B):** Concentration dependent LGAC secretion, Values are means+SD of LGAC cell response to each treatment expressed as (BhexTreatment-BhexCCh-)/(BhexCCh+-BhexCCh-)*100%. CCh-

group response is defined as 0% and CCh+ group response is defined as 100%; N=3. * P < 0.05,**P < 0.01, *** P < 0.001.

Figure 12. Lacritin and Lac-ELPs stimulate β-hexosaminidase secretion in a time and dose dependent manner. β-hexosaminidase secreted into the supernatant culture media was measured by its catalytic activity against substrate 4-methylumbelliferyl N-acetylb-D-glucosaminide (4MUGlcNAc). Activity was normalized to OD465nm/μg protein using BCA assay. Results from three individual cell preparations were analyzed. Each treatment was triplicated under every preparation. Figure was shown as cell response % compared to Carbachol stimulation and plain medium treatment. Significance was analyzed using two-way ANOVA. **(A):** LGACs were treated with 20μM, 10μM, 1μM and 0.1μM of Lac-V96, lacritin, V96 or controls for 1h at 37°C. 10μM and 20 μM Lac-V96 and lacritin significantly enhanced β-hexosaminidase secretion compared to V96 group, showing 20-30% LGAC reponse of positive control carbachol group. **(B):** LGACs were treated with 10μM Lac-V96, lacritin, V96 or controls for 0min, 30min, 1h, 2h and 4h. Lac-V96 and lacritin started stimulating β-hexosaminidase secretion as early as 30min and reached a plateau at 1h. **(C):** LGACs were treated with 20μM Lac-I96, Lac-V96, Lac-S96, Lac-S48I48 or lacritin for 1h at 37°C. *p<0.05, **p<0.01, ***p<0.001, ****p<0.0001. Each treatment is triplicated each time and whole β-Hexosaminidase secretion assays were repeated 3 times (N=3, n=3). LGAC cell response under each condition is compared to CCh+ (100%) minus CCh- response (0%).

Figure 13. Lac-ELP and Lac stimulate Syn-GFP secretion. In vitro activity of purified proteins was measured by β-hexosaminidase assay and syncollin-GFP secretion assay using primary rabbit lacrimal gland acinar cells (LGACs). Previous studies have shown that both β-hexosaminidase and syncollin-GFP can be secreted from rabbit lacrimal gland acinar cells in primary culture on stimulation with secretagogs. **(A):** schematic outline of LGAC, N: nucleus, L: lumenal regions, SVs: secretory vesicles. **(B):** 50μM CCh+, Lac-V96, Lac or V96 was added into Ad-Syn-GFP (green) and LifeAct-RFP (red) double transduced LGACs.Time-lapse pictures were taken using Zeiss LSM 510 Meta NLO (Thornwood, NY) confocal imaging system. Scale bar: 5μm, *:Lumenal regions, arrows: morphology change in LGAC lumen and Syncollin-GFP secretory vesicles.

Figure 14. Lac-V96 induces chronic Syn-GFP secretion and F-actin remodeling LGACs were transduced with adenovirus Ad-Syn-GFP and Ad-LifeAct-RFP to investigate the

changes in secretion marker protein Syncollin-GFP (green) secretion and actin filaments (red) located beneath the apical and basal membrane during exocytosis evoked by the Lac-V96 and lacritin using time-lapse confocal fluorescence microscopy. **(A):** Structure model of LGAC. F-actin are more enriched underneath apical membrane. **(B):** While positive control muscarinic agonist carbachol (100μM) acutely (0-15min) increased significant apical actin filament turnover and also promoted transient actin assembly around apparent fusion intermediates (B1-B4); Lac-V96 (20μM) exhibits a much milder and chronic effect on LGAC morphology (B5-B8). However, one can still observe increased irregularity in the continuity of apical actin filaments and formation of actin-coated structures beneath the apical and also basal membrane (purple arrows). The lumenal regions in LGACs were distinguished by *. L: lumen; SV: secretion vesicle

Figure 15. Lac-ELPs and lacritin triggers transient cytoplasmic Ca2+ wave in HCE-T cells but not in LGACs. (A1): Acute stimulation with carbachol (10μM) induced Ca2+ oscillation in LGACs. **(A2):** Carbachol titration (0.1μM, 1μM, 10μM, 100μM, 1mM and 1mM) triggered concentration dependent Ca2+ wave in HCE-T cells. **(B1):** NaCl Ringer solution did not trigger Ca2+ wave in HCE-T cells. **(B2&B3):** EGF (10ng/ml) or lacritin (10μM) triggered 3-4 fold intracellular Ca2+ increase in HCE-T cells. **(B4):** Lac-S48I48 (40μM×2) triggered 4-6 fold intracellular Ca2+ increase in HCE-T cells. **(C):** Summary of Ca2+ response in LGACs and HCE-T cells induced by treatment. *Fluorescence intensity change in ten individual cells were analyzed and plotted as (Ft-F0)/F0. Representative maximum cell response images were shown. HCE-T cells were rinsed twice with dPBS (Ca^{2+} and Mg^{2+} free) and incubated at 37°C for 20 minutes in fresh KSFM medium without BPE or EGF containing 2.5μM Fluo-4 AM. The cells were then rinsed twice with NaCl Ringer buffer (145mM NaCl, 5mM KCl, 1mM CaCl2, 1mM KH2PO4, 1mM MgCl2, 10mM glucose, and 10mM HEPES, osmolarity 300, pH 7.4) and kept in the same buffer at room temperature for 30 minutes. For Ca^{2+} free medium, 1mM Ca^{2+} was replaced with 0.5mM EGTA. The data are presented as percentage change in fluorescence intensity at each time point (F_t) to the first time point (F_0) reading: $(F_t-F_0)/F_0\times100\%$.

Figure 16. Lacritin is susceptible to protease. (A): Time dependent degradation of purified lacritin. Up: SDS-PAGE stained with coomassie blue showing disappearing of lacritin band; lower: one-phase decay fitting curve of lacritin degradation, $t_{1/2}$=23.7h (R^2=0.99). **(B):** Lacritin degradation can be inhibited by protease inhibitor cocktail. **(C):** Western blot of purified

lacritin probed with anti-lacritin antibody. **(D):** MALDI-TOF analysis of lacritin degradation product. **(E):** Examples of possible cutting sites within lacritin sequence. *Truncation products following degradation were assigned by MALDI-TOF MS by comparison of measured with predicted mass to charge ratios (m/z) with +1 charge ionization ($[M + H]^+$). Corresponding sequences are shown. Bold and underlined sequence: Syndecan-1 binding site. Blue: residual thrombin cleavage site. Red: possible cutting site. ***$p<0.001$

DETAILED DESCRIPTION OF THE INVENTION

All references cited herein are incorporated by reference in their entirety as though fully set forth. Unless defined otherwise, technical and scientific terms used herein have the same meaning as commonly understood by one of ordinary skill in the art to which this invention belongs. Singleton et al., *Dictionary of Microbiology and Molecular Biology 3rd ed.*, J. Wiley & Sons (New York, NY 2001); March, *Advanced Organic Chemistry Reactions, Mechanisms and Structure 5th ed.*, J. Wiley & Sons (New York, NY 2001); and Sambrook and Russell, *Molecular Cloning: A Laboratory Manual 3rd ed.*, Cold Spring Harbor Laboratory Press (Cold Spring Harbor, NY 2001), *Remington's Pharmaceutical Sciences*, by E. W. Martin, Mack Publishing Co., Easton, Pa., 15th Edition (1975), describes compositions and formulations suitable for pharmaceutical delivery of the inventive compositions described herein provide one skilled in the art with a general guide to many of the terms used in the present application.

One skilled in the art will recognize many methods and materials similar or equivalent to those described herein, which could be used in the practice of the present invention. Indeed, the present invention is in no way limited to the methods described herein. For purposes of the present invention, the following terms are defined below.

"Administering" and/or "administer" as used herein refer to any route for delivering a pharmaceutical composition to a patient. Routes of delivery may include non-invasive peroral (through the mouth), topical (skin), transmucosal (nasal, buccal/sublingual, vaginal, ocular and rectal) and inhalation routes, as well as parenteral routes, and other methods known in the art. Parenteral refers to a route of delivery that is generally associated with injection, including intraorbital, infusion, intraarterial, intracarotid, intracapsular, intracardiac, intradermal, intramuscular, intraperitoneal, intrapulmonary, intraspinal, intrasternal, intrathecal, intrauterine, intravenous, subarachnoid, subcapsular, subcutaneous, transmucosal, or transtracheal. Via the

parenteral route, the compositions may be in the form of solutions or suspensions for infusion or for injection, or as lyophilized powders.

"Modulation" or "modulates" or "modulating" as used herein refers to upregulation (i.e., activation or stimulation), down regulation (i.e., inhibition or suppression) of a response or the two in combination or apart.

"Pharmaceutically acceptable carriers" as used herein refer to conventional pharmaceutically acceptable carriers useful in this invention.

"Promote" and/or "promoting" as used herein refer to an augmentation in a particular behavior of a cell or organism.

"Subject" as used herein includes all animals, including mammals and other animals, including, but not limited to, companion animals, farm animals and zoo animals. The term "animal" can include any living multi-cellular vertebrate organisms, a category that includes, for example, a mammal, a bird, a simian, a dog, a cat, a horse, a cow, a rodent, and the like. Likewise, the term "mammal" includes both human and non-human mammals.

"Therapeutically effective amount" as used herein refers to the quantity of a specified composition, or active agent in the composition, sufficient to achieve a desired effect in a subject being treated. A therapeutically effective amount may vary depending upon a variety of factors, including but not limited to the physiological condition of the subject (including age, sex, disease type and stage, general physical condition, responsiveness to a given dosage, desired clinical effect) and the route of administration. One skilled in the clinical and pharmacological arts will be able to determine a therapeutically effective amount through routine experimentation.

"Treat," "treating" and "treatment" as used herein refer to both therapeutic treatment and prophylactic or preventative measures, wherein the object is to prevent or slow down (lessen) the targeted condition, disease or disorder (collectively "ailment") even if the treatment is ultimately unsuccessful. Those in need of treatment may include those already with the ailment as well as those prone to have the ailment or those in whom the ailment is to be prevented.

The lacrimal gland-cornea axis plays a critical role in maintaining ocular health. While avascular cornea serves as both protective barrier and main refractive element of the visual system, lacrimal gland is the major organ secreting key proteins and electrolytes into the tear

film that overspreads the cornea and conjunctiva. Dry eye syndrome is a multifactorial disease of the tears and ocular surface causing visual disturbance and tear film instability. Accordingly to report, severe dry eye disease (DED) affects approximately 5 million Americans above 50 years and its global prevalence ranges from 5% to 35%. Great strides have been made to treat dry eye syndrome and DED through lubricating ocular surface with artificial tears, conserving the secreted tears using tear plugs and eye-shields, or targeting the associated ocular surface inflammation such as Cyclosporin eye-drops. Nevertheless, there still remains a continued demand for efficient, sustained and targeted novel dry eye syndrome and DED therapy.

Ocular drug delivery remains challenging due to the unique ocular anatomy and physiology. Blinking, tear film, and various layers of corneal cells all lead to reduced bioavailability for topical ocular administration. Conventional eye drops are washed away from the eye within minutes after ocular administration, and less than 2% of the medication is absorbed. Due to rapid clearance, ocular drug formulations must be given frequently, every 2 to 8 hours. Further, effective dry eye therapy requires economic process of manufacture, long-term drug stability inside appropriate vehicle and non-invasive prolonged controlled release of the drug to target site. A promising development of safe and effective drug delivery systems is biocompatible polymers, which offer the versatility to remodel drug delivery vesicle structure and further tailor drug release kinetics. Recently, macromolecular self-assemble nanoparticles are emerging as attractive candidates for therapeutic applications.

Elastin-like-polypeptides (ELPs) are one type of such biomaterials. These proteins are members of a larger class of bioresponsive protein polymers that are macromolecules responsive to small environmental changes, for instance temperature or pH. Inspired from human tropoelastin, ELPs have unique properties that promote phase separation, recombinant expression, protein purification, and self-assembly of nanostructures. The polypeptides are biodegradable, biocompatible polymers with temperature-sensitive phase behavior. ELPs are soluble in aqueous solutions below their transition temperature and collapse and aggregate under hydrophobic forces above their critical transition temperature. Importantly, this type of phase transition can be exploited for the development of fusion proteins that are highly soluble at room temperature, but undergo reversible assembly of micron size particles on the ocular surface. These dynamic chemical characteristics can be captured in fusion proteins containing

therapeutically effective compounds, thereby allowing retention of biopharmaceuticals in the eye longer than conventional application techniques.

One therapeutically effective compound for use in treating dry eye syndrome is lacritin. lacritin is a 138 amino acid, 12.3 kDa glycoprotein (Uniparc ID NO. Q9GZZ8) secreted in human tears. One of the 4-5% proteins that are downregulated in dry eye syndromes, lacritin is a highly glycosylated tear protein showing prosecretory and mitogenetic activity for corneal epithelial cells. Detected by 2-D PAGE, nano-LC-MS/MS and SELDI studies, lacritin shows a common downregulation in blepharitis vs normal tears. *In vivo* studies of lacritin on New Zealand white rabbits shows that eyes treated three times a day for two weeks display a steady rise in tearing that is sustained for at least one week after the last treatment and is well tolerated when topically applied in rabbits. Current ongoing and future research is being carried out to formulate lacritin as a topical eye drop as an effective treatment for dry eye syndrome. However, these rabbit studies have demonstrated that significant effects with lacritin require application of the protein to the ocular surface at least three times a day via eye drops.

The inventors have exploited the features of ELPs in creating a fusion protein containing lacritin, to effectively stimulate ocular surface healing and tear production. By fusing a small library of various ELPs to lacritin, the inventors characterized the phase transition temperatures for the resulting lacritin-ELP constructs and demonstrated that the lacritin contained therein is capable of actively stimulating the tear secretion of primary lacrimal gland acinar cells from rabbits. The most commonly used ELPs consist of pentapeptide repeats of $(VPGX_{aa}G)_n$ where X_{aa}, the guest residue, is any amino acid and n represents the number of repeats in the ELP. ELPs exhibit the unique property of inverse temperature phase transition; they are soluble in aqueous solution below their inverse transition temperature (*Tt*) and undergo an aqueous demixing above their *Tt*, resulting in the formation of an insoluble, polymer-rich 'coacervate' phase. This novel application of ELPs exploits their characteristic phase behavior to slow clearance of biologically active proteins from the eye, while also providing a versatile liquid-solid medium scaffold as support for retaining these compounds in the eye.

Described herein are various aspects of the present invention. In one embodiment, the present invention provides an isolated fusion protein including a bioresponse protein polymer conjugated to a therapeutic protein. In another embodiment, the isolated fusion protein contains

a bioresponse protein polymer that is an elastin-like polypeptide (ELP). In another embodiment, the ELP includes the motif $(Val\text{-}Pro\text{-}Gly\text{-}X_{aa}\text{-}Gly)_n$, where n is between 10 and 300 repeat units and X_{aa} is a natural or synthetic amino acid. In another embodiment, the ELP includes the motif $(Val\text{-}Pro\text{-}Gly\text{-}X_{aa}\text{-}Gly)_n$, where n is between 10-50, 50-100, 100-150, 150-200, 200-250, 250-300 and/or 300-400 repeat units and X_{aa} is a natural or synthetic amino acid. In other embodiments, X_{aa} is serine, isoleucience, or valine. In one embodiment, n is 96 and X_{aa} is valine.

In another embodiment, the therapeutic protein is lacritrin, a functional equivalent or active fragment thereof. In another embodiment, the lacritrin, functional equivalent or active fragment thereof is human lacritrin. In another embodiment, the lacritrin, functional equivalent or active fragment thereof is an amino acid sequence with 70, 75, 80, 85, 90, 95, 99, or 100% similarity to SEQ ID NO: 3. In another embodiment, the lacritrin, functional equivalent or active fragment thereof is amino acid sequence SEQ ID NO: 4, SEQ ID NO: 5, SEQ ID NO: 6, SEQ ID NO: 7, or SEQ ID NO: 8. In another embodiment, the bioresponse protein polymer and therapeutic protein are conjugated via a linker peptide. In another embodiment, the linker peptide is the amino acid sequence: SEQ ID NO: 9. In another embodiment, the bioresponse protein polymer is ELP, the therapeutic protein is lacritrin, and the ELP is conjugated to the lacritrin via a linker peptide. In another embodiment, the isolated fusion protein includes the amino acid sequence: SEQ ID NO: 4, SEQ ID NO: 5, SEQ ID NO: 6, SEQ ID NO: 7, or SEQ ID NO: 8, conjugated to amino acid motif $[VPGX_{aa}G]_n$, wherein n is 96 and X_{aa} is valine. In other embodiments, the therapeutic protein is Restasis (cyclosporin), α-Crystallin, Ocriplasmin, Ranibizumab, aflibercept, iSONEP, or Volociximab.

In other embodiments, ELPs are composed of simple pentapeptide repeat $(VPGX_{aa}G)_n$, where the 'guest residue' X_{aa} can be any amino acid and n controls the peptide length. In other embodiments, ELPs possess inverse temperature phase transition behavior, are soluble in aqueous solutions below their transition temperature (*Tt*), and/or self-assemble into various-sized particles above *Tt*. In other embodiments, *Tt* can be precisely modulated by adjusting the length of the pentapetides repeats and the hydrophobicity of the guest residue. In certain embodiments, *Tt* is calculated according to the following equation:

$$T_t = m \, \mathrm{Log}_{10}[C_{ELP}] + b$$

wherein C_{ELP} (μM) is the ELP concentration, m is the slope (°C per Log_{10}[μM]), and b (°C) is the transition temperature at 1 μM. In other embodiments, the ELPs include at least two

monomeric amino acid motifs with different guest residues, $(VPGX_{aa}1G)_{n1}(VPGX_{aa}2G)_{n2}$, where n1 or n2 are each between 10 and 300 repeat units and X_{aa} is a natural or synthetic amino acid. In another embodiment, the ELP includes the motif $(Val\text{-}Pro\text{-}Gly\text{-}X_{aa}\text{-}Gly)_n$, where n1 or n2 are each between 10-50, 50-100, 100-150, 150-200, 200-250, 250-300 and/or 300-400 repeat units and X_{aa} is a natural or synthetic amino acid. In other embodiments, X_{aa} is serine, isoleucience, or valine. In one embodiment, n is 48 and X_{aa} is valine.

In another aspect of the present invention, described herein is an isolated nucleotide encoding a fusion protein that includes a bioresponse protein polymer conjugated to a therapeutic protein. In another embodiment, the bioresponse protein polymer is a member of the group of elastins, resilins, collagens, slik- and/or elastin-like polypeptides. In another embodiment, the bioresponse protein polymer is an elastin-like polypeptide (ELP). In another embodiment, the ELP includes the motif $(VPGX_{aa}G)_n$, where n is between 10 and 300 repeat units and X_{aa} is a natural or synthetic amino acid. In another embodiment, the ELP includes the motif $(Val\text{-}Pro\text{-}Gly\text{-}X_{aa}\text{-}Gly)_n$, where n is between 10-50, 50-100, 100-150, 150-200, 200-250, 250-300 and/or 300-400 repeat units and X_{aa} is a natural or synthetic amino acid. In other embodiments, X_{aa} is serine, isoleucience, or valine. In one embodiment, n is 96 and X_{aa} is valine. In another embodiment, the therapeutic protein is lacritrin, a functional equivalent or active fragment thereof. In another embodiment, the lacritrin, functional equivalent or active fragment thereof is human lacritrin In another embodiment, the lacritrin, functional equivalent or active fragment thereof is an amino acid sequence with 70, 75, 80, 85, 90, 95, 99, or 100% similarity to SEQ ID NO: 3. In another embodiment, the lacritrin, functional equivalent or active fragment thereof is amino acid sequence SEQ ID NO: 4, SEQ ID NO: 5, SEQ ID NO: 6, SEQ ID NO: 7, or SEQ ID NO: 8. In another embodiment, the isolated nucleotide encoding a fusion protein includes polynucleotide sequence SEQ ID NO: 1 or SEQ ID NO:2. In another embodiment, the bioresponse protein polymer is ELP, the therapeutic protein is lacritrin, and the ELP is conjugated to the lacritrin via a linker peptide. In another embodiment, the linker peptide is the amino acid sequence: SEQ ID NO: 9. In another embodiment, the bioresponse protein polymer and therapeutic protein are conjugated via a linker peptide. In another embodiment, the bioresponse protein polymer is ELP, the therapeutic protein is lacritrin, and the ELP is conjugated to the lacritrin via a linker peptide. In another embodiment, the isolated fusion protein includes the amino acid sequence: SEQ ID NO: 4, SEQ ID NO: 5, SEQ ID NO: 6, SEQ

ID NO: 7, or SEQ ID NO: 8, conjugated to amino acid motif $[VPGX_{aa}G]_n$, wherein n is 96 and X_{aa} is valine. n other embodiments, the therapeutic protein is Restasis (cyclosporin), α-Crystallin, Ocriplasmin, Ranibizumab, aflibercept, iSONEP, or Volociximab. In another embodiment, the isolated nucleotide is constructed using recursive directional ligation.

In other embodiments, the ELPs are fusion proteins including Lac-ELP fusion proteins. In other embodiments, the Lac-ELP fusion proteins are Lac-I96, Lac-V96, Lac-S96, and/or Lac-S48I48. In other embodiments, the Lac-ELPs are purified by inverse phase transition cycling (ITC), which can further be purified using size exclusion chromatography polishing to remove ELP tag. In another embodiment, free lacritin can be released from purified lacritin-ELP via thrombin cleavage. In other embodiments, Lac-ELPs pre-assemble into 10-60 nm nanoparticles. Above *Tt*, Lac-I96 and Lac-V96 form micron-sized coacervate while Lac-S48I48 assembles into 100-180 nm micelles. In other embodiments, ELPs are also capable of self-assembling into stable micelles around physiological temperature, such as 37°C. In other embodiments, ELPs organized as stable micelles are used as a drug delivery vehicle, which may further modulate biodistribution and pharmacokinetics of the protein *in vivo*. In other embodiments, ELPs are applied as a drug delivery vehicle for a therapeutic such as Restasis (cyclosporin), α-Crystallin, Ocriplasmin, Ranibizumab, aflibercept, iSONEP, Volociximab, Sirolimus (rapamycin), Pazopanib, Vatalanib, AL39324, ATG-3, JSM6427, Fasudil, ATS907, AR-12286, K-115, and/or Carbachol.

In another aspect of the present invention, described herein are ELPs that can be used as a purification tag. In one embodiment, the present invention includes a method of using an ELP in a purification process, including: a) providing a sample including a ELP construct, b) inducing phase transition in the sample by adding 0 to 20 M NaCl and heating to temperatures up to about 10, 20, 30, 35, 37, 40, or 45°C, b) centrifuging the sample at 5,000, 6,000, 7,000, 8,000, 9,000 or 10,000 g, c) discarding the supernatant, and d) cooling remaining pellet to about, 1, 2, 3, 4, 5, or 6-10°C. In one embodiment, the sample is further agitated into a solution. In one embodiment, repeated cycles of hot and cold centrifugation are further applied, including 1, 2, 3, 4, 5, 6, 7, 8, 9 or 10 repetitions. In another aspect of the present invention, ELPs that can be used as a purification tag for lacritin, thioredoxin (Trx), chloramphenicol acetyltransferase (CAT), calmodulin (CaM), green fluorescent protein (GFP), and/or Knob.

In another aspect of the present invention, described herein is a method of treating a disease and/or condition in a human subject, which includes providing a quantity of a composition, wherein the composition includes a fusion protein, the fusion protein including a bioresponse protein polymer conjugated to a therapeutic protein; and treating a human subject by administering a therapeutically effective dosage of the composition to the subject, thereby treating the subject. In another embodiment, the human subject is afflicted with a disease and/or condition affecting the organs of the circulatory system, digestive system, endocrine system, integumentary system, lymphatic system, immune system, musculoskeletal system, nervous system, reproductive system, respiratory system, and/or urinary system. Examples include the skin, stomach, intestines, pancreas, liver, and/or brain. In another embodiment, the human subject is in need of treatment for an eye disease and/or condition selected from the group consisting of: acanthamoeba keratitis, allergies, amblyopia, Bell's palsy, blepharitis, cataracts, chalazion, color blindness, corneal ulcer, detached retina, dry eye syndrome, keratoconjunctivitis sicca, eye occlusions, eye twitching, macular hole, nystagmus, ocular migraine, ocular rosacea, optic neuritis, optic neuropathy, photophobia, pinguecula and pterygium, ptosis, Sjogren's syndrome, strabismus, stye, subconjunctival hemorrhage, uveitis, CMV retinitis, conjunctivitis, diabetic retinopathy, eye herpes, glaucoma, karatoconus, macular degeneration, macular dystrophy, ocular hypertension, retinitis pigmentosa, and/or Stargardt's disease. In other embodiments, the drug delivery vehicle is used in combination with a contact lens. In another embodiment, the bioresponse protein polymer is ELP, the therapeutic protein is lacritrin, and the ELP is conjugated to the lacritrin via a linker peptide.

In another aspect of the present invention, described herein is a pharmaceutical composition, which includes a bioresponse protein polymer conjugated to a therapeutically effective protein and a pharmaceutically acceptable carrier. In another embodiment, bioresponse protein polymer is ELP, the therapeutic protein is lacritrin, and the ELP is conjugated to the lacritrin via a linker peptide.

EXAMPLES

The following examples are provided to better illustrate the claimed invention and are not to be interpreted as limiting the scope of the subject matter. To the extent that specific materials are mentioned, it is merely for purposes of illustration and is not intended to limit the invention.

One skilled in the art may develop equivalent means, compositions or reactants without the exercise of inventive capacity and without departing from the scope of the present invention.

Example 1
Bioresponse protein polymers, generally

ELPs are repeated pentameric peptides, $(VPGX_{aa}G)_n$. These peptides have characteristic inverse phase transition temperatures, T_t, above which they phase separate from aqueous solution. By choosing the identity of X_{aa} and the length n, ELPs of different T_t can be efficiently and precisely biosynthesized (Tables 1 and 2). Genetically engineered ELPs are pharmacologically relevant, being monodisperse, biodegradable, and biocompatible. The present invention harnesses these features of bioresponsive protein polymers to control ocular clearance (Fig 1B, C).

To reduce the frequency of dosing, lacritin has been genetically fused with ELPs of different transition temperatures that are above and below the ocular surface temperature (Table 2). One example fusion protein, lacritin-V96, is soluble at room temperature and administered to the eye, upon which the body temperature raises them above their transition temperature. This process induces the formation of adhesive ELP aggregates, which slows or prevents ocular clearance. Free, active lacritin is expected to be in equilibrium with the ELP aggregates and extends the period of treatment from a single drop. ELPs with a transition temperature greater than 37°C are expected to clear quickly from the eye; however, ELPs with transition temperature between room temperature (25°C) and body temperature (37°C) are expected to drain slowly from the eye.

Table 1. Examples of of ELP protein polymers

Label	Amino acid sequence	*MW (kD)	Target behavior in body	**Assembly temperature (°C)	***Hydrodynamic Radius at 37 °C, R_h=(nm)
I96	$G(VPGIG)_{96}Y$	40.9	microparticle depot	20	>> 1,000
S96	$G(VPGSG)_{96}Y$	38.5	soluble control	56	4.2 ± 1.8
S48I48	$G(VPGSG)_{48}(VPGIG)_{48}Y$	39.6	nanoparticle	25	21.8 ± 1.5

*Molecular weight estimated for expressed gene product, as confirmed using MALDI-TOF mass spectrometry
**Assembly temperature determined using optical density at 350 nm on a temperature gradient of 1 °C min^{-1}
***Radii determined using dynamic light scattering at 25 uM ELP in phosphate buffered saline.

Table 2. Lacritin-ELP constructs evaluated

Protein Name	**lacritin-ELP amino acid sequence	Approximate MW (kD)	*T_t (°C)	Expected ocular clearance
Lac-V96	MEDASSDSTGADPAQEAGTSKPNEEISGPAEPASPPETTTTAQETSAA AVQGTAKVTSSRQELNPLKSIVEKSILLTEQALAKAGKGMHGGVPG GKQFIENGSEFAQKLLKKFSLLKPWA-GLVPR|GS-G[VPGVG]$_{96}$ Y	52.5	**26.8**	slow
Lac-I96	MEDASSDSTGADPAQEAGTSKPNEEISGPAEPASPPETTTTAQETSAA AVQGTAKVTSSRQELNPLKSIVEKSILLTEQALAKAGKGMHGGVPG GKQFIENGSEFAQKLLKKFSLLKPWA-GLVPR|GS-G[VPGIG]$_{96}$ Y	50	**10**	fast
Lac-S96	MEDASSDSTGADPAQEAGTSKPNEEISGPAEPASPPETTTTAQETSAA AVQGTAKVTSSRQELNPLKSIVEKSILLTEQALAKAGKGMHGGVPG GKQFIENGSEFAQKLLKKFSLLKPWA-GLVPR|GS-G[VPGSG]$_{96}$ Y	50	**60**	fast

*As observed for Lac_V96 and expected based on the approximate transition temperature for I96 and S96.
** Amino-terminal lacritin with the signal peptide removed followed by an underlined thrombin cleavage site, followed by a carboxy terminal ELP.

Example 2
Characterization of lacritin-ELP conjugate assembly and bioactivity

The inventors cloned (Figure 3A) and purified lacritin-ELP conjugates (Table 2). One of these conjugates, Lac-V96, has been extensively characterized through proteolytic cleavage via thrombin. A purified ELP fusion proteins (Lac-V96), a purified ELP (V96), and the purified cleaved lacritin (Lac) are all depicted (Figure 4A, 5A). The molecular mass for these constructs was confirmed using mass spectrometry (Figure 4B, 5B, Table 3). The ELP lacritin fusion protein Lac-V96 was able to undergo temperature dependent phase separation (Figure 6); furthermore, Lac-V96 is soluble at room temperature and phase separates above 30°C. More importantly, the inventors have applied this lacritin fusion protein to successfully induce expression of an enzyme marker associated with secretion, beta hexosaminidase, in primary cells isolated from rabbit lacrimal gland (LGACs).

Example 3
Constructing genes encoding for lacritin-ELPs

Genetic engineering can be used to prepare repetitive polypeptides of specific chain length. In this approach, oligonucleotide cassettes encoding the monomer gene for the pentapeptide ELP is ligated into a specially modified cloning vector, such as pet25b+. Restriction enzymes are selected RE1 and RE2, which cleave the monomer genes as

demonstrated in Figure 10B. The cloning vector with the monomer gene is digested with both RE1 and RE2 to produce an insert, which is gel purified and ligated into a separate preparation of vector linearized by digestion with only RE1. This approach leads to the controlled dimerization of the synthetic gene. This technique can be repeated until an ELP of desired chain length is formed. After formation of a library of synthetic genes encoding ELPs of different lengths and guest residues (X_{aa}), selected ELPs are transferred onto a plasmid at an RE1 cut site to the carboxy terminus of a lacritin gene (Figure 10B). Following every ligation, bacterial colonies are grown up in a 4 mL culture and harvested for plasmid DNA. The DNA is then screened by diagnostic digestion using XbaI and BamHI for the correct insertion of both the lacritin and ELP genes. Positive plasmids are then sent for DNA sequencing from the T7 promoter and terminator sequences, which is used to confirm the presence of a ribosome binding sequence, a start codon, an in frame lacritin gene, an in frame thrombin cleavage site, an inframe ELP, and an in frame stop codon. Successfully sequenced plasmids are then moved to expression bacterial cultures.

Example 4
Purification of lacritin-ELP fusion proteins

Purified plasmids (Figure 3A) are transferred into an expression host optimized for the production of repetitive sequences, the BLR(DE3)™ (Novagen). The inventors identified a critical production stage, whereby reducing the incubation temperature to 30 degrees Celsius for 24 hours is important to prevent premature cleavage of ELPs and lacritin. ELPs and lacritin-ELPs are purified using inverse phase transition cycling. Briefly, this method makes use of the ELP phase separation to induce selected precipitation of ELP fusion proteins using centrifugation. The phase transition temperature can be induced using a mild combination of 0 to 3 M NaCl and heating to temperatures up to about 37°C. This causes the phase separation of ELPs, which are centrifuged under about 10,000 g. The supernatant, which includes bacterial contaminants, is discarded. Next, the ELP pellet is cooled to 4°C and agitated gently until it returns to solution. The redissolved ELP is again centrifuged to discard any remaining protein

contaminants. As needed, this cycle of hot and cold centrifugation is repeated between 3 and 6 times to produce pure fusion constructs.

Example 5
Lac-ELPs and ELPs are purified by Inverse Transition Cycling (ITC)

In another example of the versatility of bioresponse polymers, ELPs can used as purification tag to extract soluble fusion proteins from *E.coli* debris due to their unique reversible inverse phase transition behavior. Lacritin has been previously purified using intein system, which requires multiple steps of chromatography. The inventors herein describe an alternative purification approach using ELPs. With IPTG induction, Lac-I96, Lac-V96, Lac-S96 and Lac-S48I48 can achieve satisfactory yield of more than 40mg/L. MALDI-TOF analysis and western blotting with anti-lacritin antisera further confirmed successful construction of Lac-ELPs (Figure Figure 15C). Interestingly, after ITC purification, the inventors observed two major bands on SDS-PAGE of purified Lac-ELPs (Figure 5A), upper band around 52kD and lower band around 40kD, which suggested there was pre-mature cleavage of lacritin from the fusion construct. Further degradation study confirmed this observation (Figure 16A). The inventors utilized Superose size exclusion column to remove free ELP tags (Figure 3B). Internal lacritin control was liberated from ELP tag via cleavage at designed thrombin recognition site encoded between the two moieties (Figure 1A and 2A). Similar to previous reports, lacritin ran higher on SDS-PAGE than expected M.W. 12kD (Figure 4A and 5A).

Using above method, Lac-ELPs, ELPs and lacritin can reach more than 95% purity on SDS-PAGE stained with coomassie blue (Figure 4A and 5A) The inventors also noticed several smaller MW bands (around 10kD) in purified lac-ELP and lacritin products (Figure 4A, 5A, and 8C). Analysis of MALDI-TOF data indicated that these difference size fragments released from lac-ELPs are multiple sites within the lacritin-thrombin region of the fusion protein may be susceptible to enzymatic attack by proteases or act as a protease itself (Figure 16D&E).

More specifically, ELPs I96, V96, S96 and S48I48 were expressed in BLR (DE3) E. coli cells (Novagen Inc., Milwaukee, WI). Briefly, after overnight start culture, protein was expressed for 24 h in an orbital shaker at 37 °C at 250 rpm. Cell culture were harvested and re-suspended in phosphate buffer saline (PBS). After sonication and removing insoluble cell debris and nucleic, ELPs were purified from clarified cell supernatant by inverse transition cycling

(ITC)[i] as previous reported until ELP purity was determined to be approximately 99% pure by SDS-PAGE gels stained with $CuCl_2$.

Lac-ELPs were expressed in BLR (DE3) E. coli cells using IPTG induction. Briefly, after overnight starter culture, cell pellet was inoculated into 1L TB medium and grew at 37 °C until OD600nm reached 0.5. 500ul of 1M IPTG stock solution was added into cell culture and temperature was decreased to 25°C to optimize protein expression. After 5h induction, cells were harvested and purified using ITC. Due to fast degradation of Lac-ELP, fusion protein was further polished by using Superose size exclusion column at 4°C. After balancing the column with PBS (Ph7.4), 100mg Lac-ELP was then loaded onto the column and washed out by isocratic flow of PBS at 0.5ml/min. Peak 1 was collected and concentrated using Amicon Ultra 10Kd. Free lacritin is released by thrombin cleavage of Lac-ELP fusion protein. Briefly, 300ul thrombin beads slurry (Sigma-Aldrich) was added into 200mg ITC purified Lac-ELP and incubated at room temperature for overnight. After pelleting down thrombin beads at 2,500rpm, solution was warmed up to 37°C and centrifuged at 4,000 rpm for 10min to remove phase transitioned ELP tag. Supernatant after spin was concentrated using Amicon Ultra 3Kd. Protein concentrations were determined by UV-visible spectroscopy at 280 nm (εELP=1285$M^{-1}cm^{-1}$, εLac-ELP=6990$M^{-1}cm^{-1}$, εLac=5500$M^{-1}cm^{-1}$). Protein molecular weight is further confirmed by MALDI-TOF analysis.

Example 6

Assessing the purity and molecular weight for ELP fusion proteins

Purified proteins were further characterized by SDS-PAGE and MALDI-TOF analysis. The temperature-dependent phase transition behavior of both ELPs and Lac-ELPs was characterized by measuring the optical density at 350 nm (OD350 nm) as a function of solution temperatures between 15 and 85°C in a DU800 UV-visible spectrophotometer.

More specifically, ELP and ELP fusion proteins, are run on a standard SDS-PAGE apparatus. ELPs on PAGE can be stained and imaged using copper chloride. In addition to purified ELP and ELP-lacritin, thrombin can be added to the fusion proteins. After incubation under standard conditions, this process liberates the free lacritin (Figure 1A, 2A, 4A and 5A). Although lacritin is approximately 12 kDa, it is has been reported to run on PAGE as a band around 18 kDa, which was observed by the inventors. The resulting gel depicts the purity of the peptides purified using ELP phase separation (Figure 4A and 5A).

Further confirming the identity of these gene products, the specific protein spots are isolated and characterized using matrix assisted laser desorption ion time of flight mass spectrometry (MALDI-TOF) (Figure 4B and 5B). The resulting masses are consistent with the expected protein mass to a high degree of accuracy (Table 3).

Table 3. MALDI-TOF analysis of purified ELP and lacritin fusion proteins

Protein	Expected Mass (kD)	MALDI-TOF result(kD)
Lac-V96	52.52	52.29
V96	39.55	39.21
Lac	12.85	12.73

Example 7

Measurement of phase transition temperature for ELP fusion proteins

ELP transition temperatures are determined on a Beckman DU800 UV-VIS spectrophotometer under a temperature gradient of 1°C per minute in PBS. The transition temperature, by turbidometric analysis, is defined as the maximum first derivative of the optical density at 350 nm. ELP transition temperatures are functions of the logarithm of concentration; therefore, a range of sample concentrations from 5 to 100 μM ELP are typically observed and fit to the following equation:

$$T_t = m \, \mathrm{Log}_{10}[C_{ELP}] + b$$

Where C_{ELP} (μM) is the ELP concentration, m is the slope (°C per Log_{10}[μM]), and b (°C) is the transition temperature at 1 μM. The transition temperatures for an ELP with and without fusion to a lacritin protein domain are indicated, which demonstrate that there is a measureable, but minimal decrease in the transition temperature (Figure 8A-D). Further, it is observed that lacritin undergoes degradation at 37°C (Figure 7A-C).

Typically, PBS solutions of protein sample (100μM, 50μM, 25μM, 10μM and 5μM) were heated at 1°C/min between 10°C and 85°C. T_t under each concentration is defined as the maximum first derivative of turbidity change. Particle size distribution of Lacritin, ELP and Lac-ELP fusions was measured as a function of temperature increase by dynamic light scattering (DLS). Briefly, protein samples were prepared at 25μM in PBS and filtered through a 20 nm filter (Whatman Anodisc) at 4°C. Autocorrelation functions were collected using a DynaPro-LSR dynamic light scattering Wyatt Plate Reader (Wyatt Technology, Santa Barbara, CA). Light

scattering data were collected at regular temperature intervals (1°C) as solutions were heated from 5 to 60°C. The results were analyzed using a Rayleigh sphere model and fitted into either a regularization or cumulant algorithm based on the sum-of-squares value. Critical micelle temperature (CMT) for each protein construct was defined as the lowest temperature at which the Rh is significantly greater than the average monomer Rh.

Example 8
Lacritin moiety influences phase transition behavior of parent ELPs

As ELP fusion protein, Lac-ELP would be expected to undergo phase transition like parent ELPs, one can characterize the influence of fusion lacritin moiety on *Tt* of attached ELPs. Figure 2B and Figure 8 showed inverse phase transition characterization of all expressed ELPs and lac-ELP fusion proteins at a concentration of 5, 10, 25, 50 and 100 μM in phosphate buffered saline (PBS) over the experimentally accessible temperature range of 10-90°C. As described, *Tt* of ELPs could be predicted by a simple equation, which accounts for the ELP concentration and its length: *Tt* = m Log10[CELP] + b, where CELP (μM) is the ELP concentration, m is the slope (°C per Log10[μM]), and b (°C) is the transition temperature at 1 μM. Comparison of lacritin, Lac-V96 and V96 phase transition curve at 25μM (Figure 8A and 8B) demonstrated maintenance of the phase transition behavior of parent ELPs.

However, a 5°C decrease in *Tt* at 25μM was observed for the fusion protein. Interestingly, Δ*Tt* of Lac-S48I48 and Lac-S96 was much more dramatic compared to S48I48 and S96 (Figure 8C and 8D). While S48I48 exhibited one smooth micelle formation and one sharp bulk phase transition, only one sharp phase transition around 15°C was noticed with Lac-S48I48, which was 60°C lower than bulk phase transition temperature of S48I48 (Figure 8D). On the contrary, Lac-S96 completely abolished phase transition behavior of parent S96 within accessible temperature range of 10-90°C (Figure 8C).

Example 9
Lac-ELPs pre-assemble into nano-sized particles

Phase transition characterization results suggested the fusion lacritin moiety may interact with each other in a random/organized pattern other rather simply staying as monomers. One can further characterize the self-assembly property of purified Lac-ELPs using Dynamic Light

Scattering (DLS). As shown in Figure 9A, free lacritin exhibited as 2-3nm monomers between 5°C and 60°. While S96 stayed stable as 2-3nm monomers within experimental temperature range, Lac-S96 pre-assembled as 30-40nm particles (Figure 9C). Lac-V96 and Lac-I96 similarly exhibited as 30-40nm pre-assembled particles until bulk phase transition above *Tt* (Figure (B). S48I48 was chosen as our micelle scaffold. Remarkably, as different from sharp phase transition of I96 and V96 below 37°C, S48I48 assembled from 2-3nm monomers into 20nm micelles above its critical micelle temperature (CMT) at around 26°C (Figure 9D). Same as other Lac-ELPs, Lac-S48I48 preassemble into 30-40nm particles even at 5°C. As temperature was raised, Lac-S48I48 aggregated into 140-150nm mono-dispersed particles above its *Tt* (Figure 9D). Interestingly, native ELPs by themselves do not preassemble as their fusion constructs.

The DLS observations were further supported by high-resolution TEM and Cryo-TEM images of the corresponding nanoparticles. While S48I48 formed perfect micelle structure (Figure 9E&H), Lac-S48I48 presented a much larger size in its nanostructure, which was around 60-70nm in diameter (Figure 9F&I). Discrepancy of micelles diameter measured using three techniques may come from the hydrophobicity of the fusion protein. As DLS measures hydrodynamic radius of the particle, lacritin moiety may exist in its most extended conformation in the solution and thus gave a 130-140nm Rh reading. Both TEM and Cryo-TEM measured dry samples so that only the most hydrophobic core was shown in the figures. Due to fast degradation of Lac-S48I48, both TEM and Cryo-TEM images of Lac-S48I48 also showed partially degraded product: S48I48 micelles.

Example 10

Measurement of secretion of beta hexosaminidase from primary lacrimal gland cells

Primary rabbit lacrimal gland acinar cells (LGAC) are used for *in vitro* secretion assay. Lacrimal acini were isolated and cultured for 2-3 days. Cells prepared in this way aggregate into acinus-like structures; individual cells within these structures display distinct apical and basolateral domains and maintain a robust secretory response. Total protein is quantified by Biorad assay and secreted protein is quantified by β-hexosaminidase assay. Briefly, primary rabbit acinar cells are seeded in 12-well plate 2 days before test. 2 hours before testing, old medium is replaced by 600 ul fresh PCM. Medium and cells are incubated at 37°C for 2 hours. After collecting a sample of medium before secretion, ELP or lacritin ELP in PBS is added into

each well and incubated at 37 °C for 30 min. All the samples are aggressively vortexed and centrifuged at 4°C, 12,000 rpm for 5 min. For Biorad assay, before and after secretion media samples are tested on 96-well plates in triplicate. For measurement of the β-hexosaminidase activity, 4-methylumbelliferyl N-acetyl-β-D-glucosaminide is used as a substrate in triplicate. Carbachol is used as a positive control for secretion; furthermore, specific secretion is normalized to the controls with and without carbachol (CCh+, CCh-) (Figure 10A and 12). The results show that ELP-lacritin retains biological activity in an physiologically relevant cell type, as demonstrated by changes in secretion of proteins delivered via Ad-Syn-GFP or LifeAct-RFP reporter constucts transfection into LGACs (Figure 13). Changes in luminal regions and secretory vesicles was observed following ELP-lacritin and LAC administration. These results were further confirmed via direct measurement of protein secretion assays of rabbit LGACs, following ELP-lacritin and LAC stimulation (Figure 12).

Example 11

Lac-ELPs and lacritin stimulate β-hexosaminidase secretion in rabbit LGACs in a time and dose dependent manner

In another example, a well-established *in vitro* rabbit LGAC secretion model to evaluate prosecretory function of lacritin and its Lac-ELP fusion constructs. Figure 11 summarizes the β-hexosaminidase secretion results of acute Lac-ELPs and lacritin stimulation on rabbit LGACs. As internal positive control, 100μM carbachol significantly stimulated secretion during the 4h treatment time range. Compared to V96, Lac-V96 and lacritin significantly stimulated secretion at a concentration of 10μM ($p<0.01$) and 20μM ($p<0.001$) (Figure 11A); apparent effects at 1μM and 0.1μM were not statistically significant. When treating LGACs with Lac-V96 and lacritin for 0-4h at a concentration of 10μM, significant secretion effect was observed after 30min treatment and reached the peak at 1h ($p<0.0001$); after 1h, β-hexosaminidase secretion slower down (Figure 11B). The inventors further compared LGACs response to Lac-ELPs with different hydrophobicity and conformation. While difference between Lac-I96 and Lac-V96 groups were marginal, Lac-S96 group exhibited a slight higher β-hexosaminidase secretion level and Lac-S48I48 group showed lowest response. This difference may come from the

NGSEFAQKLL residues of lacritin sequence which is required for Syndecan-1 binding, which is believed to be crucial in downstream signal transduction. Since Lac-S96 is in its most soluble and extended conformation at 37°C (Figure 8C), no downstream protein-protein binding was blocked by the ELP tag. Due to phase transition at 37°C, Lac-I96 and Lac-V96 formed micron-sized coacervates (Figure 8B), so that binding of lacritin to Syndecan was not as efficient. The most interesting result comes from Lac-S48I48. Though it did form micelle with lacritin on the corona as designed (Figure 8D & Figure 9), this construct showed the least activity. It is possible that NGSEFAQKLL residues at the C-terminus of lacritin were buried in the inter-section of micelle, which made them difficult to be recognized by the receptors.

Example 12

Lac-ELPs and lacritin stimulate chronic F-actin remodeling around LGAC lumen and enhanced secretory vesicle formation

In response to secretagogues, LGACs exocytose the contents of mature secretory vesicles containing tear proteins at their apical membranes into lumen area. Spurred by understanding the cellular mechanism of Lac-ELP and lacritin triggered secretion, the inventors utilized live LGACs time-lapse confocal fluorescence microscopy imaging to investigate changes of actin filaments located beneath the apical membrane during exocytosis evoked by Lac-ELP and lacritin (20μM). For live cell imaging, rabbit lacrimal acini seeded on Matrigel-covered glass-bottomed round 35 mm dishes (MatTek, Ashland MA) at a density of 4×10^6 cells per dish for 2 days were co-transduced with Ad-Syn-GFP and Ad-LifeAct-RFP at MOI of 6 for each for 2 hours. Cells were then rinsed and cultured in fresh medium for overnight to allow protein expression. Dual transduction efficiency (as measured by RFP-actin expression) ranged from 80-90% in each experiment. On day 3, lacrimal acini were analyzed by time-lapse confocal fluorescence and DIC microscopy using Zeiss Multiple Time Series V3.2 software modules. Live cell analyses were performed at 37°C. For time-lapse analysis, acini of similar size (4-6 cells arranged around a central lumen) were chosen. DIC images and RFP, GFP fluorescence were acquired simultaneously using the 488 line of the Argon Laser.

Similar to other epithelial cells, actin filaments in LGACs are primarily enriched beneath the apical plasma membrane and less abundant beneath basolateral membranes. Here, the inventors transduced LGACs with high efficiency (80-90%) replication-defective adenovirus

(Ad) encoding RFP-actin (Ad-LifeAct-RFP) to label the actin filament array in lacrimal acini and measured its dynamics change during stimuli. Adenovirus encoding cytosolic protein Syn-GFP (Ad-Syn-GFP) was double transduced. Images obtained for different treatments were shown for plain PCM medium/CCh- (Figure 14B), carbachol (100μM) and Lac-V96 (20μM). Image acquisition of treated acini was initiated 30-60 seconds after treatment addition, due to the time required to refocus. In the absence of any treatment, there was little global remodeling of apical or basolateral actin filaments; only subtle basal release of a few SVs at the apical membrane were detected (Figure 14B CCh-). While positive control carbachol (100μM) acutely (0-15min) increased significant apical actin filament turnover and promoted transient actin assembly around apparent fusion intermediates (Figure 14B CCh+); Lac-V96 (20μM) exhibited a milder and more chronic effect on LGAC morphology change (Figure 14B Lac-V96 20μM). After a lag time for about 20min, 2 types of significant cellular changes were observed in LGACs perfused by Lac-V96: (1) increased irregularity in the continuity of apical actin filaments and formation of actin-coated structures beneath the apical and also basal membrane (purple arrows).

Example 13

Lac-ELPs and lacritin triggers transient cytosolic Ca2+ wave in HCE-T cells but not LGACs

The ability of actin filaments to remodel rapidly in response to changes in intracellular signaling is essential for their participation in exocytosis. Results from β-hexosaminidase secretion and confocal imaging studies show that Lac-ELP and lacritin trigger different cellular response compared to carbachol (Figure 11 and 14). Moreover, our β-hexosaminidase secretion result shows the minimal therapeutic concentration of lacritin is 10μM, which is more than 100 fold of previous reported 10-100nM dose required for peroxidase secretion. Without being bound by any particular theory, different receptor expression levels on rabbit and rat LGACs, may display differences in early signal transduction pathway participating in Lac-ELPs/lacritin triggered secretion. In the lacrimal gland, cholinergic agonists stimulate protein secretion by activating phospholipase C to break down phosphatidylinositol bisphosphate into 1,4,5-inositol trisphosphate(1,4,5-IP3) and diacylglycerol (DAG). 1,4,5-IP3 causes release of Ca2+ from intracellular stores. This Ca2+, perhaps in conjunction with calmodulin, activates specific protein kinases that may be involved in secretion. As a positive control used in this study, carbachol triggered intracellular Ca2+ wave in LGACs at an optimal concentration of 10-100μM

(Figure 15A1). Supramaximal concentrations of carbachol caused a decreased response (data not shown). Ca2+ intensity elevated around 50-100%, with 50% of total acini responded to the stimuli. Although small intra-acini variance was observed, reflecting as a different Ca2+ intensity change, all acini responded to exogenous carbachol simultaneously in a twinkling scintillation pattern. On the contrast, neither Lac-ELPs nor Epidermal growth factor (EGF) was capable of evoking the same Ca2+ reaction in LGACs, which suggested Lac-ELPs and lacritin may trigger different signal transduction pathway other than utilizing second messenger Ca2+. It is possible that intracellular Ca2+ change was too low to be detected, on the basis that Lac-ELPs/lacritin caused lower β-hexosaminidase secretion in LGACs than carbachol (Figure 11).

Example 14
Application of Lac-ELPs to human corneal cells

Described herein is application of Lac-ELPs to corneal cells. SV40-immortalized HCE-T cells were grown to 80% confluent on glass bottom 35-mm dish in keratinocyte-SFM media (Life Technologies, Rockville, MD) containing bovine pituitary extract (50μg/ml), EGF (5ng/ml) and penicillin/streptomycin. To optimize cell responsiveness to EGF and lacritin-ELPs, cells were starved with EGF and BPE free medium for 24 hours before experimentation.

The inventors observed the same Ca2+ wave pattern in HCE-T cells treated with Lac-ELPs and lacritin (Figure 15B3&B4). Interestingly, second messenger Ca2+ wrote a different code in HCE-T cells: instead of simultaneous twinkling scintillation, an obvious propagation wave of "brighten up" was observed across the cell sheet.

Compared to LGACs, elevation of intracellular Ca2+ concentration in HCE-T cells was sharper and decreased more smoothly, with a maximum 5 fold fluorescence increase in lacritin (10μM) and Lac-S48I48 (40μM) treating groups. Percentage of total responding cells was depending on lacritin/Lac-ELPs concentration (Figure 15C). Moreover, HCE-T cells appeared to have "memory" for exogenous Lac/Lac-ELPs treatment, as treating the same group of cells for the second time with the same concentration of proteins, Ca2+ influx was higher (Figure 15B4). The same Ca2+ wave pattern was observed in carbachol (Figure 15A2) and EGF treatment groups (Figure 15B2). While carbachol exhibited a concentration dependent effect; reaction of HCE-T cells to EGF was more biphasic, with maximum response recorded at 10ng/ml (Figure

15C). [Ca2+] elevation in HCE-T cells depended on extracellular-cytosol [Ca2+] gradient, as cells bathed in w/o Ca2+ solution did not respond to the same stimuli.

Example 15
Biostability of lacritin

Lacritin crystals have been developed but are not yet suitable for X-ray diffraction. Without signal peptide, lacritin protein sequence itself has a calculated isoelectric point (pI) of 5.1715. Using ExPASy amino sequence composition analysis, composition of lacritin contains 10.9% Ser, 8.4% Thr, 9.2% Lys. With 10% Lys content, lacritin could easily be a serine protease target. At the same time, lacritin contains one His, thirteen Ser and three Asp, it may also exhibit autolysis property similar to trypsin. The described *in vitro* degradation results of purified lacritin show that half-life of lacritin is only 24 hours (Figure 16A), which makes its purification a challenge.

As thermo-responsive biopolymer, ELPs show unique potential as a polypeptide "tag" for protein purification and as a carrier for therapeutic protein cargo. Compared with traditional His-tag and intein system, ELP system shows a more economic purification budget with satisfactory yield. In addition, scale-up of this purification method is easy because it is not limited by resin capacity. The method Inverse transition cycling (ITC) exploits the observation that proteins or peptides that are fused to a stimulus responsive ELP retain this behavior in the complex milieu of contaminating cellular components. In the described results, all control ELPs (V96, S96, I96, S48I48) show a yield of 50-100mg/L (Figure 5A). Due to fast degradation and pre-mature cleavage of ELP tag, a size-exclusion polishing step is required for lac-ELPs. But yield of the fusion protein is still over 30mg/L. Removing ELP tag to release free lacritin is as simple as to trigger ELP phase transition and centrifuge it out of solution after thrombin cleavage (Figure 5A). The inventors used thrombin kit from Sigma with thrombin attached to the agarose beads, thus during low speed centrifugation, thrombin was also removed from the supernatant, leaving only soluble lacritin.

Example 16
Signalling pathways involved in prosecretory activity

There are many therapeutics with great potential for ophthalmology but cannot be delivered in sufficiently high concentrations into the eye at the site of required action because of their improper size. The inventors have shown that fusion of lacritin with different ELPs, can improve *in vitro* pharmacokinetics and thus enhance therapeutic efficacy. Three types of ELP tags have been chosen to fulfill this aim: In the simplest form, S96 tag is fused to lacritin as a soluble macromolecular carrier. I96 and V96 as two hydrophobic tags with different *Tt* under 37°C so that fusion protein forms a viscous coacervate, which may be used as insoluble drug depot when locally delivered at desired site. In a more sophisticated design, nanoscale self-assembly S48I48 block copolymer is chosen to assist Lac-ELP assemble into spherical micelles. Peroxidase secretion by rat lacrimal gland has been widely used for measuring protein secretion *in vitro*. However, it is not secreted by rabbit lacrimal gland, the most widely used animal model *in vivo* for evaluating secretion. β-hexosaminidase is present in both human and rabbit tear fluid and is secreted from rabbit lacrimal gland acinar cells in primary culture on stimulation with secretagogs . In this study, the inventors utilized this model to quantitatively evaluate prosecretory activity of Lac-ELPs and lacritin. Optimal rabbit LGACs response was observed after 1 hour Lac-ELP or lacritin treatment in a dose dependent manner, both showing 30-40% response compared to carbachol group.

To identify the impact of exogenous recombinant lac-ELP and lacritin on morphology change and mature secretion vesicle formation of LGACs, the inventors double transduced LGACs with adenovirus Ad-LifeAct-RFP (F-actin marker) and Ad-Syn-GFP (secretion protein marker) to observe cell response using confocal microscope. Ad-syncollin-GFP was generated and for amplification, QB1 cells, a derivative of HEK293 cells, were infected with Ad-syncollin-GFP and grown at 37°C and 5% CO2 in DMEM (high glucose) containing 10% fetal bovine serum for 66 hours until completely detached from the flask surface. The Adeno-X™ virus purification kit was used for virus purification and the Adeno-X™ rapid titer kit for viral titration.

While carbachol triggered immediate intense F-actin remodeling beneath both apical and basal membrane of LGAC luminal region, Lac-ELPs and lacritin demonstrated a milder and more chronic effect, which suggests Lac-ELPs and lacritin signaling may involve other pathways other than activating muscarinic type 3 acetylcholine receptors (M3R). The inventors investigated signal transduction pathways triggered by Lac-ELP/lacritin stimuli by recording

cytosolic Ca2+ wave change in LGACs and SV-40 transduced human corneal epithelial cells (HCE-Ts) stained with intracellular calcium indicator Fluo-4AM. While 10μM carbachol treatment significantly elevated cytosolic Ca2+ level in LGACs, Ca2+ change in LGACs in regards to lacritin and Lac-ELPs treatments were hardly detected. Interestingly, Ca2+ wave propagation in HCE-T cells can be triggered by 10μM lacritin/Lac-ELPs. Taken together, the prosecretory and elevating cytosolic [Ca2+] activities of Lac-ELPs supported our hypothesis that ELPs are promising as an ocular drug delivery carrier.

A better understanding of the complex spatiotemporal Ca2+ signal pattern in LGACs and HCE-T cells might therefore shed light on intracellular processes influencing lacritin and Lac-ELPs activity. The Ca2+ signaling results show that lacritin/Lac-ELPs did not exhibit the same Ca2+ oscillation pattern in LGACs as carbachol. Without being bound by any particular theory, this suggests a different downstream signaling pathway may be involved in its prosecretory activity. As a key regulator in maintaining corneal epithelial cell proliferation and migration, EGF was included in the Ca2+ signaling study, which acts in a paracrine fashion on epithelial cells proliferation via orchestrated calcium influx from intracellular calcium stores and extracellular space. EGF, carbachol and lacritin/Lac-ELPs exhibited similar Ca2+ wave pattern on HCE-T cells, which prompt us start wondering which cell receptors were involved in carbachol and EGF signaling. It is well known that carbachol stimulates tear fluid production through the activation of muscarinic receptors.

Compared to conventional synthetic low molecular weight drugs, proteins are more unstable during their storage and administration and susceptible to denaturation during the drug production process. Our degradation study of lacritin is an example of this concept.

Example 17
Discussion

To achieve minimal invasive means for the delivery of therapeutic proteins to treat dry eye disease is one of the challenges of ophthalmology. One obstacle of ocular drug delivery is the anatomical and physiological barriers in the eye and low bioavailability of present medications. Biodegradable polymer-based drug delivery systems show considerable promise for the treatment of ocular diseases by providing a sustained-release platform.

The results described herein demonstrate successful bioconstruction of lac-ELPs with versatile ELP tags and allowed us to potentially modulate in vitro and in vivo pharmacokinetic profile of native lacritin. β-hexosaminidase secretion results from our in vitro rabbit model also show promising therapeutic potential of lacritin-ELPs. Hydrophobicity of ELP tag did not show a significant impact on β-hexosaminidase secretion results. However, multivalent presentation of lacritin on the corona of ELP micelle decreased efficiency of lacritin proseretory activity. Lacritin-ELPs and lacritin induce chronic F-actin remodeling around acinar lumen and elevated mature secretion vesicle formation. Lac-ELPs and lacritin triggers transient Ca2+ waves in SV40-transduced Human Epithelial Cells (HCE-Ts).

The results herein described demonstrate construction of a lacritin-ELP fusion protein with biocompatible phase transition behavior without retardation of effective biological activity. The fusion protein imparts the thermo-responsive property of the ELP and prosecretory function of lacritin, which has great potential for controlling ocular bioavailability. This use of ELPs for constructing thermo-responsive ophthalmic drugs opens new possibilities for the treatment of dry eye disease.

The various methods and techniques described above provide a number of ways to carry out the invention. Of course, it is to be understood that not necessarily all objectives or advantages described may be achieved in accordance with any particular embodiment described herein. Thus, for example, those skilled in the art will recognize that the methods can be performed in a manner that achieves or optimizes one advantage or group of advantages as taught herein without necessarily achieving other objectives or advantages as may be taught or suggested herein. A variety of advantageous and disadvantageous alternatives are mentioned herein. It is to be understood that some preferred embodiments specifically include one, another, or several advantageous features, while others specifically exclude one, another, or several disadvantageous features, while still others specifically mitigate a present disadvantageous feature by inclusion of one, another, or several advantageous features.

Furthermore, the skilled artisan will recognize the applicability of various features from different embodiments. Similarly, the various elements, features and steps discussed above, as well as other known equivalents for each such element, feature or step, can be mixed and matched by one of ordinary skill in this art to perform methods in accordance with principles

described herein. Among the various elements, features, and steps some will be specifically included and others specifically excluded in diverse embodiments.

Although the invention has been disclosed in the context of certain embodiments and examples, it will be understood by those skilled in the art that the embodiments of the invention extend beyond the specifically disclosed embodiments to other alternative embodiments and/or uses and modifications and equivalents thereof.

Many variations and alternative elements have been disclosed in embodiments of the present invention. Still further variations and alternate elements will be apparent to one of skill in the art. Among these variations, without limitation, are the methods of preparing, isolating, or purifying fusion proteins containing bioresponse proteins polymers and/or therapeutic proteins, functional equivalents, and/or active fragments thereof, methods of treating various disease and/or conditions using fusion proteins, including types of diseases, conditions and/or target organ(s) that relate to the teachings of the invention, techniques and composition and use of solutions used therein, and the particular use of the products created through the teachings of the invention. Various embodiments of the invention can specifically include or exclude any of these variations or elements.

In some embodiments, the numbers expressing quantities of ingredients, properties such as concentration, reaction conditions, and so forth, used to describe and claim certain embodiments of the invention are to be understood as being modified in some instances by the term "about." Accordingly, in some embodiments, the numerical parameters set forth in the written description and attached claims are approximations that can vary depending upon the desired properties sought to be obtained by a particular embodiment. In some embodiments, the numerical parameters should be construed in light of the number of reported significant digits and by applying ordinary rounding techniques. Notwithstanding that the numerical ranges and parameters setting forth the broad scope of some embodiments of the invention are approximations, the numerical values set forth in the specific examples are reported as precisely as practicable. The numerical values presented in some embodiments of the invention may contain certain errors necessarily resulting from the standard deviation found in their respective testing measurements.

In some embodiments, the terms "a" and "an" and "the" and similar references used in the context of describing a particular embodiment of the invention (especially in the context of

certain of the following claims) can be construed to cover both the singular and the plural. The recitation of ranges of values herein is merely intended to serve as a shorthand method of referring individually to each separate value falling within the range. Unless otherwise indicated herein, each individual value is incorporated into the specification as if it were individually recited herein. All methods described herein can be performed in any suitable order unless otherwise indicated herein or otherwise clearly contradicted by context. The use of any and all examples, or exemplary language (e.g. "such as") provided with respect to certain embodiments herein is intended merely to better illuminate the invention and does not pose a limitation on the scope of the invention otherwise claimed. No language in the specification should be construed as indicating any non-claimed element essential to the practice of the invention.

Groupings of alternative elements or embodiments of the invention disclosed herein are not to be construed as limitations. Each group member can be referred to and claimed individually or in any combination with other members of the group or other elements found herein. One or more members of a group can be included in, or deleted from, a group for reasons of convenience and/or patentability. When any such inclusion or deletion occurs, the specification is herein deemed to contain the group as modified thus fulfilling the written description of all Markush groups used in the appended claims.

Preferred embodiments of this invention are described herein, including the best mode known to the inventor for carrying out the invention. Variations on those preferred embodiments will become apparent to those of ordinary skill in the art upon reading the foregoing description. It is contemplated that skilled artisans can employ such variations as appropriate, and the invention can be practiced otherwise than specifically described herein. Accordingly, many embodiments of this invention include all modifications and equivalents of the subject matter recited in the claims appended hereto as permitted by applicable law. Moreover, any combination of the above-described elements in all possible variations thereof is encompassed by the invention unless otherwise indicated herein or otherwise clearly contradicted by context.

Furthermore, numerous references have been made to patents and printed publications throughout this specification. Each of the above cited references and printed publications are herein individually incorporated by reference in their entirety.

In closing, it is to be understood that the embodiments of the invention disclosed herein are illustrative of the principles of the present invention. Other modifications that can be

employed can be within the scope of the invention. Thus, by way of example, but not of limitation, alternative configurations of the present invention can be utilized in accordance with the teachings herein. Accordingly, embodiments of the present invention are not limited to that precisely as shown and described.

THE CLAIMS

1. An isolated fusion protein comprising:

a bioresponse protein polymer, and

a therapeutic protein conjugated to the bioresponse protein polymer.

2. The isolated fusion protein of claim 1, wherein the bioresponse protein polymer comprises an elastin-like polypeptide (ELP).

3. The isolated fusion protein of claim 2, wherein the ELP comprises amino acid motif $(Val\text{-}Pro\text{-}Gly\text{-}X_{aa}\text{-}Gly)_n$, where n comprises 10 to 300 units and X_{aa} is a natural or synthetic amino acid.

4. The isolated fusion protein of claim 3, wherein n is 96 and X_{aa} is serine, valine, or isoleucine.

5. The isolated fusion protein of claim 1, wherein the therapeutic protein comprises lacritrin, a functional equivalent or active fragment thereof.

6. The isolated fusion protein of claim 5, wherein the lacritrin, functional equivalent or active fragment thereof comprises human lacritrin.

7. The isolated fusion protein of claim 5, wherein the lacritrin, functional equivalent or active fragment thereof comprises amino acid sequence: SEQ ID NO: 3, SEQ ID NO: 4, SEQ ID NO: 5, SEQ ID NO: 6, SEQ ID NO: 7, or SEQ ID NO: 8.

8. The isolated fusion protein of claim 1, wherein the bioresponse protein polymer and therapeutic protein are conjugated via a linker peptide.

9. The isolated fusion protein of claim 8, wherein the linker peptide comprises amino acid sequence: SEQ ID NO: 9.

10. The isolated fusion protein of claim 1, wherein the bioresponse protein polymer is ELP, the therapeutic protein is lacritrin, and the ELP is conjugated to the lacritrin via a linker peptide.

11. An isolated nucleotide encoding a fusion protein comprising:

a bioresponse protein polymer, and

a therapeutic protein conjugated to the bioresponse protein polymer.

12. The isolated nucleotide of claim 11, wherein the bioresponse protein polymer comprises an elastin-like polypeptide (ELP).

13. The isolated nucleotide of claim 12, wherein the ELP comprises amino acid motif (Val-Pro-Gly-X_{aa}-Gly)$_n$, where n comprises 10 to 300 repeat units and X_{aa} is a natural or synthetic amino acid.

14. The isolated nucleotide of claim 11, wherein the therapeutic protein comprises lacritrin, a functional equivalent or active fragment thereof.

15. A method of constructing the isolated nucleotide of claim 11 using recursive directional ligation.

16. A method of treating a disease and/or condition in a human subject, comprising:

providing a quantity of a composition, wherein the composition comprises a fusion protein, the fusion protein comprising a bioresponse protein polymer and a therapeutic protein conjugated to the bioresponse protein polymer; and

treating a human subject by administering a therapeutically effective dosage of the composition to the subject, thereby treating the subject.

17. The method of claim 16, wherein the human subject is in need of treatment for an eye disease and/or condition selected from the group consisting of: acanthamoeba keratitis, allergies, amblyopia, Bell's palsy, blepharitis, cataracts, chalazion, color blindness, corneal ulcer, detached retina, dry eye syndrome, keratoconjunctivitis sicca, eye occlusions, eye twitching, macular hole,

nystagmus, ocular migraine, ocular rosacea, optic neuritis, optic neuropathy, photophobia, pinguecula, pterygium, ptosis, Sjogren's syndrome, strabismus, stye, subconjunctival hemorrhage, uveitis, CMV retinitis, conjunctivitis, diabetic retinopathy, eye herpes, glaucoma, karatoconus, macular degeneration, macular dystrophy, ocular hypertension, retinitis pigmentosa, and/or Stargardt's disease.

18. The method of claim 16, wherein the bioresponse protein polymer comprises an elastin-like polypeptide (ELP), the therapeutic protein comprises lacritrin, and the ELP is conjugated to the lacritrin via a linker peptide.

19. A pharmaceutical composition comprising:

a bioresponse protein polymer;

a therapeutic protein conjugated to the bioresponse protein polymer; and

a pharmaceutically acceptable carrier.

20. The pharmaceutical composition of claim 19, wherein the bioresponse protein polymer comprises an elastin-like polypeptide (ELP), the therapeutic protein comprises lacritrin, and the ELP is conjugated to the lacritrin via a linker peptide.

ABSTRACT

Described herein are bioresponsive protein polymers for therapeutic applications, including delivery to physiologically demanding environments, such as the eye surface. Bioresponsive protein polymers can be fused with biopharmaceuticals using genetic engineering techniques for enhanced therapeutic activity. In certain embodiments, the unique temperature-sensitive phase separation properties of bioresponsive protein polymers, allows generation of therapeutics resistant to ocular clearance. Such fusion proteins containing bioresponsive protein polymers and biopharmaceuticals allow retention of drugs in the eye for much longer periods of time. Improved biostability and bioavailability improves drug efficacy, while reducing cost and eliminating the need for repeated drug application

Figure 1

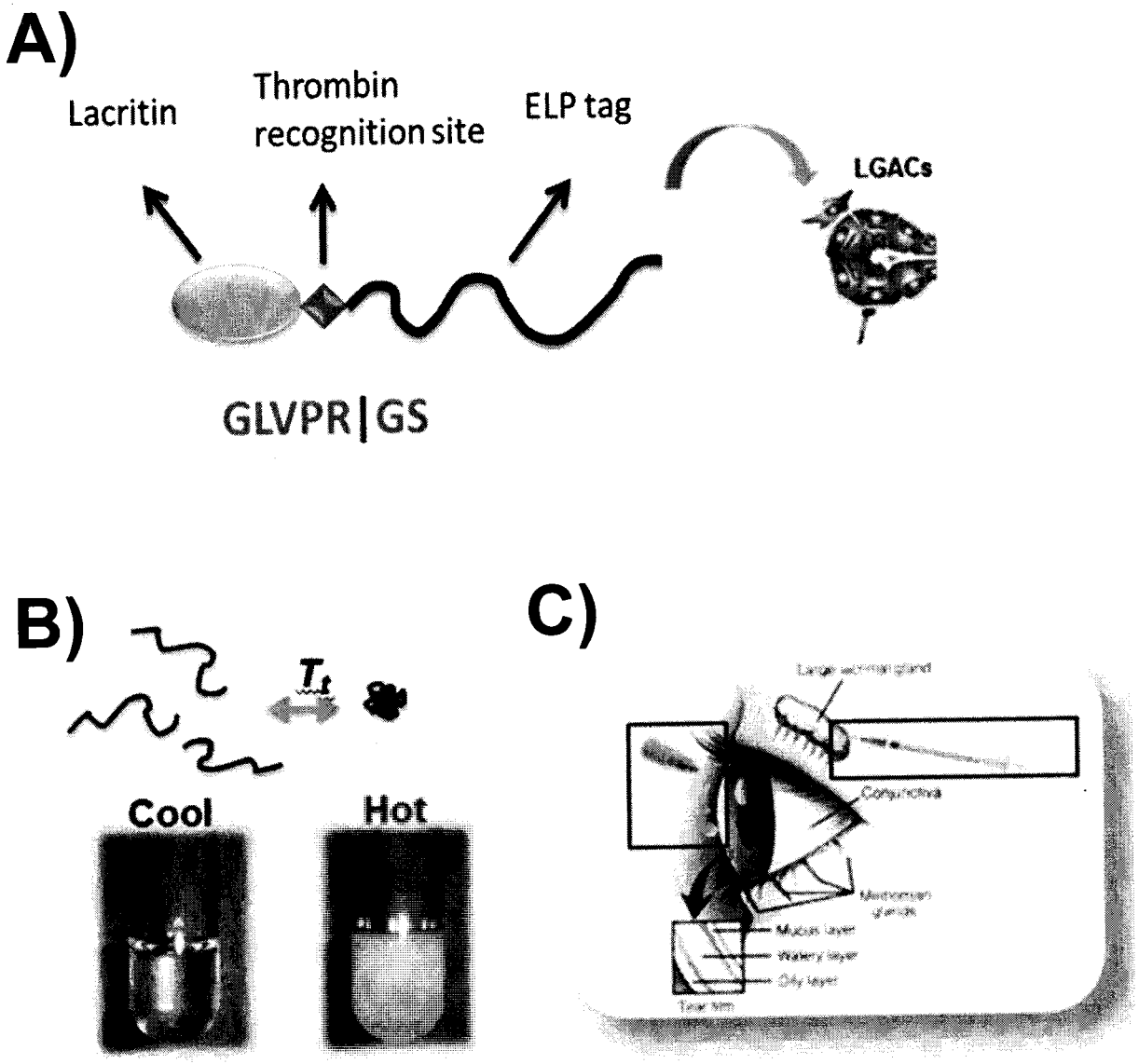
A)
Lacritin
Thrombin recognition site
ELP tag
LGACs
GLVPR|GS
B)
T_t
Cool
Hot
C)
Conjunctiva
Mucin layer
Watery layer
Oily layer

Figure 2

A

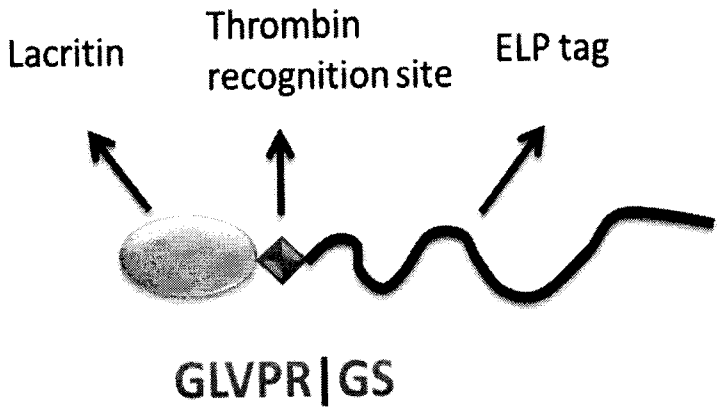

B

Hydrophobicity

Micelle Monomer

Name	I96	Lac-I96	V96	Lac-V96	S96	Lac-S96	S48I48	Lac-S48I48	Lacritin
Sequence	$G(VPGIG)_{96}$	Lac-Thrombin-$G(VPGIG)_{96}$	$G(VPGVG)_{96}$	Lac-Thrombin-$G(VPGVG)_{96}$	$G(VPGSG)_{96}$	Lac-Thrombin-$G(VPGSG)_{96}$	$G(VPGSG)_{48}(VPGIG)_{48}$	Lac-Thrombin-$G(VPGSG)_{48}(VPGIG)_{48}$	Lac
m/z	40.9	53.9	39.6	52.5	38.4	51.4	39.7	52.6	12.9
$[M+H]^+$	39.2	53.1	39.2	52.3	38.9	51.1	39.5	52.2	12.7
$25\mu M\_T_t$ (°C)	19.5	14.5	31.6	26.8	57.6	NA	26.6 / 75.0	18.7	NA

Figure 3

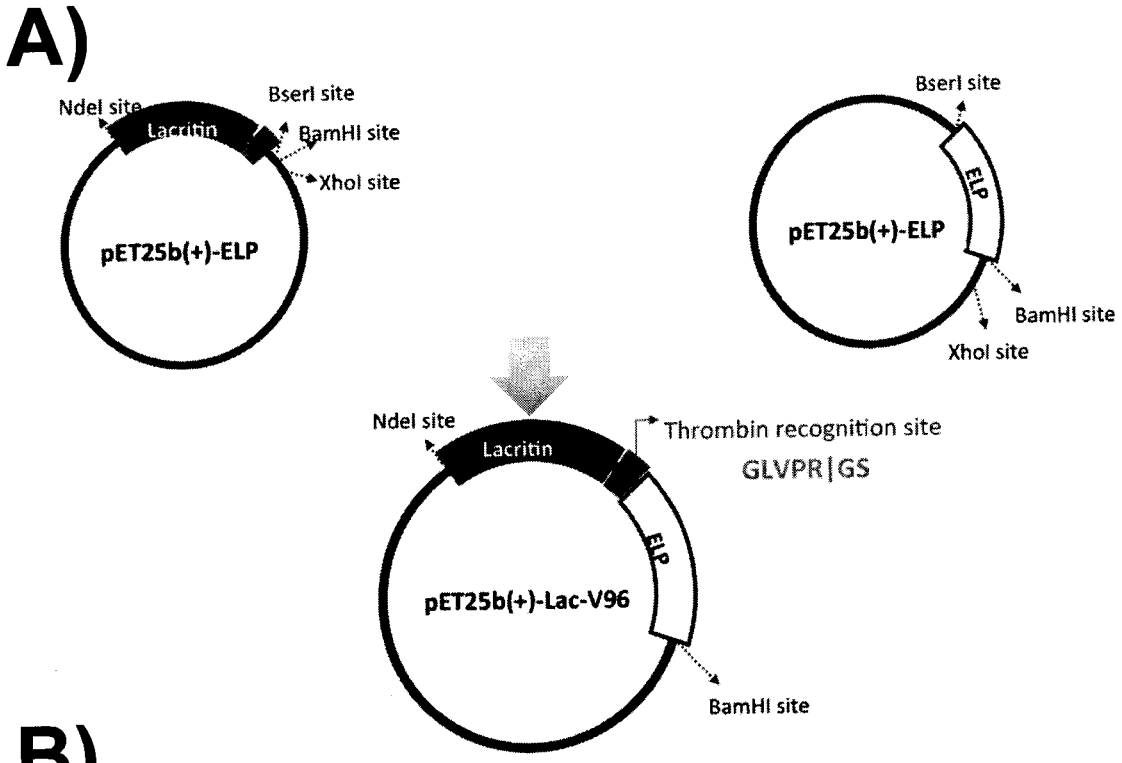
A)
NdeI site
Lacritin
BserI site
BamHI site
XhoI site
pET25b(+)-ELP
BserI site
ELP
pET25b(+)-ELP
BamHI site
XhoI site
NdeI site
Lacritin
Thrombin recognition site
GLVPR|GS
ELP
pET25b(+)-Lac-V96
BamHI site

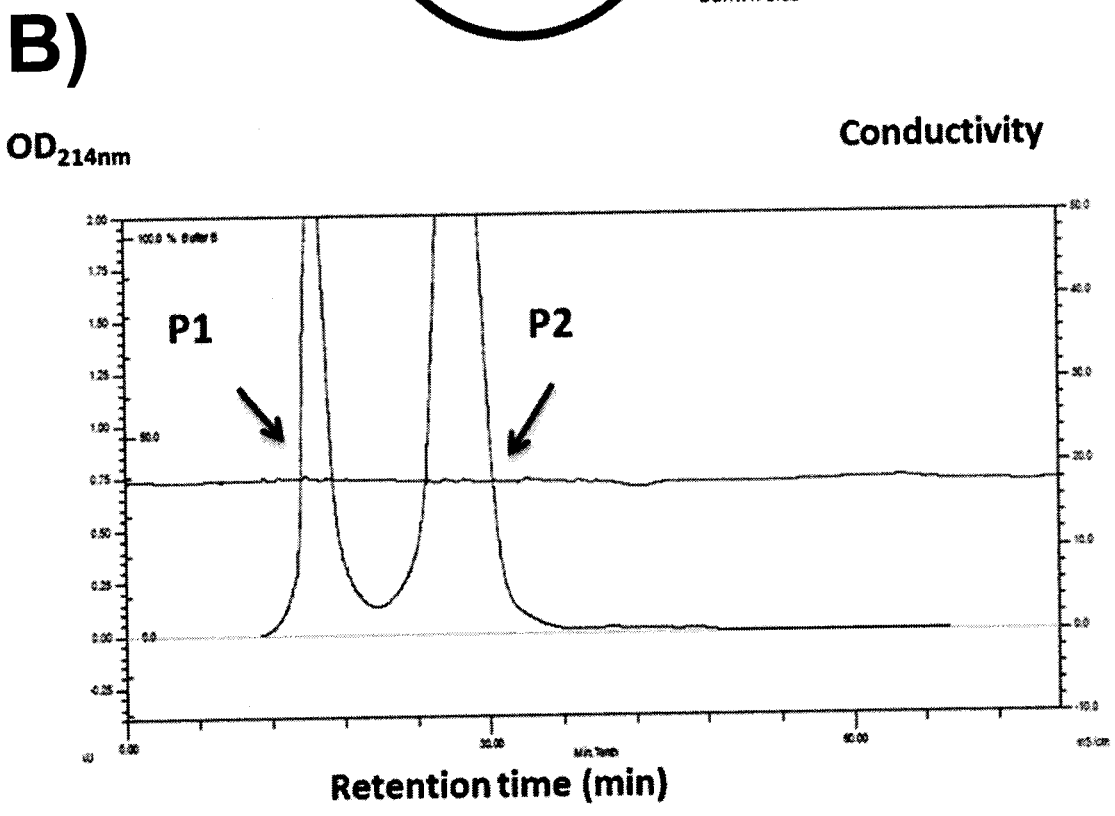
B)
OD214nm
Conductivity
P1
P2
Retention time (min)

Figure 4

A)

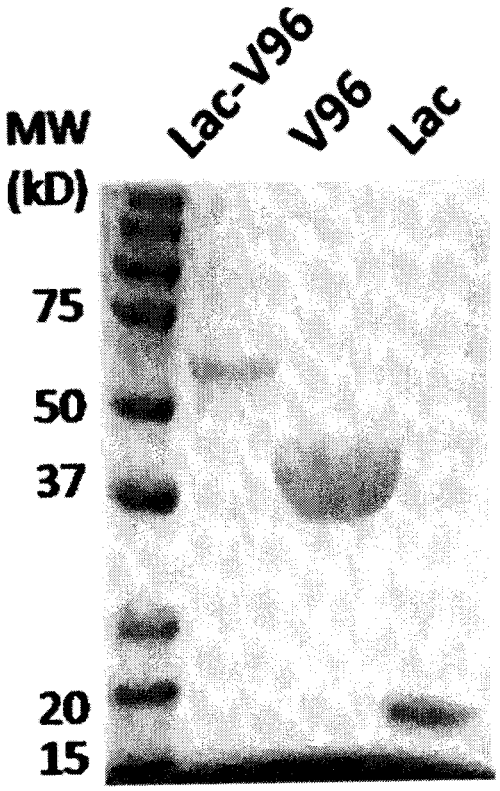
MW
(kD)
Lac-V96
V96
Lac
75
50
37
20
15

B)

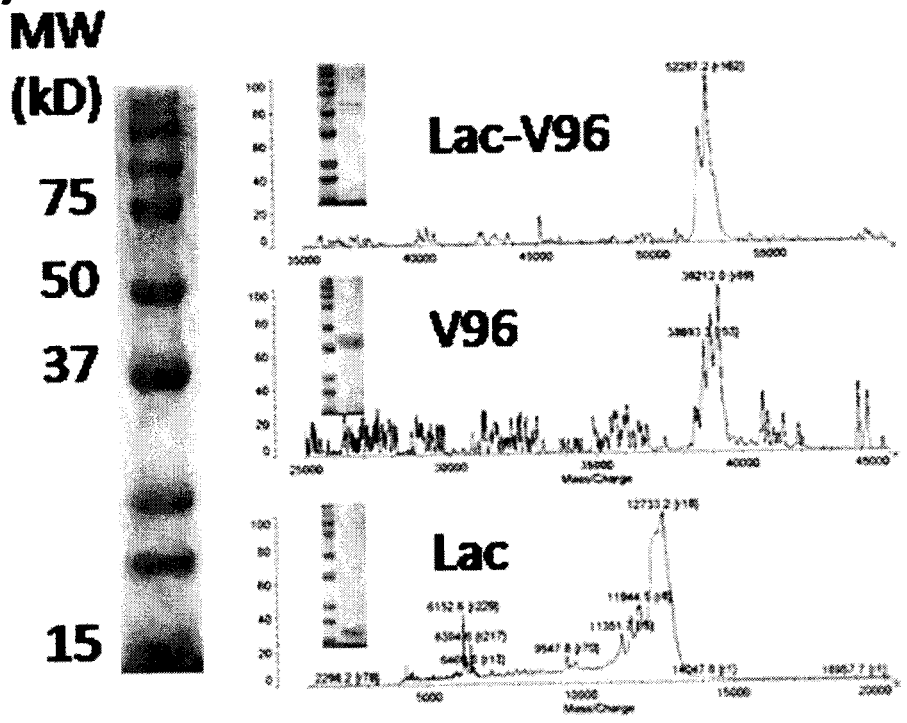
MW
(kD)
75
50
37
15
Lac-V96
V96
Lac

Figure 5

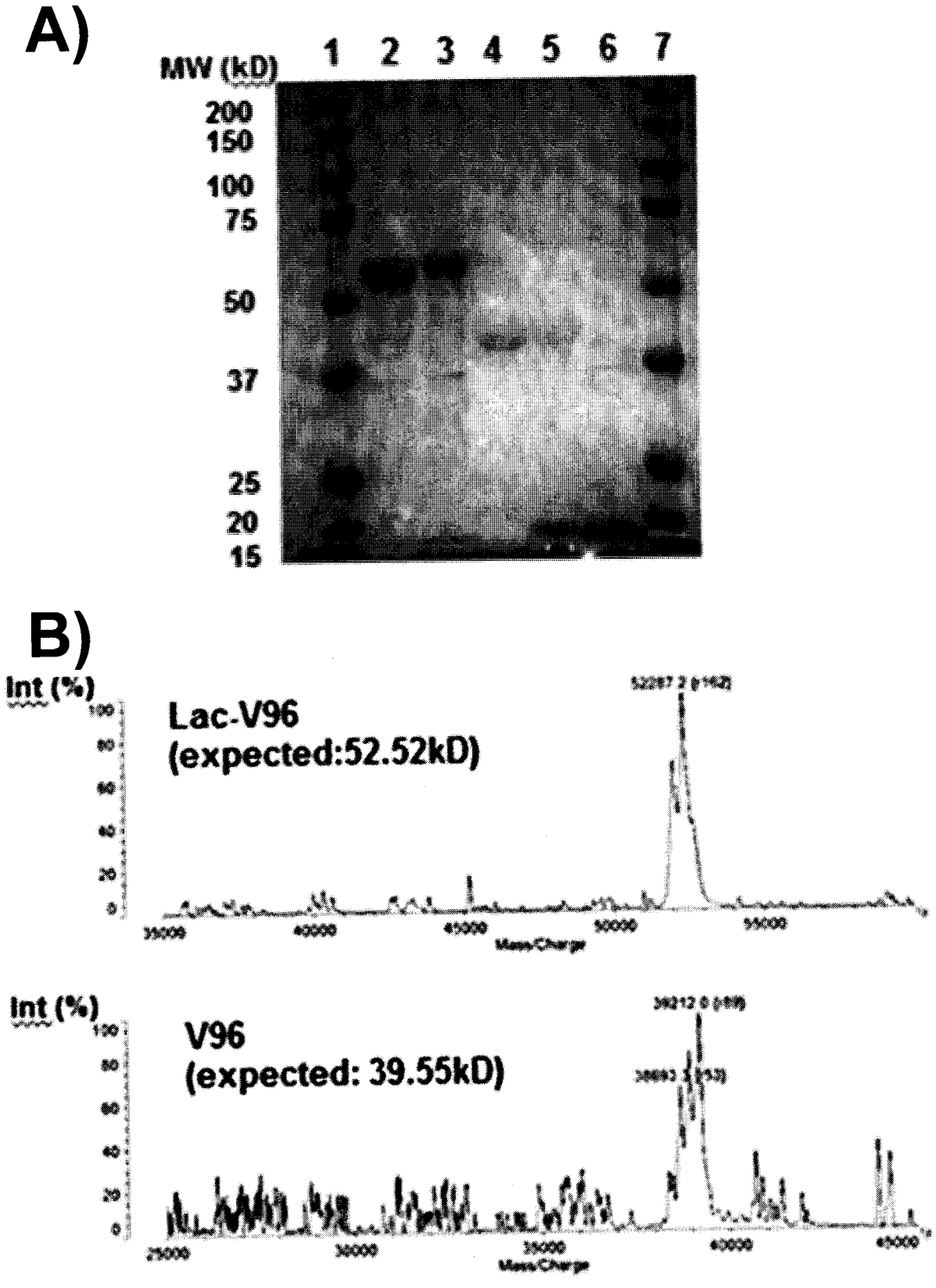
A)
MW (kD)
1 2 3 4 5 6 7
200
150
100
75
50
37
25
20
15
B)
Int (%)
Lac-V96
(expected:52.52kD)
Mass/Charge
Int (%)
V96
(expected: 39.55kD)
Mass/Charge

Figure 6

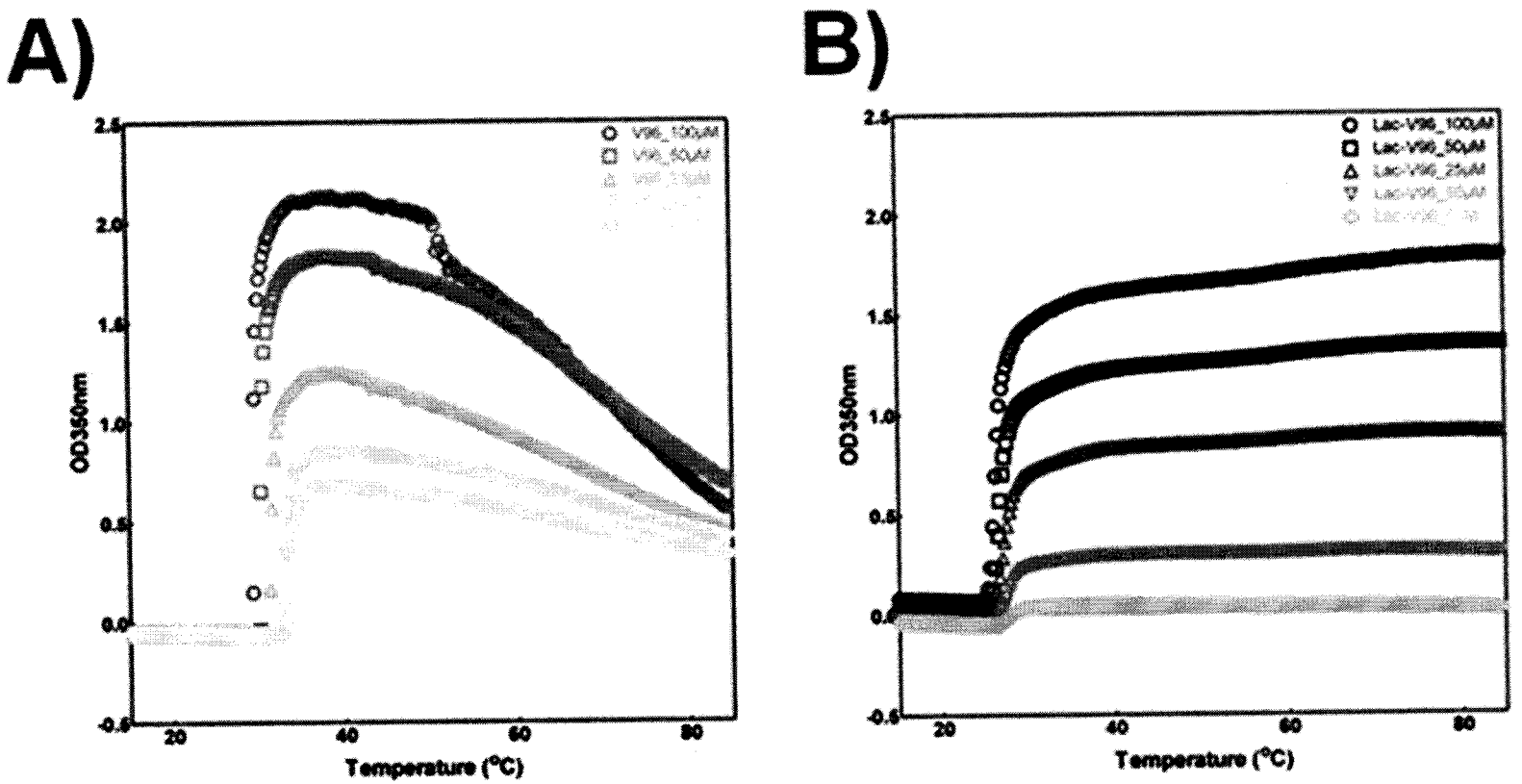
A)
B)
OD350nm
Temperature (°C)
Lac-V96_100μM
Lac-V96_50μM
Lac-V96_25μM

Figure 6

C)

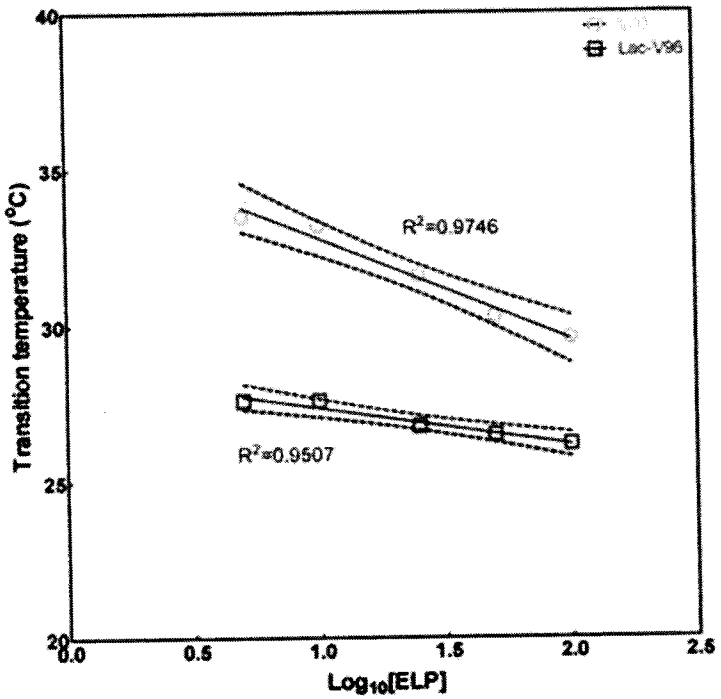
Lac-V96
R^2=0.9746
R^2=0.9507
Transition temperature (°C)
Log_{10}[ELP]
40
35
30
25
20
0.0
0.5
1.0
1.5
2.0
2.5

D)

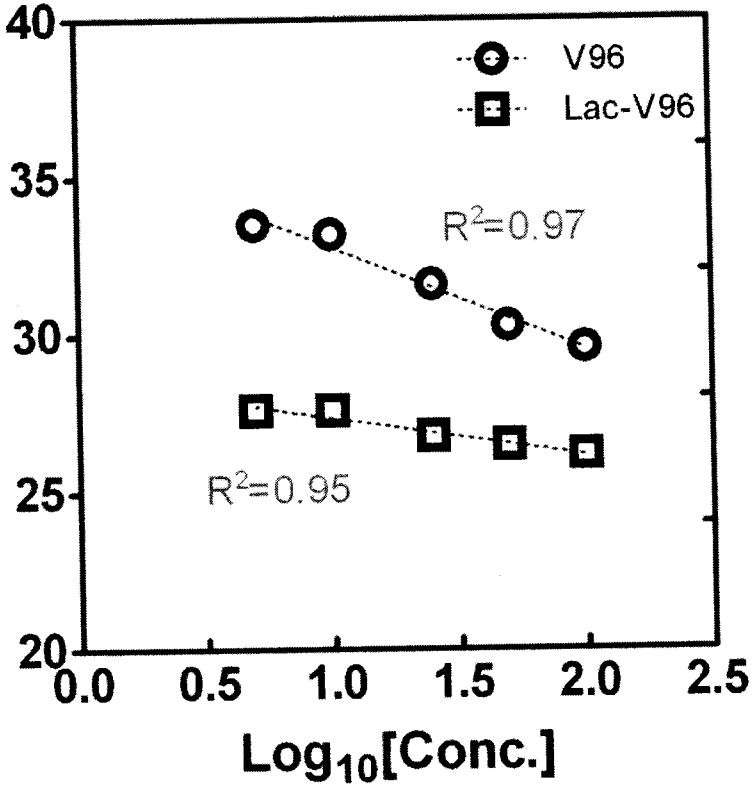
V96
Lac-V96
R^2=0.97
R^2=0.95
40
35
30
25
20
0.0
0.5
1.0
1.5
2.0
2.5
Log_{10}[Conc.]

Figure 7

A)

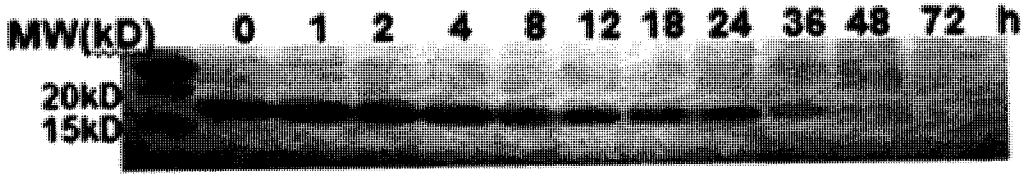

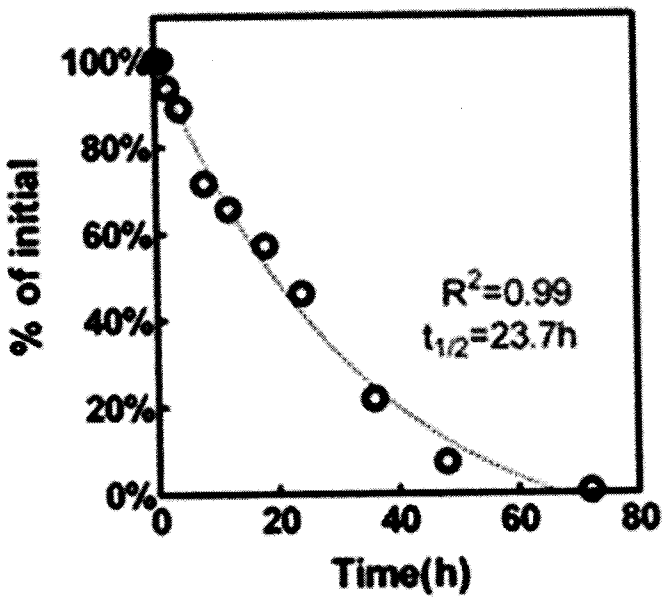

B) GEDASSDSTGADPAQEAGTSKPNEEISGPAEPASPPETTTTAQETSAAAVQGTAKVTS
SRQELNPLKSIVEKSILLTEQALAKAGKGMHGGVPGGKQFIENGSEFAQKLLKKFSLL
KPWAGLVPRGSG(VPGVG)$_{96}$Y

Figure 7

C)

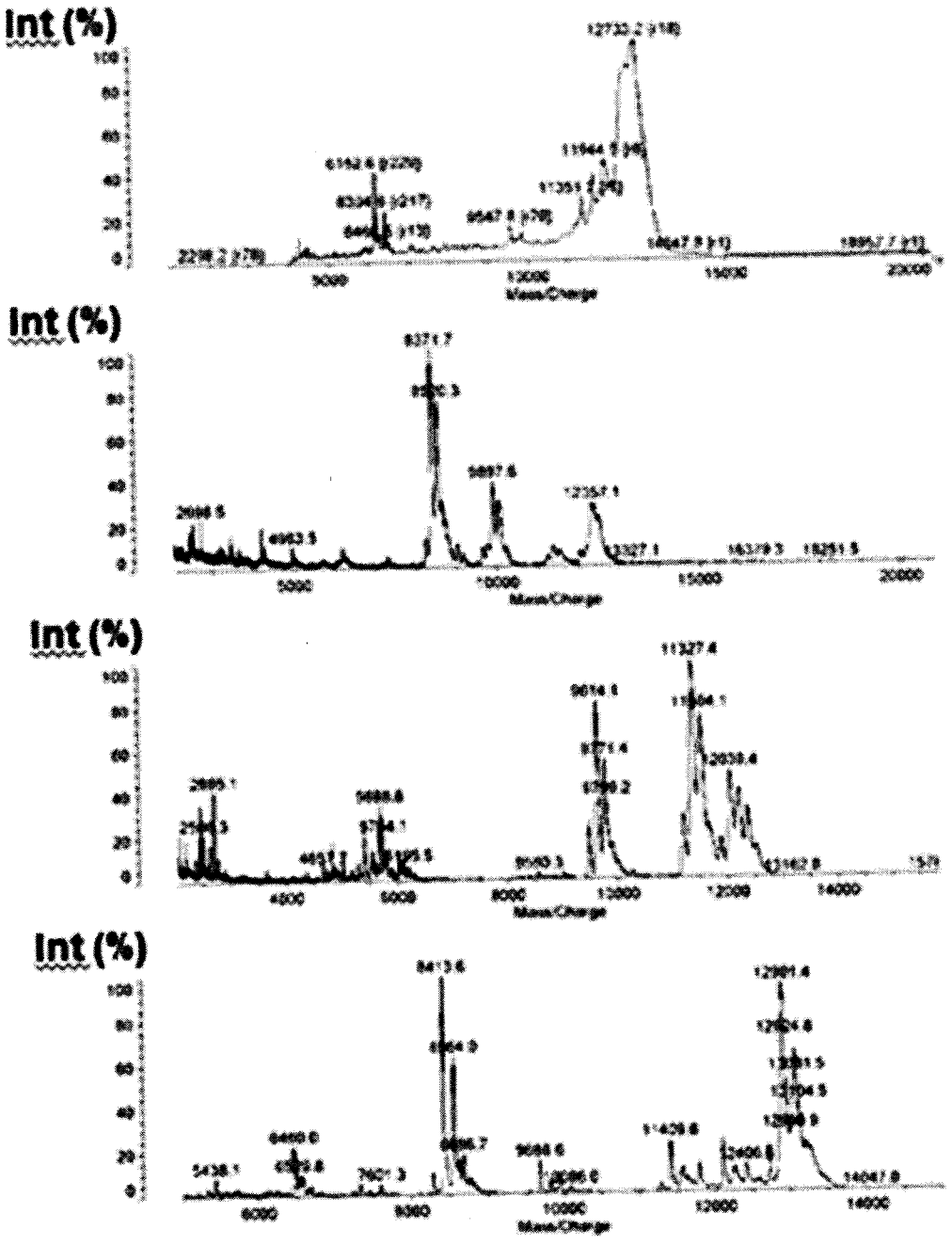
Int (%)
Mass/Charge
Int (%)
Mass/Charge
Int (%)
Mass/Charge
Int (%)
Mass/Charge

Figure 8

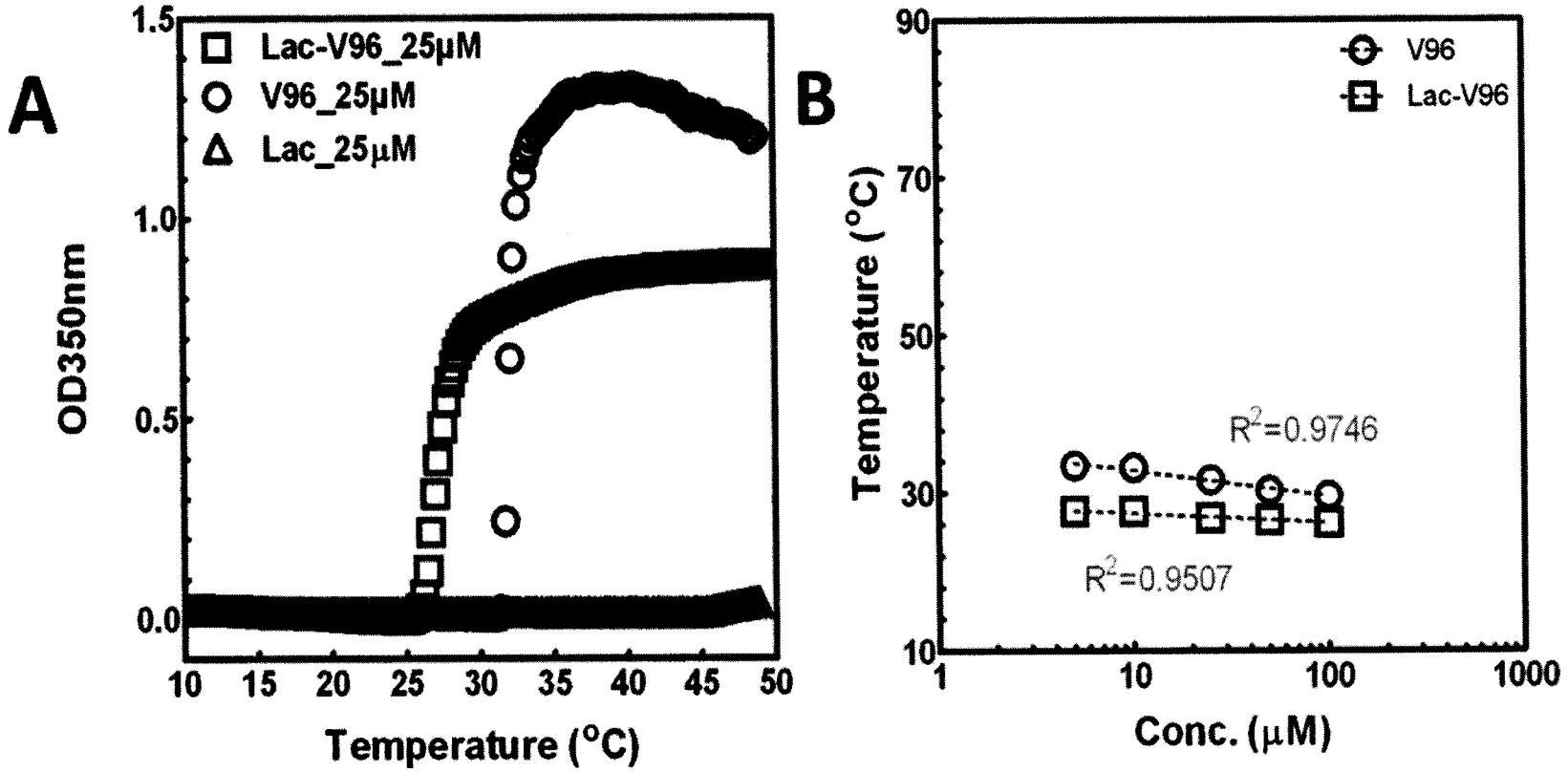
A
Lac-V96_25μM
V96_25μM
Lac_25μM
OD350nm
Temperature (°C)
B
V96
Lac-V96
R2=0.9746
R2=0.9507
Temperature (°C)
Conc. (μM)

Figure 8

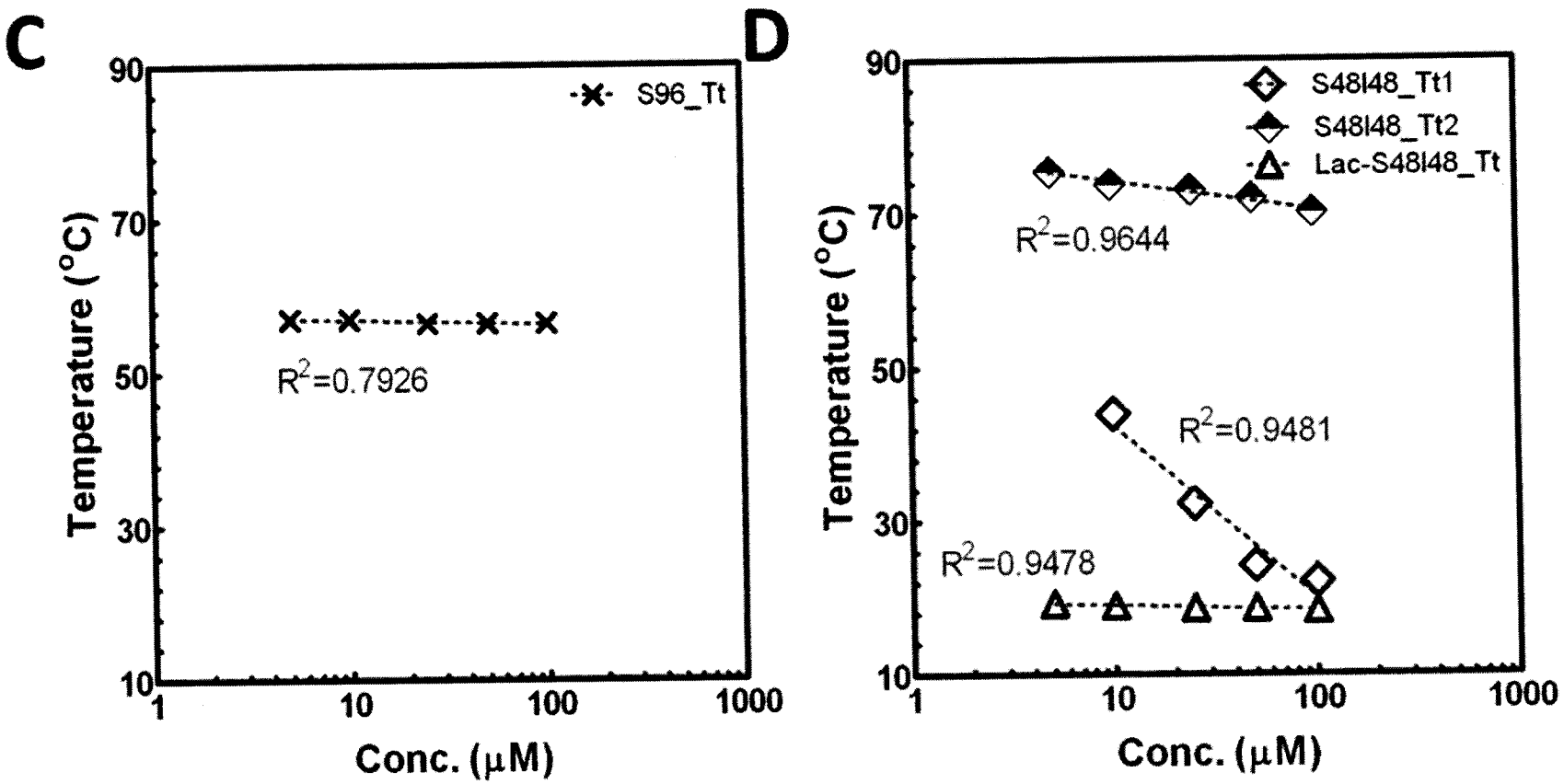
C
D
90
70
50
30
10
Temperature (°C)
1
10
100
1000
Conc. (μM)
S96_Tt
R2=0.7926
S48I48_Tt1
S48I48_Tt2
Lac-S48I48_Tt
R2=0.9644
R2=0.9481
R2=0.9478

Figure 9

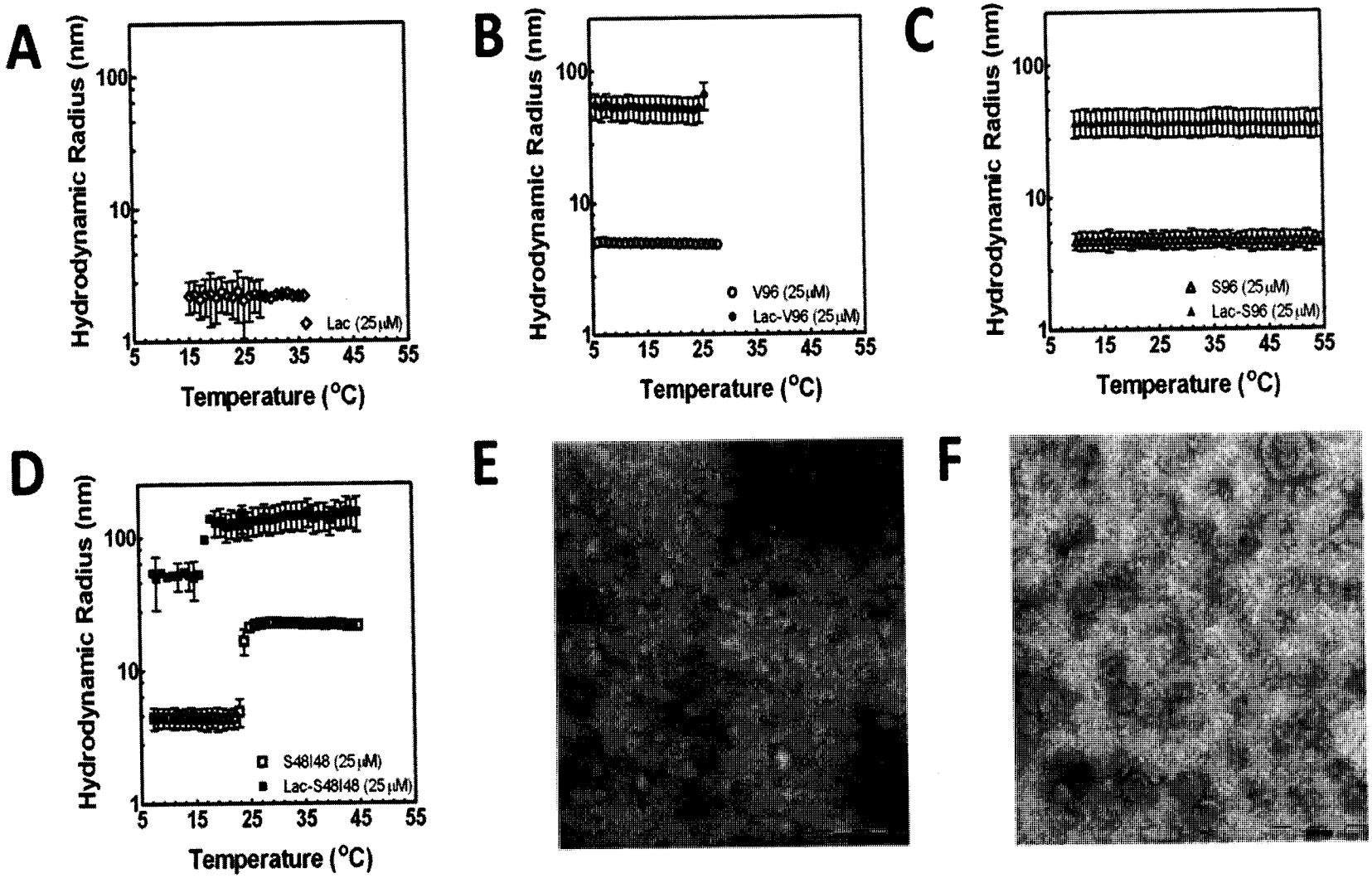
A
Hydrodynamic Radius (nm)
100
10
1
5
15
25
35
45
55
Temperature (°C)
Lac (25μM)
B
Hydrodynamic Radius (nm)
100
10
1
5
15
25
35
45
55
Temperature (°C)
V96 (25μM)
Lac-V96 (25μM)
C
Hydrodynamic Radius (nm)
100
10
1
5
15
25
35
45
55
Temperature (°C)
S96 (25μM)
Lac-S96 (25μM)
D
Hydrodynamic Radius (nm)
100
10
1
5
15
25
35
45
55
Temperature (°C)
S48I48 (25μM)
Lac-S48I48 (25μM)
E
F

Figure 9

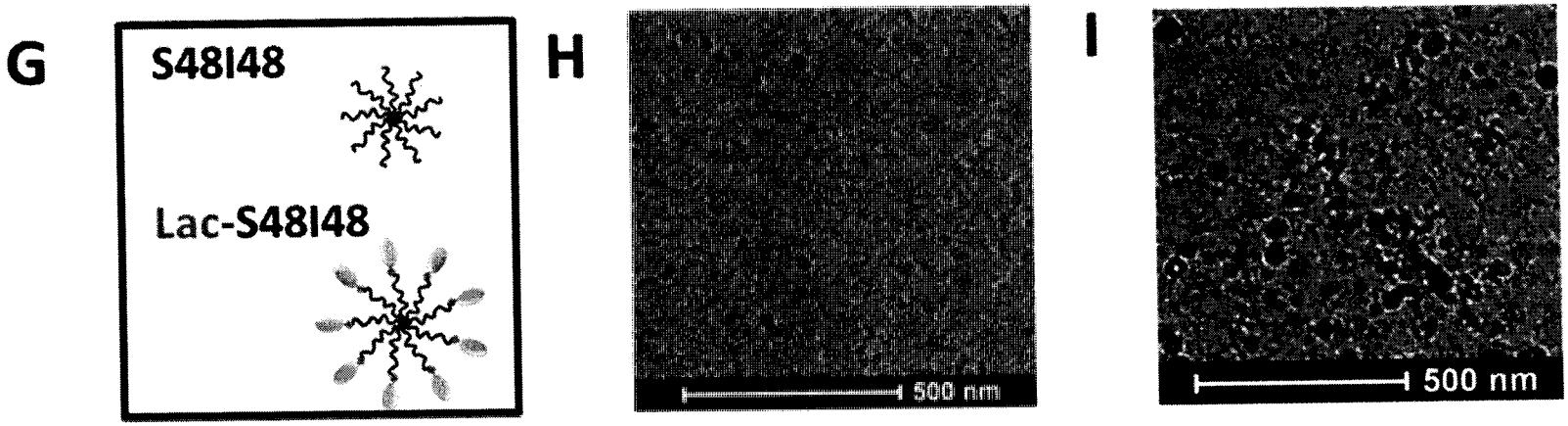

Figure 10

A)

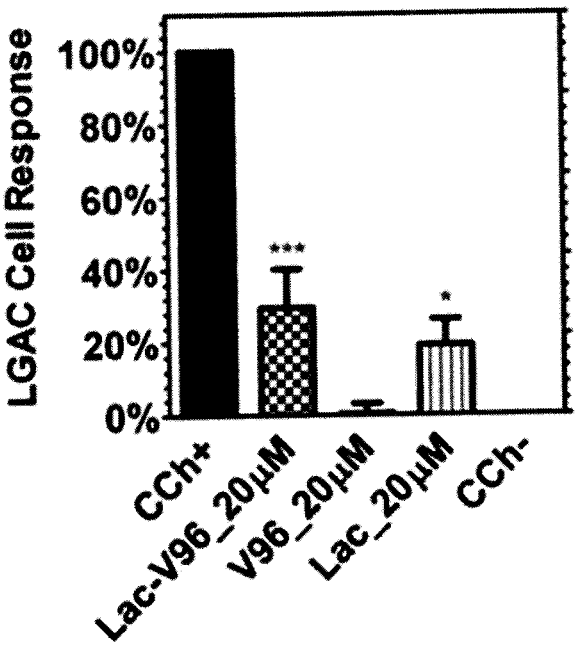
LGAC Cell Response
100%
80%
60%
40%
20%
0%
***
*
CCh+
Lac-V96_20µM
V96_20µM
Lac_20µM
CCh-

B)

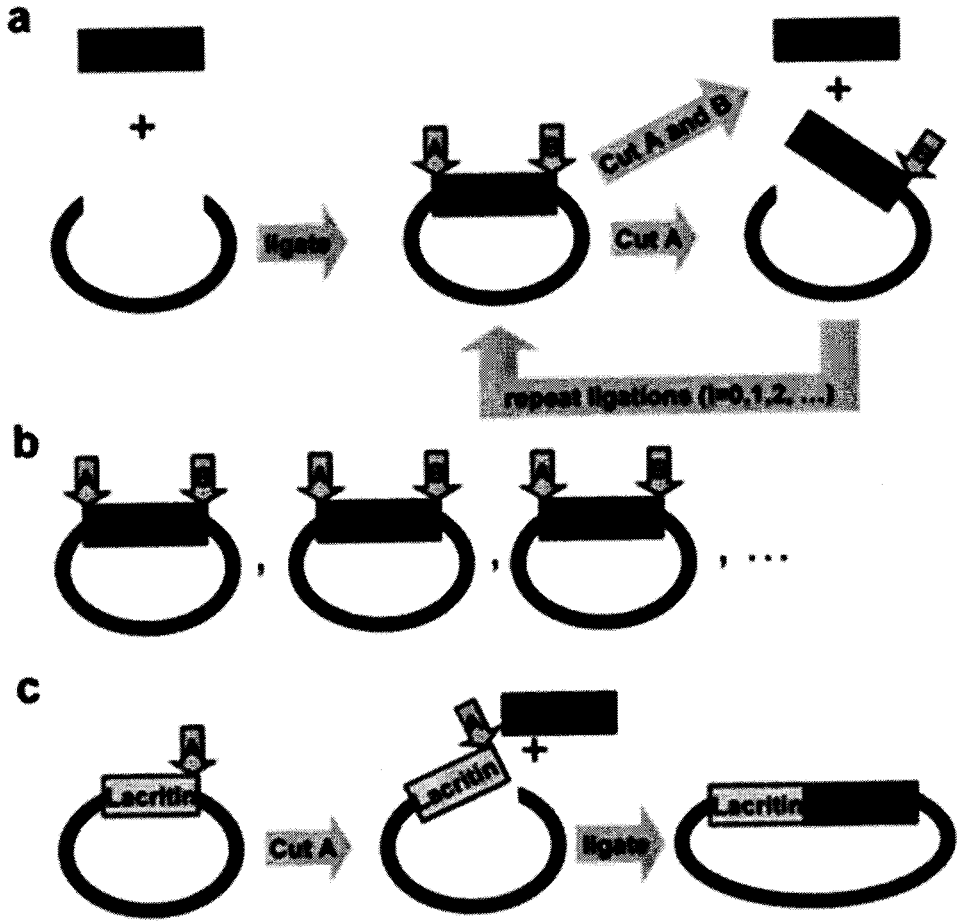
a
+
ligate
Cut A and B
Cut A
+
repeat ligations (i=0,1,2, ...)
b
c
Lacritin
Cut A
Lacritin
+
ligate
Lacritin

Figure 11

A

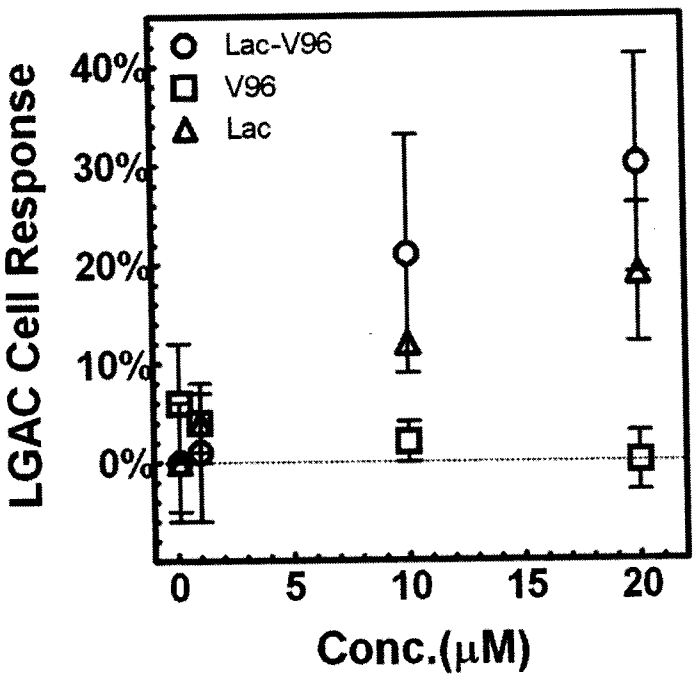

Conc. (μM)	Lac-V96&V96	Lacritin&V96	Lac-V96&Lacritin
0.1	ns	ns	ns
1	ns	ns	ns
10	*	*	ns
20	***	***	ns

B

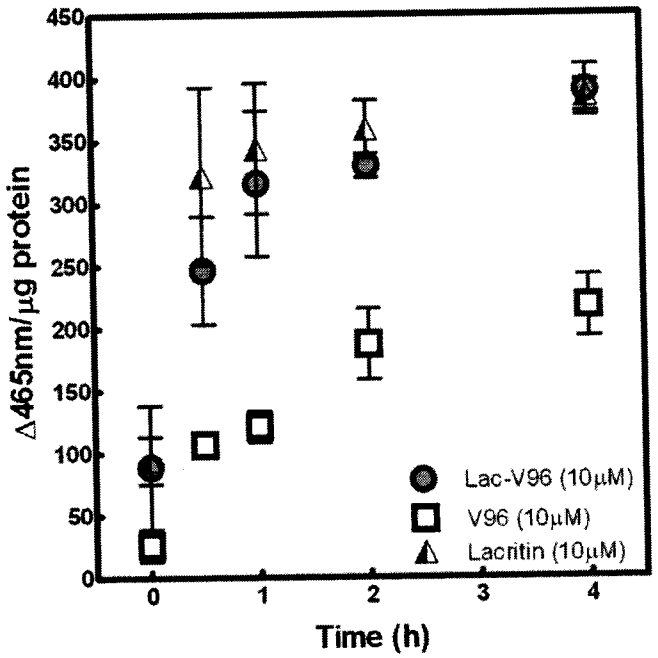

Time (h)	Lac-V96&V96	Lacritin&V96	Lac-V96&Lacritin
0	ns	ns	ns
0.5	***	****	ns
1	****	****	ns
2	***	****	ns
4	****	****	ns

Figure 12

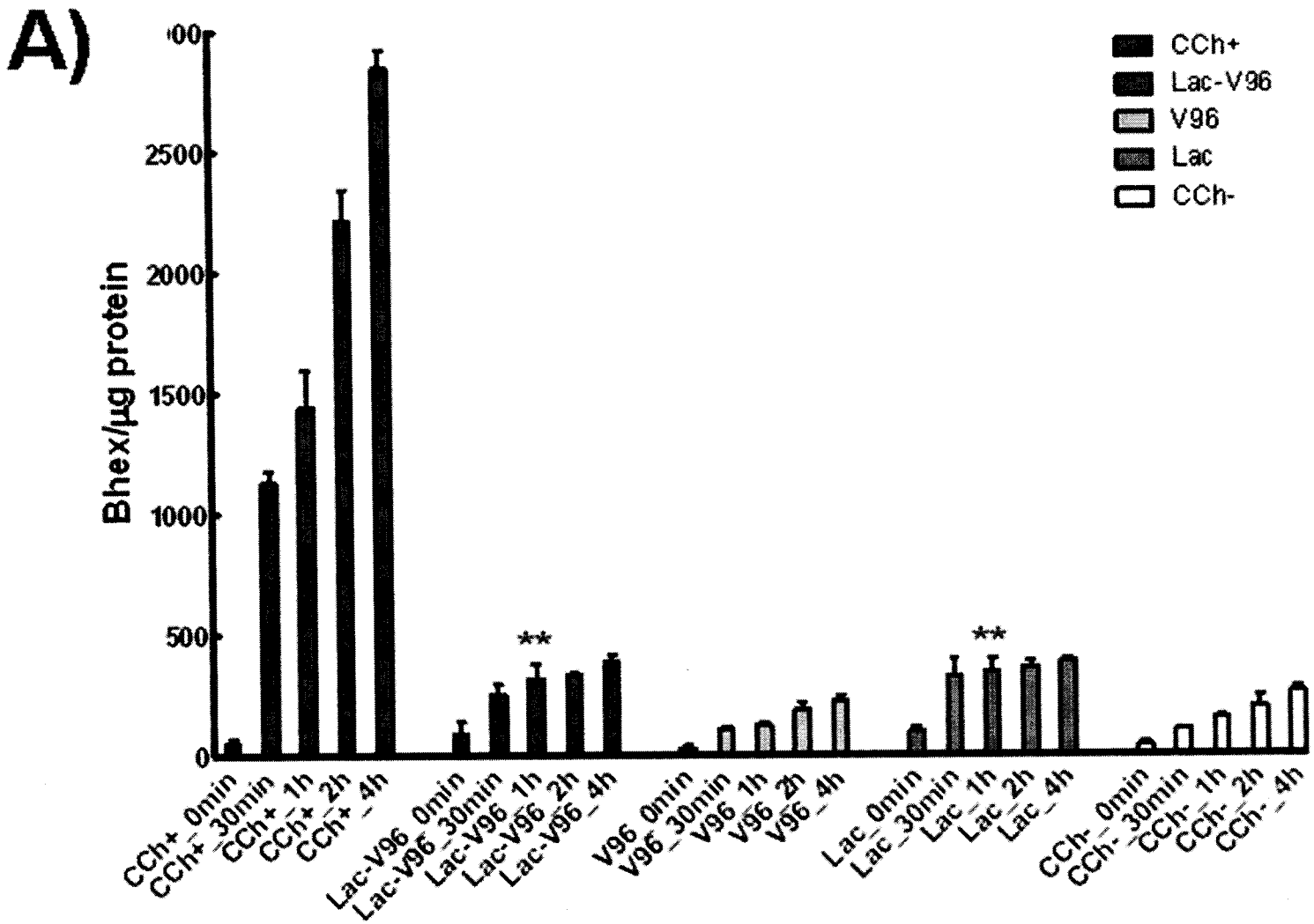
A)
Bhex/µg protein
3000
2500
2000
1500
1000
500
0
CCh+
Lac-V96
V96
Lac
CCh-
**
**
CCh+_0min
CCh+_30min
CCh+_1h
CCh+_2h
CCh+_4h
Lac-V96_0min
Lac-V96_30min
Lac-V96_1h
Lac-V96_2h
Lac-V96_4h
V96_0min
V96_30min
V96_1h
V96_2h
V96_4h
Lac_0min
Lac_30min
Lac_1h
Lac_2h
Lac_4h
CCh-_0min
CCh-_30min
CCh-_1h
CCh-_2h
CCh-_4h

Figure 12

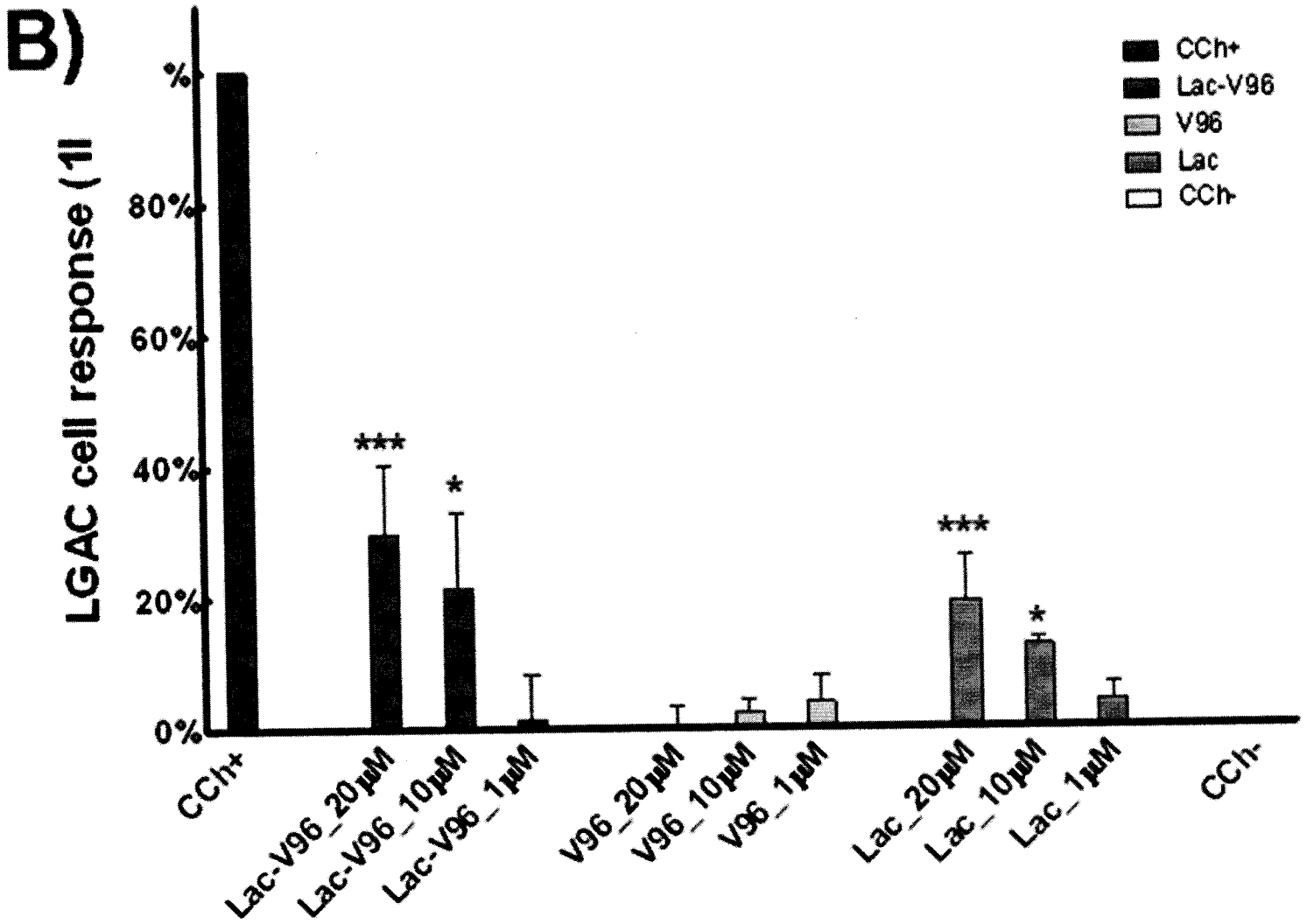
B)
LGAC cell response (1I
%
80%
60%
40%
20%
0%
***
*
***
*
CCh+
Lac-V96
V96
Lac
CCh-
CCh+
Lac-V96_20µM
Lac-V96_10µM
Lac-V96_1µM
V96_20µM
V96_10µM
V96_1µM
Lac_20µM
Lac_10µM
Lac_1µM
CCh-

Figure 13

A)

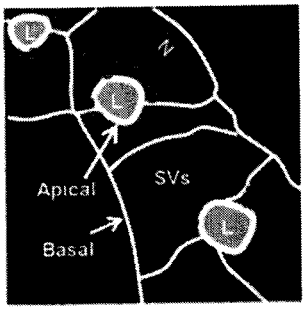

B)

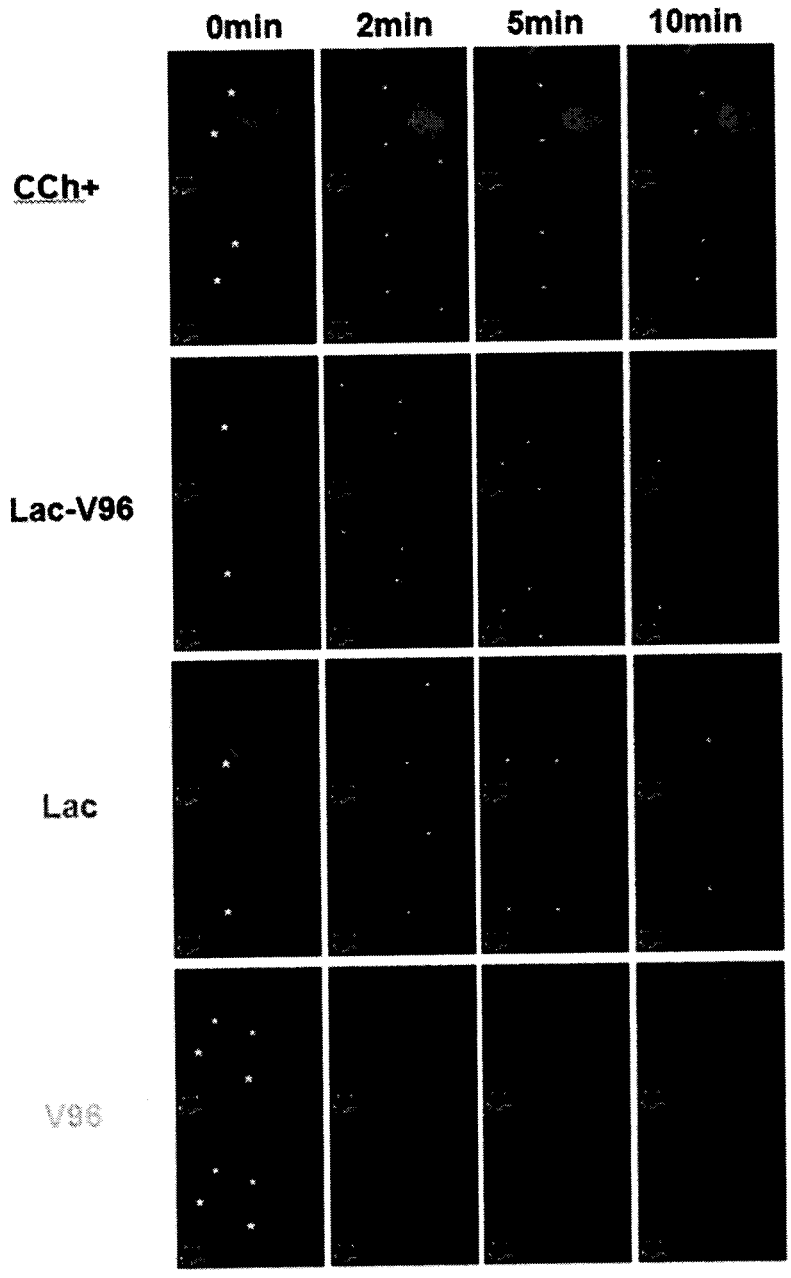

Figure 14

A)

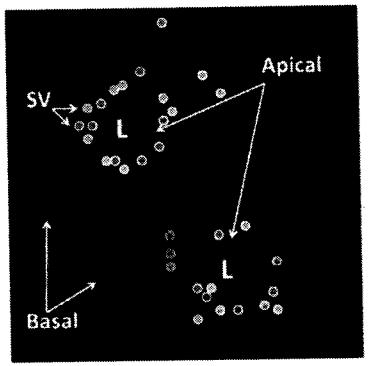
SV
Apical
L
L
Basal

B)

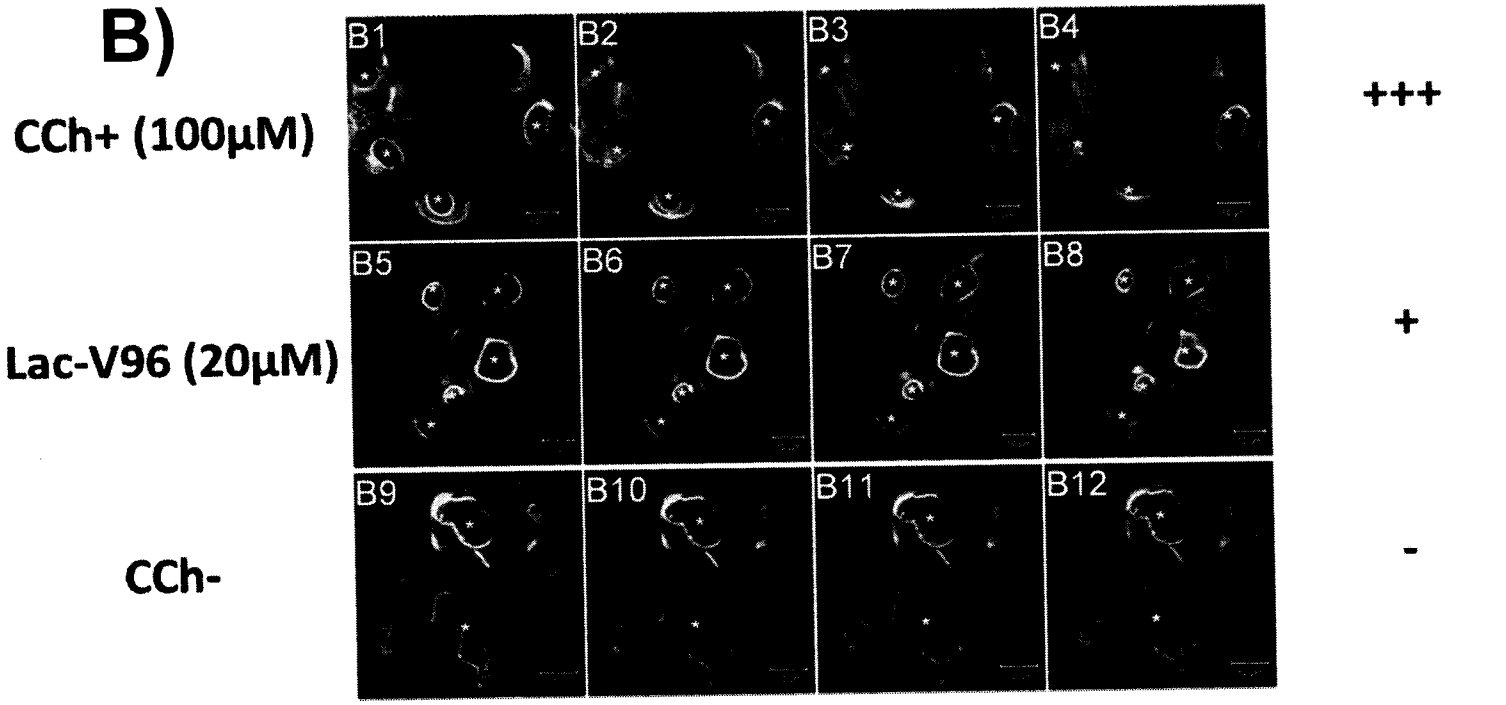
0sec
626sec
1564sec
2440sec
Response
CCh+ (100µM)
Lac-V96 (20µM)
CCh-
B1
B2
B3
B4
B5
B6
B7
B8
B9
B10
B11
B12
+++
+
-

Figure 15

A1

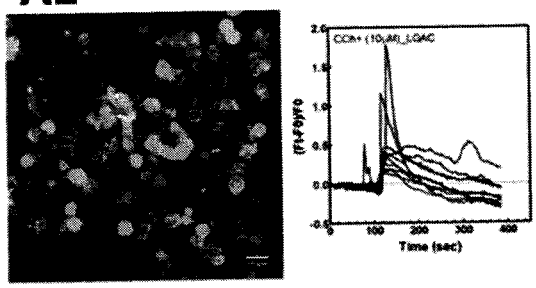

A2

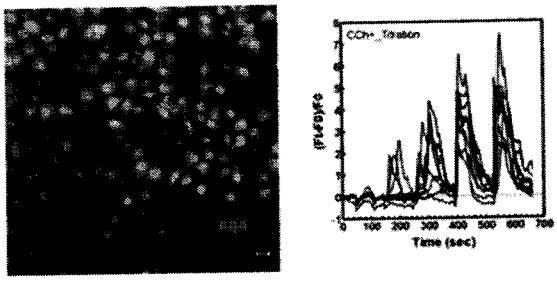

B1

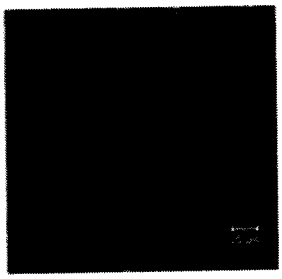

B2

B3

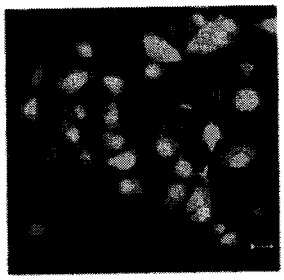

B4

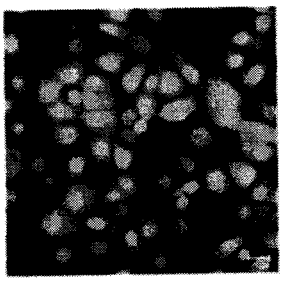

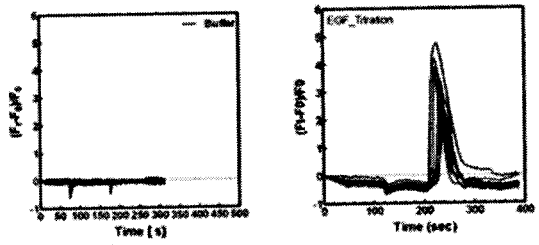

C

	LGAC		HCE-T	
	Pattern	% cell response	Pattern	% cell response
Medium	NA	NA	NA	NA
CCh+	Spark, Oscillation Biphasic	50%	Spark, Wave Conc. dependent	10%-90%
EGF	NA	NA	Spark, Wave Biphasic	10%-50%
Lacritin	NA	NA	Spark, Wave Conc. dependent	10%-90%
Lac-ELP	NA	NA	Spark, Wave Conc. dependent	10%-90%

Figure 16

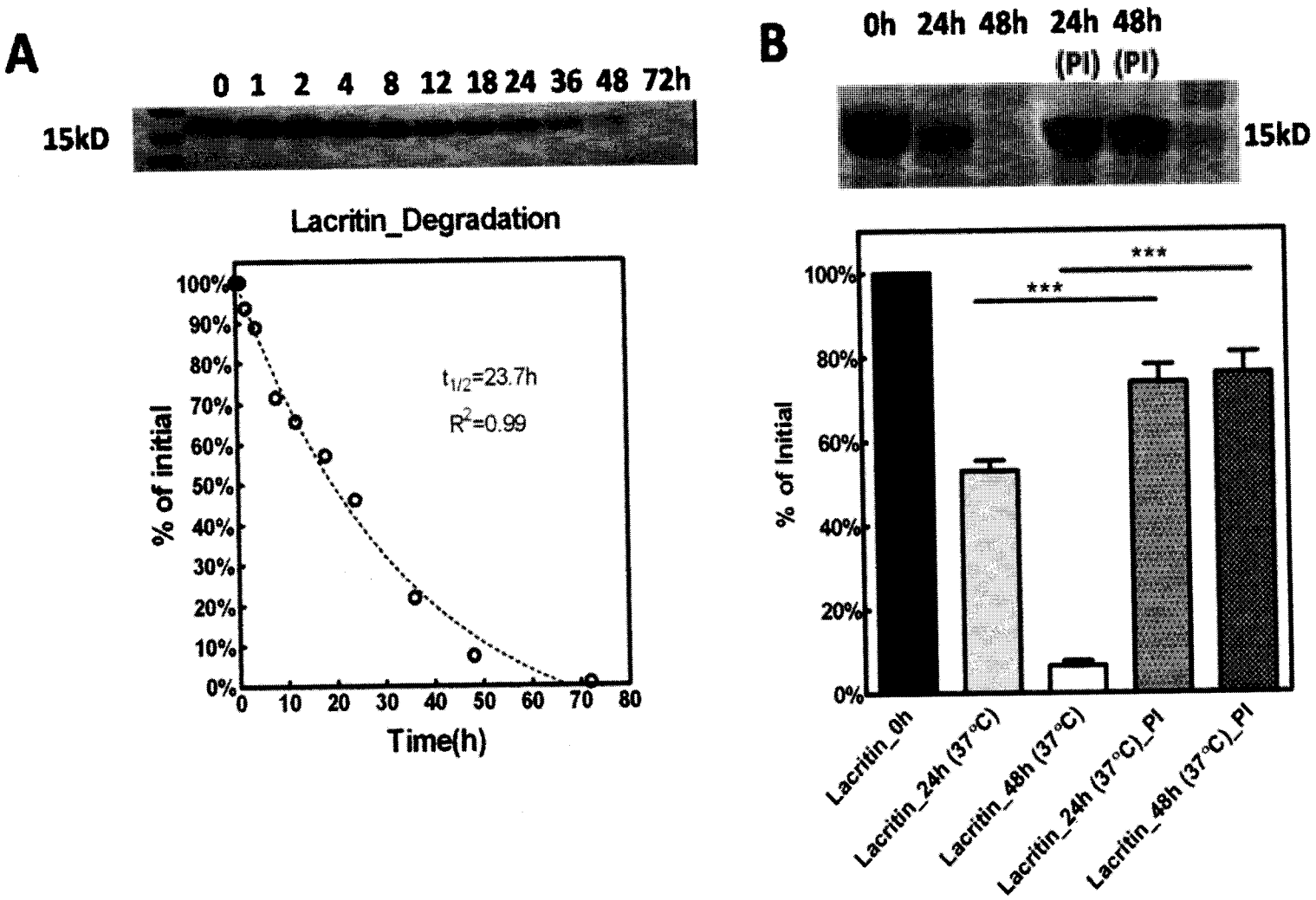
A
0 1 2 4 8 12 18 24 36 48 72h
15kD
Lacritin_Degradation
% of initial
Time(h)
$t_{1/2}$=23.7h
R^2=0.99
B
0h 24h 48h 24h 48h
(PI) (PI)
15kD
% of Initial
***
***
Lacritin_0h
Lacritin_24h (37°C)
Lacritin_48h (37°C)
Lacritin_24h (37°C)_PI
Lacritin_48h (37°C)_PI

Figure 16

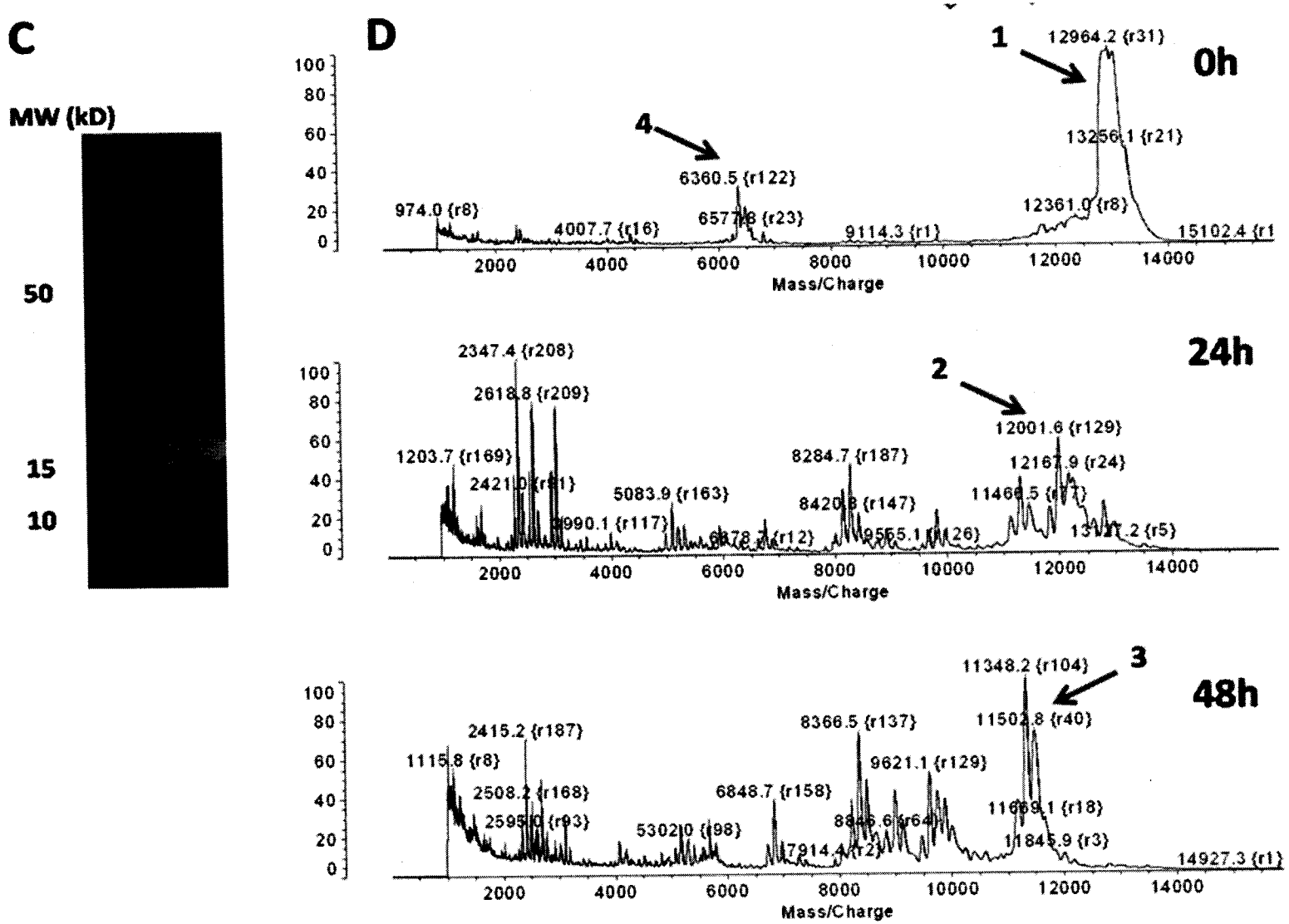
C
MW (kD)
50
15
10
D
0h
1
12964.2 {r31}
4
6360.5 {r122}
13256.1 {r21}
974.0 {r8}
4007.7 {r16}
12361.0 {r8}
9114.3 {r1}
15102.4 {r1
Mass/Charge
24h
2
2347.4 {r208}
2618.8 {r209}
12001.6 {r129}
1203.7 {r169}
8284.7 {r187}
5083.9 {r163}
Mass/Charge
48h
3
11348.2 {r104}
2415.2 {r187}
8366.5 {r137}
1115.8 {r8}
9621.1 {r129}
2508.2 {r168}
6848.7 {r158}
11845.9 {r3}
14927.3 {r1}
Mass/Charge

Figure 16

E

	Sequence	m/z	$[M+H]^+$
1	MGEDASSDSTGADPAQEAGTSKPNEEISGPAEPASPPETTTTAQETSAAA VQGTAKVTSSRQELNPLKSIVEKSILLTEQALAKAGKGMHGGVPGGKQFIE **NGSEFAQKLL**KKFSLLKPWAGLVPR|	12.97	12.96
2	MGEDASSDSTGADPAQEAGTSKPNEEISGPAEPASPPETTTTAQETSAAA VQGTAKVTSSRQELNPLKSIVEKSILLTEQALAKAGKGMHGGVPGGKQFIE **NGSEFAQKLL**KKFSLL|K|	11.97/ 12.09	12.00
3	MGEDASSDSTGADPAQEAGTSKPNEEISGPAEPASPPETTTTAQETSAAA VQGTAKVTSSRQELNPLKSIVEKSILLTEQALAKAGKGMHGGVPGGKQFIE **NGSEFAQKLL**K|K|	11.38/ 11.51	11.35/ 11.47/ 11.50
4	|PNEEISGPAEPASPPETTTTAQETSAAAVQGTAKVTSSRQELNPLKSIVEK SILLTEQALAK|	6.42	6.36

PATENT

IN THE UNITED STATES PATENT & TRADEMARK OFFICE

In re Application of	: MACKAY, John Andrew *et al.*
Application No.	: To be assigned
Filing Date	: July 26, 2012
Title	: CONTROLLED RELEASE OF OCULAR BIOPHARMACEUTICALS USING BIORESPONSIVE PROTEIN POLYMERS
Attorney Docket No.	: 065715-000038US00
Date	: July 26, 2012

Commissioner for Patents
P.O. Box 1450
Alexandria, VA 22313-1450

STATEMENT TO SUPPORT FILING AND SUBMISSION IN ACCORDANCE WITH 37 C.F.R. §§ 1.821-1.825

Dear Sir:

Attached is a computer readable form ("txt" file) of the "Sequence Listing," as well as a paper copy of the "Sequence Listing," disclosed in the above-identified patent application. Applicants respectfully submit that the content of the attached paper copy and the attached computer readable form of the Sequence Listing, submitted in accordance with 37 C.F.R. § 1.821(c) and (e), respectively, are the same.

If it should be determined, for any reason, that an insufficient fee has been paid, please charge any insufficiency to Deposit Account No. 50-4166.

Respectfully submitted,
John Andrew MacKay
NIXON PEABODY LLP

By _____
Stephen W. Chen
Registration No. 60,629

555 West Fifth Street, 46th Floor
Los Angeles, California 90013
Telephone: (213) 629-6000
Facsimile: (213) 629-6001

SEQUENCE LISTING

<110> University of Southern California
MACKAY, John A.
WANG, Wan

<120> CONTROLLED RELEASE OF OCULAR BIOPHARMACEUTICALS USING BIORESPONSIVE PROTEIN POLYMERS

<130> 065715-000038US00

<150> 61/511,928
<151> 2011-07-26

<160> 9

<170> PatentIn version 3.5

<210> 1
<211> 406
<212> DNA
<213> Homo sapiens

<400> 1
catatggaag acgcttcttc tgactctacc ggtgctgacc cggctcagga agctggtacc 60

tctaaaccga acgaagaaat ctctggtccg gctgaaccgg cttctccgcc ggaaaccacc 120

accaccgctc aggaaacctc tgctgctgct gttcagggta ccgctaaagt tacctcttct 180

cgtcaggaac tgaacccgct gaaatctatc gttgaaaaat ctatcctgct gaccgaacag 240

gctctggcta aagctggtaa aggtatgcac ggtggtgttc cgggtggtaa acagttcatc 300

gaaaacggtt ctgaattcgc tcagaaactg ctgaaaaaat tctctctgct gaaaccgtgg 360

gctggtctgg ttccgcgtgg ttctggttac tgatctcctc ggatcc 406

<210> 2
<211> 508
<212> DNA
<213> Homo sapiens

<400> 2
gcagattctg tggttatact cactcctcat cccaaagaat gaaatttacc actctcctct 60

tcttggcagc tgtagcaggg gccctggtct atgctgaaga tgcctcctct gactcgacgg 120

gtgctgatcc tgcccaggaa gctgggacct ctaagcctaa tgaagagatc tcaggtccag 180

cagaaccagc ttcaccccca gagacaacca caacagccca ggagacttcg gcggcagcag 240

ttcaggggac agccaaggtc acctcaagca ggcaggaact aaaccccctg aaatccatag 300

tggagaaaag tatcttacta acagaacaag cccttgcaaa agcaggaaaa ggaatgcacg 360

gaggcgtgcc aggtggaaaa caattcatcg aaaatggaag tgaatttgca caaaaattac 420

tgaagaaatt cagtctatta aaaccatggg catgagaagc tgaaaagaat gggatcattg 480

gacttaaagc cttaaatacc cttgtagc 508

<210> 3
<211> 138
<212> PRT
<213> Homo sapiens

<400> 3

```
Met Lys Phe Thr Thr Leu Leu Phe Leu Ala Ala Val Ala Gly Ala Leu
1               5                  10                  15

Val Tyr Ala Glu Asp Ala Ser Ser Asp Ser Thr Gly Ala Asp Pro Ala
            20                  25                  30

Gln Glu Ala Gly Thr Ser Lys Pro Asn Glu Glu Ile Ser Gly Pro Ala
        35                  40                  45

Glu Pro Ala Ser Pro Pro Glu Thr Thr Thr Thr Ala Gln Glu Thr Ser
    50                  55                  60

Ala Ala Ala Val Gln Gly Thr Ala Lys Val Thr Ser Ser Arg Gln Glu
65                  70                  75                  80

Leu Asn Pro Leu Lys Ser Ile Val Glu Lys Ser Ile Leu Leu Thr Glu
                85                  90                  95

Gln Ala Leu Ala Lys Ala Gly Lys Gly Met His Gly Gly Val Pro Gly
            100                 105                 110

Gly Lys Gln Phe Ile Glu Asn Gly Ser Glu Phe Ala Gln Lys Leu Leu
        115                 120                 125

Lys Lys Phe Ser Leu Leu Lys Pro Trp Ala
    130                 135
```

<210> 4
<211> 118
<212> PRT
<213> Homo sapiens

<400> 4

```
Asp Ala Ser Ser Asp Ser Thr Gly Ala Asp Pro Ala Gln Glu Ala Gly
1               5                  10                  15

Thr Ser Lys Pro Asn Glu Glu Ile Ser Gly Pro Ala Glu Pro Ala Ser
            20                  25                  30

Pro Pro Glu Thr Thr Thr Thr Ala Gln Glu Thr Ser Ala Ala Ala Val
        35                  40                  45
```

```
Gln Gly Thr Ala Lys Val Thr Ser Ser Arg Gln Glu Leu Asn Pro Leu
    50                  55                  60

Lys Ser Ile Val Glu Lys Ser Ile Leu Leu Thr Glu Gln Ala Leu Ala
65                  70                  75                  80

Lys Ala Gly Lys Gly Met His Gly Gly Val Pro Gly Gly Lys Gln Phe
                85                  90                  95

Ile Glu Asn Gly Ser Glu Phe Ala Gln Lys Leu Leu Lys Lys Phe Ser
            100                 105                 110

Leu Leu Lys Pro Trp Ala
        115
```

<210> 5
<211> 120
<212> PRT
<213> Homo sapiens

<400> 5

```
Met Glu Asp Ala Ser Ser Asp Ser Thr Gly Ala Asp Pro Ala Gln Glu
1               5                   10                  15

Ala Gly Thr Ser Lys Pro Asn Glu Glu Ile Ser Gly Pro Ala Glu Pro
            20                  25                  30

Ala Ser Pro Pro Glu Thr Thr Thr Thr Ala Gln Glu Thr Ser Ala Ala
        35                  40                  45

Ala Val Gln Gly Thr Ala Lys Val Thr Ser Ser Arg Gln Glu Leu Asn
    50                  55                  60

Pro Leu Lys Ser Ile Val Glu Lys Ser Ile Leu Leu Thr Glu Gln Ala
65                  70                  75                  80

Leu Ala Lys Ala Gly Lys Gly Met His Gly Gly Val Pro Gly Gly Lys
                85                  90                  95

Gln Phe Ile Glu Asn Gly Ser Glu Phe Ala Gln Lys Leu Leu Lys Lys
            100                 105                 110

Phe Ser Leu Leu Lys Pro Trp Ala
        115                 120
```

<210> 6
<211> 121
<212> PRT
<213> Homo sapiens

<400> 6

```
Met Gly Glu Asp Ala Ser Ser Asp Ser Thr Gly Ala Asp Pro Ala Gln
1               5                  10                  15

Glu Ala Gly Thr Ser Lys Pro Asn Glu Glu Ile Ser Gly Pro Ala Glu
            20                  25                  30

Pro Ala Ser Pro Pro Glu Thr Thr Thr Thr Ala Gln Glu Thr Ser Ala
        35                  40                  45

Ala Ala Val Gln Gly Thr Ala Lys Val Thr Ser Ser Arg Gln Glu Leu
    50                  55                  60

Asn Pro Leu Lys Ser Ile Val Glu Lys Ser Ile Leu Leu Thr Glu Gln
65                  70                  75                  80

Ala Leu Ala Lys Ala Gly Lys Gly Met His Gly Gly Val Pro Gly Gly
                85                  90                  95

Lys Gln Phe Ile Glu Asn Gly Ser Glu Phe Ala Gln Lys Leu Leu Lys
            100                 105                 110

Lys Phe Ser Leu Leu Lys Pro Trp Ala
        115                 120
```

<210> 7
<211> 117
<212> PRT
<213> Homo sapiens

<400> 7

```
Met Gly Glu Asp Ala Ser Ser Asp Ser Thr Gly Ala Asp Pro Ala Gln
1               5                  10                  15

Glu Ala Gly Thr Ser Lys Pro Asn Glu Glu Ile Ser Gly Pro Ala Glu
            20                  25                  30

Pro Ala Ser Pro Pro Glu Thr Thr Thr Thr Ala Gln Glu Thr Ser Ala
        35                  40                  45

Ala Ala Val Gln Gly Thr Ala Lys Val Thr Ser Ser Arg Gln Glu Leu
    50                  55                  60

Asn Pro Leu Lys Ser Ile Val Glu Lys Ser Ile Leu Leu Thr Glu Gln
65                  70                  75                  80

Ala Leu Ala Lys Ala Gly Lys Gly Met His Gly Gly Val Pro Gly Gly
```

85 90 95

Lys Gln Phe Ile Glu Asn Gly Ser Glu Phe Ala Gln Lys Leu Leu Lys
100 105 110

Lys Phe Ser Leu Leu
115

<210> 8
<211> 112
<212> PRT
<213> Homo sapiens

<400> 8

Met Gly Glu Asp Ala Ser Ser Asp Ser Thr Gly Ala Asp Pro Ala Gln
1 5 10 15

Glu Ala Gly Thr Ser Lys Pro Asn Glu Glu Ile Ser Gly Pro Ala Glu
20 25 30

Pro Ala Ser Pro Pro Glu Thr Thr Thr Thr Ala Gln Glu Thr Ser Ala
35 40 45

Ala Ala Val Gln Gly Thr Ala Lys Val Thr Ser Ser Arg Gln Glu Leu
50 55 60

Asn Pro Leu Lys Ser Ile Val Glu Lys Ser Ile Leu Leu Thr Glu Gln
65 70 75 80

Ala Leu Ala Lys Ala Gly Lys Gly Met His Gly Gly Val Pro Gly Gly
85 90 95

Lys Gln Phe Ile Glu Asn Gly Ser Glu Phe Ala Gln Lys Leu Leu Lys
100 105 110

<210> 9
<211> 8
<212> PRT
<213> Homo sapiens

<400> 9

Gly Leu Val Pro Arg Gly Ser Gly
1 5

Electronic Acknowledgement Receipt

EFS ID:	13350172
Application Number:	13559053
International Application Number:	
Confirmation Number:	2080
Title of Invention:	CONTROLLED RELEASE OF OCULAR BIOPHARMACEUTICALS USING BIORESPONSIVE PROTEIN POLYMERS
First Named Inventor/Applicant Name:	John Andrew MacKay
Customer Number:	106303
Filer:	Stephen Weihung Chen/Marina Der Tatevossian
Filer Authorized By:	Stephen Weihung Chen
Attorney Docket Number:	065715-000038US00
Receipt Date:	26-JUL-2012
Filing Date:	
Time Stamp:	16:18:30
Application Type:	Utility under 35 USC 111(a)

Payment information:

Submitted with Payment	yes
Payment Type	Deposit Account
Payment was successfully received in RAM	$655
RAM confirmation Number	3410
Deposit Account	504166
Authorized User	

The Director of the USPTO is hereby authorized to charge indicated fees and credit any overpayment as follows:

Charge any Additional Fees required under 37 C.F.R. Section 1.17 (Patent application and reexamination processing fees)

Charge any Additional Fees required under 37 C.F.R. Section 1.19 (Document supply fees)

Charge any Additional Fees required under 37 C.F.R. Section 1.21 (Miscellaneous fees and charges)

File Listing:

Document Number	Document Description	File Name	File Size(Bytes)/ Message Digest	Multi Part /.zip	Pages (if appl.)
1	Application Data Sheet	ADS_USC038US00.pdf	679866 d513e979374f78b1ff4b24931ea8113c9134f2a3	no	4
Warnings:					
Information:					
2	Miscellaneous Incoming Letter	SequenceListingStatement_038US00.pdf	17350 43f66a4e9d13d7cd7b286940ac5de28c72dbd315	no	1
Warnings:					
Information:					
3	Sequence Listing	SequenceListing_USC038US0.pdf	18352 796c380ecbbae68d695dedc6eb807715098b770f	no	5
Warnings:					
Information:					
4	Sequence Listing (Text File)	SequenceListing_USC038US0.txt	8483	no	0
Warnings:					
Information:					
5		NonProvisional_038US00.pdf	971315 38160455967a6e805471a2a101ce0ef76503b7fd	yes	63

Multipart Description/PDF files in .zip description

Document Description	Start	End
Specification	1	36
Claims	37	39
Abstract	40	40
Drawings-only black and white line drawings	41	63

Warnings:					
Information:					
6	Fee Worksheet (SB06)	fee-info.pdf	37183 40c98f2c17c3b9eb64026dbb0417988e2bcc5061	no	2
Warnings:					

Information:	
Total Files Size (in bytes):	1732549

This Acknowledgement Receipt evidences receipt on the noted date by the USPTO of the indicated documents, characterized by the applicant, and including page counts, where applicable. It serves as evidence of receipt similar to a Post Card, as described in MPEP 503.

New Applications Under 35 U.S.C. 111

If a new application is being filed and the application includes the necessary components for a filing date (see 37 CFR 1.53(b)-(d) and MPEP 506), a Filing Receipt (37 CFR 1.54) will be issued in due course and the date shown on this Acknowledgement Receipt will establish the filing date of the application.

National Stage of an International Application under 35 U.S.C. 371

If a timely submission to enter the national stage of an international application is compliant with the conditions of 35 U.S.C. 371 and other applicable requirements a Form PCT/DO/EO/903 indicating acceptance of the application as a national stage submission under 35 U.S.C. 371 will be issued in addition to the Filing Receipt, in due course.

New International Application Filed with the USPTO as a Receiving Office

If a new international application is being filed and the international application includes the necessary components for an international filing date (see PCT Article 11 and MPEP 1810), a Notification of the International Application Number and of the International Filing Date (Form PCT/RO/105) will be issued in due course, subject to prescriptions concerning national security, and the date shown on this Acknowledgement Receipt will establish the international filing date of the application.

US 20130210747A1

(19) **United States**

(12) **Patent Application Publication**

Hamm-Alvarez et al.

(10) **Pub. No.: US 2013/0210747 A1**

(43) **Pub. Date: Aug. 15, 2013**

(54) **METHODS AND THERAPEUTICS COMPRISING LIGAND-TARGETED ELPS**

(71) Applicant: **University of Southem California**, (US)

(72) Inventors: **Sarah Hamm-Alvarez**, Pasadena, CA (US); **John Andrew MacKay**, Pasadena, CA (US); **Guoyong Sun**, Mission Viejo, CA (US); **Pang-Yu Hsueh**, San Jose, CA (US)

(73) Assignee: **UNIVERSITY OF SOUTHERN CALIFORNIA**, Los Angeles, CA (US)

(21) Appl. No.: **13/764,476**

(22) Filed: **Feb. 11, 2013**

Related U.S. Application Data

(60) Provisional application No. 61/598,298, filed on Feb. 13, 2012, provisional application No. 61/664,619, filed on Jun. 26, 2012.

Publication Classification

(51) **Int. Cl.**
A61K 47/48 (2006.01)

(52) **U.S. Cl.**
CPC ***A61K 47/48292*** (2013.01)
USPC **514/21.2**; 530/353; 536/23.5; 435/69.1; 435/375; 514/20.8; 435/348; 435/325; 435/353; 435/366; 435/254.2; 435/252.33; 435/252.3; 435/252.35; 435/369; 435/352; 435/357; 435/365; 435/363; 435/367; 435/254.21; 435/254.22; 435/254.23

(57) **ABSTRACT**

Disclosed herein are novel methods and compositions for targeting drug delivery systems to specific cells. One aspect relates to a drug delivery system comprising an elastin-like peptide (ELP) component and a ligand selected from the group consisting of mIgA and knob capable of either drug encapsulation or drug attachment. Further aspects relate to drug delivery systems comprising an elastin-like peptide (ELP) component and a ligand; wherein the ligand specifically binds to a receptor selected from the group consisting of CAR and pIgR. Further aspects include the novel transcytosing properties of the elastin-like peptide and the ligand, knob. Also provided are methods and pharmaceutical compositions comprising the disclosed therapeutics.

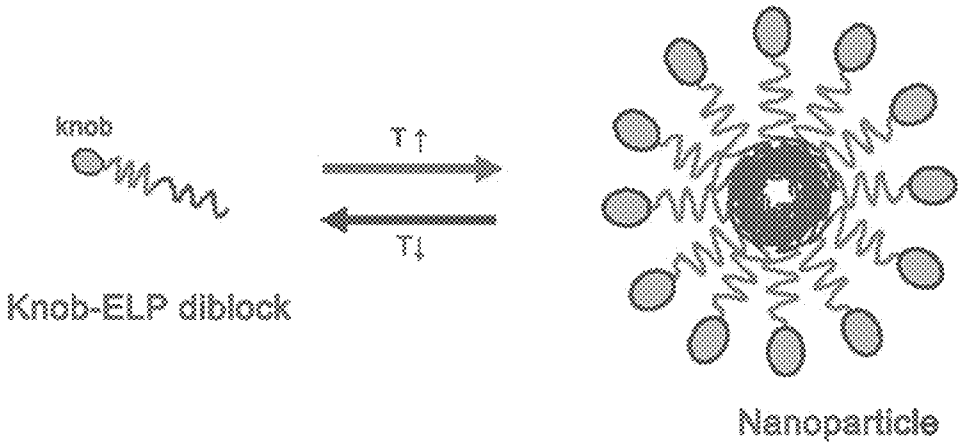

Fig. 1

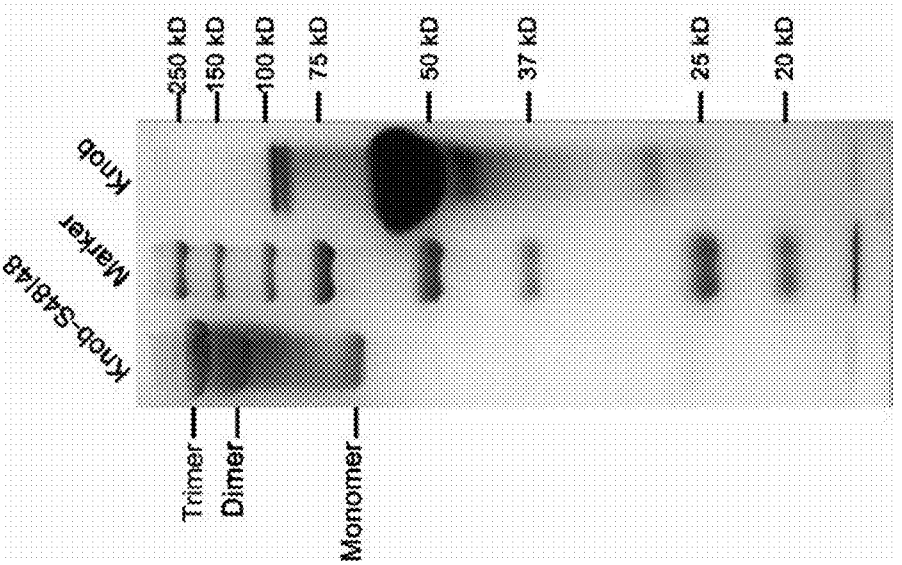
250 kD
150 kD
100 kD
75 kD
50 kD
37 kD
25 kD
20 kD
Knob
Marker
Knob-S48I48
Trimer
Dimer
Monomer

Fig. 3

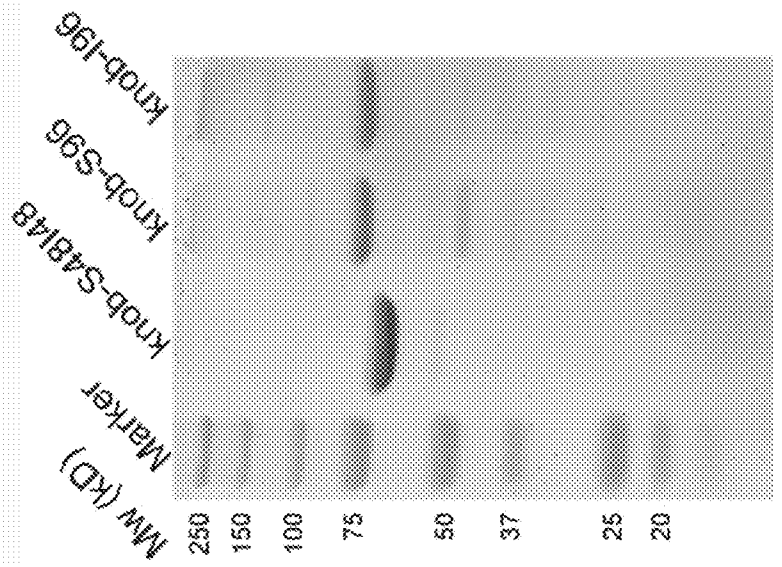
MW (kD)
Marker
Knob-S48I48
Knob-S96
Knob-196
250
150
100
75
50
37
25
20

Fig. 2

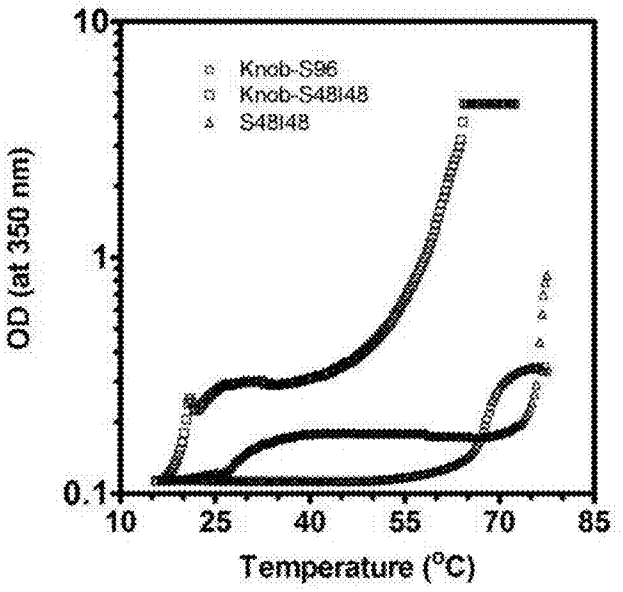
10
1
0.1
OD (at 350 nm)
Knob-S96
Knob-S48I48
S48I48
10
25
40
55
70
85
Temperature (°C)

Fig. 4

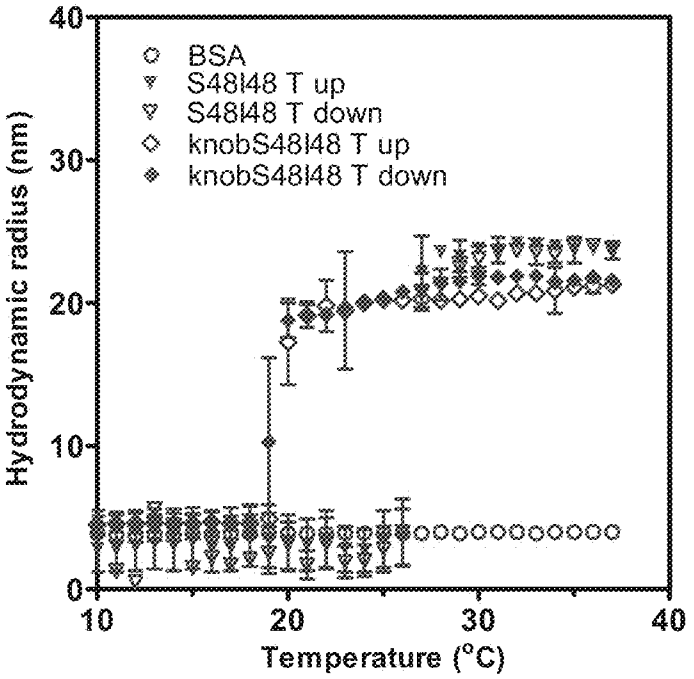
BSA
S48I48 T up
S48I48 T down
knobS48I48 T up
knobS48I48 T down
Hydrodynamic radius (nm)
Temperature (°C)
0
10
20
30
40

Fig. 5A

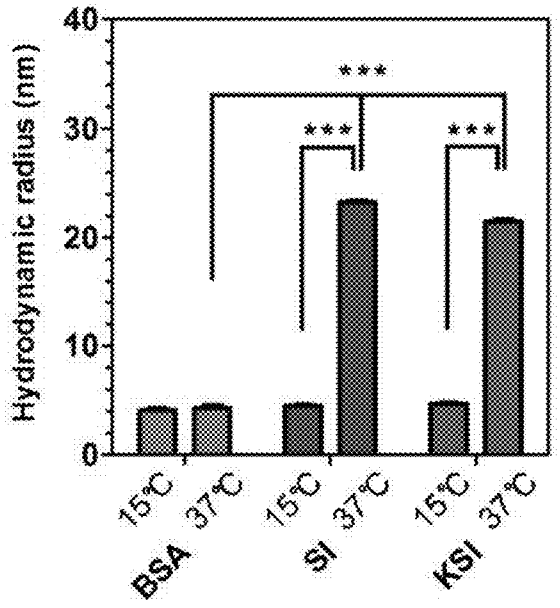
Hydrodynamic radius (nm)
***
***
***
15°C
37°C
BSA
SI
KSI
0
10
20
30
40

Fig. 5B

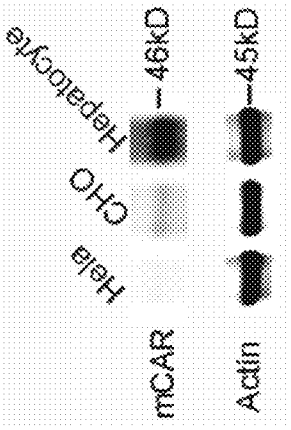
Hepatocyte
CHO
Hela
mCAR
Actin
46kD
45kD

Fig. 7

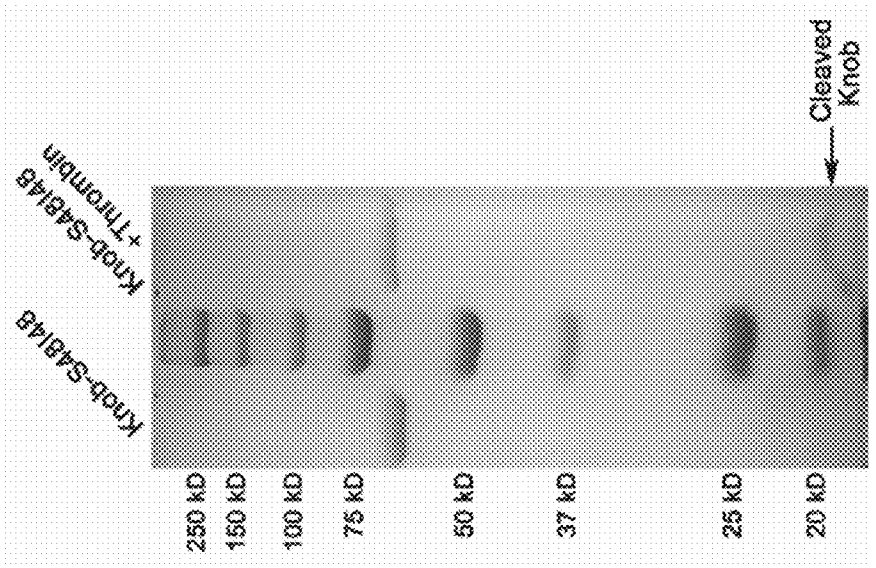
Knob-SAB1A8
Knob-SAB1A8
+Thrombin
Cleaved Knob
250 kD
150 kD
100 kD
75 kD
50 kD
37 kD
25 kD
20 kD

Fig. 6

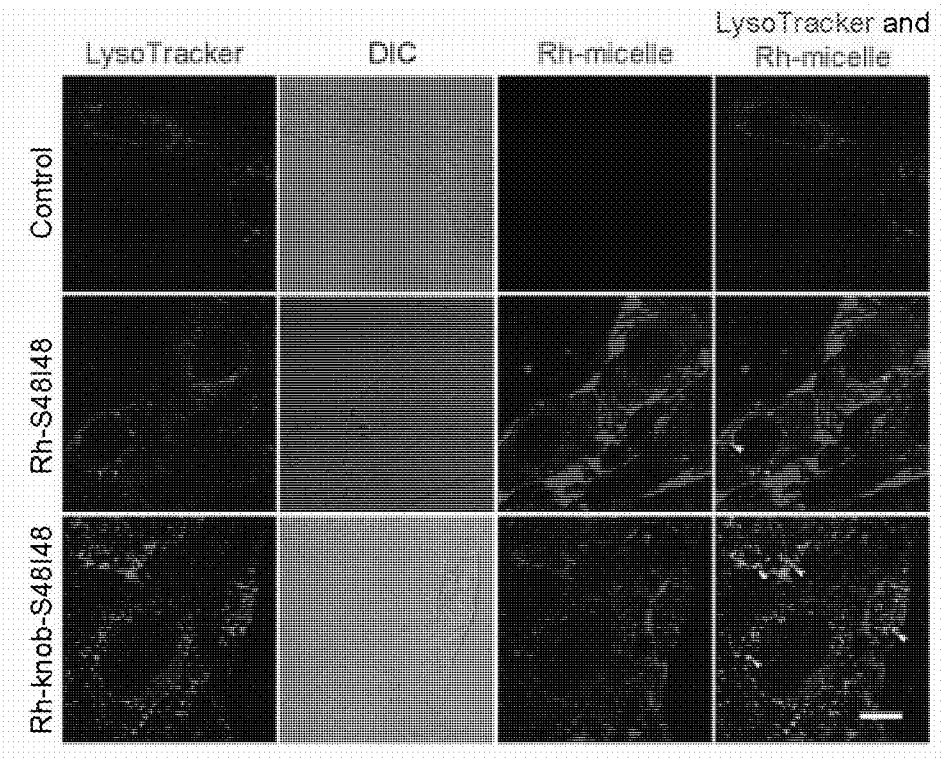
LysoTracker
DIC
Rh-micelle
LysoTracker and Rh-micelle
Control
Rh-S48I48
Rh-knob-S48I48

Fig. 8

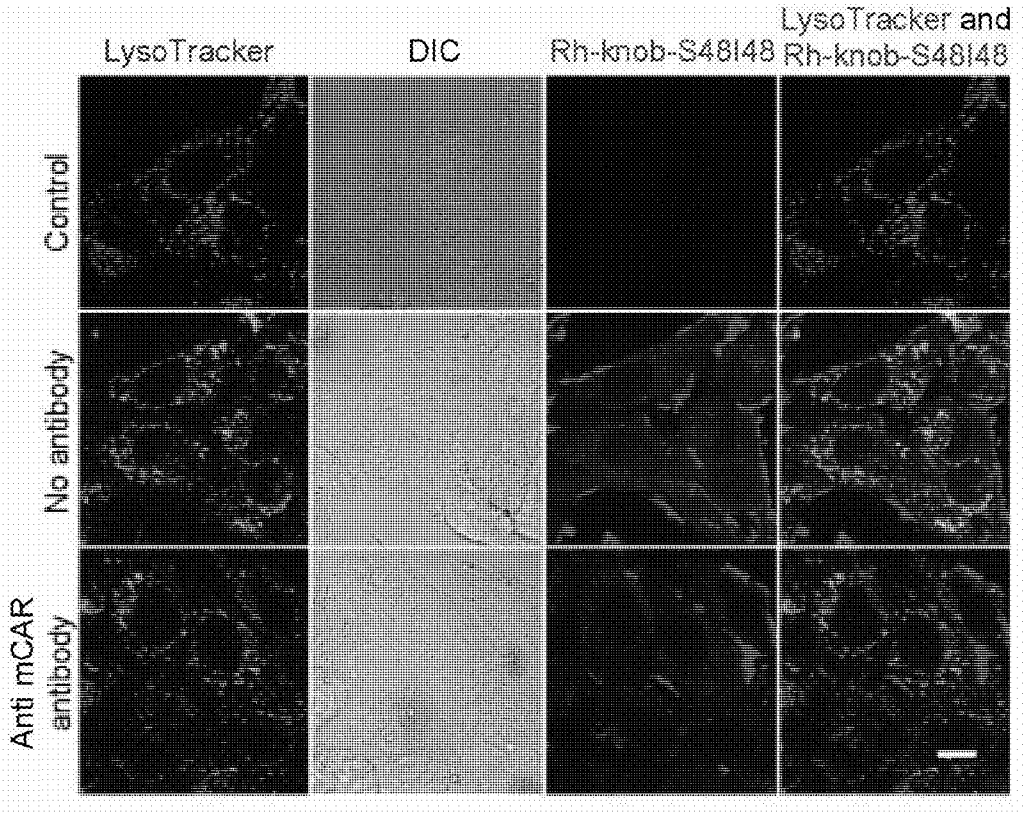
LysoTracker
DIC
Rh-knob-S48I48
LysoTracker and Rh-knob-S48I48
Control
No antibody
Anti mCAR antibody

Fig. 9

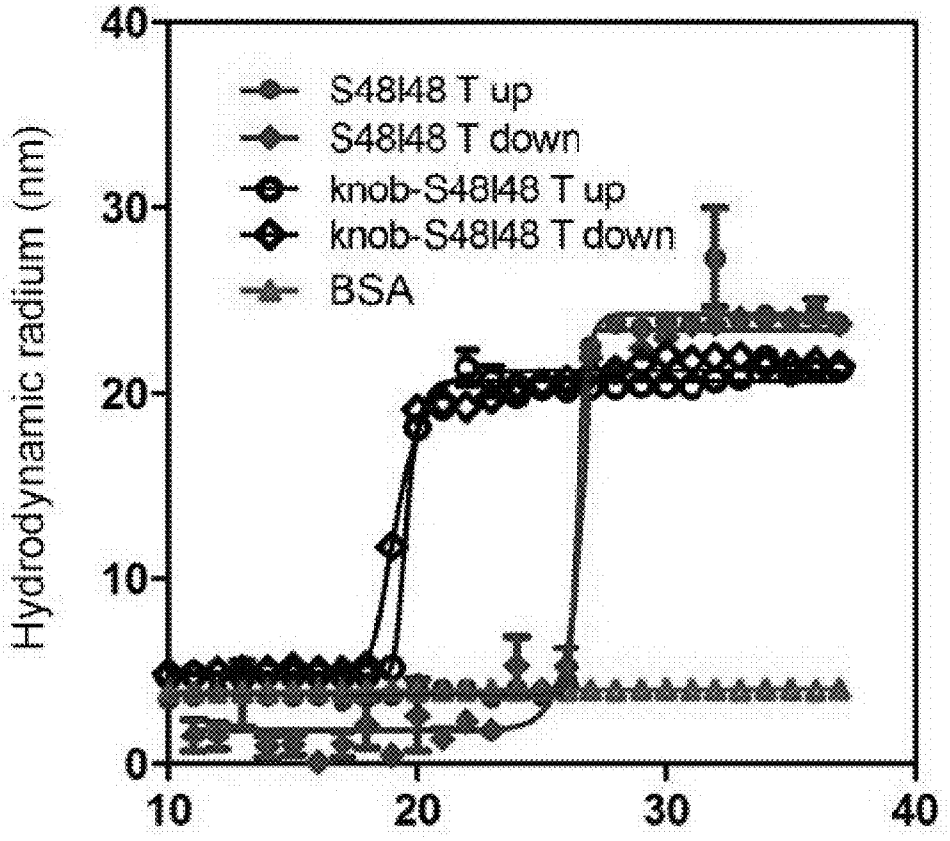
Hydrodynamic radium (nm)
40
30
20
10
0
10
20
30
40
S48I48 T up
S48I48 T down
knob-S48I48 T up
knob-S48I48 T down
BSA

Fig. 10

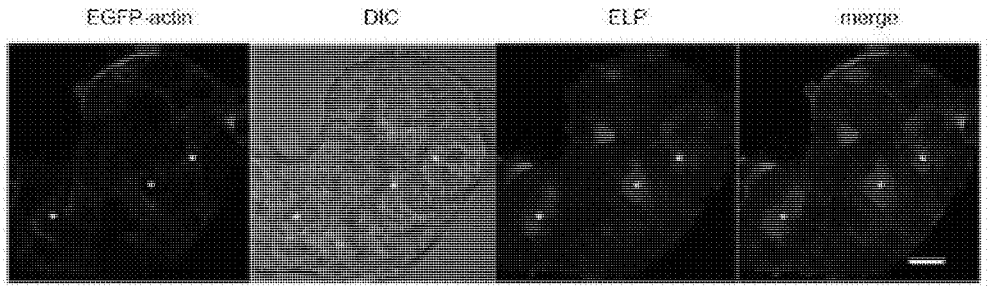

*lumena. Scale bar: 10 μm

Fig. 11

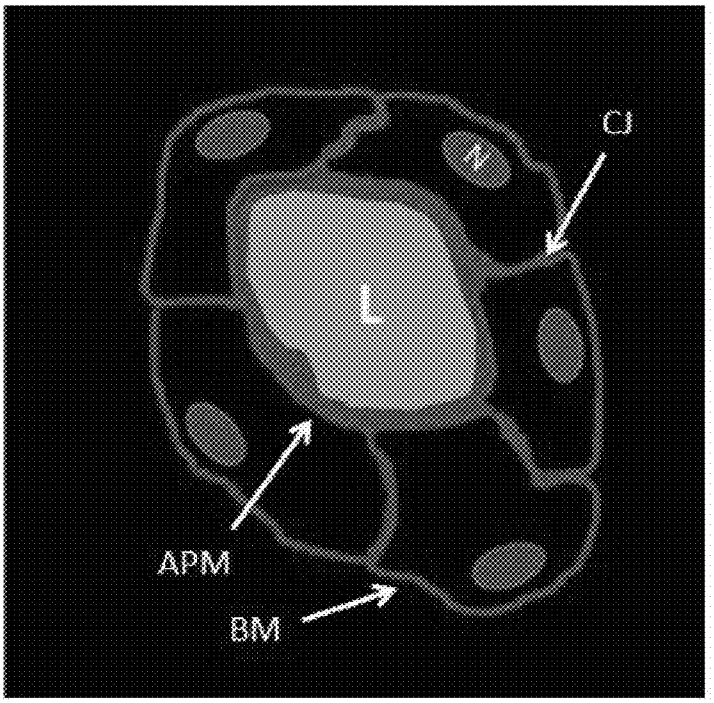

L: acinar lumena
N: nucleus
APM: apical membrane
BM: basal-lateral membrane
CJ: cell junction

Fig. 12

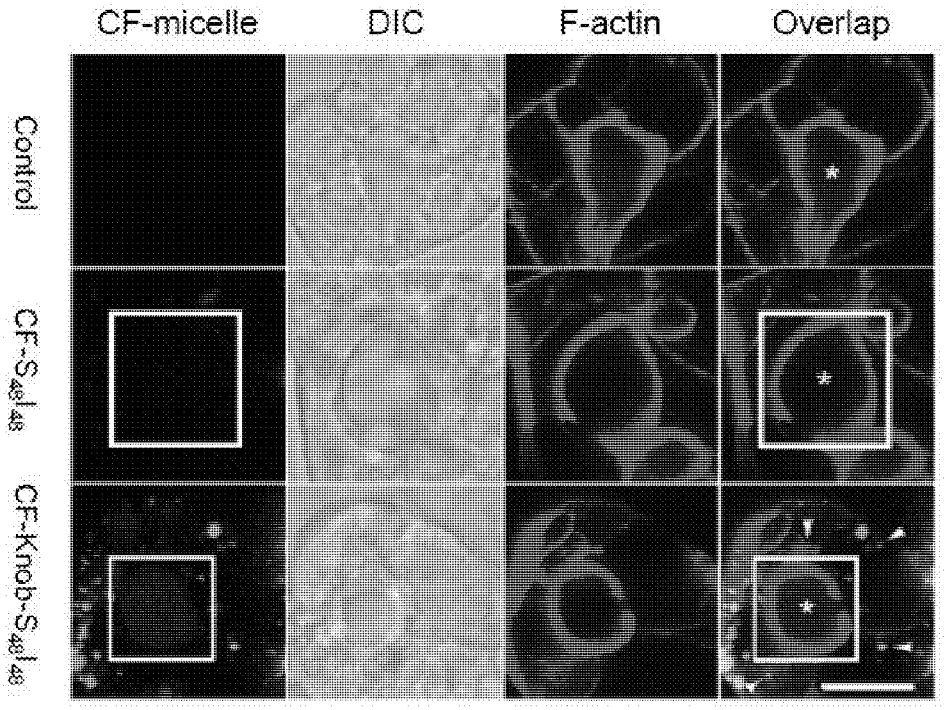
CF-micelle
DIC
F-actin
Overlap
Control
CF-S48I48
CF-Knob-S48I48

Fig. 13

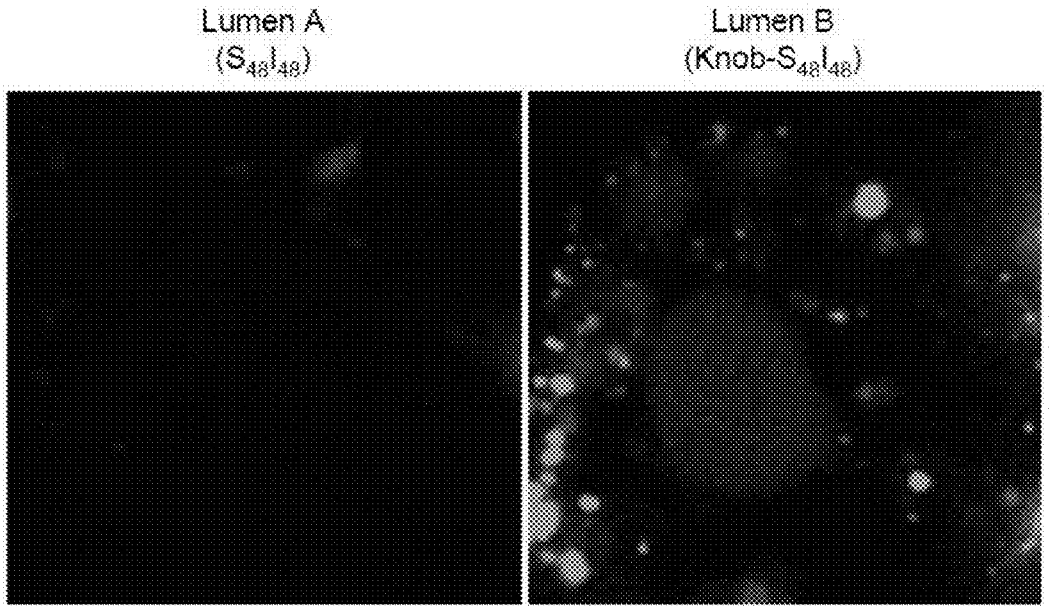

Fig. 14

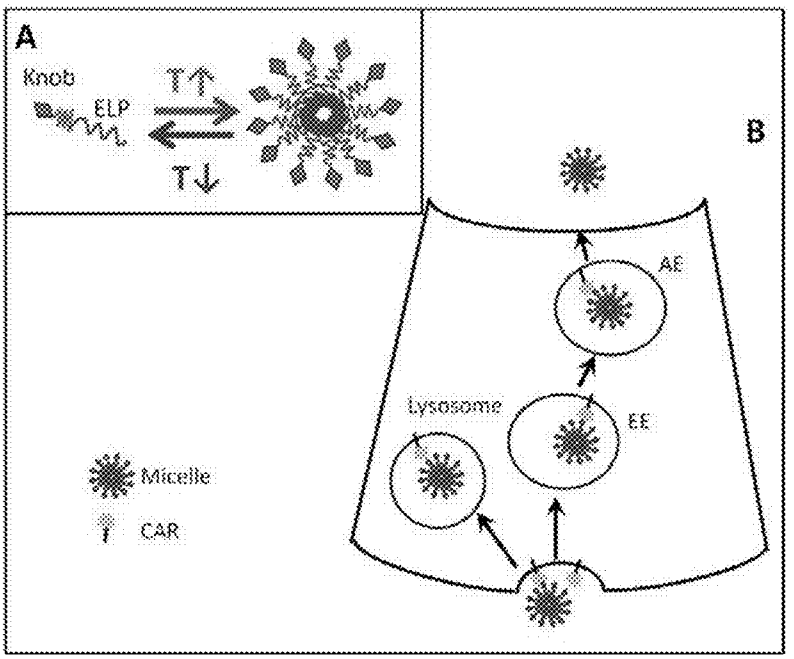

Fig. 15

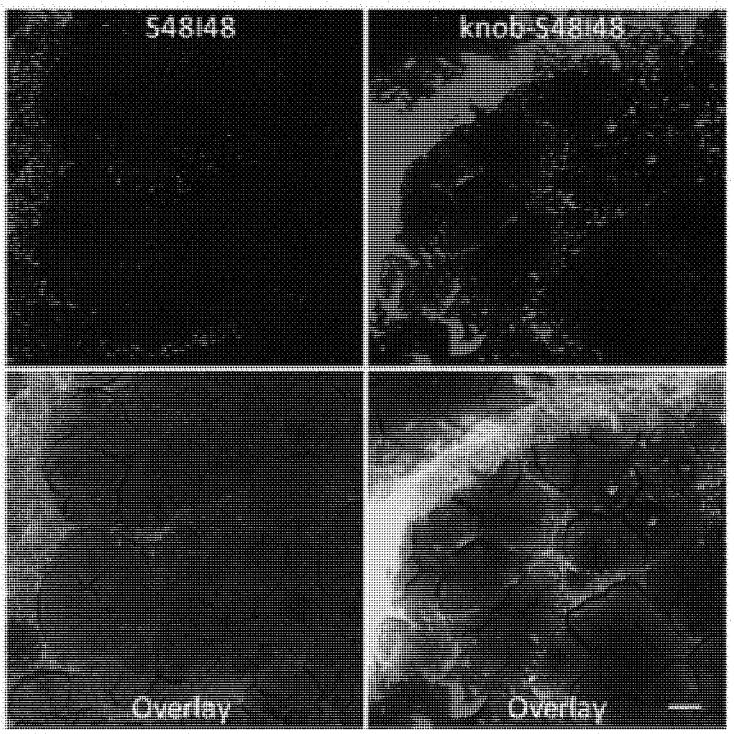

Fig. 16

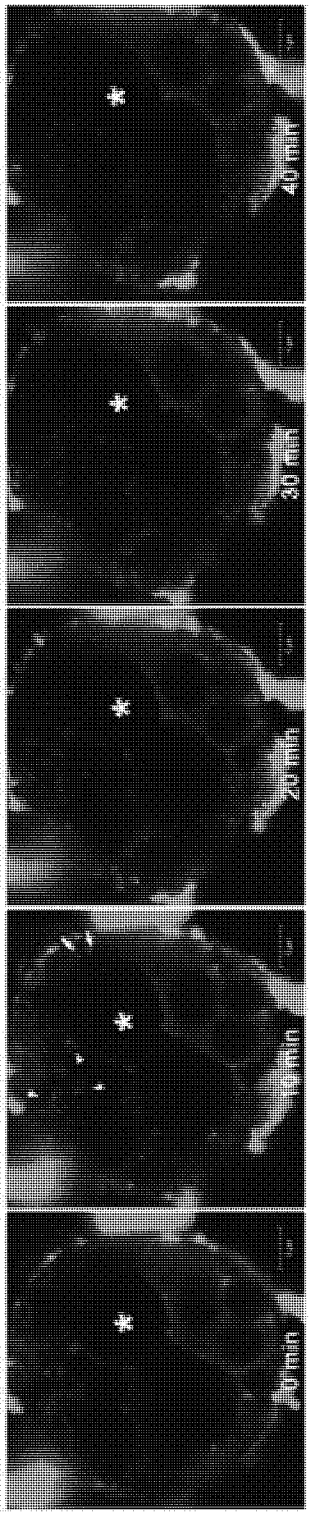

Fig. 17

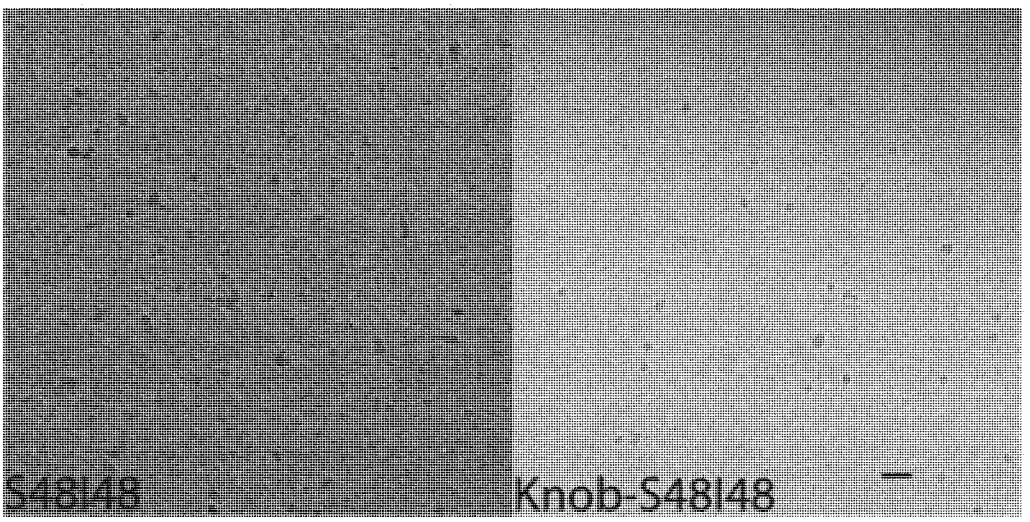

Fig. 18A

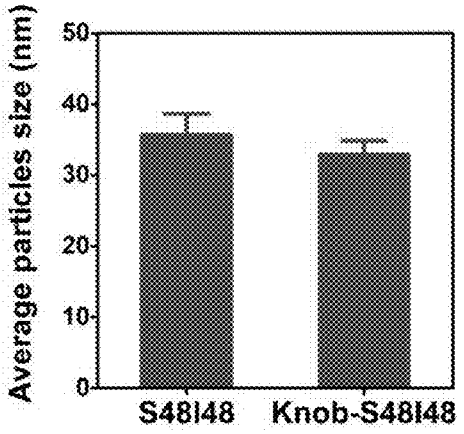

Fig. 18B

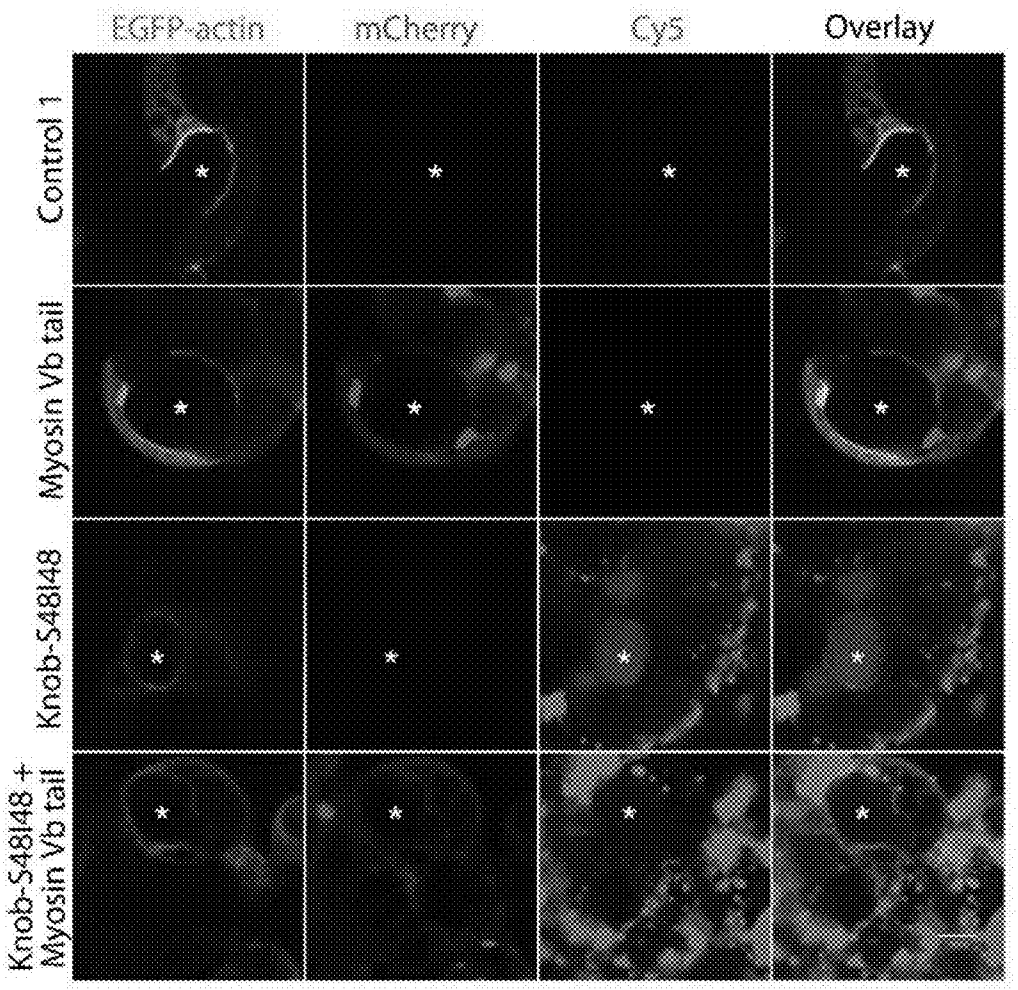
EGFP-actin
mCherry
Cy5
Overlay
Control 1
Myosin Vb tail
Knob-S48I48
Knob-S48I48 + Myosin Vb tail

Fig. 19

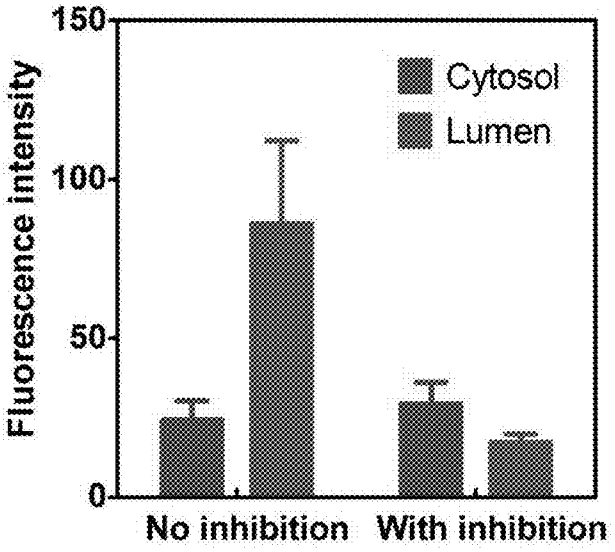

Fig. 20A

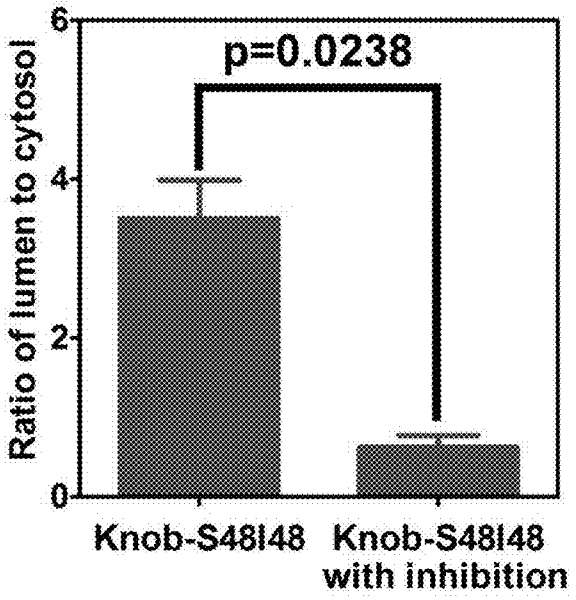

Fig. 20B

METHODS AND THERAPEUTICS COMPRISING LIGAND-TARGETED ELPS

CROSS-REFERENCE TO RELATED APPLICATIONS

[0001] This application claims the benefit under 35 U.S.C. §119(e) to U.S. Provisional Application Ser. No. 61/598,298, filed Feb. 13, 2012, and U.S. Provisional Application Ser. No. 61/664,619, filed Jun. 26, 2012, each of which are hereby incorporated by reference in their entirety.

STATEMENT OF GOVERNMENT SUPPORT

[0002] The presently disclosed subject matter was made with United States Government support under Grant Nos. EY017293-S1, EY017293 and 5-P30-CA14089, awarded by the National Institutes of Health (NIH). The United States Government has certain rights in the presently disclosed subject matter.

BACKGROUND

[0003] Drug delivery to the eye (e.g. to retina, choroid, vitreous and optic nerve) is important for treating several disorders such as age-related macular degeneration, diabetic retinopathy, retinal venous occlusions, retinal arterial occlusion, macular edema, postoperative inflammation, infection, dryness, uveitis retinitis, proliferative vitreoretinopathy and glaucoma. Due to anatomic membrane barriers (i.e. cornea, conjunctiva and sclera) and the lacrimal drainage it can be quite challenging to target drugs and achieve therapeutic drug concentrations in the anterior parts of the eye after topical drug administration. Reaching the posterior part of the eye is an even more challenging task because of the anatomical and physiological barriers segregating this part of the eye from the anterior segment. Since those barriers cannot be altered with non-invasive methods, there is a need in the art for improved methods and pharmaceutical compositions that increase ocular bioavailability.

[0004] There is a need in the art for improved noninvasive, safe and patient-friendly drug delivery systems that are specific and effective for targeted delivery to the eye. In general, drugs can enter the eye via three distinctive routes, i.e. a) through conjunctiva/sclera after topical application, b) from the anterior part after topical application, and c) from the systemic circulation after topical application, parenteral, oral, and intranasal or other administration routes that deliver drugs to the blood circulation. Then drugs can be delivered to the eye via invasive methods such as direct drug injection into the vitreous humor or subconjunctival injections. Invasive methods can cause discomfort for the patient and can also lead to complications that are even more serious than the disease being treated. In most cases, topical or systemic administration is used to treat posterior diseases despite limited bioavailability from these formulations. There is also a need for sustained retention of drugs administered by topical administration onto the ocular surface since many diseases including inflammatory or infectious diseases require a greater drug concentration than can be achieved by infrequent topical administration due to issues with rapid clearance.

[0005] In the past few decades, research has focused on drug loaded nanoparticles, such as liposomes, micelles, dendrimers and polymersomes. Relatively few drug carriers have been approved for use in humans, which suggests that better strategies and materials may be required to generate successful nanomedicines. Traditional drug delivery systems have a number of deficiencies including a lack of targeted delivery, high toxicity, low cellular uptake, and poor biocompatibility. Therefore, there is a need in the art for improved drug delivery systems targeted to parts of the eye.

SUMMARY

[0006] Disclosed herein are novel methods and compositions for targeting therapeutics to specific cells. One aspect relates to a therapeutic agent comprising an elastin-like peptide (ELP) component and a ligand selected from the group consisting of mIgA and knob. Previous reports indicated that the fiber knob of adenovirus serotype 5 (Ad5) exhibits a high efficiency of internalization in liver after intravenous injection in mice (J. Virol. 78:6431-6438 (2004)). Both hepatocytes and lacrimal gland acinar cells (LGACs), also very efficiently transduced with Ad5 in a unique fiber-dependent pathway, display a very high level of coxsackie-adenovirus receptor (CAR) expression. Although CAR remains surface-associated in most cells, Applicants' research shows internalization of Ad5 in these cells is through a CAR-mediated and fiber-dependent endocytic pathway (J. Virol. 80:11833-11861 (2006)).

[0007] To develop new treatments for diseases of the lacrimal gland, new drug vehicles are required that are biocompatible, biodegradable and easily modified with bioactive peptides. An emerging approach to this challenge employs genetically engineered polypeptides to drive the assembly of nanostructures. Elastin-like-polypeptides possess unique phase transition behavior, that mediates self-assembly of nanoparticles.

[0008] A second aspect relates to a therapeutic agent comprising an elastin-like peptide (ELP) component and a ligand; wherein the ligand specifically binds to a receptor selected from the group consisting of CAR (GenBank acc.no. AF 200465.1) and pIgR (NCBI Reference Sequence NM_002644.3).

[0009] A further aspects relates to a method for delivering a therapeutic agent comprising an elastin-like peptide (ELP) to a cell, said method comprising: administering an (ELP) component and a ligand component to the cell; wherein the ligand component specifically binds to a receptor selected from the group consisting of CAR and pIgR.

[0010] Still further, there is provided a method for delivering a therapeutic agent comprising an elastin-like peptide (ELP) to a cell, said method comprising: administering an (ELP) component and a ligand component to the cell; wherein the ligand component is selected from the group consisting of mIgA and knob.

[0011] In another aspect, a method for delivering a drug to the luminal area of the lacrimal gland by transcytosis is provided, the method comprising, consisting essentially, or yet further consisting of, contacting the lacrimal gland with one or more of a drug delivery agent, a polynucleotide, or a composition, as described herein, wherein the ligand component specifically binds to a CAR and/or pIgR receptor; and/or wherein the ligand component is mIgA and/or knob. The contacting can be in vitro or in vivo. In one embodiment, the drug is in contact with the ocular surface of the eye. Transcytosis allows the durg to have access to the ocular surface of the eye. The transcytosis property enables treatment of the surface of the eye for a variety of conditions like dry eye, scleritis, and the like.

[0012] In yet another aspect, provided is a method for treating a disease of the lacrimal gland, comprising, or alternatively consisting essentially of, or yet further consisting of, administering to a patient in need of such treatment one or more of a drug delivery agent, a polynucleotide, or a compositions, wherein the ligand component specifically binds to a CAR and/or pIgR receptor; and/or wherein the ligand component is mIgA and/or knob, thereby treating the patient. In one aspect, the disease is cancer.

[0013] In certain embodiments, the cell is any cell that expresses a CAR or pIGR receptor. Non-limiting examples include liver, heart, lacrimal gland, salivary gland, lung, brain, pancreatic acinar tissue, prostate or mucosal cells. In a related embodiment, the cell is the lacrimal acinar cell of the lacrimal gland (LGAC). CAR is detected in liver and lacrimal gland as well as in human umbilical vein endothelial cells and pancreatic acinar tissue (acinar cells and islets), as well as in prostate. Most mucosal epithelial cells display pIgR including the cells lining the gut, pulmonary epithelial cells, acinar cells (salivary, lacrimal gland) and other barrier epithelial tissues responsible for maintaining mucosal immunity. Accordingly, in one embodiment, the drug is released from interstitial to luminal surfaces on a mucosal epithelial cell.

BRIEF DESCRIPTION OF THE FIGURES

[0014] FIG. **1** is a schematic representation of knob-ELP fusion peptides. Full-length knob was expressed at the N-terminus of diblock ELPs. A thrombin cleavage site was engineered between the knob domain and the diblock ELP. The designed diblock knob-ELP can assemble into a nanoparticle, mediated by the first ELP phase transition of the diblock ELP. Above the first transition temperature, knob-ELP will reversibly self-assemble into a nanoparticle.

[0015] FIG. **2** shows denaturing SDS-PAGE for knob-ELPs. The knob-I96, knob-S96 and knob-S48I48 were purified by inverse phase transition cycling (ITC) and resolved by SDS-PAGE stained with Coomassie brilliant blue. The molecular weights of marker proteins lane are 250, 150, 100, 75, 50, 37, 25 and 20 kD, as listed.

[0016] FIG. **3** shows non-denatured-PAGE of knob-S48I48. The knob-S48I48 was mixed with non-denaturing sample buffer (without 2-mercapto-ethanol) and resolved by PAGE. The gel was then stained with Coomassie brilliant blue. The molecular weights of the marker lanes are 250, 150, 100, 75, 50, 37, 25 and 20 kD (from top to bottom), respectively.

[0017] FIG. **4** shows temperature-dependence of the optical density for ELP fusion peptides. Phase transition behavior of knob-S96, S48I48 and knob-S48I48. Each sample was diluted to 25 μM in PBS at 4° C. The OD of samples at 350 nm was measured using a spectrophotometer with increasing temperatures from 15 to 80° C.

[0018] FIG. **5**A-B shows the temperature-dependent assembly and disassembly for ELP fusion peptides. Dynamic light scattering was used to characterize S48I48 and knob-S48I48. (A) S48I48 and knob-S48I48 were diluted at 25 μM in PBS and passed through a 20 nm filter at 4° C. before measurement in a DynaPro plate reader. Readings were taken starting with an increase from 10° C. to 37° C. and then a decrease from 37° C. to 10° C. BSA was only measured from 10° C. to 37° C. (B) Statistical comparison for nanoparticles radius for BSA, S48I48 and knob-S48I48 at 15° C. and 37° C. *** indicates $p<0.01$ as determined using the Tukey post-hoc test.

[0019] FIG. **6** shows proteolytic release of knob from knob-ELP. Left lane is knob-S48I48 before cleavage and right lane is knob-S48I48 after incubation with thrombin overnight at room temperature. The gel was stained by Coomassie brilliant blue. The position of the cleaved knob domain near 20 kD is shown in the right lane.

[0020] FIG. **7** shows murine hepatocytes expresses coxsackie adenovirus receptor (CAR). Hepatocytes, CHO, and Hela cells were lysed with SDS-PAGE sample buffer and CAR expression detected with western blot via primary goat anti mouse CAR and mouse anti-actin antibodies, as well as secondary IRDye®800 donkey anti-goat and IRDye® 700 goat anti-mouse antibodies.

[0021] FIG. **8** demonstrates live cell imaging of cellular uptake for ELP and knob-ELP nanoparticles. Transformed mouse hepatocytes grown on 35 mm glass-bottomed dishes were incubated in medium containing 10 μM rhodamine-conjugated S48I48 or knob-S48I48 (red) with 75 nM LysoTracker green (green) at 37° C. for 30 minutes and imaged using confocal microscopy. Knob-S48I48 exhibited markedly more co-localization with LysoTracker green while S48I48 exhibited more apparent surface association. The arrows indicated the internalized nanoparticles co-localized with lysosome. Scale bar: 10 μm.

[0022] FIG. **9** shows competitive binding and uptake of knob-S48I48 with anti-mouse CAR antibody. Live cell imaging was performed on transformed mouse hepatocytes grown on 35 mm glass-bottomed dishes were pre-incubated with 20 μg/mL anti-mouse CAR antibody at 37° C. for 30 minutes. Rhodamine-conjugated knob-S48I48 (red, 10 μM) with LysoTracker green (green) was added into the medium. After 30 minutes the cells were rinsed with fresh warm medium and imaged using confocal microscopy. Scale bar: 10 μm.

[0023] FIG. **10** shows self-assembly or disassembly of nanoparticles above or below their phase transition temperatures. S48I48 and Knob-S48I48 were passed through a 20 nm microfilter at 4° C. in PBS and characterized by dynamic light scattering spectroscopy (DynaPro plate reader). Readings were taken starting with an increase from 10° C. to 37° C. and then decrease from 37° C. to 10° C. BSA was only measured from 10° C. to 37° C.

[0024] FIG. **11** shows knob-ELP nanoparticles transcytosed in LGACs. Scale bar represents 10 μM.

[0025] FIG. **12** shows a schematic representation of reconstituted LG acinar cluster. L represents acinar lumena. N represents cell nucleus. APM represents apical membrane. BM represents basal-lateral membrane. CJ represents cell junction.

[0026] FIG. **13** shows intracellular uptake of carboxyfluorescein (CF)-conjugated ELPs in lacrimal gland acinar cells. Unlike CF-S48I48, CF-Knob-S48I48 exhibits strong internalization which was shown in green in reconstituted LGACs. Also endocytosed CF-Knob-S48I48 was transcytosed into reconstituted acinar lumen which was stained by expressed Lifeact-RFP proteins (red).

[0027] FIG. **14** shows lumen A (S48I48, left panel) and lumen B (Knob-S48I48, right panel). Arrowheads indicate internalized nanoparticels (Knob-S48I48). The symbol "*" indicates lumen. Box indicates luminal area of LGACs. Scale bar represents 10 μm.

[0028] FIG. **15**A-B is a schematic representation showing knob-S48I48 nanoparticles targeted to CAR in LGACs.

[0029] FIG. **16** shows the in vivo retention of knob-S48I48 in the LG of BALB/c mice.

[0030] FIG. **17** shows the basal-to-apical transport of Cy5-Knob-S48I48 in primary cultures of Lacrimal Gland Acinar Cells (LGACs).

[0031] FIG. **18**A-B shows the spherical morphology of S48I48 protein polymer nanoparticles with and without the Knob domain. FIG. **18**A shows the Cryo-transmission electron microscopy (TEM) imaging of S48I48 and Knob-S48I48 (Scale bar: 100 nm) and FIG. **18**B shows the average particles sizes measured by Image J.

[0032] FIG. **19** shows the overexpression of Myosin Vb tail suppresses accumulation of knob-S48I48 nanopraticles at the acinar lumen. mCherry myosin Vb tail (red), an inhibitor of LGAC transcytosis from basolateral to apical membranes, significantly reduces the transcytosis of knob-S48I48 (purple). Green label associated with expression of EGFP-actin denotes the organization of the actin cytoskeleton while *, lumenal area of LGACs, surrounded by apical plasma membrane.

[0033] FIG. **20**A-B shows the quantitative suppression of transcytosis of knob-S48I48 nanoparticles by myosin Vb overexpression. FIG. **20**A shows the quantification of fluorescence intensity via Image J in the lumen vs. the cytosol for LGACs incubated with or without inhibition of myosin Vb tail and FIG. **20**B shows the ratio of lumen to cytosol.

DETAILED DESCRIPTION

Definitions

[0034] The practice of the present invention will employ, unless otherwise indicated, conventional techniques of tissue culture, immunology, molecular biology, microbiology, cell biology and recombinant DNA, which are within the skill of the art. See, e.g., Sambrook et al., (1989) Molecular Cloning: A Laboratory Manual, 2nd edition; Ausubel et al., eds. (1987) Current Protocols In Molecular Biology; MacPherson, B. D. Hames and G. R. Taylor eds., (1995) PCR 2: A Practical Approach; Harlow and Lane, eds. (1988) Antibodies, A Laboratory Manual; Harlow and Lane, eds. (1999) Using Antibodies, a Laboratory Manual; and R. I. Freshney, ed. (1987) Animal Cell Culture.

[0035] All numerical designations, e.g., pH, temperature, time, concentration, and molecular weight, including ranges, are approximations which are varied (+) or (−) by increments of 1.0 or 0.1, as appropriate. It is to be understood, although not always explicitly stated that all numerical designations are preceded by the term "about". It also is to be understood, although not always explicitly stated, that the reagents described herein are merely exemplary and that equivalents of such are known in the art.

[0036] As used in the specification and claims, the singular form "a," "an" and "the" include plural references unless the context clearly dictates otherwise.

[0037] As used herein, the term "comprising" is intended to mean that the compositions and methods include the recited elements, but do not exclude others. "Consisting essentially of" when used to define compositions and methods, shall mean excluding other elements of any essential significance to the combination when used for the intended purpose. Thus, a composition consisting essentially of the elements as defined herein would not exclude trace contaminants or inert carriers. "Consisting of" shall mean excluding more than trace elements of other ingredients and substantial method steps. Embodiments defined by each of these transition terms are within the scope of this invention.

[0038] A "composition" is also intended to encompass a combination of active agent and another carrier, e.g., compound or composition, inert (for example, a detectable agent or label) or active, such as an adjuvant, diluent, binder, stabilizer, buffers, salts, lipophilic solvents, preservative, adjuvant or the like. Carriers also include pharmaceutical excipients and additives proteins, peptides, amino acids, lipids, and carbohydrates (e.g., sugars, including monosaccharides, di-, tri-, tetra-, and oligosaccharides; derivatized sugars such as alditols, aldonic acids, esterified sugars and the like; and polysaccharides or sugar polymers), which can be present singly or in combination, comprising alone or in combination 1-99.99% by weight or volume. Exemplary protein excipients include serum albumin such as human serum albumin (HSA), recombinant human albumin (rHA), gelatin, casein, and the like. Representative amino acid/antibody components, which can also function in a buffering capacity, include alanine, glycine, arginine, betaine, histidine, glutamic acid, aspartic acid, cysteine, lysine, leucine, isoleucine, valine, methionine, phenylalanine, aspartame, and the like. Carbohydrate excipients are also intended within the scope of this invention, examples of which include but are not limited to monosaccharides such as fructose, maltose, galactose, glucose, D-mannose, sorbose, and the like; disaccharides, such as lactose, sucrose, trehalose, cellobiose, and the like; polysaccharides, such as raffinose, melezitose, maltodextrins, dextrans, starches, and the like; and alditols, such as mannitol, xylitol, maltitol, lactitol, xylitol sorbitol (glucitol) and myoinositol.

[0039] The term "pharmaceutically acceptable carrier" (or medium), which may be used interchangeably with the term biologically compatible carrier or medium, refers to reagents, cells, compounds, materials, compositions, and/or dosage forms that are not only compatible with the cells and other agents to be administered therapeutically, but also are, within the scope of sound medical judgment, suitable for use in contact with the tissues of human beings and animals without excessive toxicity, irritation, allergic response, or other complication commensurate with a reasonable benefit/risk ratio. Pharmaceutically acceptable carriers suitable for use in the present invention include liquids, semi-solid (e.g., gels) and solid materials (e.g., cell scaffolds and matrices, tubes sheets and other such materials as known in the art and described in greater detail herein). These semi-solid and solid materials may be designed to resist degradation within the body (non-biodegradable) or they may be designed to degrade within the body (biodegradable, bioerodable). A biodegradable material may further be bioresorbable or bioabsorbable, i.e., it may be dissolved and absorbed into bodily fluids (water-soluble implants are one example), or degraded and ultimately eliminated from the body, either by conversion into other materials or breakdown and elimination through natural pathways.

[0040] As used herein, the term "patient" or "subject" intends an animal, a mammal or yet further a human patient. For the purpose of illustration only, a mammal includes but is not limited to a human, a feline, a canine, a simian, a murine, a bovine, an equine, a porcine or an ovine.

[0041] The term "purified protein or peptide" as used herein, is intended to refer to a composition, isolatable from other components, wherein the protein or peptide is purified to any degree relative to its naturally-obtainable state. A purified protein or peptide therefore also refers to a protein or peptide, free from the environment in which it may naturally occur.

[0042] The term "therapeutic" refers to an agent or component capable of inducing a biological effect in vivo and/or in vitro. The biological effect may be useful for treating and/or preventing a condition, disorder, or disease in a subject or patient. A therapeutic may include, without limitation, a small molecule, a nucleic acid, or a polypeptide.

[0043] The term "coxsackievirus and adenovirus receptor" or "CAR" refers to a high affinity receptor that is present in many human tissues, including liver, heart, lacrimal gland, salivary gland, lung, and brain, pancreas and prostate.

[0044] The term "Polymeric Immunoglobulin Receptor" or "pIgR" refers to a high affinity receptor that is expressed by human mucosal cells.

[0045] "LGAC" or "lacrimal gland acinar cell" is a specific cell type of the lacrimal gland that expresses CAR and pIgR on the cell surface. These cells are also sometimes referred to lacrimal acinar epithelial cells.

[0046] This disclosure relates to genetically engineered polypeptide nanoparticles targeted to lacrimal gland acinar cells. To develop new treatments for disease of the lacrimal gland, new drug carriers are required that are biocompatible and easily modified with bioactive peptides. An emerging solution to this challenge utilizes genetically engineered polypeptides to drive the assembly of nanostructures. Elastin-like-polypeptide engages in a unique phase transition behavior, which can mediate self-assembly of nanoparticles. Described herein is a class of diblock ELP fusion proteins with high affinity peptides which are intended for targeting of lacrimal gland acinar cells (LGAC). The diblock mIgA-ELP fusion proteins are able to self assemble to nanoparticles, which can be utilized for gene therapy and drug delivery to LGAC and other mucosal epithelial cells.

[0047] As used herein, the term "biological equivalent thereof" is used synonymously with "equivalent" unless otherwise specifically intended. When referring to a reference protein, polypeptide or nucleic acid, intends those having minimal homology while still maintaining desired structure or functionality. Unless specifically recited herein, it is contemplated that any polynucleotide, polypeptide or protein mentioned herein also includes equivalents thereof. For example, an equivalent intends at least about 60%, or 65%, or 70%, or 75%, or 80% homology or identity and alternatively, at least about 85%, or alternatively at least about 90%, or alternatively at least about 95%, or alternatively 98% percent homology or identity and exhibits substantially equivalent biological activity to the reference protein, polypeptide or nucleic acid. Alternatively, a biological equivalent is a peptide encoded by a nucleic acid that hybridizes under stringent conditions to a nucleic acid or complement that encodes the peptide. Hybridization reactions can be performed under conditions of different "stringency". In general, a low stringency hybridization reaction is carried out at about 40° C. in about 10×SSC or a solution of equivalent ionic strength/temperature. A moderate stringency hybridization is typically performed at about 50° C. in about 6×SSC, and a high stringency hybridization reaction is generally performed at about 60° C. in about 1×SSC. Hybridization reactions can also be performed under "physiological conditions" which is well known to one of skill in the art. A non-limiting example of a physiological condition is the temperature, ionic strength, pH and concentration of Mg^{2+} normally found in a cell.

[0048] A polynucleotide or polynucleotide region (or a polypeptide or polypeptide region) having a certain percentage (for example, about 60%, 65%, 70%, 75%, 80%, 85%, 90%, 95% or 97%) of "sequence identity" to another sequence means that, when aligned, that percentage of bases (or amino acids) are the same in comparing the two sequences. The alignment and the percent homology or sequence identity can be determined using software programs known in the art, for example those described in Current Protocols in Molecular Biology (Ausubel et al., eds. 1987) Supplement 30, section 7.7.18, Table 7.7.1. Preferably, default parameters are used for alignment. A preferred alignment program is BLAST, using default parameters. In particular, preferred programs are BLASTN and BLASTP, using the following default parameters: Genetic code=standard; filter=none; strand=both; cutoff=60; expect=10; Matrix=BLOSUM62; Descriptions=50 sequences; sort by =HIGH SCORE; Databases=non-redundant, GenBank+EMBL+DDBJ+PDB+GenBank CDS translations+SwissProtein+SPupdate+PIR. Details of these programs can be found at the following Internet address: ncbi.nlm.nih.gov/cgi-bin/BLAST.

[0049] "Homology" or "identity" or "similarity" refers to sequence similarity between two peptides or between two nucleic acid molecules. Homology can be determined by comparing a position in each sequence which may be aligned for purposes of comparison. When a position in the compared sequence is occupied by the same base or amino acid, then the molecules are homologous at that position. A degree of homology between sequences is a function of the number of matching or homologous positions shared by the sequences. An "unrelated" or "non-homologous" sequence shares less than 40% identity, or alternatively less than 25% identity, with one of the sequences of the present invention.

[0050] An "equivalent" of a polynucleotide or polypeptide refers to a polynucleotide or a polypeptide having a substantial homology or identity to the reference polynucleotide or polypeptide. In one aspect, a "substantial homology" is greater than about 60%, 65%, 70%, 75%, 80%, 85%, 90%, 95% or 98% homology.

[0051] As used herein, "expression" refers to the process by which polynucleotides are transcribed into mRNA and/or the process by which the transcribed mRNA is subsequently being translated into peptides, polypeptides, or proteins. If the polynucleotide is derived from genomic DNA, expression may include splicing of the mRNA in an eukaryotic cell.

[0052] The term "encode" as it is applied to polynucleotides refers to a polynucleotide which is said to "encode" a polypeptide if, in its native state or when manipulated by methods well known to those skilled in the art, it can be transcribed and/or translated to produce the mRNA for the polypeptide and/or a fragment thereof. The antisense strand is the complement of such a nucleic acid, and the encoding sequence can be deduced therefrom.

[0053] "Regulatory polynucleotide sequences" intends any one or more of promoters, operons, enhancers, as know to those skilled in the art to facilitate and enhance expression of polynucleotides.

[0054] An "expression vehicle" is a vehicle or a vector, non-limiting examples of which include viral vectors or plasmids, that assist with or facilitate expression of a gene or polynucleotide that has been inserted into the vehicle or vector.

[0055] A "delivery vehicle" is a vehicle or a vector that assists with the delivery of an exogenous polynucleotide into

a target cell. The delivery vehicle may assist with expression or it may not, such as traditional calcium phosphate transfection compositions.

[0056] A "composition" is intended to mean a combination of active agent and another compound or composition, inert (for example, a solids support or pharmaceutically acceptable carrier) or active, such as an adjuvant.

[0057] A "pharmaceutical composition" is intended to include the combination of an active agent with a carrier, inert or active, making the composition suitable for diagnostic or therapeutic use in vitro, in vivo or ex vivo.

[0058] "An effective amount" refers to the amount of an active agent or a pharmaceutical composition sufficient to induce a desired biological and/or therapeutic result. That result can be alleviation of the signs, symptoms, or causes of a disease, or any other desired alteration of a biological system. The effective amount will vary depending upon the health condition or disease stage of the subject being treated, timing of administration, the manner of administration and the like, all of which can be determined readily by one of ordinary skill in the art.

[0059] As used herein, the terms "treating," "treatment" and the like are used herein to mean obtaining a desired pharmacologic and/or physiologic effect. The effect may be prophylactic in terms of completely or partially preventing a disorder or sign or symptom thereof, and/or may be therapeutic in terms of a partial or complete cure for a disorder and/or adverse effect attributable to the disorder.

[0060] As used herein, to "treat" further includes systemic amelioration of the symptoms associated with the pathology and/or a delay in onset of symptoms. Clinical and sub-clinical evidence of "treatment" will vary with the pathology, the subject and the treatment.

[0061] "Administration" can be effected in one dose, continuously or intermittently throughout the course of treatment. Methods of determining the most effective means and dosage of administration are known to those of skill in the art and will vary with the composition used for therapy, the purpose of the therapy, the target cell being treated, and the subject being treated. Single or multiple administrations can be carried out with the dose level and pattern being selected by the treating physician. Suitable dosage formulations and methods of administering the agents are known in the art. Route of administration can also be determined and method of determining the most effective route of administration are known to those of skill in the art and will vary with the composition used for treatment, the purpose of the treatment, the health condition or disease stage of the subject being treated, and target cell or tissue. Non-limiting examples of route of administration include oral administration, nasal administration, injection, topical application, intrapentoneal, intravenous and by inhalation. An agent of the present invention can be administered for therapy by any suitable route of administration. It will also be appreciated that the preferred route will vary with the condition and age of the recipient, and the disease being treated.

[0062] The agents and compositions of the present invention can be used in the manufacture of medicaments and for the treatment of humans and other animals by administration in accordance with conventional procedures, such as an active ingredient in pharmaceutical compositions.

[0063] As used herein, the term "detectable label" intends a directly or indirectly detectable compound or composition that is conjugated directly or indirectly to the composition to be detected, e.g., N-terminal histadine tags (N-His), magnetically active isotopes, e.g., ^{115}Sn, ^{117}Sn and ^{119}Sn, a non-radioactive isotopes such as ^{13}C and ^{15}N, polynucleotide or protein such as an antibody so as to generate a "labeled" composition. The term also includes sequences conjugated to the polynucleotide that will provide a signal upon expression of the inserted sequences, such as green fluorescent protein (GFP) and the like. The label may be detectable by itself (e.g. radioisotope labels or fluorescent labels) or, in the case of an enzymatic label, may catalyze chemical alteration of a substrate compound or composition which is detectable. The labels can be suitable for small scale detection or more suitable for high-throughput screening. As such, suitable labels include, but are not limited to magnetically active isotopes, non-radioactive isotopes, radioisotopes, fluorochromes, luminescent compounds, dyes, and proteins, including enzymes. The label may be simply detected or it may be quantified. A response that is simply detected generally comprises a response whose existence merely is confirmed, whereas a response that is quantified generally comprises a response having a quantifiable (e.g., numerically reportable) value such as an intensity, polarization, and/or other property. In luminescence or fluorescence assays, the detectable response may be generated directly using a luminophore or fluorophore associated with an assay component actually involved in binding, or indirectly using a luminophore or fluorophore associated with another (e.g., reporter or indicator) component.

[0064] Examples of luminescent labels that produce signals include, but are not limited to bioluminescence and chemiluminescence. Detectable luminescence response generally comprises a change in, or an occurrence of, a luminescence signal. Suitable methods and luminophores for luminescently labeling assay components are known in the art and described for example in Haugland, Richard P. (1996) Handbook of Fluorescent Probes and Research Chemicals (6^{th} ed.). Examples of luminescent probes include, but are not limited to, aequorin and luciferases.

[0065] Examples of suitable fluorescent labels include, but are not limited to, fluorescein, rhodamine, tetramethylrhodamine, eosin, erythrosin, coumarin, methyl-coumarins, pyrene, Malacite green, stilbene, Lucifer Yellow, Cascade Blue™, and Texas Red. Other suitable optical dyes are described in the Haugland, Richard P. (1996) Handbook of Fluorescent Probes and Research Chemicals (6^{th} ed.).

[0066] In another aspect, the fluorescent label is functionalized to facilitate covalent attachment to a cellular component present in or on the surface of the cell or tissue such as a cell surface marker. Suitable functional groups, including, but not are limited to, isothiocyanate groups, amino groups, haloacetyl groups, maleimides, succinimidyl esters, and sulfonyl halides, all of which may be used to attach the fluorescent label to a second molecule. The choice of the functional group of the fluorescent label will depend on the site of attachment to either a linker, the agent, the marker, or the second labeling agent.

Elastin-Like Polypeptides (ELPs)

[0067] Elastin-like-polypeptides (ELPs) are a genetically engineered polypeptide with unique phase behavior (see for e.g. S. R. MacEwan, et al., Biopolymers 94(1) (2010) 60-77) which promotes recombinant expression, protein purification and self-assembly of nanostructures (see for e.g. A. Chilkoti, et al., Advanced Drug Delivery Reviews 54 (2002) 1093-

1111). ELPs are artificial polypeptides composed of repeated pentapeptide sequences, $(VPGXG)_n$ (SEQ ID. NO: 1) derived from human tropoelastin, where X is the "guest residue" Which is any amino acid. In one embodiment, X is any amino acid except proline. This peptide motif displays rapid and reversible de-mixing from aqueous solutions above a transition temperature, T_t. Below T_t, ELPs adopt a highly water soluble random coil conformation; however, above T_t, they separate from solution, coalescing into a second aqueous phase. The T_t of ELPs can be tuned by choosing the guest residue and ELP chain length as well as fusion peptides at the design level (see for e.g. MacEwan S R, et al., Biopolymers 94(1): 60-77). The ELP phase is both biocompatible and highly specific for ELPs or ELP fusion proteins, even in complex biological mixtures. Genetically engineered ELPs are monodisperse, biodegradable, non-toxic. Throughout this description, ELPs are identified by the single letter amino acid code of the guest residue followed by the number of repeat units, n. For example, S48I48 represents a diblock copolymer ELP with 48 serine (S) pentamers ($[VPGSG]_{48}$, SEQ ID. NO: 2) at the amino terminus and 48 isoleucine (I) pentamers ($[VPGIG]_{48}$, SEQ ID. NO: 3) at the carboxy terminus. A "diblock" as used herein refers to an ELP with two blocks of repeated polypeptide sequence. For example, the diblock $(VPGSG)_{48}$ $(VPGIG)_{48}$ (SEQ ID. NO: 12) comprises 48 repeated units of a polypeptide having the sequence VPGSG (SEQ ID NO: 2) and 48 repeated units of a polypeptide having the sequence VPGIG (SEQ ID. NO: 3). In one embodiment, the drug delivery agent comprises a polypeptide with the sequence of SEQ ID. NO: 12.

[0068] In further embodiments, the drug delivery agent comprises, a consisting essentially of, or yet consists of, a polypeptide with the sequence $(VPGSG)_{96}$ (SEQ ID. NO: 13) or $(VPGIG)_{96}$ (SEQ ID. NO: 14) or a biological equivalent thereof.

[0069] Described herein are ELP fusion proteins, which can be self assembled into nanoparticles. The diameter of the nanoparticle can be from about 1 to about 1000 nm or from about 1 to about 500 nm, or from about 1 to about 100 nm, or from about 1 to about 50 nm, or from about 20 to about 50 nm, or from about 30 to about 50 nm, or from about 35 to about 45 nm. In one embodiment, the diameter is about 40 nm. These nanoparticles can be high efficiently internalized into LGAC. The fusion proteins are composed of elastin-like-polypeptides and high affinity polypeptides. These fusion proteins can be expressed from a variety of expression systems known to those skilled in the art and easily purified by the phase transition behavior of ELPs. These ELP fusion proteins are able to conjugate small molecules, such as, for example, chemotherapeutic agents, anti-inflammation agents, antibiotics and polypeptides and other water soluble drugs. In addition, the ELP nanoparticles are useful for carrying DNA, RNA, protein and peptide-based therapeutics.

[0070] ELPs have potential advantages over chemically synthesized polymers as drug delivery agents. First, because they are biosynthesized from a genetically encoded template, ELPs can be made with precise molecular weight. Chemical synthesis of long linear polymers does not typically produce an exact length, but instead a range of lengths. Consequently, fractions containing both small and large polymers yield mixed pharmacokinetics and biodistribution. Second, ELP biosynthesis produces very complex amino acid sequences with nearly perfect reproducibility. This enables very precise selection of the location of drug attachment. Thus drug can be selectively placed on the corona, buried in the core, or dispersed equally throughout the polymer. Third, ELP can self assemble into multivalent nanoparticles that can have excellent site-specific accumulation and drug carrying properties. Fourth, because ELP are designed from native amino acid sequences found extensively in the human body they are biodegradable, biocompatible, and tolerated by the immune system. Fifth, ELPs undergo an inverse phase transition temperature, T_t, above which they phase separate into large aggregates. By localized heating, additional ELP can be drawn into the target site, which may be beneficial for increasing drug concentrations.

[0071] A therapeutic such as a drug, for example, may be attached to the ELP through cysteine, lysine, glutamic acid or aspartic acid residues present in the polymer. In some embodiments, the cysteine, lysine, glutamic acid or aspartic acid residues are generally present throughout the length of the polymer. In some embodiments, the cysteine, lysine, glutamic acid or aspartic acid residues are clustered at the end of the polymer. In some embodiments of the presently described subject matter, therapeutics are attached to the cysteine residues of the ELP using thiol reactive linkers. In some embodiments of the presently described subject matter, therapeutics are attached to the lysine residues of the high molecular weight polymer sequence using NHS (N-hydroxysuccinimide) chemistry to modify the primary amine group present on these residues. In some embodiments of the presently described subject matter, therapeutics are attached to the glutamic acid or aspartic acid residues of the ELP using EDC (1-Ethyl-3-[3-dimethylaminopropyl]carbodiimide Hydrochloride) chemistry to modify the carboxylic acid group present on the ELP residues.

[0072] The therapeutic associated with the ELP may be hydrophobic or hydrophilic. Which the drug is hydrophobic, attachment to the terminus of the ELP may facilitate formation of the multivalent nanoparticle. The number of drug particles attached to the ELP can be from about 1 to about 30, or from about 1 to about 10, or about 1, 2, 3, 4, 5, 6, 7, 8, 9, or 10. In some embodiments, the attachment points for a therapeutic are equally distributed along the backbone of the ELP, and the resulting drug-ELP is prevented from forming nanoparticle structures under physiological salt and temperature conditions.

[0073] In addition to therapeutics, the ELPs may also be associated with a detectable label that allows for the visual detection of in vivo uptake of the ELPs. Suitable labels include, for example, fluorescein, rhodamine, tetramethylrhodamine, eosin, erythrosin, coumarin, methyl-coumarins, pyrene, Malacite green, Alexa-Fluor®, stilbene, Lucifer Yellow, Cascade Blue™, and Texas Red. Other suitable optical dyes are described in Haugland, Richard P. (1996) Molecular Probes Handbook.

[0074] In certain embodiments, the ELP components include polymeric or oligomeric repeats of the pentapeptide VPGXG (SEQ ID. NO: 1), where the guest residue X is any amino acid, that in one aspect, excludes proline. X may be a naturally occurring or non-naturally occurring amino acid. In some embodiments, X is selected from alanine, arginine, asparagine, aspartic acid, cysteine, glutamic acid, glutamine, glycine, histidine, isoleucine, leucine, lysine, methionine, phenylalanine, serine, threonine, tryptophan, tyrosine and valine. In some embodiments, X is a natural amino acid other than proline or cysteine.

[0075] The guest residue X may be a non-classical (non-genetically encoded) amino acid. Examples of non-classical amino acids include: D-isomers of the common amino acids, 2,4-diaminobutyric acid, α-amino isobutyric acid, A-aminobutyric acid, Abu, 2-amino butyric acid, γ-Abu, ϵ-Ahx, 6-amino hexanoic acid, Aib, 2-amino isobutyric acid, 3-amino propionic acid, ornithine, norleucine, norvaline, hydroxyproline, sarcosine, citrulline, homocitrulline, cysteic acid, t-butylglycine, t-butylalanine, phenylglycine, cyclohexylalanine, β-alanine, fluoro-amino acids, designer amino acids such as β-methyl amino acids, C α-methyl amino acids, N α-methyl amino acids, and amino acid analogs in general.

[0076] Selection of X is independent in each ELP structural unit (e.g., for each structural unit defined herein having a guest residue X). For example, X may be independently selected for each structural unit as an amino acid having a positively charged side chain, an amino acid having a negatively charged side chain, or an amino acid having a neutral side chain, including in some embodiments, a hydrophobic side chain.

[0077] In each embodiment, the structural units, or in some cases polymeric or oligomeric repeats, of the ELP sequences may be separated by one or more amino acid residues that do not eliminate the overall effect of the molecule, that is, in imparting certain improvements to the therapeutic component as described. In certain embodiments, such one or more amino acids also do not eliminate or substantially affect the phase transition properties of the ELP component (relative to the deletion of such one or more amino acids).

[0078] The ELP component in some embodiments is selected or designed to provide a T_t ranging from about 10 to about 80° C., such as from about 35 to about 60° C., or from about 38 to about 45° C. In some embodiments, the T_t is greater than about 40° C. or greater than about 42° C., or greater than about 45° C., or greater than about 50° C. The transition temperature, in some embodiments, is above the body temperature of the subject or patient (e.g., >37° C.) thereby remaining soluble in vivo, or in other embodiments, the T_t is below the body temperature (e.g., <37° C.) to provide alternative advantages, such as in vivo formation of a drug depot for sustained release of the therapeutic agent.

[0079] The T_t of the ELP component can be modified by varying ELP chain length, as the Tt generally increases with decreasing MW. For polypeptides having a molecular weight >100,000, the hydrophobicity scale developed by Urry et al. (PCT/US96/05186, which is hereby incorporated by reference in its entirety) is preferred for predicting the approximate T_t of a specific ELP sequence. However, in some embodiments, ELP component length can be kept relatively small, while maintaining a target T_t, by incorporating a larger fraction of hydrophobic guest residues (e.g., amino acid residues having hydrophobic side chains) in the ELP sequence. For polypeptides having a molecular weight <100,000, the T_t may be predicted or determined by the following quadratic function: $T_t=M_0+M_1X+M_2X^2$ where X is the MW of the fusion protein, and $M_0=116.21$; $M_1=-1.7499$; $M_2=0.010349$.

[0080] While the T_t of the ELP component, and therefore of the ELP component coupled to a therapeutic component, is affected by the identity and hydrophobicity of the guest residue, X, additional properties of the molecule may also be affected. Such properties include, but are not limited to solubility, bioavailability, persistence, and half-life of the molecule.

Ligands

[0081] In certain embodiments of the invention, the therapeutic agent comprises an ELP component fused or conjugated to a LGAC-targeted ligand. A LGAC-targeted ligand is a peptide, polypeptide, or molecule that targets the ELP to the LGAC. In one embodiment, the ligand component of the drug delivery agent described herein is the adenovirus knob domain, which is a LGAC-targeted ligand. This domain is represented by the protein sequence: GAITVGNKNND-KLTLWTTPAPSPNCRLNAEKDAKLTLV-LTKCGSQILATVSVLAVKGSL APISGTVQSAHLIIR-FDENGVLLNNSFLDPEYWNFRNGDLTEGTAYTNAV GFMPNLSAY PKSHGKTAKSNIVSQVYLNGDKTK-PVTLTITLNGTQETGDTTPSAYSMSFSWDWSGHN YINEIFATSSYTFSYIAQE (SEQ ID. NO: 4), or a biological equivalent thereof. The term "biological equivalent" is defined above. In one aspect, a biological equivalent is a peptide encoded by a nucleic acid that hybrizes to a nucleic acid that encodes the LGAC-targeted ligand 2 or its complement under conditions of a high stringency hybridization reaction, that is performed at about 60° C. in about 1×SSC that has substantial identical biological activity to the above-noted sequence. In one embodiment, the knob ligand comprises a polypeptide having the sequence of SEQ ID. NO: 4 or a biological equivalent thereof.

[0082] In certain embodiments, the ELP comprises knob or a polypeptide with at least 80% identity to knob. Alternatively, the polypeptide has about at least 85% or about at least 90% or about at least 95%, or about at least 99% identity to knob.

[0083] In further embodiments, the ELP comprises a mIgA ligand or double mIgA ligand. This ligand is represented by the amino acid sequence: TWASRQEPSQGTTTFAVTS (SEQ ID. NO: 5) or a biological equivalent thereof. In one embodiment, the mIgA ligand comprises a polypeptide having the sequence of SEQ ID. NO: 5 or a biological equivalent thereof. The term "biological equivalent" is defined above. In one aspect, a biological equivalent is a peptide encoded by a nucleic acid that hybrizes to a nucleic acid that encodes the mIgA ligand or double mIgA ligand or its complement under conditions of a high stringency hybridization reaction, that is performed at about 60° C. in about 1×SSC that has substantial identical biological activity to the above-noted sequence. In certain embodiments, the ELP comprises the mIgA ligand or a polypeptide with at least 80% identity to mIgA. Alternatively, the polypeptide has about at least 85% or about at least 90% or about at least 95%, or about at least 99% identity to mIgA. The term "mIgA" refers to the pIgR-binding site in the Cα3 domain of dimeric human IgA. The Cα3 domain is represented by the protein sequence: RP EVHLLPPPSE ELALNELVTL TCLARGFSPK DVLVRWLQGS QEL-PREKYLT WASRQEPSQG TTTFAVTSIL RVAAED-WKKG DTFSCMVGHE ALPLAFTQKT ID (SEQ ID. NO: 6) (See for e.g. Frank W. Putnam, et al. J. Biol. Chem. 254, 2865-2874).

Expression of Recombinant Proteins

[0084] ELPs and other recombinant proteins described herein can be prepared by expressing polynucleotides encoding the polypeptide sequences of this invention in an appropriate host cell, i.e., a prokaryotic or eukaryotic host cell This can be accomplished by methods of recombinant DNA technology known to those skilled in the art. It is know to those

skilled in the art that modifications can be made to any peptide to provide it with altered properties. Polypeptides of the invention can be modified to include unnatural amino acids. Thus, the peptides may comprise D-amino acids, a combination of D- and L-amino acids, and various "designer" amino acids (e.g., β-methyl amino acids, C-α-methyl amino acids, and N-α-methyl amino acids, etc.) to convey special properties to peptides. Additionally, by assigning specific amino acids at specific coupling steps, peptides with α-helices, β turns, β sheets, α-turns, and cyclic peptides can be generated. Generally, it is believed that beta-turn spiral secondary structure or random secondary structure is preferred.

[0085] The ELPs can be expressed and purified from a suitable host cell system. Suitable host cells include prokaryotic and eukaryotic cells, which include, but are not limited to bacterial cells, yeast cells, insect cells, animal cells, mammalian cells, murine cells, rat cells, sheep cells, simian cells and human cells. Examples of bacterial cells include *Escherichia coli, Salmonella enterica* and *Streptococcus gordonii*. In one embodiment, the host cell is *E. coli*. The cells can be purchased from a commercial vendor such as the American Type Culture Collection (ATCC, Rockville Md., USA) or cultured from an isolate using methods known in the art. Examples of suitable eukaryotic cells include, but are not limited to 293T HEK cells, as well as the hamster cell line BHK-21; the murine cell lines designated NIH3T3, NS0, C127, the simian cell lines COS, Vero; and the human cell lines HeLa, PER.C6 (commercially available from Crucell) U-937 and Hep G2. A non-limiting example of insect cells include *Spodoptera frugiperda*. Examples of yeast useful for expression include, but are not limited to *Saccharomyces, Schizosaccharomyces, Hansenula, Candida, Torulopsis, Yarrowia*, or *Pichia*. See e.g., U.S. Pat. Nos. 4,812,405; 4,818,700; 4,929,555; 5,736,383; 5,955,349; 5,888,768 and 6,258,559.

Protein Purification

[0086] The phase transition behavior of the ELPs allows for easy purification. The ELPs may also be purified from host cells using methods known to those skilled in the art. These techniques involve, at one level, the crude fractionation of the cellular milieu to polypeptide and non-polypeptide fractions. Having separated the polypeptide from other proteins, the polypeptide of interest may be further purified using chromatographic and electrophoretic techniques to achieve partial or complete purification (or purification to homogeneity). Analytical methods particularly suited to the preparation of a pure peptide or polypeptide are filtration, ion-exchange chromatography, exclusion chromatography, polyacrylamide gel electrophoresis, affinity chromatography, or isoelectric focusing. A particularly efficient method of purifying peptides is fast protein liquid chromatography or even HPLC. In the case of ELP compositions protein purification may also be aided by the thermal transition properties of the ELP domain as described in U.S. Pat. No. 6,852,834.

[0087] Generally, "purified" will refer to a protein or peptide composition that has been subjected to fractionation to remove various other components, and which composition substantially retains its expressed biological activity. Where the term "substantially purified" is used, this designation will refer to a composition in which the protein or peptide forms the major component of the composition, such as constituting about 50%, about 60%, about 70%, about 80%, about 90%, about 95% or more of the proteins in the composition.

[0088] Various methods for quantifying the degree of purification of the protein or peptide will be known to those of skill in the art in light of the present disclosure. These include, for example, determining the specific activity of an active fraction, or assessing the amount of polypeptides within a fraction by SDS/PAGE analysis. A preferred method for assessing the purity of a fraction is to calculate the specific activity of the fraction, to compare it to the specific activity of the initial extract, and to thus calculate the degree of purity, herein assessed by a "-fold purification number." The actual units used to represent the amount of activity will, of course, be dependent upon the particular assay technique chosen to follow the purification and whether or not the expressed protein or peptide exhibits a detectable activity.

[0089] Various techniques suitable for use in protein purification will be well known to those of skill in the art. These include, for example, precipitation with ammonium sulfate, PEG, antibodies and the like or by heat denaturation, followed by centrifugation; chromatography steps such as ion exchange, gel filtration, reverse phase, hydroxylapatite and affinity chromatography; isoelectric focusing; gel electrophoresis; and combinations of such and other techniques. As is generally known in the art, it is believed that the order of conducting the various purification steps may be changed, or that certain steps may be omitted, and still result in a suitable method for the preparation of a substantially purified protein or peptide.

Pharmaceutical Compositions

[0090] Pharmaceutical compositions are further provided. The compositions comprise a carrier and ELPs as described herein. The carriers can be one or more of a solid support or a pharmaceutically acceptable carrier. In one aspect, the compositions are formulated with one or more pharmaceutically acceptable excipients, diluents, carriers and/or adjuvants. In addition, embodiments of the compositions include ELPs, formulated with one or more pharmaceutically acceptable auxiliary substances.

[0091] The invention provides pharmaceutical formulations in which the one or more of an isolated polypeptide of the invention, an isolated polynucleotide of the invention, a vector of the invention, an isolated host cell of the invention, or an antibody of the invention can be formulated into preparations for injection in accordance with the invention by dissolving, suspending or emulsifying them in an aqueous or nonaqueous solvent, such as vegetable or other similar oils, synthetic aliphatic acid glycerides, esters of higher aliphatic acids or propylene glycol; and if desired, with conventional additives such as solubilizers, isotonic agents, suspending agents, emulsifying agents, stabilizers and preservatives or other antimicrobial agents. A non-limiting example of such is a antimicrobial agent such as other vaccine components such as surface antigens, e.g. a Type IV Pilin protein (see Jurcisek and Bakaletz (2007) J. of Bacteriology 189(10):3868-3875) and antibacterial agents.

[0092] Aerosol formulations provided by the invention can be administered via inhalation. For example, embodiments of the pharmaceutical formulations of the invention comprise a compound of the invention formulated into pressurized acceptable propellants such as dichlorodifluoromethane, propane, nitrogen and the like.

[0093] Embodiments of the pharmaceutical formulations of the invention include those in which the ELP is formulated in an injectable composition. Injectable pharmaceutical for-

mulations of the invention are prepared as liquid solutions or suspensions; or as solid forms suitable for solution in, or suspension in, liquid vehicles prior to injection. The preparation may also be emulsified or the active ingredient encapsulated in liposome vehicles in accordance with other embodiments of the pharmaceutical formulations of the invention.

[0094] Suitable excipient vehicles are, for example, water, saline, dextrose, glycerol, ethanol, or the like, and combinations thereof. In addition, if desired, the vehicle may contain minor amounts of auxiliary substances such as wetting or emulsifying agents or pH buffering agents. Methods of preparing such dosage forms are known, or will be apparent upon consideration of this disclosure, to those skilled in the art. See, e.g., Remington's Pharmaceutical Sciences, Mack Publishing Company, Easton, Pa., 17th edition, 1985. The composition or formulation to be administered will, in any event, contain a quantity of the compound adequate to achieve the desired state in the subject being treated.

[0095] Routes of administration applicable to the methods and compositions described herein include intranasal, intramuscular, subcutaneous, intradermal, topical application, intravenous, nasal, oral, inhalation, intralacrimal, retrolacrimal profusal along the duct, intralacrimal, and other enteral and parenteral routes of administration. Routes of administration may be combined, if desired, or adjusted depending upon the agent and/or the desired effect. An active agent can be administered in a single dose or in multiple doses. Embodiments of these methods and routes suitable for delivery, include systemic or localized routes. In one embodiment, the composition comprising the ELP is administered intralacrimally through injection. In further embodiments, the composition is administered systemically, topically on top of the eye, by retrolacrimal profusion, or intranasally.

Treatment of Disease

[0096] Methods and compositions disclosed herein are useful in treating disorders of the eye. The lacrimal gland acinar cell targeted ELPs provide a site-specific target therapeutic. Accordingly, these ELP nanoparticles may be useful to encapsulate or attach drugs for treating disorders localized to the eye. By way of example, these disorders can include, age-related macular degeneration, Sjögren's syndrome, autoimmune exocrinopathy, diabetic retinopathy, graft versus host disease (exocrinopathy associated with) retinal venous occlusions, retinal arterial occlusion, macular edema, postoperative inflammation, uveitis retinitis, proliferative vitreoretinopathy and glaucoma. In one embodiment, the disease is Sjögren's syndrome. In another embodiment, the disease is keratoconjunctivitis sicca (dry eye). In another embodiment the disease is scleritis. In another embodiment the disease is glaucoma.

Combination Treatments

[0097] Administration of the therapeutic agent or substance of the present invention to a patient will follow general protocols for the administration of that particular secondary therapy, taking into account the toxicity, if any, of the treatment. It is expected that the treatment cycles would be repeated as necessary. It also is contemplated that various standard therapies, as well as surgical intervention, may be applied in combination with the described therapy.

Example 1

ELPs Comprising Targeting Ligands

[0098] Since discovered a half century ago, human adenovirus has attracted attention because different types cause significant levels of respiratory, ocular, and gastrointestinal disease. Because of its pathological effects, a significant amount of information is therefore available on its mode of interaction with cells. Adenovirus serotype 2 and serotype 5 within subgroup C, the best understood types of this virus, attach to cells through the initial binding of the fiber protein to the cell-surface coxsackievirus and adenovirus receptor (CAR). CAR is a 46-kDa high affinity receptor that is present in many human tissues, including liver, heart, lacrimal gland, lung, and brain and which is thought to function as a cell adhesion protein. Upon surface binding, adenovirus entry in most cells is facilitated through interaction of an additional adenoviral capsid protein, the penton base, with integrin receptors on the plasma membrane, a process facilitating efficient entry via endocytosis. This mechanism, which occurs in cells expressing the most abundant CAR protein in the body, has been reported to deliver a region of the fiber capsid protein, the knob, to a subcellular degradative compartment. After entry, through either fiber/knob- or penton-dependent interactions, mechanisms have been described for the subsequent interactions between the virus and other intracellular transport machinery, which facilitate efficient trafficking of the viral DNA to the nucleus. For these and other reasons, most notably the ability of adenovirus to transduce non-dividing cells, adenovirus serotype 5 and other serotypes have been explored as vectors for gene therapy. However, despite their relatively efficient cellular endocytosis and gene transfer, viral vectors in general have intrinsic drawbacks, such as limited opportunities for repeat administrations due to acute inflammatory responses and delayed humoral or cellular immune responses. In addition, some viral vectors integrate DNA into the genome, resulting in insertional mutagenesis.

[0099] In the past few decades, numerous research groups have focused on drug carriers, such as liposomes, micelles, dendrimers, and polymersomes. Relatively few drug carriers have been approved for use in humans, which suggests that better strategies and materials may be required to generate successful nanomedicines. One emerging strategy is to design genetically engineered protein polymers that self-assemble directly into nanoparticles. For example, the elastin-like-polypeptides (ELP) are a genetically engineered polypeptide with unique phase behavior, which promotes recombinant expression, protein purification and self-assembly of nanostructures. Genetically engineered ELPs are biodegradable and biocompatible. ELPs are composed of the repeated amino acid sequence $(VPGXG)_n$ (SEQ ID. NO: 1), where the hydrophobicity of X determines the polypeptide phase behavior. Exemplified herein, ELPs are identified by the single letter amino acid code of the guest residue followed by the number of repeat units, n. For example, S48I48 represents a diblock copolymer ELP with 48 serine (S) pentamers at the amino terminus and 48 isoleucine (I) pentamers at the carboxy terminus.

[0100] Lacrimal acinar epithelial cells exhibit a unique fiber-dependent internalization mechanism for adenovirus type 5, and this internalization mechanism can be recapitulated by the knob domain of the fiber protein. This mechanism seems to operate in hepatocytes as well to enable internaliza-

tion of free knob protein to intracellular degradative compartments. This is in contrast to other demonstrations that fiber is responsible only for the initial binding of adenovirus to the cell via CAR, and not for internalization, which is driven by the penton base capsid protein and integrin receptors on the plasma membrane, a process facilitating efficient entry. Some studies have recently shown that CAR, which is a cell adhesion protein and thought to be largely surface associated, can in fact be endocytosed. Altogether these studies suggest that in certain cells, such as acinar cells and hepatocytes where CAR is highly abundant, that a subpopulation may serve as an internalization receptor when bound to fiber or knob proteins. The physiological relevance of this endocytotic population of CAR in these cells is so far unknown. To exploit this apparent CAR internalization pathway and high affinity interaction with viral proteins for drug delivery while minimizing the use of the entire viral capsid, described herein is the development of a simple gene product that assembles nanoparticles decorated with the knob domain of adenovirus fiber protein. The most significant advantages of this platform include: (i) compatibility with genetic engineering; (ii) no bioconjugate chemistry is required to link fusion proteins to the nanoparticle; (iii) and the resulting polypeptides assemble into nanoparticles that are monodisperse, multivalent, and biodegradable. These particles are predominantly composed of diblock copolymers of ELP. ELP block copolymers self-assemble multimeric nanoparticles above a transition temperature that can be controlled by adjusting their hydrophobicity and molecular weight (FIG. **1**). Above the critical temperature for the ELP diblock copolymer, the knob-ELP fusion protein also assembles nanoparticles. It was investigated whether nanocarriers displaying the knob domain may exhibit selective internalization into tissues expressing unique CAR-dependent endoyctosis of fiber and knob. Described herein are the biophysical properties and cellular uptake of a knob-ELP, which self assembles nanoparticles that have potential applications for drug delivery and gene therapy.

Materials and Reagents

[0101] TB dry powder growth medium was purchased from MO BIO Laboratories, Inc. (Carlsbad, Calif.). NHS-Rhodamine was purchased from Thermo Fisher Scientific (Rockford, Ill.). Thrombin CleanCleave™ Kit, Polyethylenimine, Copper Chloride and insulin were obtained from Sigma-Aldrich (St. Louis, Mo.). The knob domain gene sequence was ordered from Integrated DNA Technologies (Coralville, Iowa). LysoTracker Green CN 26 was purchased from Invitrogen (Carlsbad, Calif.). Goat anti-mouse CAR antibody was obtained from R&D Systems (Minneapolis, Minn.). IRDye®800-conjugated donkey anti-goat second antibody was purchased from Rockland (Gilbertsville, Pa.). Blocking buffer was purchased from Li-COR Biosciences (Lincoln, Nebr.). The QIAprep Spin Miniprep Kit and QIAquick Gel Extraction Kit were purchased from Qiagen (Valencia, Calif.).

Knob-ELP Vector Design

[0102] The plasmids encoding ELP were designed similarly to those reported previously (see, for e.g., A. Chilkoti, et al., Advanced Drug Delivery Reviews 54 (2002) 1093-1111 and J. R. McDaniel, et al., Biomacromolecules 11(4) (2010) 944-952 which is incorporated by reference). The knob domain gene sequence was designed with restriction enzyme NdeI and BamHI at 5' and 3' of the knob gene respectively. A thrombin amino acid recognition site (GLVPRGS; SEQ ID. NO: 7) was incorporated between the knob sequence and the ELP sequence. A recognition site for BseRI was also incorporated to facilitate the insertion of ELP genes with complementary two base pair 5' overhang(s). The plasmids containing genes that encode for ELP and knob were double digested by BseRI and BssHII, and the DNA pieces containing ELP and knob were purified using a gel extraction kit and then ligated together. Successful clones were confirmed by diagnostic DNA digestion, DNA sequencing, and mass spectrometry of the polypeptide gene products.

Purification of ELP Fusion Proteins

[0103] *E. coli* strain BLR (Novagen Inc., Milwaukee, Wis.) was transformed with the modified pET-25(+) expression vectors containing the ELP or knob-ELP genes. The bacteria were grown overnight in 5 mL TB dry medium supplemented with 1 μg/mL ampicillin in an orbital shaker at 37° C. Then bacteria were centrifuged down, and the pellet was resuspended in 2 liters TB dry medium and cultured for 24 hours in an orbital shaker at 37° C. The bacteria were again harvested by centrifugation at 4° C. and resuspended in phosphate buffer saline (PBS). The bacteria were lysed by discontinuous pulsed ultrasonication in an ice-water bath. The insoluble debris was removed from the lysate by centrifugation and nucleic acids were precipitated by adding polyethylenimine (0.5% w/v final concentration) and removed by centrifugation at 4° C. From the clarified bacterial lysates, the ELPs and knob-ELPs were purified by inverse transition cycling (ITC), which has been described previously [20-22]. Briefly, ELP solutions were warmed at room temperature and NaCl was added (1-3 M final concentration) to induce the ELP phase separation. The aggregated ELP fusion polypeptides were separated from the lysate by centrifugation at room temperature. The ELP pellet was resolubilized in PBS within an ice-water bath. The resolubilized ELP solution was centrifuged at 4° C. to remove remaining aggregated proteins. It was previously reported that purification cycles were repeated for two to six rounds as needed to purify various ELP fusion proteins (See, for e.g., D. E. Meyer, et al., Nature Biotechnology 17 (1999) 1112-111520, and K. Trabbic-Carlson, et al., Protein Sci 13(12) (2004) 3274-3284 which is herein incorporated by reference). In this study, the purification cycle was repeated five times to remove nearly all of the contaminating *E. coli* proteins, which was essential because contaminants may aggregate during heating and bias the hydrodynamic radius. The purity of purified knob-ELP was measured using SDS-PAGE in a 10% gel. After electrophoresis, the gel was stained with Coomassie brilliant blue.

Characterization of Knob-ELP

[0104] As described above, the knob-ELP was designed as a fusion protein consisting of a knob domain and an ELP. To study these multifunctional polypeptides, they were characterized by non-denaturing PAGE, turbidometric analysis of their temperature-dependent phase behavior, and dynamic light scattering. Native fiber/knob proteins are trimeric; therefore, the ability of knob-ELPs to self-associate was characterized using non-denaturing PAGE. Knob-S48I48 and recombinant knob was mixed with sample buffer without 2-mercaptoethanol, and then loaded onto a 10% polyacrylamide gel without SDS at 4° C. At this temperature, the ELP

nanoparticles remain dissociated, which enables the polypeptides to enter the gel. After three hours of electrophoresis, the gel was stained with Coomassie brilliant blue.

[0105] To explore the temperature-dependent phase behavior of the ELPs, optical density and hydrodynamic radius were observed over a range of temperatures. Knob-596, S48I48 and knob-S48I48 were diluted to 25 μM in PBS on ice and the absorbance at 350 nm was monitored with a DU800 UV-Vis spectrophotometer (Beckman Coulter, Brea, Calif.) at a temperature gradient of 1° C./minute. For dynamic light scattering studies, S48I48 and knob-S48I48 were diluted to 25 μM in PBS and passed through 20 nm membrane filters at 4° C., and BSA, a protein with a similar molecular to knob-S48I48 was used as a control. Then 90 μL sample of was transferred into a 384 well microplate and covered with 20 μL mineral oil. The microplate and mineral oil were pre-chilled at 4° C. at least for 1 hour. The microplate was centrifuged at 4° C. to remove air bubbles from samples before and after addition of mineral oil. Then the sample was measured in a DynaPro plate reader (Wyatt Inc., Santa Barbara, Calif.) at temperature intervals of 1° C. The resulting hydrodynamic radii were collected and analyzed by Dynamics (Wyatt Inc., Santa Barbara, Calif.). The measurements were repeated three times and particle radius for BSA, S48I48 and knob-S48I48 at 15° C. and 37° C. were analyzed by a one-way analysis of variance (R^2=1.000, p=10^{-20}, n=18).

Thrombin Cleavage of Knob-ELP

[0106] A thrombin recognition site was designed between the knob domain and ELP sequence (Table 1), which was cleaved by thrombin (Sigma-Aldrich, St. Louis, Mo.). Thrombin immobilized on agarose beads was centrifuged to remove the storage buffer and washed with cleavage buffer (from the thrombin cleavage kit). The knob-S48I48 was then diluted with cleavage buffer to 1 mg/mL and suspended with thrombin agarose slurry for 24 hours at room temperature. After incubation, the thrombin agarose beads were removed by centrifugation. The cleaved knob (21.7 kD) was resolved by SDS-PAGE and gels were stained with Coomassie brilliant blue. The SDS-PAGE gel was scanned with a Molecular Imager Gel Doc XR System (Bio-Rad, Hercules, Calif.) and analyzed with software Quantity one (Bio-Rad).

TABLE 1

Summary of Expressed Polypeptides

Peptide label	*Amino acid sequence	**Critical aggregation temperature (° C.)	Expected molecular weight (kD)	*** Measured molecular weight (kD)	**** Hydrodynamic radius (nm) at 37° C.
knob-S96	knob-$(VPGSG)_{96}$Y (SEQ ID. NO: 8)	68.2	60.179	—	5.3
knob-I96	knob-$(VPGIG)_{96}$Y (SEQ ID. NO: 9)	—	62.682	—	—
knob-S48I48	knob-G$(VPGSG)_{48}(VPGIG)_{48}$Y (SEQ ID. NO: 10)	19.5	61.431	61.241	21.7
S48I48	G$(VPGSG)_{48}(VPGIG)_{48}$Y (SEQ ID. NO: 10)	26.5	39.643	39.670	23.7

*Knob amino acid sequence with thrombin cleavage site underlined:
GAITVGNKNNDKLTLWTTPAPSPNCRLNAEKDAKLTLVLTKCGSQILATVSVLAVKGSLAPISGTVQSAHLIIRFDENGVLLNNSFLDPEYWNFRNG
DLTEGTAYTNAVGFMPNLSAYPKSHGKTAKSNIVSQVYLNGDKTKPVTLTITLNGTQETGDTTPSAYSMSFSWDWSGHNYINEIFATSSYTFSYIAQ
EGLVPRGSG (SEQ ID. NO: 11)
**determined using optical density by UV-Vis spectrophotometer.
***determined using MALDI mass spectrometry.
****determined using dynamic light scattering.

Self-Assembly or Disassembly of Nanoparticles-Above/Below their Phrase Transition Temperatures

TABLE 2

Summary of Expressed Polypeptides

Peptide	Amino acid sequence	Measured molecular weight (kDa)	Transition Temperature (° C.) T1	T2
S48I48	G$(VPGSG)_{48}(VPGIG)_{48}$Y (SEQ ID. NO: 10)	39.67	26.5	75
knob-S48I48	knob-G$(VPGSG)_{48}(VPGIG)_{48}$Y (SEQ ID. NO: 10)	61.24	19.5	60

Conjugation with NHS-Rhodamine

[0107] To track cellular uptake, the ELPs S48I48 and knob-S48I48 were conjugated with a detectable label, NHS-Rhodamine (Thermo Fisher Scientific Inc, Rockford, Ill.) via covalent modification of primary amines at the amino end of the peptide. For S48I48, the only available amine is at the amino terminus; however, knob-S48I48 has an additional 11 lysine residues that may be sites of modification. The conjugation was performed in 100 mM borate buffer for 2 hours at 4° C., and the conjugated ELP was separated by size exclusion chromatography on a PD10 desalting column (GE Healthcare, Piscataway, N.J.).

Cellular Uptake of Knob-ELP/ELP

[0108] Hepatocytes were expected to be enriched in the CAR receptor, according to previous reports (see, for e.g., J. Xie, L. et al., J. Virol. 80(23) (2006) 11833-11851). To confirm this, a western blot was performed on a murine hepatocyte cell-line. CHO cells were used as a negative control. 2×10^4 cells were mixed with SDS-PAGE sample buffer and heated above 95° C. for 5 minutes. CAR was detected by western blotting using a goat anti-mouse CAR antibody as the primary antibody and IRDye®800-conjugated donkey anti-goat antibody as the secondary antibody. The result was scanned using an Odyssey® Imaging System (Li-COR, Lincoln, Nebr., USA) and quantified with the Odyssey® 1.1 software.

[0109] To observe uptake into mouse hepatocytes, cells were cultured on 35 mm glass coverslip-bottomed dishes with medium [(DMEM (4.5 g/L) containing 10% fetal bovine serum, 5 μg/ml insulin, and 0.02 μg/ml epidermal growth factor]. Uptake studies were conducted when hepatocytes reached 70% confluence. After washing with warm fresh medium, hepatocytes were cultured in medium containing 10 μM of either S48I48 or knob-S48I48 conjugated with rhodamine, and 75 nM LysoTracker green. After 30 minutes incubation at 37° C., the cells were rinsed with warm fresh medium to remove the free knob-ELP/ELP in the medium. Next cells were incubated with 75 nM LysoTracker green in a 37° C. incubation chamber. The chamber is mounted on a Zeiss LSM 510 Meta confocal microscope system, which is equipped with argon and red and green HeNe lasers and mounted on a vibration-free table.

[0110] To demonstrate the specificity of knob-ELP internalization for the CAR pathway, hepatocytes were pre-bound with goat anti-mouse CAR antibody. After confirming that the goat anti-mouse CAR antibody has a high affinity with the mouse hepatocytes, the anti-mouse CAR antibody (0.2 mg/mL) was diluted with warm medium 10-fold and incubated with the hepatocytes for 30 minutes at 37° C. Knob-S48I48 conjugated with rhodamine was then added to the medium at a concentration of 10 μM. After 30 minutes incubation with knob-S48I48 and 75 nM LysoTracker green, the hepatocytes were rinsed, then incubated in fresh warm medium with 75 nM LysoTracker green and imaged as described above.

Example 2

Transcytosis of Knob-ELPs to Lacrimal Gland Acinar Lumen

[0111] Intracellular uptake of carboxyfluorescein (CF)-conjugated ELPs in lacrimal gland acinar cells (LGACs) is shown in FIG. **13**. Unlike CF-S48I48, CF-Knob-S48I48 exhibits strong internalization which was shown in green in reconstituted LGACs. FIG. **13** shows that endocytosed CF-Knob-S48I48 was transcytosed into reconstituted acinar lumen which was stained by expressed Lifeact-RFP proteins (red). Lumen A (S48I48) and lumen B (Knob-S48I48) are shown in FIG. **14**. Internalized knob-S48I48 was transcytosed into the luminal area of LGACs as shown in lumen B.

[0112] In a separate experiment the basal-to-apical transport of Cy5-Knob-S48I48 in primary cultures of Lacrimal Gland Acinar Cells (LGACs) was observed. As shown in FIG. **17**, uptake of Cy5-Knob-S48I48 in LGACs with overexpressed RFP-Rab5a. Rabbit LGACs were transduced on day 2 with Adenovirus encoding RFP-Rab5a (red) in order to stain early endosome structures. After 16-18 hours LGACs were incubated with 30 μM Cy5-Knob-S48I48 (green) at 37° C. for 10 min before imaging by confocal microscopy over 40 min. In FIG. **17**, asterisks denote the acinar lumen, and the arrowheads indicate the dynamic fusion of early endosomes containing Cy5-Knob-S48I48 nanoparticles internalized from the basolateral membrane. The transcytosis experiments were conducted in primary rabbit lacrimal gland acinar cells (LGACs). LGACs were isolated and maintained in a laminin-based primary culture system and grown on the 35 mm petri dishes for 2 to 3 days. These culture conditions let LGACs reconstitute polarity, establish lumina, and format secretory vesicles. The dishes were pre-coated with commercial matrigel (BD Sciences, Franklin Lakes, N.J.). The dishes were incubated with 1 mL matrigel at 1:50 dilution with ice cold medium at 37° C. for 30 min and the dishes were emptied prior to adding cells. Female New Zealand White rabbits weighing between 1.8 and 2.2 kg were obtained from Irish Farms (Norco, Calif.). Before the experiment, the LGACs were pre-incubated at the second day with baculovirus encoding RFP-Rab5a overnight, which can indicate basolateral and apical early endosomes of rabbit LGACs. Cy5 labelled knob-S48I48 (Cy5 knob-S48I48) was utilized in the transcytosis experiment. 30 μM Cy5-knob-S48I48 diluted in the same medium as cell cultured at 4° C. and then warmed to 37° C. and added into dishes. The cells were cultured with Cy5 knob-ELPs in a 37° C. incubator with 5% CO_2. After 10 minutes incubation, the LGACs were washed with fresh warm medium three times to remove the free Cy5-knob-S48I48 in the medium. Then the cells were incubated with fresh warm medium in a 37° C. incubation chamber. The chamber is mounted on a Zeiss LSM 510 Meta confocal microscope system, which is equipped with argon and red and green He—Ne lasers and mounted on a vibration-free table.

[0113] It was also found that overexpression of Myosin Vb tail suppresses accumulation of knob-S48I48 nanopraticles at the acinar lumen. A mCherry myosin Vb tail, an inhibitor of LGAC transcytosis from basolateral to apical membranes, was found to significantly reduce the transcytosis of knob-S48I48 (FIG. **19**). Quantification of these results is shown in FIG. **20**A-B. For this experiment, LGACs were pre-infected with adenovirus mCherry-Myosin Vb tail. To obtain the indication of lumen area of LGACs, the cells were also pre-infected with Adenovirus EGFP-actin and helper virus at a 37° C. incubator with 5% CO_2 overnight. To avoid the clash of fluorescence colours, the knob-S48I48 used in transcytosis inhibition was conjugated with Cy5. The LGACs were grown on 35 mm glass-bottomed dishes for two days. Adenovirus EGFP-actin and helper virus with or without adenovirus mCherry Myosin Vb tail were added into dishes and cultured overnight. After waiting for expression of fluorescence, con-

focal microscopy was used to make sure adenovirus mCherry-myosin Vb tail and adenovirus EGFP-actin grow in LGACs. On the third day, knob-S48I48 conjugated with Cy5 was then mixed with the cold medium at a concentration of 30 μM, warmed to 37° C. and then added into dishes. After 60 minutes incubation in a 37° C. incubator with 5% CO_2, LGACs were thoroughly rinsed with fresh warm medium then immediately imaged under a Zeiss LSM 510 Meta confocal microscope system, which is equipped with argon and red and green He—Ne lasers and mounted on a vibration-free table. All images were captured under the confocal microscope and processed using ImageJ (NIH, USA).

[0114] FIG. **15** shows a schematic representation showing knob-S48I48 nanoparticles targeted to CAR in LGACs. As depicted in FIG. **15**A, Knob-S48I48 reversibly assembles into micelles or disassembles into peptide monomers in response to temperature. Knob-S48I48 contains a full-length Ad5 knob domain at its N-terminus followed by a thrombin cleavage site and the protein polymer S48I48. FIG. **15**B depicts multivalent knob-S48I48 nanoparticles associate with the CAR, abundantly expressed on the cellular surface of hepatocytes and LGACs, and followed by internalization via CAR-mediated endocytosis. Endocytosed Knob-S48I48 nanoparticles are transported to early endosomes in LGACs, which is followed by basal-to-apical transport to the acinar lumen, a process called transcytosis. In reconstituted rabbit LGACs, internalized knob-S48I48 nanoparticles are shuttled between basal early endosomes, apical early endosomes, and sorting endosomes.

In Vivo Retention of Knob-S48I48 in the LG of BALB/c Mice.

[0115] Twelve-week-old male BALB/c mice were administered, by intra-lacrimal gland injection, 5 μL of 50 μM rhodamine-labelled S48I48 or rhodamine-labelled knob-S48I48 (red) combined with 50 μg CF-dextran (10 kD, green). After 1 h, mice were euthanized and the glands were retrieved, embedded into the O.C.T. compound (Tissue-Tek), and frozen on dry ice. The frozen tissue blocks were cut into 10 μm thick sections and imaged using confocal fluorescence microscopy. The white arrows indicate endocytosed S48I48 or knob-S48I48 nanoparticles. The bar represents 10 μm. Mouse LGs injected with rhodamine-labelled knob-S48I48 display stronger apical-membrane/luminal accumulation, surface association, and internalization than did untargeted S48I48. This data is shown in FIG. **16**. For this experiment, the mice were euthanatized by intraperitoneal injection with 55 mg ketamine and 14 mg xylazine per kilogram of body weight, followed by cervical dislocation. 5 μL of 50 μM rhodamine labelled knob-S48I48 or S48I48 was injected into the lacrimal glands of mice. After 60 minutes, the tear was collected from one eye of mouse by adding Carbachol into the related lacrimal gland. For another gland, it was removed after the tear collection was done at the first eye. After removal, LGs were snap frozen and stored on the dry ice. The frozen glands were cut into 10 μm thick sections and mounted on glass slides. Then the sections were examined with a confocal laser scanning microscope (LSM) at excitation wavelengths of 488 and 534 nm.

Knob-ELP Purification

[0116] A series of ELPs were genetically engineered, expressed in *E. coli*, and purified using the ELP temperature-dependent phase transition property (Table 1). The purified material was characterized for molecular weight and purity using SDS-PAGE and matrix assisted laser desorption ion mass spectrometry (FIG. **2**, Table 1). Three fusion peptides with knob were prepared, knob-S96, knob-S48I48, and knob-I96. The ELPs S96 and 196 have a high and low transition temperature respectively; however, they do not form nanoparticles (data not shown). In contrast, the ELP S48I48 was shown to form nanoparticles at physiological temperatures (Table 1). Each of these fusion peptides appears as a major band around 60 kD (FIG. **2**), which corresponds to the predicted and observed molecular weights as determined using mass spectrometry (Table 1). Some contaminating *E. coli* proteins appear to co-purify with both knob-I96 and knob-S96 but not knob-S48I48. Although not essential for this study, the non-chromatographic purification of proteins fused to ELPs represents a powerful advantage of this approach.

Characterization of Knob-ELP

[0117] To determine if the knob-ELP fusion peptides exist in a trimeric form, as they do for native adenovirus as required for appropriate CAR binding, non-denaturing gel electrophoresis was performed (FIG. **3**). Knob-S48I48 surprisingly showed three strong bands around 60 kD, 120 kD and 180 kD, which indicated monomer, dimer and trimer forms of knob-ELP. For comparison, a recombinant knob purified using nickel affinity chromatography (without ELP) was also confirmed to form predominantly trimers. The recombinant knob lane indicates several minor bands, with molecular weights slightly lower than knob. These minor bands may come from partial proteolysis of knob. This data suggests that the ELP architecture may influence the native quaternary structure of fused proteins domains, whereby block copolymers that assemble nanoparticles (S48I48) also promote formation of native trimers. So the recombinant knob-ELP has properties similar to those of the native knob.

[0118] To characterize the ELP behavior of the knob fusion peptides, the transition temperatures were identified by optical density (FIG. **4**) and the assembly of nanoparticles was confirmed using dynamic light scattering. Knob-596, a monoblock ELP, only exhibits one increase in optical density over a temperature gradient at a temperature well above physiological conditions. Knob-196 also shows a single increase in optical density; however, due to the hydrophobicity of the isoleucine X residue, this fusion peptide phase-separates near room temperature. In contrast, the diblock ELP Knob-S48I48 displayed two phase transition temperatures, one around 19.5° C. and another around 60° C. Qualitatively, this behavior is similar to S48I48, which has two transition temperatures at 26.5 and 75° C. For knob-S48I48, at temperatures below 19.5° C., the polypeptides are free in solution; however, between 19.5 and about 40° C. the peptides are presumed to form nanoparticles. Above 60° C., the S48 block phase separates, and nanoparticles are not stable. By comparing the critical aggregation temperatures of knob-S48I48 and S48I48, it can be easily observed that the knob domain slightly depresses the nanoparticle assembly temperature (Table 1).

[0119] While optical density is useful to determine the temperature of assembly, dynamic light scattering is necessary to verify the size and formation of stable nanoparticles. Upon heating, both S48I48 and knob-S48I48 self-assemble into nanoparticles and this assembly was shown to be reversible upon cooling (FIG. **5**(A)). When the temperature increased

from 10 to 37° C., both knob-S48I48 and S48I48 transitioned from unimers to nanoparticles, of a radius previously shown to be nanoparticles (see, for e.g., M. R. Dreher, et. al. J Am Chem Soc 130(2) (2008) 687-694). This assembly is reversible, and the nanoparticles were disassembled into unimers when temperature decreased from 37 to 10° C. It was shown by DLS that S48I48 and knob-S48I48 self-assemble into nanoparticles with a diameter consistent with micelles as reported (see, for e.g., M. R. Dreher, et. al. J Am Chem Soc 130(2) (2008) 687-694). At physiological temperature (37° C.), the hydrodynamic radii of S48I48 and knob-S48I48 nanoparticles were 23.7 and 21.7 nm respectively. As observed using dynamic light scattering, the critical nanoparticle temperature (CNT) for knob-ELP is 19.5° C. while ELP without knob is 26.5° C. This downward shift in CNT is consistent with that observed by optical density (FIG. **4**). While the addition of knob to the ELP lowers the nanoparticle assembly temperature, it did not change the hydrodynamic radius. The control BSA exhibits a stable size around 4 nm, the same as the unimers of knob-S48I48 and S48I48, because BSA does not have any phase transition behavior. The ANOVA results (FIG. **5**(B)) indicate that BSA, S48I48 and knob-S48I48 have similar sizes at 15° C., while the particles size of S48I48 and knob-S48I48 had a significantly larger radii at 37° C. compared with BSA ($p<0.01$).

[0120] S48I48 protein polymer nanoparticles with and without the Knob domain were viewed by cryo-transmission electron microscopy (TEM) imaging. Cryo-TEM specimens were prepared using FEI Vitrobot (Hillsboro, Oreg.). ELP solutions were kept in an ice bath (4° C.) before processing. A typical procedure involves first loading ~6 uL of the sample on a TEM grid coated with a lacey carbon film (LC325-Cu, Electron Microscopy Sciences). Then, the specimen was carefully blotted under 95% humidity following blotting parameters that were preset depending on the viscosity and concentration of the studied sample. The blotted grid was immediately transferred into liquid ethane, and stored in liquid nitrogen environment. Micrographs were acquired using FEI Tecnai 12 TWIN transmission electron microscope equipped with 16 bit 2Kx2K FEI eagle bottom mount camera (Hillsboro, Oreg.). All images were captured under 100 kV accelerating voltage and processed using ImageJ (NIH, USA). As shown in FIG. **18**B, the particles were found to have an average particle size from about 30-40 nm.

Cleavage of Knob-ELP

[0121] To determine if these ELPs can be utilized as a strategy to purify free knob, a thrombin recognition site was incorporated into the construct between knob and the ELP (Table 1). The knob-S48I48 construct was incubated with a thrombin cleavage solution, which partially cleaved the fusion peptide, as validated by a band near 20 kD (FIG. **6**). Since the thrombin recognition site can be cleaved, there exists the possibility of harvesting recombinant knob from knob-ELP fusion peptides. More importantly, the molecular weight bands resulting from cleavage of knob from ELP further confirm the successful expression of the knob-ELP constructs.

Cellular Uptake

[0122] To determine if knob-mediated internalization is conferred to knob-ELP fusion peptides, live cell uptake experiments were conducted to study the internalization of knob-S48I48 into a hepatocyte cell line. This study was carried out in transformed mouse hepatocytes because of the high expression of CAR, which has been hypothesized to mediate the novel fiber and knob-dependent endocytotic uptake that has been observed. Prior to uptake studies, it was necessary to confirm that the hepatocyte cell line does express CAR (FIG. **7**). A western blot comparing CAR expression in three representative and commonly utilized cell types indicated that hepatocyte lysates showed very strong immunoreactivity around 46 kD in mouse hepatocyte cell lysate only, which is the correct molecular weight for CAR. CHO cell lysates showed a slight band and there was no expression detectable in Hela cell lysates.

[0123] Having demonstrated that the hepatocyte cell line expresses CAR, a rhodamine-labeled knob-S48I48 was employed to explore uptake via the CAR pathway. A rhodamine-labeled S48I48 was used as a control for cell-surface binding of ELPs. With 30 minutes incubation at 37° C., there was a significant cellular uptake of knob-S48I48 (FIG. **8**). For reference, LysoTracker green was used to stain low pH lysosomes inside the cells. A control sample without ELP shows no signal (absence of red labeling). In contrast, both knob-S48I48 and S48I48 can be clearly seen at the surface of the hepatocytes. Compared with S48I48, knob-S48I48 exhibited much stronger punctate red fluorescence inside hepatocyte cells, and S48I48 exhibited slightly more intense fluorescence on the cell surface. Both the intracellular fluorescence of knob-S48I48 and S48I48 that was seen was co-localized with low pH compartments; however, only knob-S48I48 showed an abundant punctate intracellular fluorescence labeling pattern (FIG. **8**).

[0124] Having demonstrated an effect of the fused knob domain on the cellular internalization of the fluorescent label, a competitive binding study was used to determine the specificity of uptake for the CAR pathway (FIG. **9**). Pre-incubation with anti-mouse CAR antibody reduced the intracellular punctate fluorescence associated with intracellular knob-S48I48 nanoparticles relative to the signal detected in hepatocytes without antibody pre-binding. This result suggests the anti-mouse CAR antibody blocks or alters the internalization of knob-S48I48 into hepatocytes. Incubation with a non-specific antibody similarly did not affect knob-S48I48 uptake (data not shown). In conjunction with the previous experiment, this data supports a model of uptake of knob-ELP nanoparticles via a unique CAR-mediated endocytotic pathway.

[0125] To develop a novel targeted drug carrier, the knob domain of fiber protein from adenovirus 5 was fused with a diblock ELP capable of assembling nanoparticles. Plasmids encoding knob-ELP and ELP were constructed and purified from *E. coli*. Non-denaturing PAGE demonstrated that knob-ELP fusion peptides form trimeric and dimeric quaternary structures, which is a property of the native knob. Dynamic light scattering indicated that both knob-S48I48 and S48I48 can self-assemble into compact nanoparticles, with hydrodynamic diameters around 40 nm. The critical nanoparticle temperature of S48I48 and knob-S48I48 were 26.5 and 19.5° C. respectively. Cellular uptake experiments indicated that both S48I48 and knob-S48I48 bind a hepatocyte cell line; however, the knob-S48I48 showed more intracellular vesicular uptake, specifically into lysosomal compartments. A competitive binding experiment with anti mouse CAR antibody blocks the internalization of knob-S48I48, suggesting that uptake is mediated by knob-CAR binding and endocytosis.

Unlike adenovirus, this simplified fusion peptide lacks many of the capsid proteins responsible for immunogenicity; furthermore, the knob-domain lacks the adenoviral RGD motif that targets integrins. As such, these polypeptide nanoparticles are a potentially useful new class of drug carriers that target a unique uptake mechanism, which is differentially expressed throughout the body.

[0126] It should be understood that although the present invention has been specifically disclosed by preferred embodiments and optional features, modification, improvement and variation of the inventions embodied therein herein disclosed may be resorted to by those skilled in the art, and that such modifications, improvements and variations are considered to be within the scope of this invention such as for example, embodiments described in Appendix A attached hereto. The materials, methods, and examples provided here are representative of preferred embodiments, are exemplary, and are not intended as limitations on the scope of the invention.

[0127] The invention has been described broadly and generically herein. Each of the narrower species and subgeneric groupings falling within the generic disclosure also form part of the invention. This includes the generic description of the invention with a proviso or negative limitation removing any subject matter from the genus, regardless of whether or not the excised material is specifically recited herein.

[0128] In addition, where features or aspects of the invention are described in terms of Markush groups, those skilled in the art will recognize that the invention is also thereby described in terms of any individual member or subgroup of members of the Markush group.

[0129] All publications, patent applications, patents, and other references mentioned herein are expressly incorporated by reference in their entirety, to the same extent as if each were incorporated by reference individually. In case of conflict, the present specification, including definitions, will control.

SEQUENCE LISTING

<160> NUMBER OF SEQ ID NOS: 14

<210> SEQ ID NO 1
<211> LENGTH: 5
<212> TYPE: PRT
<213> ORGANISM: Artificial Sequence
<220> FEATURE:
<223> OTHER INFORMATION: Description of Artificial Sequence: Synthetic peptide
<220> FEATURE:
<221> NAME/KEY: MOD_RES
<222> LOCATION: (4)..(4)
<223> OTHER INFORMATION: Any amino acid

<400> SEQUENCE: 1

Val Pro Gly Xaa Gly
1 5

<210> SEQ ID NO 2
<211> LENGTH: 240
<212> TYPE: PRT
<213> ORGANISM: Artificial Sequence
<220> FEATURE:
<223> OTHER INFORMATION: Description of Artificial Sequence: Synthetic polypeptide

<400> SEQUENCE: 2

Val Pro Gly Ser Gly Val Pro Gly Ser Gly Val Pro Gly Ser Gly Val
1 5 10 15

Pro Gly Ser Gly Val Pro Gly Ser Gly Val Pro Gly Ser Gly Val Pro
20 25 30

Gly Ser Gly Val Pro Gly Ser Gly Val Pro Gly Ser Gly Val Pro Gly
35 40 45

Ser Gly Val Pro Gly Ser Gly Val Pro Gly Ser Gly Val Pro Gly Ser
50 55 60

Gly Val Pro Gly Ser Gly Val Pro Gly Ser Gly Val Pro Gly Ser Gly
65 70 75 80

Val Pro Gly Ser Gly Val Pro Gly Ser Gly Val Pro Gly Ser Gly Val
85 90 95

Pro Gly Ser Gly Val Pro Gly Ser Gly Val Pro Gly Ser Gly Val Pro

-continued

```
            100                 105                 110

Gly Ser Gly Val Pro Gly Ser Gly Val Pro Gly Ser Gly Val Pro Gly
        115                 120                 125

Ser Gly Val Pro Gly Ser Gly Val Pro Gly Ser Gly Val Pro Gly Ser
    130                 135                 140

Gly Val Pro Gly Ser Gly Val Pro Gly Ser Gly Val Pro Gly Ser Gly
145                 150                 155                 160

Val Pro Gly Ser Gly Val Pro Gly Ser Gly Val Pro Gly Ser Gly Val
                165                 170                 175

Pro Gly Ser Gly Val Pro Gly Ser Gly Val Pro Gly Ser Gly Val Pro
            180                 185                 190

Gly Ser Gly Val Pro Gly Ser Gly Val Pro Gly Ser Gly Val Pro Gly
        195                 200                 205

Ser Gly Val Pro Gly Ser Gly Val Pro Gly Ser Gly Val Pro Gly Ser
    210                 215                 220

Gly Val Pro Gly Ser Gly Val Pro Gly Ser Gly Val Pro Gly Ser Gly
225                 230                 235                 240


<210> SEQ ID NO 3
<211> LENGTH: 240
<212> TYPE: PRT
<213> ORGANISM: Artificial Sequence
<220> FEATURE:
<223> OTHER INFORMATION: Description of Artificial Sequence: Synthetic
      polypeptide

<400> SEQUENCE: 3

Val Pro Gly Ile Gly Val Pro Gly Ile Gly Val Pro Gly Ile Gly Val
1               5                   10                  15

Pro Gly Ile Gly Val Pro Gly Ile Gly Val Pro Gly Ile Gly Val Pro
            20                  25                  30

Gly Ile Gly Val Pro Gly Ile Gly Val Pro Gly Ile Gly Val Pro Gly
        35                  40                  45

Ile Gly Val Pro Gly Ile Gly Val Pro Gly Ile Gly Val Pro Gly Ile
    50                  55                  60

Gly Val Pro Gly Ile Gly Val Pro Gly Ile Gly Val Pro Gly Ile Gly
65                  70                  75                  80

Val Pro Gly Ile Gly Val Pro Gly Ile Gly Val Pro Gly Ile Gly Val
                85                  90                  95

Pro Gly Ile Gly Val Pro Gly Ile Gly Val Pro Gly Ile Gly Val Pro
            100                 105                 110

Gly Ile Gly Val Pro Gly Ile Gly Val Pro Gly Ile Gly Val Pro Gly
        115                 120                 125

Ile Gly Val Pro Gly Ile Gly Val Pro Gly Ile Gly Val Pro Gly Ile
    130                 135                 140

Gly Val Pro Gly Ile Gly Val Pro Gly Ile Gly Val Pro Gly Ile Gly
145                 150                 155                 160

Val Pro Gly Ile Gly Val Pro Gly Ile Gly Val Pro Gly Ile Gly Val
                165                 170                 175

Pro Gly Ile Gly Val Pro Gly Ile Gly Val Pro Gly Ile Gly Val Pro
            180                 185                 190

Gly Ile Gly Val Pro Gly Ile Gly Val Pro Gly Ile Gly Val Pro Gly
        195                 200                 205

Ile Gly Val Pro Gly Ile Gly Val Pro Gly Ile Gly Val Pro Gly Ile
```

-continued

```
    210                 215                 220

Gly Val Pro Gly Ile Gly Val Pro Gly Ile Gly Val Pro Gly Ile Gly
225                 230                 235                 240


<210> SEQ ID NO 4
<211> LENGTH: 195
<212> TYPE: PRT
<213> ORGANISM: Human adenovirus

<400> SEQUENCE: 4

Gly Ala Ile Thr Val Gly Asn Lys Asn Asn Asp Lys Leu Thr Leu Trp
1               5                   10                  15

Thr Thr Pro Ala Pro Ser Pro Asn Cys Arg Leu Asn Ala Glu Lys Asp
            20                  25                  30

Ala Lys Leu Thr Leu Val Leu Thr Lys Cys Gly Ser Gln Ile Leu Ala
        35                  40                  45

Thr Val Ser Val Leu Ala Val Lys Gly Ser Leu Ala Pro Ile Ser Gly
    50                  55                  60

Thr Val Gln Ser Ala His Leu Ile Ile Arg Phe Asp Glu Asn Gly Val
65                  70                  75                  80

Leu Leu Asn Asn Ser Phe Leu Asp Pro Glu Tyr Trp Asn Phe Arg Asn
                85                  90                  95

Gly Asp Leu Thr Glu Gly Thr Ala Tyr Thr Asn Ala Val Gly Phe Met
            100                 105                 110

Pro Asn Leu Ser Ala Tyr Pro Lys Ser His Gly Lys Thr Ala Lys Ser
        115                 120                 125

Asn Ile Val Ser Gln Val Tyr Leu Asn Gly Asp Lys Thr Lys Pro Val
    130                 135                 140

Thr Leu Thr Ile Thr Leu Asn Gly Thr Gln Glu Thr Gly Asp Thr Thr
145                 150                 155                 160

Pro Ser Ala Tyr Ser Met Ser Phe Ser Trp Asp Trp Ser Gly His Asn
                165                 170                 175

Tyr Ile Asn Glu Ile Phe Ala Thr Ser Ser Tyr Thr Phe Ser Tyr Ile
            180                 185                 190

Ala Gln Glu
        195


<210> SEQ ID NO 5
<211> LENGTH: 19
<212> TYPE: PRT
<213> ORGANISM: Artificial Sequence
<220> FEATURE:
<223> OTHER INFORMATION: Description of Artificial Sequence: Synthetic
      peptide

<400> SEQUENCE: 5

Thr Trp Ala Ser Arg Gln Glu Pro Ser Gln Gly Thr Thr Thr Phe Ala
1               5                   10                  15

Val Thr Ser


<210> SEQ ID NO 6
<211> LENGTH: 104
<212> TYPE: PRT
<213> ORGANISM: Homo sapiens

<400> SEQUENCE: 6

Arg Pro Glu Val His Leu Leu Pro Pro Pro Ser Glu Glu Leu Ala Leu
```

-continued

```
1               5                   10                  15

Asn Glu Leu Val Thr Leu Thr Cys Leu Ala Arg Gly Phe Ser Pro Lys
            20                  25                  30

Asp Val Leu Val Arg Trp Leu Gln Gly Ser Gln Glu Leu Pro Arg Glu
        35                  40                  45

Lys Tyr Leu Thr Trp Ala Ser Arg Gln Glu Pro Ser Gln Gly Thr Thr
    50                  55                  60

Thr Phe Ala Val Thr Ser Ile Leu Arg Val Ala Ala Glu Asp Trp Lys
65                  70                  75                  80

Lys Gly Asp Thr Phe Ser Cys Met Val Gly His Glu Ala Leu Pro Leu
                85                  90                  95

Ala Phe Thr Gln Lys Thr Ile Asp
            100


<210> SEQ ID NO 7
<211> LENGTH: 7
<212> TYPE: PRT
<213> ORGANISM: Artificial Sequence
<220> FEATURE:
<223> OTHER INFORMATION: Description of Artificial Sequence: Synthetic
      peptide

<400> SEQUENCE: 7

Gly Leu Val Pro Arg Gly Ser
1               5


<210> SEQ ID NO 8
<211> LENGTH: 481
<212> TYPE: PRT
<213> ORGANISM: Artificial Sequence
<220> FEATURE:
<223> OTHER INFORMATION: Description of Artificial Sequence: Synthetic
      polypeptide

<400> SEQUENCE: 8

Val Pro Gly Ser Gly Val Pro Gly Ser Gly Val Pro Gly Ser Gly Val
1               5                   10                  15

Pro Gly Ser Gly Val Pro Gly Ser Gly Val Pro Gly Ser Gly Val Pro
            20                  25                  30

Gly Ser Gly Val Pro Gly Ser Gly Val Pro Gly Ser Gly Val Pro Gly
        35                  40                  45

Ser Gly Val Pro Gly Ser Gly Val Pro Gly Ser Gly Val Pro Gly Ser
    50                  55                  60

Gly Val Pro Gly Ser Gly Val Pro Gly Ser Gly Val Pro Gly Ser Gly
65                  70                  75                  80

Val Pro Gly Ser Gly Val Pro Gly Ser Gly Val Pro Gly Ser Gly Val
                85                  90                  95

Pro Gly Ser Gly Val Pro Gly Ser Gly Val Pro Gly Ser Gly Val Pro
            100                 105                 110

Gly Ser Gly Val Pro Gly Ser Gly Val Pro Gly Ser Gly Val Pro Gly
        115                 120                 125

Ser Gly Val Pro Gly Ser Gly Val Pro Gly Ser Gly Val Pro Gly Ser
    130                 135                 140

Gly Val Pro Gly Ser Gly Val Pro Gly Ser Gly Val Pro Gly Ser Gly
145                 150                 155                 160

Val Pro Gly Ser Gly Val Pro Gly Ser Gly Val Pro Gly Ser Gly Val
                165                 170                 175
```

-continued

```
Pro Gly Ser Gly Val Pro Gly Ser Gly Val Pro Gly Ser Gly Val Pro
            180                 185                 190

Gly Ser Gly Val Pro Gly Ser Gly Val Pro Gly Ser Gly Val Pro Gly
        195                 200                 205

Ser Gly Val Pro Gly Ser Gly Val Pro Gly Ser Gly Val Pro Gly Ser
    210                 215                 220

Gly Val Pro Gly Ser Gly Val Pro Gly Ser Gly Val Pro Gly Ser Gly
225                 230                 235                 240

Val Pro Gly Ser Gly Val Pro Gly Ser Gly Val Pro Gly Ser Gly Val
                245                 250                 255

Pro Gly Ser Gly Val Pro Gly Ser Gly Val Pro Gly Ser Gly Val Pro
            260                 265                 270

Gly Ser Gly Val Pro Gly Ser Gly Val Pro Gly Ser Gly Val Pro Gly
        275                 280                 285

Ser Gly Val Pro Gly Ser Gly Val Pro Gly Ser Gly Val Pro Gly Ser
    290                 295                 300

Gly Val Pro Gly Ser Gly Val Pro Gly Ser Gly Val Pro Gly Ser Gly
305                 310                 315                 320

Val Pro Gly Ser Gly Val Pro Gly Ser Gly Val Pro Gly Ser Gly Val
                325                 330                 335

Pro Gly Ser Gly Val Pro Gly Ser Gly Val Pro Gly Ser Gly Val Pro
            340                 345                 350

Gly Ser Gly Val Pro Gly Ser Gly Val Pro Gly Ser Gly Val Pro Gly
        355                 360                 365

Ser Gly Val Pro Gly Ser Gly Val Pro Gly Ser Gly Val Pro Gly Ser
    370                 375                 380

Gly Val Pro Gly Ser Gly Val Pro Gly Ser Gly Val Pro Gly Ser Gly
385                 390                 395                 400

Val Pro Gly Ser Gly Val Pro Gly Ser Gly Val Pro Gly Ser Gly Val
                405                 410                 415

Pro Gly Ser Gly Val Pro Gly Ser Gly Val Pro Gly Ser Gly Val Pro
            420                 425                 430

Gly Ser Gly Val Pro Gly Ser Gly Val Pro Gly Ser Gly Val Pro Gly
        435                 440                 445

Ser Gly Val Pro Gly Ser Gly Val Pro Gly Ser Gly Val Pro Gly Ser
    450                 455                 460

Gly Val Pro Gly Ser Gly Val Pro Gly Ser Gly Val Pro Gly Ser Gly
465                 470                 475                 480

Tyr


<210> SEQ ID NO 9
<211> LENGTH: 481
<212> TYPE: PRT
<213> ORGANISM: Artificial Sequence
<220> FEATURE:
<223> OTHER INFORMATION: Description of Artificial Sequence: Synthetic
      polypeptide

<400> SEQUENCE: 9

Val Pro Gly Ile Gly Val Pro Gly Ile Gly Val Pro Gly Ile Gly Val
1               5                   10                  15

Pro Gly Ile Gly Val Pro Gly Ile Gly Val Pro Gly Ile Gly Val Pro
            20                  25                  30
```

-continued

```
Gly Ile Gly Val Pro Gly Ile Gly Val Pro Gly Ile Gly Val Pro Gly
        35                  40                  45

Ile Gly Val Pro Gly Ile Gly Val Pro Gly Ile Gly Val Pro Gly Ile
    50                  55                  60

Gly Val Pro Gly Ile Gly Val Pro Gly Ile Gly Val Pro Gly Ile Gly
65                  70                  75                  80

Val Pro Gly Ile Gly Val Pro Gly Ile Gly Val Pro Gly Ile Gly Val
                85                  90                  95

Pro Gly Ile Gly Val Pro Gly Ile Gly Val Pro Gly Ile Gly Val Pro
            100                 105                 110

Gly Ile Gly Val Pro Gly Ile Gly Val Pro Gly Ile Gly Val Pro Gly
        115                 120                 125

Ile Gly Val Pro Gly Ile Gly Val Pro Gly Ile Gly Val Pro Gly Ile
    130                 135                 140

Gly Val Pro Gly Ile Gly Val Pro Gly Ile Gly Val Pro Gly Ile Gly
145                 150                 155                 160

Val Pro Gly Ile Gly Val Pro Gly Ile Gly Val Pro Gly Ile Gly Val
                165                 170                 175

Pro Gly Ile Gly Val Pro Gly Ile Gly Val Pro Gly Ile Gly Val Pro
            180                 185                 190

Gly Ile Gly Val Pro Gly Ile Gly Val Pro Gly Ile Gly Val Pro Gly
        195                 200                 205

Ile Gly Val Pro Gly Ile Gly Val Pro Gly Ile Gly Val Pro Gly Ile
    210                 215                 220

Gly Val Pro Gly Ile Gly Val Pro Gly Ile Gly Val Pro Gly Ile Gly
225                 230                 235                 240

Val Pro Gly Ile Gly Val Pro Gly Ile Gly Val Pro Gly Ile Gly Val
                245                 250                 255

Pro Gly Ile Gly Val Pro Gly Ile Gly Val Pro Gly Ile Gly Val Pro
            260                 265                 270

Gly Ile Gly Val Pro Gly Ile Gly Val Pro Gly Ile Gly Val Pro Gly
        275                 280                 285

Ile Gly Val Pro Gly Ile Gly Val Pro Gly Ile Gly Val Pro Gly Ile
    290                 295                 300

Gly Val Pro Gly Ile Gly Val Pro Gly Ile Gly Val Pro Gly Ile Gly
305                 310                 315                 320

Val Pro Gly Ile Gly Val Pro Gly Ile Gly Val Pro Gly Ile Gly Val
                325                 330                 335

Pro Gly Ile Gly Val Pro Gly Ile Gly Val Pro Gly Ile Gly Val Pro
            340                 345                 350

Gly Ile Gly Val Pro Gly Ile Gly Val Pro Gly Ile Gly Val Pro Gly
        355                 360                 365

Ile Gly Val Pro Gly Ile Gly Val Pro Gly Ile Gly Val Pro Gly Ile
    370                 375                 380

Gly Val Pro Gly Ile Gly Val Pro Gly Ile Gly Val Pro Gly Ile Gly
385                 390                 395                 400

Val Pro Gly Ile Gly Val Pro Gly Ile Gly Val Pro Gly Ile Gly Val
                405                 410                 415

Pro Gly Ile Gly Val Pro Gly Ile Gly Val Pro Gly Ile Gly Val Pro
            420                 425                 430

Gly Ile Gly Val Pro Gly Ile Gly Val Pro Gly Ile Gly Val Pro Gly
        435                 440                 445
```

-continued

```
Ile Gly Val Pro Gly Ile Gly Val Pro Gly Ile Gly Val Pro Gly Ile
    450                 455                 460

Gly Val Pro Gly Ile Gly Val Pro Gly Ile Gly Val Pro Gly Ile Gly
465                 470                 475                 480

Tyr


<210> SEQ ID NO 10
<211> LENGTH: 482
<212> TYPE: PRT
<213> ORGANISM: Artificial Sequence
<220> FEATURE:
<223> OTHER INFORMATION: Description of Artificial Sequence: Synthetic
      polypeptide

<400> SEQUENCE: 10

Gly Val Pro Gly Ser Gly Val Pro Gly Ser Gly Val Pro Gly Ser Gly
1               5                   10                  15

Val Pro Gly Ser Gly Val Pro Gly Ser Gly Val Pro Gly Ser Gly Val
            20                  25                  30

Pro Gly Ser Gly Val Pro Gly Ser Gly Val Pro Gly Ser Gly Val Pro
        35                  40                  45

Gly Ser Gly Val Pro Gly Ser Gly Val Pro Gly Ser Gly Val Pro Gly
    50                  55                  60

Ser Gly Val Pro Gly Ser Gly Val Pro Gly Ser Gly Val Pro Gly Ser
65                  70                  75                  80

Gly Val Pro Gly Ser Gly Val Pro Gly Ser Gly Val Pro Gly Ser Gly
                85                  90                  95

Val Pro Gly Ser Gly Val Pro Gly Ser Gly Val Pro Gly Ser Gly Val
            100                 105                 110

Pro Gly Ser Gly Val Pro Gly Ser Gly Val Pro Gly Ser Gly Val Pro
        115                 120                 125

Gly Ser Gly Val Pro Gly Ser Gly Val Pro Gly Ser Gly Val Pro Gly
    130                 135                 140

Ser Gly Val Pro Gly Ser Gly Val Pro Gly Ser Gly Val Pro Gly Ser
145                 150                 155                 160

Gly Val Pro Gly Ser Gly Val Pro Gly Ser Gly Val Pro Gly Ser Gly
                165                 170                 175

Val Pro Gly Ser Gly Val Pro Gly Ser Gly Val Pro Gly Ser Gly Val
            180                 185                 190

Pro Gly Ser Gly Val Pro Gly Ser Gly Val Pro Gly Ser Gly Val Pro
        195                 200                 205

Gly Ser Gly Val Pro Gly Ser Gly Val Pro Gly Ser Gly Val Pro Gly
    210                 215                 220

Ser Gly Val Pro Gly Ser Gly Val Pro Gly Ser Gly Val Pro Gly Ser
225                 230                 235                 240

Gly Val Pro Gly Ile Gly Val Pro Gly Ile Gly Val Pro Gly Ile Gly
                245                 250                 255

Val Pro Gly Ile Gly Val Pro Gly Ile Gly Val Pro Gly Ile Gly Val
            260                 265                 270

Pro Gly Ile Gly Val Pro Gly Ile Gly Val Pro Gly Ile Gly Val Pro
        275                 280                 285

Gly Ile Gly Val Pro Gly Ile Gly Val Pro Gly Ile Gly Val Pro Gly
    290                 295                 300
```

-continued

```
Ile Gly Val Pro Gly Ile Gly Val Pro Gly Ile Gly Val Pro Gly Ile
305                 310                 315                 320

Gly Val Pro Gly Ile Gly Val Pro Gly Ile Gly Val Pro Gly Ile Gly
                325                 330                 335

Val Pro Gly Ile Gly Val Pro Gly Ile Gly Val Pro Gly Ile Gly Val
            340                 345                 350

Pro Gly Ile Gly Val Pro Gly Ile Gly Val Pro Gly Ile Gly Val Pro
        355                 360                 365

Gly Ile Gly Val Pro Gly Ile Gly Val Pro Gly Ile Gly Val Pro Gly
    370                 375                 380

Ile Gly Val Pro Gly Ile Gly Val Pro Gly Ile Gly Val Pro Gly Ile
385                 390                 395                 400

Gly Val Pro Gly Ile Gly Val Pro Gly Ile Gly Val Pro Gly Ile Gly
                405                 410                 415

Val Pro Gly Ile Gly Val Pro Gly Ile Gly Val Pro Gly Ile Gly Val
            420                 425                 430

Pro Gly Ile Gly Val Pro Gly Ile Gly Val Pro Gly Ile Gly Val Pro
        435                 440                 445

Gly Ile Gly Val Pro Gly Ile Gly Val Pro Gly Ile Gly Val Pro Gly
    450                 455                 460

Ile Gly Val Pro Gly Ile Gly Val Pro Gly Ile Gly Val Pro Gly Ile
465                 470                 475                 480

Gly Tyr


<210> SEQ ID NO 11
<211> LENGTH: 203
<212> TYPE: PRT
<213> ORGANISM: Artificial Sequence
<220> FEATURE:
<223> OTHER INFORMATION: Description of Artificial Sequence: Synthetic
      polypeptide

<400> SEQUENCE: 11

Gly Ala Ile Thr Val Gly Asn Lys Asn Asn Asp Lys Leu Thr Leu Trp
1               5                   10                  15

Thr Thr Pro Ala Pro Ser Pro Asn Cys Arg Leu Asn Ala Glu Lys Asp
            20                  25                  30

Ala Lys Leu Thr Leu Val Leu Thr Lys Cys Gly Ser Gln Ile Leu Ala
        35                  40                  45

Thr Val Ser Val Leu Ala Val Lys Gly Ser Leu Ala Pro Ile Ser Gly
    50                  55                  60

Thr Val Gln Ser Ala His Leu Ile Ile Arg Phe Asp Glu Asn Gly Val
65                  70                  75                  80

Leu Leu Asn Asn Ser Phe Leu Asp Pro Glu Tyr Trp Asn Phe Arg Asn
                85                  90                  95

Gly Asp Leu Thr Glu Gly Thr Ala Tyr Thr Asn Ala Val Gly Phe Met
            100                 105                 110

Pro Asn Leu Ser Ala Tyr Pro Lys Ser His Gly Lys Thr Ala Lys Ser
        115                 120                 125

Asn Ile Val Ser Gln Val Tyr Leu Asn Gly Asp Lys Thr Lys Pro Val
    130                 135                 140

Thr Leu Thr Ile Thr Leu Asn Gly Thr Gln Glu Thr Gly Asp Thr Thr
145                 150                 155                 160

Pro Ser Ala Tyr Ser Met Ser Phe Ser Trp Asp Trp Ser Gly His Asn
```

-continued

```
                165                 170                 175

Tyr Ile Asn Glu Ile Phe Ala Thr Ser Ser Tyr Thr Phe Ser Tyr Ile
            180                 185                 190

Ala Gln Glu Gly Leu Val Pro Arg Gly Ser Gly
        195                 200


<210> SEQ ID NO 12
<211> LENGTH: 480
<212> TYPE: PRT
<213> ORGANISM: Artificial Sequence
<220> FEATURE:
<223> OTHER INFORMATION: Description of Artificial Sequence: Synthetic
      polypeptide

<400> SEQUENCE: 12

Val Pro Gly Ser Gly Val Pro Gly Ser Gly Val Pro Gly Ser Gly Val
1               5                   10                  15

Pro Gly Ser Gly Val Pro Gly Ser Gly Val Pro Gly Ser Gly Val Pro
            20                  25                  30

Gly Ser Gly Val Pro Gly Ser Gly Val Pro Gly Ser Gly Val Pro Gly
        35                  40                  45

Ser Gly Val Pro Gly Ser Gly Val Pro Gly Ser Gly Val Pro Gly Ser
    50                  55                  60

Gly Val Pro Gly Ser Gly Val Pro Gly Ser Gly Val Pro Gly Ser Gly
65                  70                  75                  80

Val Pro Gly Ser Gly Val Pro Gly Ser Gly Val Pro Gly Ser Gly Val
                85                  90                  95

Pro Gly Ser Gly Val Pro Gly Ser Gly Val Pro Gly Ser Gly Val Pro
            100                 105                 110

Gly Ser Gly Val Pro Gly Ser Gly Val Pro Gly Ser Gly Val Pro Gly
        115                 120                 125

Ser Gly Val Pro Gly Ser Gly Val Pro Gly Ser Gly Val Pro Gly Ser
    130                 135                 140

Gly Val Pro Gly Ser Gly Val Pro Gly Ser Gly Val Pro Gly Ser Gly
145                 150                 155                 160

Val Pro Gly Ser Gly Val Pro Gly Ser Gly Val Pro Gly Ser Gly Val
                165                 170                 175

Pro Gly Ser Gly Val Pro Gly Ser Gly Val Pro Gly Ser Gly Val Pro
            180                 185                 190

Gly Ser Gly Val Pro Gly Ser Gly Val Pro Gly Ser Gly Val Pro Gly
        195                 200                 205

Ser Gly Val Pro Gly Ser Gly Val Pro Gly Ser Gly Val Pro Gly Ser
    210                 215                 220

Gly Val Pro Gly Ser Gly Val Pro Gly Ser Gly Val Pro Gly Ser Gly
225                 230                 235                 240

Val Pro Gly Ile Gly Val Pro Gly Ile Gly Val Pro Gly Ile Gly Val
                245                 250                 255

Pro Gly Ile Gly Val Pro Gly Ile Gly Val Pro Gly Ile Gly Val Pro
            260                 265                 270

Gly Ile Gly Val Pro Gly Ile Gly Val Pro Gly Ile Gly Val Pro Gly
        275                 280                 285

Ile Gly Val Pro Gly Ile Gly Val Pro Gly Ile Gly Val Pro Gly Ile
    290                 295                 300

Gly Val Pro Gly Ile Gly Val Pro Gly Ile Gly Val Pro Gly Ile Gly
```

-continued

305 310 315 320

Val Pro Gly Ile Gly Val Pro Gly Ile Gly Val Pro Gly Ile Gly Val
325 330 335

Pro Gly Ile Gly Val Pro Gly Ile Gly Val Pro Gly Ile Gly Val Pro
340 345 350

Gly Ile Gly Val Pro Gly Ile Gly Val Pro Gly Ile Gly Val Pro Gly
355 360 365

Ile Gly Val Pro Gly Ile Gly Val Pro Gly Ile Gly Val Pro Gly Ile
370 375 380

Gly Val Pro Gly Ile Gly Val Pro Gly Ile Gly Val Pro Gly Ile Gly
385 390 395 400

Val Pro Gly Ile Gly Val Pro Gly Ile Gly Val Pro Gly Ile Gly Val
405 410 415

Pro Gly Ile Gly Val Pro Gly Ile Gly Val Pro Gly Ile Gly Val Pro
420 425 430

Gly Ile Gly Val Pro Gly Ile Gly Val Pro Gly Ile Gly Val Pro Gly
435 440 445

Ile Gly Val Pro Gly Ile Gly Val Pro Gly Ile Gly Val Pro Gly Ile
450 455 460

Gly Val Pro Gly Ile Gly Val Pro Gly Ile Gly Val Pro Gly Ile Gly
465 470 475 480

<210> SEQ ID NO 13
<211> LENGTH: 480
<212> TYPE: PRT
<213> ORGANISM: Artificial Sequence
<220> FEATURE:
<223> OTHER INFORMATION: Description of Artificial Sequence: Synthetic polypeptide

<400> SEQUENCE: 13

Val Pro Gly Ser Gly Val Pro Gly Ser Gly Val Pro Gly Ser Gly Val
1 5 10 15

Pro Gly Ser Gly Val Pro Gly Ser Gly Val Pro Gly Ser Gly Val Pro
20 25 30

Gly Ser Gly Val Pro Gly Ser Gly Val Pro Gly Ser Gly Val Pro Gly
35 40 45

Ser Gly Val Pro Gly Ser Gly Val Pro Gly Ser Gly Val Pro Gly Ser
50 55 60

Gly Val Pro Gly Ser Gly Val Pro Gly Ser Gly Val Pro Gly Ser Gly
65 70 75 80

Val Pro Gly Ser Gly Val Pro Gly Ser Gly Val Pro Gly Ser Gly Val
85 90 95

Pro Gly Ser Gly Val Pro Gly Ser Gly Val Pro Gly Ser Gly Val Pro
100 105 110

Gly Ser Gly Val Pro Gly Ser Gly Val Pro Gly Ser Gly Val Pro Gly
115 120 125

Ser Gly Val Pro Gly Ser Gly Val Pro Gly Ser Gly Val Pro Gly Ser
130 135 140

Gly Val Pro Gly Ser Gly Val Pro Gly Ser Gly Val Pro Gly Ser Gly
145 150 155 160

Val Pro Gly Ser Gly Val Pro Gly Ser Gly Val Pro Gly Ser Gly Val
165 170 175

Pro Gly Ser Gly Val Pro Gly Ser Gly Val Pro Gly Ser Gly Val Pro

-continued

```
            180                 185                 190

Gly Ser Gly Val Pro Gly Ser Gly Val Pro Gly Ser Gly Val Pro Gly
        195                 200                 205

Ser Gly Val Pro Gly Ser Gly Val Pro Gly Ser Gly Val Pro Gly Ser
    210                 215                 220

Gly Val Pro Gly Ser Gly Val Pro Gly Ser Gly Val Pro Gly Ser Gly
225                 230                 235                 240

Val Pro Gly Ser Gly Val Pro Gly Ser Gly Val Pro Gly Ser Gly Val
                245                 250                 255

Pro Gly Ser Gly Val Pro Gly Ser Gly Val Pro Gly Ser Gly Val Pro
            260                 265                 270

Gly Ser Gly Val Pro Gly Ser Gly Val Pro Gly Ser Gly Val Pro Gly
        275                 280                 285

Ser Gly Val Pro Gly Ser Gly Val Pro Gly Ser Gly Val Pro Gly Ser
    290                 295                 300

Gly Val Pro Gly Ser Gly Val Pro Gly Ser Gly Val Pro Gly Ser Gly
305                 310                 315                 320

Val Pro Gly Ser Gly Val Pro Gly Ser Gly Val Pro Gly Ser Gly Val
                325                 330                 335

Pro Gly Ser Gly Val Pro Gly Ser Gly Val Pro Gly Ser Gly Val Pro
            340                 345                 350

Gly Ser Gly Val Pro Gly Ser Gly Val Pro Gly Ser Gly Val Pro Gly
        355                 360                 365

Ser Gly Val Pro Gly Ser Gly Val Pro Gly Ser Gly Val Pro Gly Ser
    370                 375                 380

Gly Val Pro Gly Ser Gly Val Pro Gly Ser Gly Val Pro Gly Ser Gly
385                 390                 395                 400

Val Pro Gly Ser Gly Val Pro Gly Ser Gly Val Pro Gly Ser Gly Val
                405                 410                 415

Pro Gly Ser Gly Val Pro Gly Ser Gly Val Pro Gly Ser Gly Val Pro
            420                 425                 430

Gly Ser Gly Val Pro Gly Ser Gly Val Pro Gly Ser Gly Val Pro Gly
        435                 440                 445

Ser Gly Val Pro Gly Ser Gly Val Pro Gly Ser Gly Val Pro Gly Ser
    450                 455                 460

Gly Val Pro Gly Ser Gly Val Pro Gly Ser Gly Val Pro Gly Ser Gly
465                 470                 475                 480


<210> SEQ ID NO 14
<211> LENGTH: 480
<212> TYPE: PRT
<213> ORGANISM: Artificial Sequence
<220> FEATURE:
<223> OTHER INFORMATION: Description of Artificial Sequence: Synthetic
      polypeptide

<400> SEQUENCE: 14

Val Pro Gly Ile Gly Val Pro Gly Ile Gly Val Pro Gly Ile Gly Val
1               5                   10                  15

Pro Gly Ile Gly Val Pro Gly Ile Gly Val Pro Gly Ile Gly Val Pro
            20                  25                  30

Gly Ile Gly Val Pro Gly Ile Gly Val Pro Gly Ile Gly Val Pro Gly
        35                  40                  45

Ile Gly Val Pro Gly Ile Gly Val Pro Gly Ile Gly Val Pro Gly Ile
```

-continued

```
    50                  55                  60

Gly Val Pro Gly Ile Gly Val Pro Gly Ile Gly Val Pro Gly Ile Gly
65                  70                  75                  80

Val Pro Gly Ile Gly Val Pro Gly Ile Gly Val Pro Gly Ile Gly Val
                85                  90                  95

Pro Gly Ile Gly Val Pro Gly Ile Gly Val Pro Gly Ile Gly Val Pro
            100                 105                 110

Gly Ile Gly Val Pro Gly Ile Gly Val Pro Gly Ile Gly Val Pro Gly
        115                 120                 125

Ile Gly Val Pro Gly Ile Gly Val Pro Gly Ile Gly Val Pro Gly Ile
    130                 135                 140

Gly Val Pro Gly Ile Gly Val Pro Gly Ile Gly Val Pro Gly Ile Gly
145                 150                 155                 160

Val Pro Gly Ile Gly Val Pro Gly Ile Gly Val Pro Gly Ile Gly Val
                165                 170                 175

Pro Gly Ile Gly Val Pro Gly Ile Gly Val Pro Gly Ile Gly Val Pro
            180                 185                 190

Gly Ile Gly Val Pro Gly Ile Gly Val Pro Gly Ile Gly Val Pro Gly
        195                 200                 205

Ile Gly Val Pro Gly Ile Gly Val Pro Gly Ile Gly Val Pro Gly Ile
    210                 215                 220

Gly Val Pro Gly Ile Gly Val Pro Gly Ile Gly Val Pro Gly Ile Gly
225                 230                 235                 240

Val Pro Gly Ile Gly Val Pro Gly Ile Gly Val Pro Gly Ile Gly Val
                245                 250                 255

Pro Gly Ile Gly Val Pro Gly Ile Gly Val Pro Gly Ile Gly Val Pro
            260                 265                 270

Gly Ile Gly Val Pro Gly Ile Gly Val Pro Gly Ile Gly Val Pro Gly
        275                 280                 285

Ile Gly Val Pro Gly Ile Gly Val Pro Gly Ile Gly Val Pro Gly Ile
    290                 295                 300

Gly Val Pro Gly Ile Gly Val Pro Gly Ile Gly Val Pro Gly Ile Gly
305                 310                 315                 320

Val Pro Gly Ile Gly Val Pro Gly Ile Gly Val Pro Gly Ile Gly Val
                325                 330                 335

Pro Gly Ile Gly Val Pro Gly Ile Gly Val Pro Gly Ile Gly Val Pro
            340                 345                 350

Gly Ile Gly Val Pro Gly Ile Gly Val Pro Gly Ile Gly Val Pro Gly
        355                 360                 365

Ile Gly Val Pro Gly Ile Gly Val Pro Gly Ile Gly Val Pro Gly Ile
    370                 375                 380

Gly Val Pro Gly Ile Gly Val Pro Gly Ile Gly Val Pro Gly Ile Gly
385                 390                 395                 400

Val Pro Gly Ile Gly Val Pro Gly Ile Gly Val Pro Gly Ile Gly Val
                405                 410                 415

Pro Gly Ile Gly Val Pro Gly Ile Gly Val Pro Gly Ile Gly Val Pro
            420                 425                 430

Gly Ile Gly Val Pro Gly Ile Gly Val Pro Gly Ile Gly Val Pro Gly
        435                 440                 445
```

-continued

```
Ile Gly Val Pro Gly Ile Gly Val Pro Gly Ile Gly Val Pro Gly Ile
    450                 455                 460

Gly Val Pro Gly Ile Gly Val Pro Gly Ile Gly Val Pro Gly Ile Gly
465                 470                 475                 480
```

1. A drug delivery agent comprising an elastin-like peptide (ELP) component and a ligand component, wherein:

(a) the ligand component specifically binds to a CAR and/or pIgR receptor; and/or

(b) the ligand component is mIgA and/or knob ligand, or a biological equivalent thereof of the mIgA or knob ligand.

2. The drug delivery agent of claim **1**, further comprising a detectable label.

3. The drug delivery agent of claim **1**, further comprising a therapeutic agent.

4. The drug delivery agent of claim **3**, wherein the therapeutic agent is an anti-cancer drug.

5. The drug delivery agent of claim **1**, wherein the ELP component comprises a diblock.

6. The drug delivery agent of claim **5**, wherein the ELP component comprises a polypeptide with the sequence $(VPGSG)_{48}(VPGIG)_{48}$ (SEQ ID NO: 12).

7. The drug delivery agent of claim **1**, wherein the ELP component comprises a polypeptide with the sequence $(VPGSG)_{96}$ (SEQ ID. NO: 13).

8. The drug delivery agent of claim **1**, wherein the ELP component comprises a polypeptide with the sequence $(VPGIG)_{96}$ (SEQ ID. NO: 14).

9. The drug delivery agent of claim **1**, wherein the ligand component is a mIgA ligand.

10. The drug delivery agent of claim **9**, wherein the mIgA ligand comprises a polypeptide having the sequence of SEQ ID. NO: 5 or a biological equivalent thereof.

11. The drug delivery agent of claim **1**, wherein the ligand component is a knob ligand.

12. The drug delivery agent of claim **11**, wherein the knob ligand comprises a polypeptide having the sequence of SEQ ID. NO: 4 or a biological equivalent thereof.

13. A polynucleotide encoding the drug delivery agent of claim **1**.

14. A host cell comprising the polynucleotide of claim **13**.

15. A composition comprising a carrier and a drug delivery agent of claim **1**.

16. A method for preparing a drug delivery agent, comprising expressing the polynucleotide of claim **13**.

17. A method for preparing a drug delivery agent, comprising expressing the polynucleotide of in the host cell of claim **14**.

18. The method of claim **16**, further comprising separating or purifying the drug delivery agent.

19. A method for delivering a drug comprising an elastin-like peptide (ELP) to a cell, comprising contacting the cell with a drug delivery agent of claim **1**, wherein:

(a) the ligand component specifically binds to a CAR and/or pIgR receptor; and/or

(b) the ligand component is mIgA and/or knob ligand, or a biological equivalent thereof of the mIgA or knob ligand.

20. A method for delivering a drug to the luminal area of LGACs by transcytosis, comprising contacting the LGAC with a drug delivery agent of claim **1**, wherein:

(a) the ligand component specifically binds to a CAR and/or pIgR receptor; and/or

(b) the ligand component is mIgA and/or knob ligand, or a biological equivalent thereof of the mIgA or knob ligand.

21. The method of claim **20**, wherein the drug is in contact with the ocular surface of the eye.

22. The method of claim **20**, wherein the drug is released from interstitial to luminal surfaces on a mucosal epithelial cell.

23. The method of claim **19**, wherein the contacting is in vitro or in vivo.

24. The method of claim **19**, wherein the cell is one or more of a mucosal cell, an epithelial cell or a hepatocyte and/or contained within a lacrimal gland or tissue.

25. A method for treating a disease of the lacrimal gland, comprising administering to a patient in need of such treatment a drug delivery agent of claim **1** wherein:

(a) the ligand component specifically binds to a CAR and/or pIgR receptor; and/or

(b) the ligand component is mIgA and/or knob ligand, or a biological equivalent thereof of the mIgA or knob ligand, thereby treating the patient.

26. The method of claim **25**, wherein the disease is cancer or Sjorgren's Syndrome.

27. The method of claim **25**, wherein the administration is by inhalation or via injection.

* * * * *

Ocular delivery of a model biopharmaceutical, lacritin, using protein polymers

J. A. MacKay[1,2], W. Wang[1], P. Hsueh[1]; M. Edman-Woolcott[1]; S.F. Hamm-Alvarez[1,3]

[1]Pharmacology and Pharmaceutical Sciences, University of Southern California, Los Angeles, CA, 90033, U.S.A.; [2]Biomedical Engineering, University of Southern California, Los Angeles, CA, 90033, U.S.A.; [3]Physiology and Biophysics and Ophthalmology, University of Southern California, Los Angeles, CA, 90033, U.S.A.
jamackay@usc.edu

ABSTRACT SUMMARY

The delivery of protein and peptide therapeutics to the ocular surface remains a challenge. Due to the rapid turnover of the ocular tear film, sustained release may be necessary to maintain therapeutic concentrations. To approach this problem, we have explored the fusion of thermally-responsive protein polymers directly to therapeutic proteins. As a candidate biopharmaceutical, we have focused on lacritin, which is under evaluation as a treatment for dry eye disease (DED). Lacritin is found in human tears and has both prosecretory and mitogenic functions in the anterior segment of the eye. It is deficient in the tears of DED patients, and lacritin replacement enhances the quality of the tear film in animal models. To modulate the ocular residence time of lacritin, we have expressed it in fusion to a library of elastin-like polypeptides (ELPs). ELPs are thermally responsive protein polymers that can be tuned to phase separate when they reach the temperature of the ocular surface. Lac-ELP fusions have thermally-responsive properties similar to those of the plain ELP and also have activity in a variety of *in vitro* and *in vivo* models, including the induction of tear secretion from the lacrimal glands of non-obese diabetic (NOD) mice.

INTRODUCTION

The lacrimal gland-cornea axis plays a critical role in maintaining ocular health. While avascular cornea serves as both a protective barrier and main refractive element of the visual system, the lacrimal gland is the major organ secreting key proteins and electrolytes into the tear film that overspreads the cornea and conjunctiva [1]. Beyond a hydrating effect, tear proteins contribute to anti-microbial and anti-inflammatory defense of the exposed ocular surface [2]. DED is a multifactorial disease of the tears and ocular surface causing visual disturbance and tear film instability [3]. Accordingly to reports, severe DED affects approximately 5 million Americans above age 50 and its global prevalence ranges from 5% to 35% [3]. Traditional approaches to treat DED include lubricating the ocular surface with artificial tears, conserving the secreted tears using tear plugs and eye-shields, or treating the associated ocular surface inflammation with eye drops containing anti-inflammatory medications [4]. Nevertheless, these therapies are generally regarded as ineffective and there remains a demand for novel DED therapy.

EXPERIMENTAL METHODS

Lac-ELP genes were expressed in *E. coli* and purified by inducing ELP-mediated phase separation. This was followed by size exclusion chromatography to obtain pure material (Fig. 1b). Phase behavior of fusion proteins was characterized by optical density (Fig. 1C). *In vitro* activities were tested using rabbit lacrimal gland acinar cells and SV40-immortalized human corneal epithelial cells. *In vivo* prosecretory potential of Lac-ELPs were tested on 12-week non-obese diabetic (NOD) mice via single bonus intra-lacrimal gland injection.

RESULTS AND DISCUSSION

A novel fusion protein library based on recombinant human lacritin and elastin-like-polypeptides (ELPs) was designed as a potential therapeutic for the ocular surface. The Lacritin-ELP fusion proteins imparted thermo-sensitive assembly of viscous coacervates that may promote retention in the lacrimal gland, on the

cornea, or on contact lenses. Lac-ELP induced tear secretion from male NOD mice, which have inflammation in their lacrimal gland resulting in low tear flow (Fig. 2). Viscous coacervates Lac-V96 formed local drug depot in murine lacrimal gland near injection site (not shown). Using human corneal epithelial cells, Lac-ELPs evoked both a Ca^{2+} wave and closure of a scratch (not shown).

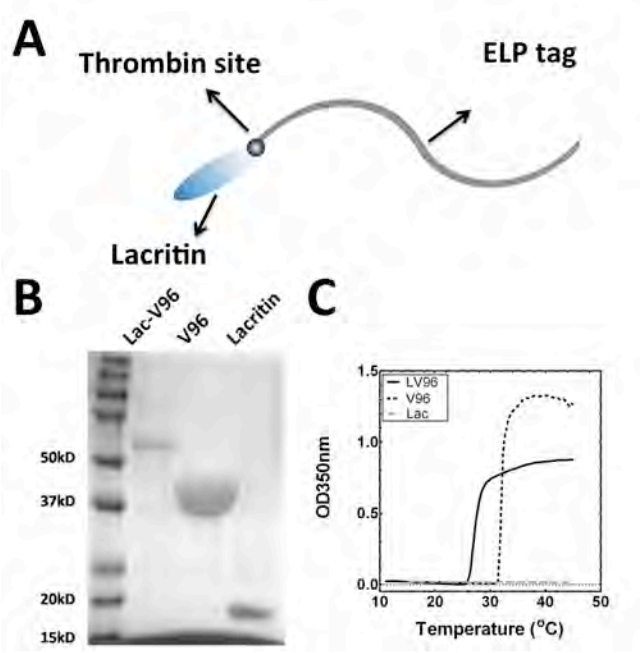

Figure 1. Purification and thermal characterization of a Lac-ELP fusion. A) Cartoon of Lac-ELP showing lacritin at the N-terminus and an ELP tag at the C-terminus of the fusion protein, with a thrombin recognition site between the two moieties. **B**) SDS-PAGE of purified Lac-ELP (LV96), ELP (V96) and lacritin (Lac). **C**) Representative transition temperatures were characterized for LV96 and V96, which phase separate above 26.8 °C and 31.6 °C respectively. These fusions would be expected to phase separate upon the eye.

CONCLUSION

Exploration of ELP-mediated retention of protein drugs in the anterior segment of the eye opens new possibilities for functionalizing peptide and protein-based therapeutics. In this abstract, we demonstrate that lacritin fusions retain both tear secretion potential and also the temperature dependence needed to enhance their retention upon administration to the eye.

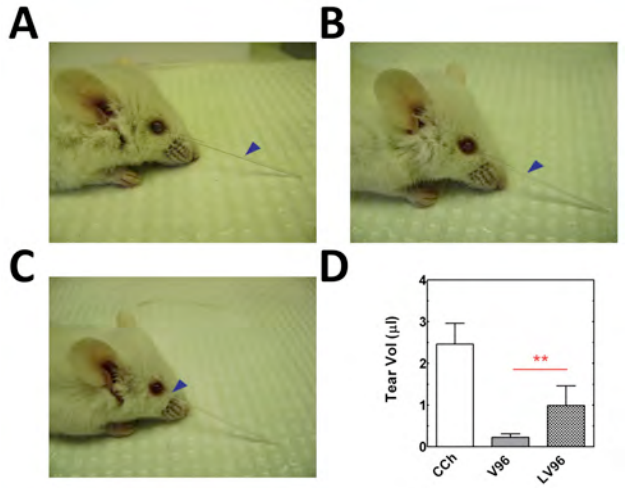

Figure 2. Lacritin ELP fusion proteins stimulate tear secretion in non-obese diabetic (NOD) mice. Representative pictures showing tear secretion stimulated by an intralacrimal gland injection of **A**) a positive control, 50 µM carbachol (CCh), **B)** 100 µM Lac-ELP (LV96), or **C**) an unmodified ELP (V96). Blue arrow: collected tear volume after 30 min. **D**) Tear volumes were quantified and showed significantly enhanced tear secretion of LV96 when compared to plain ELP V96 (**p<0.01, n=9). Data are shown as mean±S.D.

REFERENCES

[1] D.A. Dartt, Neural regulation of lacrimal gland secretory processes: relevance in dry eye diseases, Prog Retin Eye Res, 28 (2009) 155-177.

[2] G.W. Laurie, L.A. Olsakovsky, B.P. Conway, R.L. McKown, K. Kitagawa, J.J. Nichols, Dry eye and designer ophthalmics, Optom Vis Sci, 85 (2008) 643-652.

[3] N.J. Friedman, Impact of dry eye disease and treatment on quality of life, Current opinion in ophthalmology, 21 (2010) 310-316.

[4] E.K. Akpek, K.B. Lindsley, R.S. Adyanthaya, R. Swamy, A.N. Baer, P.J. McDonnell, Treatment of Sjogren's syndrome-associated dry eye an evidence-based review, Ophthalmology, 118 (2011) 1242-1252.

ACKNOWLEDGMENTS

This work was facilitated by support from the University of Southern California School of Pharmacy, The National Institutes of Health and National Eye Institute grant EY011386, the USC Whittier foundation and the USAMRAA/TATRC VRP HAD 11262019.